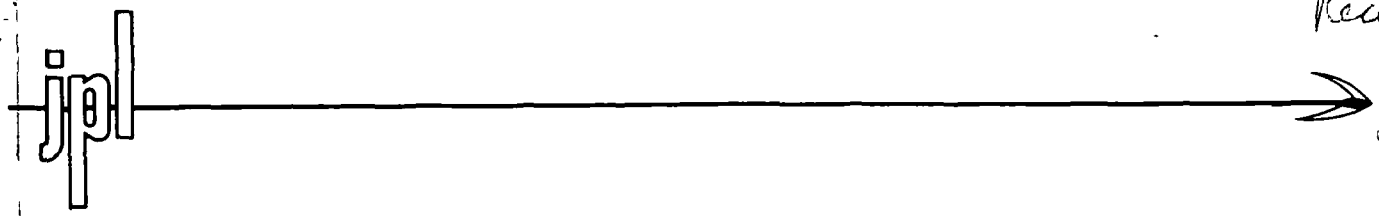

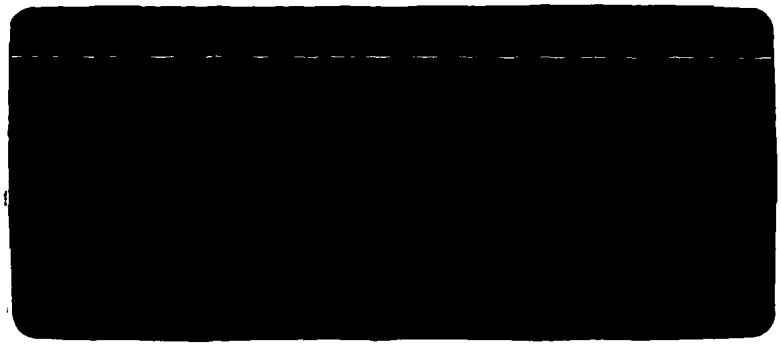

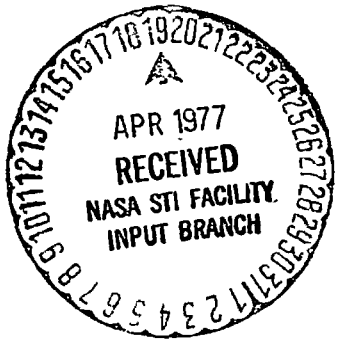

CR-152714

N77-76303

JET PROPULSION LABORATORY
CALIFORNIA INSTITUTE OF TECHNOLOGY
PASADENA, CALIFORNIA

A STUDY OF LUNAR TRAVERSE MISSIONS

JPL -

Document 760-26

16 September 1968

by the JPL Advanced Lunar Studies Team

Approved by:

J. D. Burke, Team Leader

JET PROPULSION LABORATORY
CALIFORNIA INSTITUTE OF TECHNOLOGY
PASADENA, CALIFORNIA

Copyright ©1968
Jet Propulsion Laboratory
California Institute of Technology

Prepared Under Contract No NAS7-100
National Aeronautics & Space Administration

CONTENTS

I. A STUDY OF LUNAR TRAVERSE MISSIONS 1-1

A. INTRODUCTION 1-1

II. MISSION CRITERIA 2-1

A. ASSUMPTIONS 2-1

1. Manned Operations 2-1

2. Orbital and Earth-based Surveys 2-1

B. FUNCTIONAL REQUIREMENTS 2-2

1. Sampling Mission 2-2

2. Traverse Range and Lifetime 2-3

3. Alternate Missions 2-4

4. Payload and Delivery-System Performance 2-6

III. INSTRUMENT PAYLOADS AND SCIENCE OPERATIONS 3-1

A. LUNAR MEASUREMENTS 3-1

B. MISSION OBJECTIVES 3-1

1. Primary Mission 3-1

2. Secondary Mission 3-2

C. SAMPLING REQUIREMENTS 3-3

1. Quantity and Type of Samples 3-3

2. Types of Locations for Obtaining Samples 3-3

3. Configuration of Samples 3-3

4. Additional Analysis Capability of Sampling Mission 3-4

D. GEOLOGICAL AND COMPOSITIONAL INSTRUMENTATION REQUIREMENTS 3-5

1. Types of Instrumentation Required for Lunar Volatiles 3-5

2. Types of Instrumentation Required for Traverse Geophysics 3-6

E. BIOLOGICAL INSTRUMENTATION REQUIREMENTS 3-12

1. Outgassing 3-14

2. Relation of Earth to Moon 3-14

3. Meteoritic Infall 3-14

IV. LUNAR ENVIRONMENT 4-1

A. INTRODUCTION 4-1

B. SURVEYOR TEST RESULTS 4-1

CONTENTS (contd)

V. BASELINE DESIGN 5-1

A. INTRODUCTION 5-1

1. Lunar Delivery Systems 5-1

2. Study Results of Delivery Modes 5-1

B. DESIGN CONFIGURATION 5-6

1. Integrated Spacecraft Design 5-6

2. Vehicle Performance 5-8

3. Sequence of Events 5-10

4. LRV Roving Phase Functional Block Diagram 5-15

C. LUNAR GUIDANCE AND CONTROL SUBSYSTEM 5-15

1. Remote Guidance and Control 5-15

2. Guidance and Control Subsystem Mission Requirements 5-21

3. Factors Covering Mission Requirements 5-22

D. LRV POWER SUBSYSTEM 5-29

1. Transit Operations Power Requirements 5-29

E. TELECOMMUNICATIONS SUBSYSTEM 5-37

1. Radio Frequency Subsystem (RFS) 5-37

2. Flight Command Subsystem (FCS) 5-46

3. Flight Telemetry Subsystem (FTS) 5-48

F. MOBILITY 5-60

1. Mobility Requirements 5-60

2. Mobility Performance 6-62

3. Analytical Approach 5-63

G. THERMAL CONTROL 5-83

1. Thermal Control Requirements 5-83

2. Thermal Control Design 5-85

H. SCIENCE SUBSYSTEMS 5-99

1. Instrument Payload 5-99

2. Description of Instrument Payload 5-99

I. ALTERNATE LRV DESIGN (6-wheel) 5-134

1. Design Concept 5-134

CONTENTS (contd)

J. BASELINE DELIVERY SYSTEM 5-140
1. Delivery System 5-140
2. Flight Thermal Requirements 5-161
K. LRV ADAPTATION TO APOLLO LM 5-161
1. Review 5-161
L. LARGER LRV ADAPTATION TO TITAN IIIC AND LM . . . 5-171
1. Titan IIIC LRV 5-171
M. NAVIGATION STUDIES 5-181
1. Landmark Navigation 5-181
2. Accuracy of Lunar Surface Position Determination Using Earth-Based Radio Ranging and Range-rate . . . 5-190
3. Accuracy of Lunar Surface Position Determination Using Celestial References 5-192
4. Accuracy of Inertial Guidance 5-197
N. TRADE-OFF STUDY OF MISSION PARAMETERS 5-199
1. Average Vehicle Velocity 5-199
2. Assumptions 5-206
3. Average Station Time 5-207
4. Average Step Time and Average Step Distance 5-208
5. Crater Deflection Test 5-210
O. WHEEL-SOIL INTERACTION STUDY AND TESTS 5-215
1. Soil Bearing Capacity Problem 5-215
2. Extension of Analysis 5-217
3. Testing Program 5-218
4. Pressure-Sinkage Test 5-223
5. Testing Plan and Schedule 5-228
6. Exploratory Test Results 5-229
P. OPEN DESIGN ITEMS 5-248
1. Obstacle Encounter Analysis 5-248
2. Solar Panel and High Gain Antenna Articulation 5-252

CONTENTS (contd)

Q. LRV MISSION EXTENSION 5-254
1. Preliminary Review of LRV Growth 5-254
2. Results of Review 5-254
3. Conclusions 5-255
R. SUMMARY OF LRV BASELINE DESIGN 5-257

APPENDICES

A DESCRIPTION OF NMR SPECTROMETER A-1
B DESCRIPTION OF 3-D QUADRUPOLE ION GAGE/MASS SPECTROMETER B-1
C LRV SEQUENCE OF EVENTS C-1
D SURVEYOR MIDCOURSE AND LUNAR LANDING SYSTEM D-1
E CIRCUIT LISTINGS E-1

LIST OF ILLUSTRATIONS

Figure Number	Title	Page
V-1	Payload Weight as a Function of Roving Vehicle Weight . . .	5-2
V-2	Lunar Rover for Atlas-Centaur	5-3
V-2A	LRV Mounted on LM Structure	5-4
V-3	LRV Functional Block Diagram	5-17
V-4	Electrical Power Required for G&C of Automated LRV . . .	5-19
V-5	Conceptual View of Vehicle Path Due to Non-spherical Lunar Surface	5-25
V-6	Example of Vehicle Azimuth Deflection Due to Passing Over Conical Crater	5-27
V-7	Cruise Power Profile	5-30
V-8	Average and Maximum Locomotion Power Versus Average Vehicle Speed	5-32
V-9	Weight Versus Power for RTG and Solar Panel	5-35
V-10	LRV Telecommunications Block Diagram	5-38
V-11	S-band Ranging Transponder Block Diagram	5-40
V-12	Low-gain Antenna Pattern	5-42
V-13	Frame Transmission Time Versus Gain Power Product . . .	5-52
V-14	Failure Mode on a Slope	5-67
V-15	Failure Mode Over Horizontal Terrain	5-67
V-16	Geometry of Assumed Wheel Penetration Model	5-69
V-17	Energy, Slope Distribution at 10, 30, and -30 Degrees . . .	5-73
V-18	Energy, Slope Distribution at 5, 30, and -30 Degrees	5-74
V-19	Maximum Slope Capability	5-76
V-20	LRV Suspension Spring Requirements	5-78

LIST OF ILLUSTRATIONS (contd)

Figure Number	Title	Page
V-21	Assumed Force System	5-79
V-22	Vehicle Obstacle Capability	5-80
V-23	Obstacle Capability in Soft Soil	5-82
V-24	LRV Undercarriage Clearance	5-84
V-25	Surveyor Thermal Switch	5-89
V-26	Thermal Switch on Surveyor Compartment	5-89
V-27	Typical Surveyor Switch Conductance	5-90
V-28	Dirt on Surveyor VII Alpha Scattering Instrument	5-92
V-29	Dirt on Surveyor Omni	5-93
V-30	Solar Panel Degradation	5-98
V-31	LRV Instrument Payload	5-101
V-32	Surveyor TV Camera	5-105
V-33	Variable Parameter Facsimile Camera	5-106
V-34	Facsimile Frame Format and Vidicon Frame Format	5-107
V-35	Bulk Sampler	5-111
V-36	Booms	5-112
V-37	Scoop Design	5-114
V-38	Hard-rock Drill Dump Position	5-115
V-39	Hard-rock Drill Operating Position	5-116
V-40	Auger Operating Position	5-118
V-41	Auger Stowed Position	5-119
V-42	Sample Storage System	5-122
V-43	X-ray Diffractometer	5-124
V-44	Aluminum Oxide Detector	5-131

LIST OF ILLUSTRATIONS (contd)

Figure Number	Title	Page
V-45	Six-wheel LRV for Atlas-Centaur	5-135
V-46	Six-wheel Landing Stability Boundary Estimate	5-139
V-47	Comparison of Four and Six-wheel Step Performance	5-141
V-48	Four-wheel LRV for Atlas-Centaur	5-143
V-49	Surveyor Descent Parameters	5-147
V-50	Three-sigma Ellipse Showing Prediction in Descent Velocities and Engine Cutoff Height	5-153
V-51	Engine Cutoff Altitude Versus Descent Velocity	5-155
V-52	Four-wheel Landing Stability Boundary Estimate (20-degree Slope)	5-156
V-53	Four-wheel Landing Stability Boundary Estimate (30-degree Slope)	5-157
V-54	Tire-limited Touchdown Velocity Combinations	5-160
V-55	Four-wheel LRV Mounted on LM	5-167
V-56	Six-wheel LRV Mounted on LM	5-169
V-57	Preliminary Study, Four-wheel LRV Mounted on Titan IIIC	5-173
V-58	Preliminary Study, Six-wheel LRV Mounted on Titan IIIC	5-175
V-59	Four-wheel LRV Mounted on LM (Titan IIIC)	5-177
V-60	Six-wheel LRV Mounted on LM (Titan IIIC)	5-179
V-61	Map of Mojave Desert Test Area	5-183
V-62	Air View of Test Region	5-184
V-63	Truck Used for Navigation Test	5-185
V-64	Typical Landmark	5-186
V-65	Typical Landmark	5-187
V-66	Geometry of Tracking Errors	5-193
V-67	Accuracy of Doppler Only Position Determination	5-194

LIST OF ILLUSTRATIONS (contd)

Figure Number	Title	Page
V-68	Accuracy of Position Determination Using Combined Ranging and Doppler Data	5-195
V-69	Circle of Position Determined by Single Star	5-196
V-70	Two-Star Fix	5-196
V-71	Probability Density of σ Given θ	5-199
V-72	Composite Curve for $p'\sigma$	5-202
V-73	Velocity Functions for $v(P_e, \sigma)$ for Full Range of Sigma	5-204
V-74	Average Speed as Function of Effective Power Per Wheel	5-205
V-75	Average Step Time Versus Average Vehicle Speed	5-209
V-76	Crater Deflection Test Setup	5-211
V-77	Results of Crater Deflection Tests	5-212
V-78	Results of Shallow Crater Deflection Test	5-213
V-79	Deflection Probability	5-214
V-80	Test Box	5-220
V-81	Sand Hopper in Place Over Test Box	5-221
V-82	Close-up of Sand Hopper	5-222
V-83	Control of Sand Density	5-224
V-84	Bearing Plate Configurations	5-225
V-85	Horizontal Carriage Fixture, Centered Position	5-226
V-86	Horizontal Carriage Fixture, Extreme Left Position	5-227
V-87	Test Wheels, Front View	5-230
V-88	Test Wheels, Side View	5-231
V-89	Loading Ram with Wheel Segments Attached	5-232
V-90	Loading Ram Special Loading Carriage	5-233
V-91	Wheel Sinkage Test Results	5-234

LIST OF ILLUSTRATIONS (contd)

Figure Number	Title	Page
V-92	Horizontal Surface Test (Wheel Along Slope) with Wheel Raised	5-236
V-93	Horizontal Surface Test (Wheel Along Slope) with Wheel One-third Submerged	5-237
V-94	Horizontal Surface Test (Wheel Along Slope) with Wheel Two-thirds Submerged	5-238
V-95	Fifteen-degree Sloped Surface Test (Wheel Along Slope) with Wheel Raised	5-239
V-96	Fifteen-degree Sloped Surface Test (Wheel Along Slope) with a 1.55 in. Vertical Displacement and a 1.65 in. Horizontal Displacement	5-240
V-97	Fifteen-degree Sloped Surface Test (Wheel Along Slope) with a 2.35 in. Vertical Displacement and a 2.30 in. Horizontal Displacement	5-241
V-98	Fifteen-degree Sloped Surface Test (Wheel Up-Down Slope) with Wheel Raised	5-242
V-99	Fifteen-degree Sloped Surface Test (Wheel Up-Down Slope) with a 1.50 in. Vertical Displacement and a 1.38 in. Horizontal Displacement	5-243
V-100	Load Sinkage Test Results (Circular Plates)	5-244
V-101	Load Sinkage Test Results (Rectangular Plates)	5-245
V-102	Circular Plate Test Before Loading	5-246
V-103	Circular Plate Test After Loading	5-247
V-104	Fragment and Crater Distribution	5-249
V-105	Solar Panel and High-gain Antenna Secondary Design	5-253
Appendix A		
A-1	NMR Marginal Oscillator, Schematic Diagram	A-3
A-2	NMR Spectrometer System Block Diagram	A-5

LIST OF ILLUSTRATIONS (contd)

Figure Number	Title	Page
Appendix B		
B-1	Quadrupole Electrode Structure	B-4
B-2	Ion Storage Decay Curve	B-4
B-3	Mass Spectrum	B-4
Appendix D		
D-1	Surveyor I Spacecraft Configuration	D-4
D-2	RADVS Beam Orientation	D-5
D-3	Terminal Descent Velocity Profile	D-6

LIST OF TABLES

Table Number	Title	Page
III-1	Geological and Compositional Analytical Instruments	3-7
III-2	Science Instruments for Traverse Geophysics Rover	3-13
IV-1	Soil Physical Characteristics	4-2
V-1	Weight Breakdown for LRV	5-9
V-2	Estimated Raw Power Demand From Power Source	5-34
V-3	Weight Summary for Power Subsystems	5-34
V-4	Telecommunication Design Control Table (Ranging Mode)	5-43
V-5	Telecommunication Design Control Table (Command Link)	5-47
V-6	Telecommunication Design Control Table (High-power and High-gain)	5-50
V-7	Telecommunication Design Control Table (Low-power and High-gain)	5-53
V-8	Telecommunication Design Control Table (High-power and Low-gain)	5-55
V-9	Telecommunication Design Control Table (Low-power and Low-gain)	5-57
V-10	Telecommunications Weight and Power Estimates	5-59
V-11	Mobility Characteristic Estimates	5-61
V-12	Baseline LRV Thermal Requirements for Lunar Operations	5-85
V-13	Proposed Standby Mode	5-87
V-14	Example Instrument Payload for LRV Sample Return Mission with Geological and Compositional Discriminatory Instrumentation	5-100
V-15	Photo-imaging System Requirements	5-104
V-16	Performance Capabilities of Vidicon and Facsimile Systems	5-109

LIST OF TABLES (contd)

Table Number	Title	Page
V-17	Bulk Sampler Characteristics	5-110
V-18	Furlable Boom Characteristics	5-113
V-19	Hard Rock Drill and Particulate Sampler Characteristics	5-117
V-20	Soil Auger Characteristics	5-119
V-21	Sample Handling and Storage System Characteristics	5-120
V-22	X-ray Diffractometer Characteristics	5-123
V-23	Aluminum Oxide Detector Weight Requirements	5-132
V-24	Surveyor Spacecraft Burnout Dispersions	5-148
V-25	Increase in Capability of Surveyor Propulsion System	5-149
V-26	Surveyor Retro-thrust Misalignment Data	5-151
V-27	Horizontal Velocity and Incidence Angle for Surveyor Landings (SC-1, SC-5, SC-6, and SC-7)	5-154
V-28	LRV Flight Thermal Requirements (Delivered by Atlas-Centaur)	5-162
V-29	LRV Flight Thermal Requirements (Delivered by Lunar Module)	5-165
V-30	Accuracy in Location Determinations	5-189
V-31	Speed as Function of Terrain	5-204
V-32	Average Station Time	5-207
V-33	Crater Deflection Test Dimensions of Vehicle and Crater	5-211
V-34	Test Plan for Plate Configuration	5-228
V-35	LRV Estimated Sizes	5-254
V-36	Class of Rovers	5-255
V-37	Delivery Mode Flexibility	5-256
V-38	LRV Mechanical Characteristics	5-257
V-39	LRV Guidance Characteristics	5-257

LIST OF TABLES (contd)

Table Number	Title	Page
V-40	LRV Telecommunications Characteristics	5-258
V-41	LRV Energy Characteristics	5-258
V-42	LRV Scientific Payload Characteristics	5-258
Appendix C		
C-1	Post Landing Events	C-1
C-2	Site Identification Events	C-3
C-3	Commanded Traverse Events	C-6
C-4	Science Sampling Events	C-9
C-5	Science Sample Handling Events	C-11
C-6	Lunar Night Sequence	C-12
C-7	Alternate Lunar Night Sequence with RTG	C-14
C-8	Nonstandard Sequence	C-15
C-9	Emergency Stop from "X" Reason	C-18
Appendix E		
E-1	Subsystem Number Code	E-1
E-2	Functional Block Diagram Circuit List	E-3

FOREWORD

The work here reported was done by the JPL Advanced Lunar Studies Team with support, direction and encouragement from people of NASA Headquarters, particularly Dr. Martin W. Molloy, Dr. Richard Allenby, and Col. Peter Grosz. Team members active during part or all of the year are listed on the next page, with asterisks identifying those most directly concerned with this report.

We wish to acknowledge contributions from several members of the Surveyor Project, directed by Mr. Benjamin Milwitzky, NASA, and Mr. Howard Haglund, JPL, and also to thank Dr. Wilmot Hess of MSC for his continued interest and for his invitations to those team members who have participated in the various lunar exploration-related activities of his office.

This report is not an attempt to document everything done by the team; it is specifically concerned with the mission to which we have given most attention, namely the long lunar traverse. We believe that this mission is both important and relatively poorly understood, and therefore that it deserves research and advanced development. Hopefully, our present study efforts will help to define the course of such work.

List of Advanced Lunar Study Participants

W. Ackerknecht
J Adams
V. Anthony
R. Bamford
H. Bank*
T. Barber
R. Barnett
R Brereton*
J. Bruman
J. Burke*
A. Conrad
R. Coryell*
E. Divita
L Divone
D. Elleman*
J. Eyraud
J. Garba
E Gatz
J Gerpheide
C. Giffin*
C. Gilchriest
D Green*
R. Heyser
A Hibbs
N. Horowitz*
F. Jean
J Kelley
I Kloc*
C Leising*
J. Long
A Loomis
V Magistrale
R Mankovitz
C. McCormick
W. McDonald
J. Moore
R. Morris
D. Nash
J. Porter
D Rubin*
S. Rubinstein
J. Smith*
M Smokler*
L. Stimpson
D. Stott*
E Suggs
R. Wallace
C. Wertz*
D. Young
N. Zafman

*Contributor to this report

I. A STUDY OF LUNAR TRAVERSE MISSIONS

A. INTRODUCTION

The Moon, as revealed by Ranger and Lunar Orbiter photos and Luna and Surveyor surface measurements, offers both opportunities and hazards to exploration by means of automated roving vehicles. The opportunities are becoming more and more evident as the lunar scientific program is examined in the light of recent findings about the nature of the terrestrial planets (Ref. I-1 and I-2).

For geology and geochemistry, the long traverse is important because it affords an opportunity to make observations and take samples not only in detail at particular features, but also across major regional units.

For geophysics, the traverse presents the prospect of profiling, gravimetry, geodesy and structural discrimination along major surface arcs.

For astronomy, it offers an opportunity for comparing and evaluating observatory sites.

For biology and studies of the lunar atmosphere, it can provide sampling of surface and near subsurface materials, including volatiles, from numerous different and uncontaminated environments.

In each of these disciplines and in their ensemble, the traverse (assuming proper coordination with overhead surveys and local explorations at a few sites in depth) presents an opportunity for making those critical measurements that will permit rational decisions as to the future exploration and exploitation of the Moon.

The hazards attending the long automated traverse are, however, substantial. In addition to the expected problems of spacecraft reliability over long periods in the lunar environment, the mission is subject to hazard from lunar surface characteristics not revealed by previous missions, and also from operational errors occurring in the man-machine control loop.

The purpose of the present study is to elucidate both the opportunities and the hazards. The initial reasoning which led to a concentration on the traverse mission and to the selection of a baseline system design is cited in Ref. I-3. This report summarizes progress since publication of Ref. I-3, i.e., over a period roughly coincident with Fiscal Year 1968. During the past year, the baseline vehicle design and some departures from it have been further examined. Scientific payloads for the various missions have been studied, and some of the initial design assumptions have been tested by experiment. Since one objective of the study is to identify needed advanced developments, emphasis is placed on problems considered to be poorly understood. Most of these problems now appear to relate to the systems (and their interactions) for navigation, motion control, and scientific operations on the Moon.

REFERENCE LIST

Section I

I-1. JPL ASD 900-28.
Adams, J. B., et al. "A Strategy for Scientific Exploration of the Terrestrial Planets." JPL 12 July 1967.

I-2. NASA SP-157
NASA. "1967 Summer Study of Lunar Science and Exploration." University of California, Santa Cruz, 31 July through 13 August 1967.

I-3. JPL ASD 760-5.
JPL. "A Program Analysis for Lunar Exploration." JPL 25 July 1967.

II. MISSION CRITERIA

When the traverse mission is placed in the context of an exploratory program including overhead surveys and local investigations at a few manned-landing sites, it is possible to specify the main functions of the long-range roving vehicle and its payload, and to place these functions in priority order depending on the emphasis desired in a particular mission. In Section III, representative instrument payloads for the different missions are described. This section lists the general performance criteria that appear to be basic requirements for any of the missions considered, as well as some variations in the criteria for particular mission goals.

A. ASSUMPTIONS

The unique contribution of the long-range rover to a program as defined above is the extension of direct surface measurements into regions far distant from manned landing sites.

1. Manned Operations

For this study, it is assumed that operations at manned landing sites will include:

(1) Direct observations and measurements by scientist-astronauts carrying instruments and tools

(2) Sample collection for return to Earth

(3) Emplacement of long-lived instrumentation (e.g., ALSEP).

To these operations others would be added on later expeditions, e.g., subsurface drilling and sampling, and use of mobility aids by the astronauts, permitting investigations down to a meter or so below the surface and out to a few kilometers away from each landing site.

2. Orbital and Earth-based Surveys

It is also assumed that orbital and Earth-based surveys would be made to provide the mapping and remote-sensing data necessary to tie isolated surface observations into a coherent network. The traverses would supply some elements of the required "ground truth" for these overhead surveys.

B. FUNCTIONAL REQUIREMENTS

The functional requirements for the roving system are

(1) To transport instruments, collect and identify samples, and telemeter observations to Earth during travel over distances of the order of a lunar radius

(2) To emplace instrumentation along the route, or alternatively to pause at selected points long enough to permit stationary experiments

(3) To explore unknown sites and targets of opportunity, and to evaluate and compare sites for future manned investigations in greater depth, or special purposes such as astronomy or recovery of lunar water.

1. Sampling Mission

These performance criteria are discussed in Refs. II-1 and II-3 from the standpoint of planetology, with specific reference to the Moon's place in determining the origin and constitution of the terrestrial planets. By the reasoning there presented, the priority goal of the long traverse is the collection of lunar material samples for eventual return to Earth. Of course, such samples would not be collected at random, but would be selected and identified on the basis of observations made at each sampling site. This implies that the payload must include not only sample acquisition and storage devices, but also instruments to permit selection or rejection of samples, to record all significant aspects of their surroundings, and to detect anomalous conditions that might require a change in the mission strategy.

Since a complete isotopic analysis of the samples appears impractical by remote control, the instruments mentioned would be designed more for discrimination than for analysis. Appropriate techniques, which could be reliably mechanized and would provide enough chemical and mineral discrimination to guide the sampling include·

(1) Imaging with microscopy

(2) Alpha scattering

(3) X-ray diffractometry and spectroscopy

(4) Nuclear magnetic resonance spectroscopy.

Instruments based on these and other applicable techniques are described in Section III. The more capable this array of instruments could be made the less would be the loss if retrieval and return of samples should fail. In the limit, one might ask whether sample return is really essential for isotopic analysis and dating. With present instrument technology, it is, since the elaborate and precise processes used to extract and purify the interesting elements for introduction into a mass spectrometer have not been mechanized for remote operation. A suitable subject for future study would be to compare the development of a remote solid-source mass spectrometer against the efforts required to assure rendezvous, retrieval, and return of samples from the traverse mission. Other missions without sample return are discussed in subsequent paragraphs.

2. Traverse Range and Lifetime

Another criterion that may be questioned is the range of the desired traverse. It turns out that this is not a sharply specified parameter in terms of either requirement or capability. For geology, geophysics and geochemistry, travel across large regional units of the Moon and visits to distant features are desired, giving traverse dimensions comparable to those of maria and highlands, namely several hundred kilometers. Certain geophysical experiments (e.g., seismic and gravimetric measurements) require baselines of 1000 or more kilometers for best effect. For studies of organic geochemistry and the lunar atmosphere, large excursions in latitude are desired, again pointing to a mission range of approximately 1000 kilometers. Finally, the distance from one manned landing site to another may be of this magnitude.

In terms of capability, the range is not highly constrained once it exceeds a few tens of kilometers because, at the required slow speeds (Ref. II-3 and Section V) the vehicle must have a range-independent prime power supply (e.g., solar or nuclear), and it must routinely survive the lunar night. Once these conditions are met, lifetime to wear-out rather than range becomes the dominant design consideration. By observing combinations of the mission goals, a net range of 1500 kilometers and a lifetime of one year were selected for the baseline design. This lifetime might have to be extended if the roving vehicle were expected to rendezvous with a manned landing spacecraft after a waiting period at completion of the traverse.

3. Alternate Missions

In addition to the basic sampling mission, which emphasizes geology and geochemistry, other missions have been studied.

(1) Geophysics. Geophysics could be made the main objective of a traverse. In this case, the roving vehicle would carry some of the same instruments, and it still would manipulate the lunar surface, but it would not deliver a cargo of samples. Instead, it would perform a seismic, magnetic and gravitational survey and measure the figure of the Moon along the arc of the traverse, in coordination with (a) continuous measurements at a base point such as an ALSEP site, and (b) selenodetic and other measurements from lunar orbit.

(2) In-Situ Measurements. Another alternate mission would be one in which maximum emphasis could be placed on in-situ measurements, as might be desired if the rover were sent into a region hazardous to manned-landing rendezvous. For this mission the discrimination techniques listed earlier would be replaced by analysis techniques to the extent feasible (e.g., a petrographic microscope might be used). Various combinations of such instruments are described in Section III.

(3) Dual-Operating Mode. A mission mode suggested in Ref. II-2 is the dual-operating mode, in which a roving vehicle would be designed for operation in either a manned or unmanned condition. Preliminary studies have shown that vehicles even as small as the present baseline design could physically carry a man on the Moon provided that the necessary detail design compromises proved acceptable. This could be determined by analysis, and it is intended that future studies explore some of the details. However, a more serious question arises in respect to the mission profile, or time-line. The following types of dual-mode operation have been discussed:

(a) Lunar Roving Vehicle (LRV) delivered with astronauts aboard Lunar Module (LM), used to transport men during initial extra-vehicular activities (EVA), then put in the unmanned automatic mode and sent off on long traverse

(b) LRV delivered one year ahead of men, traverse completed under remote control, rendezvous effected, vehicle put in manual mode and used by men.

Of course, combinations are conceivable, for example, after mission (b) the LRV could be sent off on another traverse. In mission (a) the chief design problem is minimizing astronaut effort required to reconfigure and check out the LRV for remote operation. In mission (b), it is to provide sufficient design margins to allow the vehicle to maintain man-rated reliability after a year of operation on the Moon.

The vehicle performance requirements of the local and long traverses are different:

(1) For manned operation, the highest safe and controllable speed is desired, because of the limited time available for EVA

(2) Mobility can be compromised, assuming that the driver can judge and avoid more hazards than a remote operator could

(3) A short-life (e.g., a few hours to one day) power supply can be used.

For remote operation

(1) Speed should be low

(2) Mobility high

(3) Power system (as well as all other systems necessary on the traverse) should have essentially unlimited lifetime.

When the dual mode was first suggested, it was viewed from the standpoint of a basic manned mission, to which the automated long traverse appeared a desirable addition. Now, it may be more appropriate to ask what is gained by adding the man-carrying feature to an automated LRV system. In recent studies, primarily because of LM payload weight and EVA timeline considerations, flying, rather than surface roving has come to be the preferred means of transport for astronauts. It is therefore necessary to compare performance, cost, and risk for the following system combinations:

(1) Automated LRV plus Lunar Flying Unit (LFU)

(2) Dual-mode LRV plus LFU

(3) Dual-mode LRV only

(4) LFU only.

Combination (1) is less advantageous than combination (2) since EVA timelines can be worked out using both types of mobile systems to permit reaching several kilometers out from the LM. Combination (3) penalizes EVA times and limits manned operating range to only a few kilometers. Combination (4) precludes the long traverse. Therefore, it appears that future studies should concentrate on the advantages and disadvantages of combinations (1) and (2) unless some overriding factor requires LFU to be eliminated.

4. Payload and Delivery-System Performance

Except for the dual-mode function, all of the previously discussed missions can be accomplished with payload masses around 100 pounds, and payload volume, power and data transfer capacities similar to those of the Surveyor spacecraft. Payload criteria are discussed further in Section III, and are also the subject of a study continuing after this report. These payloads are compatible with rover masses of 500 to 1000 pounds (Ref. II-3), such rovers can be delivered either by automated means using existing launch vehicles and spacecraft subsystems or by the manned Apollo LM. These compatible weights provide the reason for selecting an LRV baseline design near the size described in this report.

REFERENCE LIST

Section II

II-1. JPL ASD 900-28.
Adams, J. B., et al. " A Strategy for Scientific Exploration of the Terrestrial Planets." JPL 12 July 1967.

II-2. NASA SP-157.
NASA. "1967 Summer Study of Lunar Science and Exploration." University of California, Santa Cruz, 31 July through 13 August 1967.

II-3. JPL ASD 760-5.
JPL. "A Program Analysis for Lunar Exploration." JPL 25 July 1967.

III. INSTRUMENT PAYLOADS AND SCIENCE OPERATIONS

A. LUNAR MEASUREMENTS

The scientific rationale and summary of presently planned lunar missions presented in Ref. III-1 indicated that there would be no early opportunity to perform several types of high priority lunar measurements. Examples of these types of measurements are

(1) Simultaneous particle-and-field measurements on the surface and in orbit, including accurate mapping of the lunar magnetic environment

(2) Operation of a long-baseline seismic net

(3) Surface sampling, with on-site analysis and/or sample return to Earth, in Moon's polar regions and remote, rough areas

(4) Subsurface probing in regions (e.g., polar areas) where theory or observation suggests possibility of finding recoverable water

(5) Topographic mapping of selected areas in support of the above and other investigations.

This section deals mainly with item (3).

B. MISSION OBJECTIVES

The objectives listed in Ref. III-1 have been revised into two major missions:

(1) Primary mission will be to make traverses across key areas of the lunar surface and collect lunar surface samples for return to Earth

(2) Secondary mission will consist of mineral analysis, collection of non-particulate formations, collections below the surface, and detection of volatiles.

1. Primary Mission

Mission Goals. The minimum goals of this mission are as follows:

(1) Collection of 100 samples of unaltered particulate and bedrock material, each sample having a volume of 50 cc, over an extended

traverse. The samples will be identified as to location and geologic situation in which they were found.

(2) Imaging, with resolution and photometric fidelity at least equivalent to Surveyor TV, of the traverse path and sample sites.

(3) Transport of the collected samples to a point on the Moon suitable for subsequent retrieval and return to Earth. (In the present study, the retrieval point would be an equatorial manned landing site.)

2. Secondary Mission

Mission Goals. In the event that a more extensive mission is possible, the goals would be as follows:

(1) On-site chemical and mineral analysis to aid the choice of samples.

(2) Collection from sources that need to be chipped or drilled, e.g., rock fragments or outcrops.

(3) Collection of samples from below the Moon's surface.

(4) Detection of volatiles, especially water.

It should be realized that a chemical basis alone is incapable of classifying rocks. Thus, elemental analysis experiments will not distinguish crystalline rock from volcanic glass or ash with the same chemical composition, nor a physical mixture of local debris from a crystalline rock. The accepted schemes of rock classification are based on texture (the size, shape, and geometrical relation of grains in a rock) and the identification of the minerals in the rock. From these parameters, information regarding the nature, geologic history, and origin of the rock may be derived.

Local detailed surveys may be made incidental to the traverse missions for such purposes as selection of additional areas for manned landings and manned surface expeditions, or for selective geophysical measurements made on a traverse where the main objective is sampling.

C. SAMPLING REQUIREMENTS

1. Quantity and Type of Samples

The quantity and type of samples required will vary with the type of analysis to which they will be subjected. For mineralogical and chemical studies particulate samples of one gram or so will suffice. For isotope, gas, and trace element studies, solid samples of 50 to 300 grams will be needed. It is important to obtain samples that are representative of rock units encountered along the traverse path.

2. Types of Locations for Obtaining Samples

Samples should be obtained from the following types of locations (Ref. III-5):

(1) Mare surfaces

(2) Crater bottoms

(3) Highlands

(4) Ejecta blankets

(5) Subsurface (at least 3 ft deep).

3. Configuration of Samples

Because of the continuous lateral and vertical overturn by impact, centimeter-sized rock fragments in the surface debris may represent the mean composition of rocks in the sampled area, and smaller sizes may give information of broader regional significance.

Loomis and Nash (Ref. III-6 and III-7) indicate that individual rock samples or rock chips would be more desirable than drilled rock samples since drilling would destroy the details of coarse-grained textures.

It would be more desirable to collect a few large rock or rock chip samples than a large quantity of small ones. These samples should be at least golf ball size (approximately three centimeters across). However, pulverized rock samples are also desirable and would be essential for in-situ analysis. In acquiring natural particulate samples it is important to avoid fractionation to preserve the indigenous proportions of particle sizes and mineral components.

4. Additional Analysis Capability of Sampling Mission

Although the minimum objective of this particular LRV mission is to collect samples for Earth return, inclusion of analytical instruments on the payload can serve the important additional purposes of:

(1) Providing preliminary information on the mineralogical and compositional properties of the Moon along the traverse

(2) Aiding in the selection of desirable samples or sampling sites

(3) Providing some additional lunar data, e.g., geophysical, biological, atmospheric and outgassing information

(4) Providing some of the desired critical data even if rendezvous and Earth return of the samples became impossible.

The use of an X-ray diffractometer, an X-ray spectrometer and an alpha scatterer would be desirable for supplying phase and elemental analyses of the lunar particulate material and indicating mineral and compositional changes along the traverse. Any sudden changes would indicate boundaries of units and areas of interest for taking samples. Such changes might indicate types of differentiation which may be due to meteoritic impact, vulcanism, or other processes pertinent to the history of the Moon.

It is important to determine the possible roles that volatile substances have played in the lunar picture, and especially important to determine the presence of water. Outgassing may occur from various vents, rilles, and craters such as Aristarchus and Alphonsus. The sources of such volatiles and the deposits of any solid sublimates should be identified and sampled. If practical, a subsurface probe with sensors in the tip for measuring humidity and temperature gradients down to one meter in depth would be desirable.

Surveyor information has indicated that the static bearing strength of the lunar surface probably increases linearly with depth at about 3 psi/in. At this rate the force required to sink a small probe to a depth of one meter might exceed 100 lb. To overcome this problem, the probe could be driven in and out by impacting, or it could be operated like an ordinary twist drill with the displaced material being brought up to the surface and deposited around the entrance to the hole. Although it would be difficult to put sensors on the end

of this kind of a probe, it is possible that a moisture detector could be placed in a shroud which covers the hole during the drilling operation. In this manner, moisture emerging from the hole or the drillings would be detected.

D. GEOLOGICAL AND COMPOSITIONAL INSTRUMENTATION REQUIREMENTS

Instruments capable of yielding geological and compositional information, which will aid in the selection and subsequent return to Earth of samples, are listed in Table III-1. This table defines the specific measurements that each instrument can make, listed in an order starting with a gross overview (surface geometry) and proceeding toward more detail. The measurements are not necessarily listed in priority order. Scientific reasoning, concerning priority lunar and planetary surface measurements and measurement techniques, is presented in Refs. III-2, III-3, and III-4. Variations in the ultimate payload selection will be governed by the emphasis to be placed on the mission. For example, if it is desired to sample from areas of different radioisotopic content (K, U, Th) then a gamma-ray spectrometer will be required. For determining water content (in all its states) a nuclear magnetic resonance spectrometer should be used. The particular instruments selected for this baseline study payload are listed and described in Section V.

Other candidate instruments listed in Table III-1, such as the petrographic microscope, are described in Refs. III-4, III-10, and III-11, and the gamma-ray spectrometer, gamma-gamma backscatterer, gas chromatograph and mass spectrometer in Refs. III-3 and III-4. Descriptions of these instruments will not be repeated here.

The nuclear magnetic resonance spectrometer (for water detection) and the 3-D quadrupole ion gage/mass spectrometer (atmospheric analysis and water detection) have not previously been mentioned in connection with the LRV and therefore will be described in this report. Both appear promising for detection and measurement of lunar volatiles, as does the aluminum-oxide hygrometer described in Section V.

1. Types of Instrumentation Required for Lunar Volatiles

Nuclear Magnetic Resonance Spectrometer (NMR). The nuclear magnetic resonance spectrometer would be a small (probably 5 lb) fixed instrument requiring a sample, which can determine the free water (liquid state), absorbed water, or

water of hydration content of the sample. It is nondestructive to the sample so that the sample can be analyzed by other instruments or put into storage for Earth return. Principles of operation of this instrument are described in Appendix A.

3-D Quadrupole Ion Gage/Mass Spectrometer. The experimental concept described in Appendix B could be used on the LRV for the analysis of the neutral component (in contrast to ionized component) of the lunar atmosphere, of the volatile constituents of soil samples, and for the detection of outgassing (especially water) along the lunar traverse, from a drilled hole or from the drillings from the hole. The instrument proposed is a mass spectrometer recently described at the American Vacuum Society Symposium by N. R. Whetten and P. H. Dawson of the General Electric Corporation. The basic geometry of this device appears to have the capability to solve some of the following major problems plaguing mass spectrometric analysis of the lunar atmosphere:

(1) Degassing of the instrument package

(2) Sensitivity, i.e., signal-to-noise ratio

(3) Perturbation of the atmospheric composition by interaction with a hot filament source of ionizing electrons

(4) Instrument size and requirement for a magnetic field.

Operating principles and instrument details are given in Appendix B.

2. Types of Instrumentation Required for Traverse Geophysics

Traverse geophysics has a very special place in the lunar exploration program, for it can provide data towards the solution of problems that can be solved only by the combined techniques of surface mobility and geophysical instrumentation. Traverse geophysics using automated roving vehicles is not a panacea for all the problems of lunar exploration; however, it is a powerful tool for providing data on the subsurface of the Moon. When these data are correlated with lunar geology and our multiple working hypotheses, they can provide an informative picture of the possible structure and processes of the lunar crust. The choice of scientific instruments for the traverse task is quite large, because geophysical techniques and instrumentation have become more diversified through the effect of advanced technology and the revolutionary growth of

Instrument	Measurement and accuracy									Hardware status				Special requirements and remarks	Weight lb	Power w	Est time per measurement min	Telemetry requirements per measurement
[1] Instruments may be combined [2] Lunar atmosphere probably too rare for these instruments	Surface geometry	Rock fabric	Rock texture	Phase analysis	Elemental analysis	Volatile constituents	Natural radioisotopes	Surface bulk density	Atm comp, partial and total pressures	Flight	Prototype	Breadboard	Feasibility conceptual					
Photo-imaging [1]	High	High								✓				Vidicon Filters, gimbal mounts Facsimile Mast mount, filters	8	10	5-sec/frame or 8-min/360° scan	Vidicon, 600 line 2.5×10^6 bits†/frame High res Facsimile 10° × 360° scan 2.5×10^8 bits†
Petrographic mic [1]			Low	Low	Low							✓		Sample preparation 50-300μ	15	10	15 min plus 5 sec per frame	Up to 500 frames desired per sample 2.5×10^6 bits/frame
X-ray diffractometer [1]				High	Med						✓			Sample or deployment	15 } 20	45 } 45	30	6.75×10^4 bits
X-ray spectrometer [1]					Z = 11-92							✓		Sample or deployment	15 } 20	2 } 2	30	2×10^3 bits
Alpha scatterer [1]					Z = 4-17					✓				Sample or deployment	14 } 20	1 } 2	180	16 bits/chan 256 chan 4.1×10^3 bits 512 chan 8.2×10^3 bits
Gamma ray spec					K, U, Th Al, Ni, Fe		High				✓			Boom mount or deployment required	14	3	10	16 bits/chan 256 chan 4.1×10^3 bits 512 chan 8.2×10^3 bits
Magnetic mat'l pickup device				Low (mag. mat'l)	Low (mag mat'l)								✓	Deployment	(1)	(5)	1	Observe with T-V
Gamma-gamma backscatterer								To 10 cm. depth				✓		Deployment	10	3	10	(16 bits)
Gas chromatograph (to mass 300) [1]						Med (vapor)			(?)[2]		✓			Sample preparation and carrier gas	14	15	60	10^5 bits
Mass spec (to mass 300) [1]						High (vapor)			(?)[2]		✓			Sample preparation. Meas partial pres's to 10^{-14} torr	15	10	1	10^5 bits
Hygrometer [1]						H_2O (vapor)							✓	Req's sample or deployment Meas H_2O partial pres to 10^{-6} torr	1	0.4	1 or cont	(16 bits)
Nuclear magnetic resonance spectrometer [1]						H_2O (all states)						✓		Req's sample	(5)	(0.5)	(5)	(?)
3-D quadrupole (as ion gage or mass spec) [1]						High			High				✓	Monitor lunar outgassing and atmospheric constituents	(5)	(5)	Cont	(?)

( ) Indicates rough estimate

† Based on 7 bits per image point

Table III-1. Geological and Compositional Analytical Instruments

Page intentionally left blank

Page intentionally left blank

science which has taken place since 1940. For example, 10 years ago a magnetic survey was usually accomplished with a so-called field balance magnetometer. These instruments measured only one component of the earth's magnetic field, and so a magnetic survey to measure the magnitude of the geomagnetic field vector required two separate survey operations with two separate magnetometers, that is, one survey and instrument to measure the horizontal component of the geomagnetic field, and another to measure the vertical component. Today, this same operation can be carried out with one small and completely portable instrument called a proton precession magnetometer at a fraction of the time and at perhaps greater accuracy. Recent technical advances have similarly affected seismic, electrical, radioactive and gravity instruments and their application.

Although new technology has affected geophysical instrument design, and its application particularly in the sense that it makes the roving vehicle traverse geophysics mission feasible, classical geophysical experiments in magnetism, gravity and seismic prospecting appear to be most practical for the early traverse missions, as their data are more understood and interpretable in terms of terrestrial analogs. An imaging system and laser ranging experiment should also be a part of the minimum science package for the traverse geophysics mission.

An imaging system as described for the baseline payload in Section V would be suitable for the traverse geophysics task. This instrument would serve as the eyes of the rover for navigation, guidance, and positioning and, in addition, it would support the geophysical experiments by providing eyeball type geological information at each measurement site.

It has been suggested that the present absence of a strong internal magnetic field for the Moon may reduce the effectiveness of standard magnetic surveying techniques for understanding deep structural features, however, the absence of this field now may enhance the detection of remnant magnetism which could have considerable cosmogonic significance. Also, because the difference in measured susceptibility between acid and basic rocks, between nickel-iron meteorites and silicate rocks and even between chondrites and silicate rocks is large, it is probable that they have become polarized by external fields, relic lunar field, or flowage, therefore, magnetic survey techniques may prove to be a valuable

tool for mapping contacts, providing criteria for distinguishing impact and volcanic features, and in general providing new data on the structure and processes of the lunar surface.

Orthogonal Magnetometer. The traverse operation will require a three-component orthogonal magnetometer of the flux-gate, proton precession, or optical pumping type. The last two types are favored because they provide absolute magnitude data It is desirable that the magnetometer operate continuously, that is, operate both during station stops and while the rover is in traverse. An accuracy of ±5 gammas is desirable. This suggests that the magnetometer sensor must be compensated for both perm and induced magnetic interference from the roving vehicle, or else removed from its vicinity during measurements. A base control for monitoring external fluctuations and changes in the lunar magnetic field is required. This could be provided by ALSEP science or an emplaced science package containing a magnetometer. The base control station should be located in the survey or traverse area, but a separation up to 500 km could be tolerated.

The surface gravity of the Moon is only one-sixth that of the Earth, therefore, gravity anomalies on the Moon resulting from a density contrast in lunar material will comprise a larger part of the total-field measurement than similar measurements on Earth. Lunar gravity anomalies may be caused by local near-surface density contrasts in rock units, as between the regolith and basement rocks, or perhaps by regional isostatic phenomena where the Moon's crust is out of isostatic equilibrium because of ancient frozen tidal effects or crustal overloading by ejecta from large meteor impacts. The Carpathians and Apennines are possible examples of crustal overloading from the Imbrium impact event. Surface gravity data from profiles across virtually all lunar structures and contacts are desirable as these data may be critical to an understanding of the origin and evolution of these features and even the Moon itself.

Spring-Mass Gravimeter. The best gravity instrument for the traverse task is probably a conventional spring-mass gravimeter in contrast to a torsion balance or pendulum. The state-of-the-art in design of spring-mass instruments is highly advanced. Terrestrial gravimeters are required to detect changes in gravity of the order of one part in 10 million. The lunar instrument, because of the lower gravity on the Moon and the resulting higher ratio between anomaly and

total gravity, should be calibrated to detect changes of the order of one part in one million over a dynamic range of 500 milligals. Considerable care in instrument design to control long term temperature and mechanical drift will be required, for it is not likely that on the traverse mission the vehicle can be returned to a previous station to measure instrument drift.

It will be necessary to make both free-air and Bouguer corrections to the gravity observations. These corrections if not observed could mask regional trends and even local anomalies. An integrating tiltmeter supplemented with data from a base map and the imaging and tracking systems can provide the information for this correction. A terrain correction may be locally needed, also a tidal correction to account for differential alignment between the Sun, Earth and Moon will be required.

The active seismic experiment as defined here for the traverse task can be considered a shallow exploration technique for probing the uppermost kilometer of the Moon, and is designed to measure the depth of the lunar regolith and its elastic and physical properties, seismic wave velocities and rock contacts, and in general to provide subsurface data on the Moon's structure and stratification. Both refraction and reflection techniques can be useful, for one phenomenon rarely occurs without the other. The geological picture that is emerging for the lunar surface suggests a low density regolith overlying a denser unchurned basement. The study of this may present an ideal problem for the seismograph.

Seismometer. The experiment consists of a seismometer which can be deployed to the lunar surface under the rover, an auger for shot-hole preparation, and approximately 100 charges weighing 1/4 pound each for providing a seismic energy source. The charges would be activated separately by radio command from the rover. In terrestrial seismic prospecting where mobility and backtracking are not problems, the normal procedure is to use one shotpoint in conjunction with half-a-dozen or so detector-seismometers, and energy arrival times for each detector from the one source are plotted as a function of time and distance to portray refraction, reflection, and subsurface structure. On the Moon, where backtracking and locating emplaced detector-seismometers could be difficult, a suggested procedure is to emplace a series of say five charges on a rover traverse and then, from a selected position with

the seismometer on, each charge would be remotely detonated in turn. A few seconds recovery time must be allowed between detonations to avoid record wipe-out of subsequent events by the first. A shot-point spread of about 50 feet would be used at first to carefully define the average velocity in the regolith, or for precision probing for a suspected contact or structure; however, operating procedures would evolve through experience. Once the velocity function has been determined for the regolith or a particular marker bed, its depth at the other locations and during the traverse could possibly be determined from one shot-point and the reflection record. Time anomalies between the regolith and basement rocks could be very high, but between the ejecta blanket from one event and underlying ash, or say earlier ejecta, the time anomalies might be small. Therefore, timing accuracy should be controlled to at least 0.005 second and shot-point distance measured to two percent.

A laser and radio ranging experiment on the traverse mission would define a series of fixed points over the lunar surface. This type of information has a direct application to problems in selenodesy, lunar mapping, and celestial mechanics, and in addition, the experiment will provide information to assist in the free-air and Bouguer corrections for the gravity experiment. The definition of a geodetic arc for various radii of the Moon will define the size and shape of the Moon and locate frozen tidal effects. The equipment for the laser experiment would consist of a transmitter at an appropriate terrestrial observatory and a reflecting antenna and its pointing and orienting mechanism on the rover. Table III-2 summarizes the instrument requirements for the geophysical traverse.

E. BIOLOGICAL INSTRUMENTATION REQUIREMENTS

The missions previously discussed would provide planetological information relevant to the general problem of the origin of life on the terrestrial planets. A question may be raised as to whether the long traverse could also be used to make direct measurements of specific biological significance.

Table III-2. Science Instruments for Traverse Geophysics Rover

Instrument	Weight (Pounds)	Power (Watts)	Remarks
Imaging system	8	2	This instrument would provide images for guidance, navigation, and positioning of rover and in addition it would support the geophysical experiments by providing eyeball type geological information at each measurement site. Stereo, color and system resolution to at least 1/2 millimeter is desirable.
Magnetometer	6	1	This instrument on the rover would provide a profile of the magnetic intensity over various types of lunar structures and features. Instrument should have an inherent accuracy of ±5 gammas. External control by ALSEP or other station magnetometer needed.
Gravimeter	15	2	This experiment will provide information on density differences and the isostatic equilibrium of the Moon. Will be operated in a profile mode at fixed stations. Station separation will be determined from structural considerations and operating experience.
Seismometer	40	1	This experiment will determine the depth of the lunar regolith and its elastic and physical properties, seismic wave velocities and rock contacts, and in general provide subsurface data on the Moon's structure and stratification. At least 100 separate seismic events are programmed in one-quarter pound charges. Timing accuracy to 0.005 seconds and shot-point distance measurement to 2 percent are required.
Auger	10	5	Will prepare a 12 inch deep, 3 inch diameter hole for the seismic charges.
Laser and radio ranging experiment	10	2	The objective of this experiment is to determine the location and altitude of a roving vehicle gravity site by both a laser ranging instrument and radio ranging

The probability of finding life on the Moon is negligible, but a search for organic matter could be rewarding. The following paragraphs define possible sources of lunar organic material:

1. Outgassing

Recent indications from the Surveyor and Lunar Orbiter missions suggest that the Moon has undergone outgassing in the past, possibly even with the production of some (temporary) liquid water. If so, organic compounds may have been formed on the Moon by the same nonbiological processes that are believed to have been active on the primitive Earth.

2. Relation of Earth to Moon

A second source of lunar organic matter is Earth. If the theory that the Moon was once part of the Earth is correct, and if the separation of the two bodies occurred after the formation of organic matter had taken place on Earth, then the Moon could have retained some of this material.

3. Meteoritic Infall

Considerable quantities of organic matter have presumably been brought, and are still being brought, to the Moon in the form of meteoritic infall. It seems likely that most of the surface organic matter of the Moon would be from this source.

The detection and identification of organic material from any of these sources on the Moon would be of considerable biological and general scientific interest. Material from sources (1) and (2) would constitute ancient chemical fossils of a kind unknown and possibly non-existent on Earth. In addition to their biological interest, they would be of obvious importance for understanding the origin and history of the Moon. Material from source (3), if uncontaminated with (1) or (2), would provide us with samples of cosmic organic matter which, aside from their inherent interest, would be useful for establishing the level of "organic noise" that one might expect to encounter on Mars, and above which any Martian biological signal would have to be recognized.

The problem of distinguishing organic matter of these various origins, while difficult, may not be insoluble. The nature of the substances found, their amount, distribution, and associations, together with general geological evidence on the origin and history of the Moon would be important in making such

distinctions. Analyses of samples of meteoritic organic matter reaching Earth provide a basis for recognizing meteoritic organic material on the Moon. In addition, as pointed out above, it is probable that any ancient lunar organic material is buried beneath a cover of meteoritic rubble.

The instrument that seems most suitable for use on an automated LRV is a pyrolyzer combined with a gas chromatograph-mass spectrometer as developed for planetary missions. In this instrument a sample of lunar material would be heated to about 500°C and measurements would be made of the composition of the evolved gases. The instrument is further described in Ref. III-18. An experiment of this type would be of particular value on a long traverse mission, as distinct from stationary or local-area investigations, because of the opportunity for exploring wide regions as well as anomalous areas and for selecting samples of surface and subsurface materials for analysis on the basis of readings from the other instruments.

REFERENCE LIST

Section III

III-1. JPL ASD 760-5.
JPL. "A Program Analysis for Lunar Exploration." JPL 25 July 1967.

III-2. JPL TM 32-241.
Speed, R. C., Adams, J. B., Nash, D. B. "The Utility of Unmanned Probes in Lunar and Scientific Exploration." JPL July 1967.

III-3. JPL TR 32-1225.
Nash, D. B. "Sampling of Planetary Surface Solids for Unmanned In-Situ Geological and Biological Analysis: Strategy, Principles, and Instrument Requirements." JPL November 1967.

III-4. JPL ASD 760-3.
Brereton, R. G. et al. "Scientific Instruments for Lunar Exploration, Part B: Surveyors, Roving Vehicles, and Rough-Landed Probes." JPL May 1967.

III-5. NASA SP-157.
NASA. "1967 Summer Study of Lunar Science and Exploration." University of California, Santa Cruz, 31 July through 13 August 1967.

III-6. JPL Personal Interview.
Loomis, A. A. JPL June 1968.

III-7. JPL Personal Interview.
Nash, D. B. JPL June 1968.

III-8. Journal of Geophysical Research.
Adams, J. and Filice, A. "Spectral Reflectance 0.4 to 2.0 Microns of Silicate Powders," volume 5, p. 5705 through 5715. 31 August 1967.

III-9. JPL SPS 37-46.
Conel, J. E. "Emission Spectra of Silicates in the Spectral Region 8 to 14 Microns and Applications to Remote Compositional Analysis of the Moon's Surface," p. 194 and 195. JPL 31 August 1967.

III-10. JPL TR 32-785.
Loomis, A. A. "A Lunar and Planetary Petrography Experiment." JPL 1 September 1965.

III-11. JPL TM 33-353.
Loomis, A. A. "Petrographic Studies," Volume I, p. 79 through 87. JPL July 1967.

III-12. Gilvarry, J. J.
"Nature 188," p. 886.-1960.

REFERENCE LIST

Section III (contd)

III-13. Watson, K., Murray, B.C., Brown, H., J. Geophys. Res. 66, 3033 (1961)

III-14. JPL SPS 37-34
Elleman, D.D., Pearce, C.D., Manatt, S.L. Volume IV, p. 207 through 210.

III-15. Paper Presented to AAS Symposium, Las Vegas, Nev. April 68
Elleman, D.D. and Manatt, S.L. "Water Resources of the Inner Planets."

III-16. Fischer, E., Z. fur Physik
156, 26. 1959

III-17. Wuerker, R.F., Shelton, H., Langmuir, R.V.
J. Appl. Phys. 30, 342. 1959

III-18. JPL TR 32-713.
Bentley, K.E., Giffin, C.E., Whitten, D.G., Wilhite, W.F. "Detection of Life-Related Compounds on Planetary Surfaces by Gas Chromatography – Mass Spectrometry Techniques." JPL Technical Report No. 32-713, August 30, 1965.

IV. LUNAR ENVIRONMENT

A. INTRODUCTION

The simplified lunar surface model described in Ref. IV-1 was used for the baseline LRV design with the prospect that new data made available from Surveyor and Lunar Orbiter missions would permit refinement of the simplified model (see Ref. IV-2, IV-3, and IV-4).

Pending completion of the referenced lunar models (work is also in progress at MSC and USGS), JPL and MSFC have exchanged interim information described in subsequent paragraphs and in Ref. IV-8 and IV-9.

In continuing work on the vehicle-to-surface interaction, hazard probability, and navigational problems described throughout this report, emphasis is placed on four major items:

(1) Probability of unscheduled stops due to detection of hazards beyond safe mobility limits and effect of stops on step size. (cf. Sec. V. P. 1)

(2) Wheel-to-soil interaction on slopes near the angle of rest.

(3) Improved analysis and test correlations for predicting power, traction, and steering effects.

(4) Lunar thermal environment with particular reference to high-latitude operation and night survival.

B. SURVEYOR TEST RESULTS

Table IV-1 lists pertinent lunar surface information obtained from the five previous Surveyor landings. This information is the result of initial work performed by Prof. R. Scott, principal investigator for the surface sampler experiment, and by various members of the Lunar Mechanical Properties Working Group at JPL. The bulk of this information was obtained from studies of landing impact and specific science experiments conducted on Surveyor III, V, VI, and VII. Results of these studies are found in Ref. IV-2, IV-5, IV-6, IV-7, and IV-8.

Table IV-1. Soil Physical Characteristics

Characteristic	Result	Reference
Angle of internal friction	37 to 39 degrees	IV-5, page 109 and IV-6, page 87
Maximum slope of crater sides (angle of repose)	34 to 35 degrees	IV-2
Density		
(1) Top few millimeters (for thermal characteristics)	0.7 to 1.2 gm/cm^3	IV-7, page 106
(2) Below surface (for soil mechanics)	1.5 gm/cm^3	IV-5, pages 108 and 109
Cohesion	0.06 to 0.26 psi	IV-7, page 107 and IV-5, page 109
Grain size	2 to 60 microns 50% less than 10 microns	IV-6, page 87 IV-5
Permeability	1×10^{-8} to 7×10^{-8} cm/sec	IV-6, page 87
Bearing capacity (based on an 8-inch diameter footpad)		
(1) Static (average)	5 psi	IV-7, page 106
(2) Static (variable with depth)	See reference	IV-7, page 106
(a) In upper few millimeters	0.15 psi	NA
(b) At a depth of two centimeters	2.7 psi	NA
(c) At a depth of five centimeters	8.2 psi	NA
Surface Friction coefficient	0.6 to 0.8*	IV-9

*Suggested preliminary study value for adequately rough wheel or track surfaces.

REFERENCE LIST

Section IV

IV-1. JPL ASD 760-5.
JPL. "A Program Analysis for Lunar Exploration." JPL 25 July 1967.

IV-2. JPL TR 32-994.
"Lunar Slope Angles and Surface Roughness from Ranger Photographs," Choate, Raoul, June 1966.

IV-3. NASA TM X-53661.
Vaughn, Jr., O. H. "Lunar Environment: Design Criteria Model for Use in Lunar Surface Mobility Studies." NASA George C. Marshall Space Flight Center, Huntsville, Alabama. September 1967.

IV-4. JPL PD-57.
Newburn, R. "Lunar Model." JPL.

IV-5. JPL TR 32-1177.
Surveyor III Final Report.

IV-6. JPL TR 32-1246.
Surveyor V Final Report.

IV-7. JPL TR 32-1266.
Surveyor VI Final Report.

IV-8. JPL TR 32-1264, "Surveyor VII Mission Report." Parts I through III (Part II published 15 March 1968, Parts I and III publication pending winter-1968).

IV-9. JPL 760-27.
Burke, J. D. "Lunar Traverse Seminar." JPL, 16 May 1968.

V. BASELINE DESIGN

A. INTRODUCTION

In order to accomplish the roving mission objectives defined in Section II, it is necessary to combine the science requirements of Section III with appropriate roving technology in a vehicle design which can be delivered to the Moon by the various systems available for lunar exploration. This section presents revised figures based on later analysis of the design concepts given in Ref. V-1. Figure V-1 shows the range of rover weight and payload weight considered for the baseline and larger designs.

1. Lunar Delivery Systems

Types of Transport and Landing Modes. The cislunar transport and soft landing delivery modes considered available for this mission include:

(1) Automated spacecraft carrying rover as payload (rover strap-on to Surveyor-type spacecraft).

(2) Integrated rover incorporating transit, descent, and landing systems. (Figs. V-2, V-48).

(3) Manned Lunar Module (LM) carrying rover as part of payload (Fig. V-2A).

(4) Automated version of LM carrying larger rover.

(5) Automated rover launched to lunar surface from orbiting spacecraft.

Types of Injection Systems. These modes are all adaptations of two types of injection systems, the unmanned system (Atlas Centaur, Titan, etc.) and the manned system (Apollo). Recognizing the importance of flexibility to the lunar program, it was decided to explore the possibility of an adaptive roving concept, variations of which could be injected by either system and used in combination with any of these modes of delivery.

2. Study Results of Delivery Modes

Integrated Rover. Preliminary study efforts have emphasized the choice of the integrated rover since this approach appeared most economical for landing the LRV. Delivery of this same LRV by the separate automated lander or

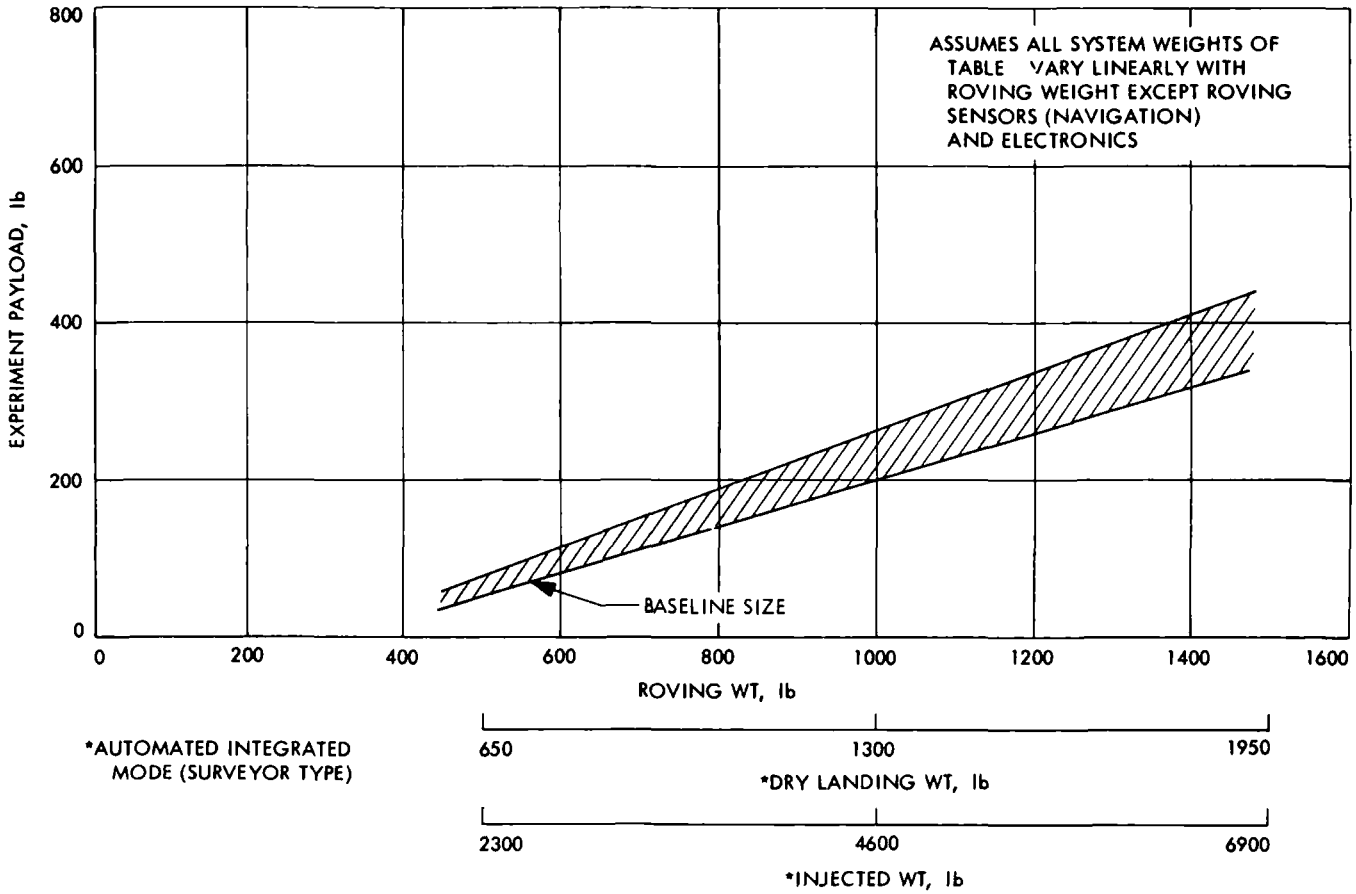

Figure V-1. Payload Weight as a Function of Roving Vehicle Weight

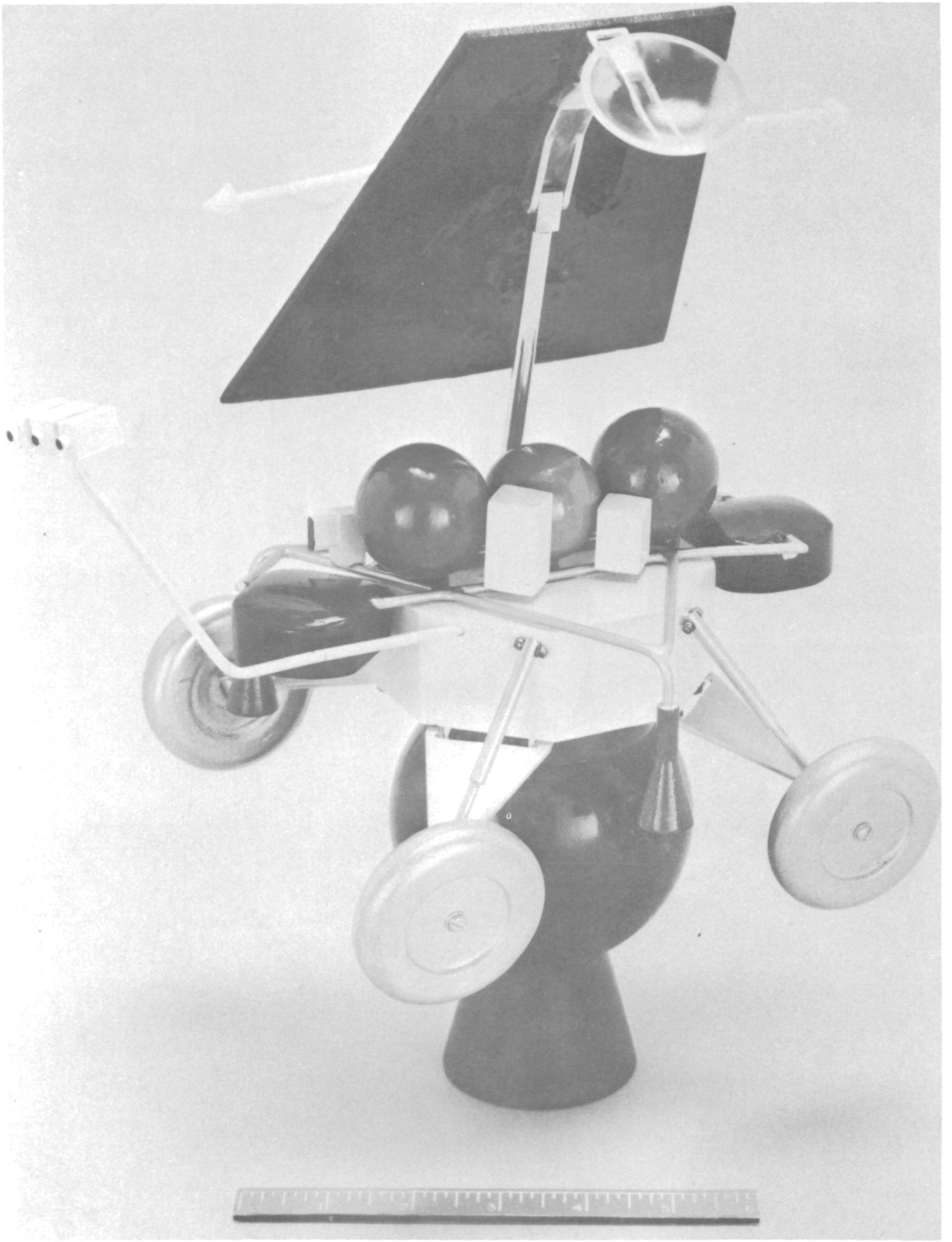

Figure V-2. Lunar Rover for Atlas-Centaur

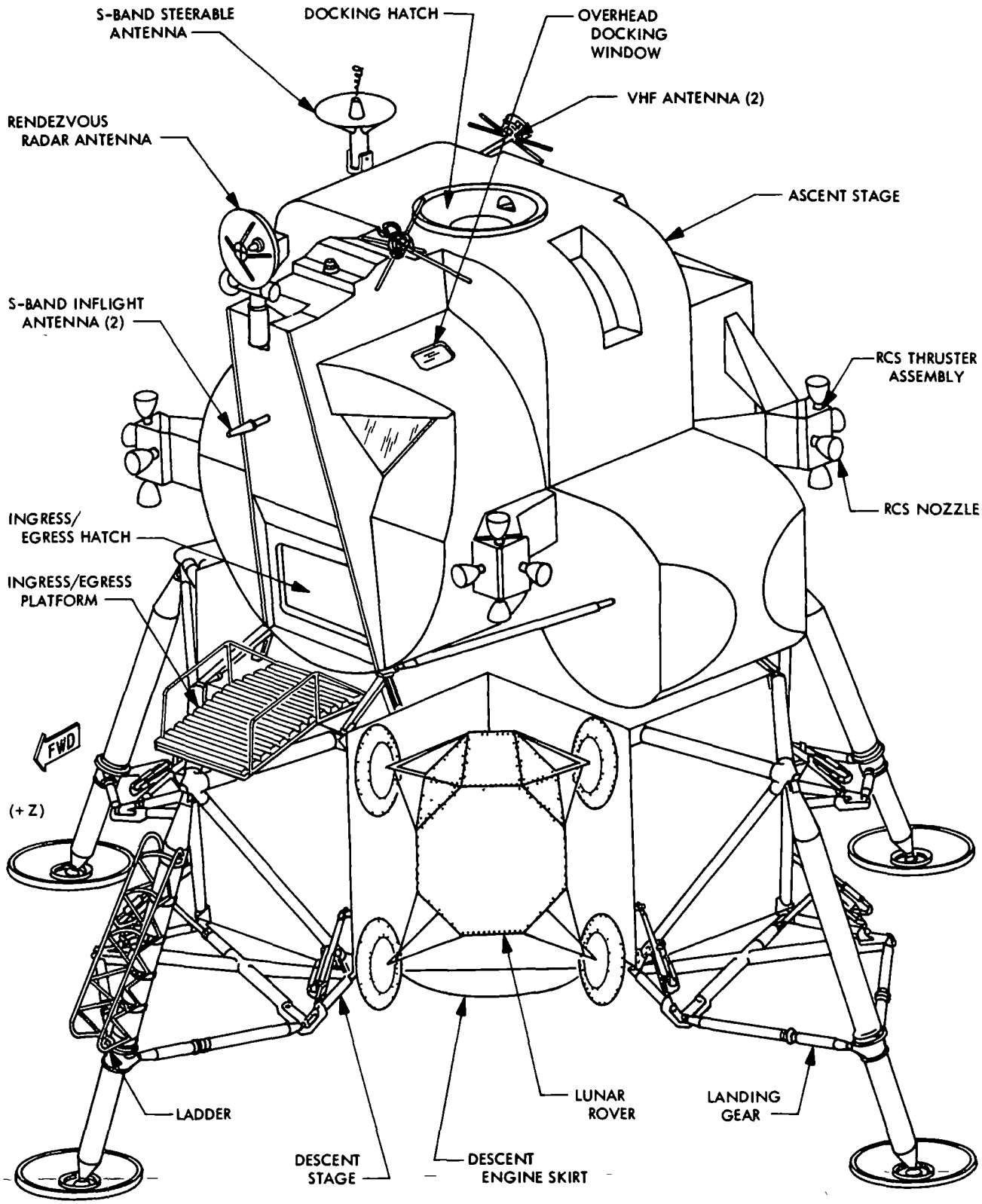

Figure V-2A. LRV Mounted on LM Structure

by manned spacecraft involves the following variations of the descent system, plus adaption to the booster, LM, or Command Service Module (CSM) constraints:

(1) Manned LM or Automated Lander. The same lunar rover with the descent systems detached.

(2) Descent from CSM in Orbit. The same lunar rover and Surveyor-type descent system incorporating a pitch-turn programmer and substituting a smaller main retro motor.

Weight and Performance Considerations. The rationale for selection of the present LRV design is described in Ref. V-1. The following considerations cause vehicle size and performance to converge toward the values chosen as the baseline for a parametric study:

(1) Performance of existing delivery systems (Atlas-Centaur and LM) implies a landed weight of 500 to 750 pounds.

Note: Throughout this section, weight means Earth weight or mass, not weight in lunar gravity.

(2) Requirements of the initial scientific mission on the long traverse are compatible with this weight. Larger payloads could be designed but it would be better to do so after gathering the critical scientific data that are the object of the baseline mission.

(3) Employment of existing delivery systems, aside from the obvious benefits in economy and reliability, permits use of accurate and detailed performance information in the baseline design study.

If the rover is launched by Atlas-Centaur and landed as a passenger on an automated Surveyor-type spacecraft it can weigh only about 200 pounds. However, as shown in Ref. V-1 if the transit and descent systems are integrated with the mobile spacecraft, it can weigh about 500 pounds. The former figure is too small for the stated scientific requirements but the latter is adequate. Figure V-1 shows instrument payload weight as a function of roving vehicle weight and injected weight

B. DESIGN CONFIGURATION

1. Integrated spacecraft design.

The design configuration developed for this vehicle adapts the major transport and descent systems of the Surveyor to soft land a four-wheeled roving vehicle on the lunar surface (Fig. V-2). It uses the Surveyor propulsion systems (vernier system and main retro motor) in combination with Surveyor radar systems (AMR and RADVS) for the descent requirements. However, it repackages the other Surveyor equipment into a single compartment above the main retro motor rather than distributed around it as in the Surveyor. This design provides an efficient body and chassis for the roving vehicle with a low center of gravity for good landing and roving stability.

Equipment Compartment Configuration. This central equipment compartment also provides a thermally controlled environment for the experiments and electronics and supports four wheels with independent springing for landing and roving. For launch these wheels are rotated to a stowed position around the main retro motor to fit within the Centaur shroud. A separable A-frame, located on top of the central compartment, carries the major descent systems including:

(1) Vernier Propulsion System. Including appropriate electronics (autopilot, etc.)

(2) Radar Descent System. Antennae plus appropriate electronics.

(3) Canopus Sensor.

The articulated solar panel and antennae (high-gain and omni) are located above the central compartment. These are arranged to permit the detachment of the A-frame and its descent systems equipment from the rover for the LM delivery mode. This also permits the jettisoning of this expended equipment after landing for the automated delivery mode. The main retro motor, which is jettisoned during descent in the normal Surveyor fashion, is located below the compartment. It contains the altitude marking radar (AMR) in the nozzle in the normal Surveyor manner along with the flight controls (electronics and gas attitude control system) which become expended equipment at the start of descent. Both are ejected upon start of the main retro motor as in the standard Surveyor AMR ejection.

The roving vehicle is powered by an electric motor in each wheel. Center point steering is also electrical, motion and steering are ground commanded.

Stereo imaging sensors plus a ranging sensor are located above the compartment for prime data and roving navigation while the other experiments are located within the compartment with access to the front, side or bottom as required.

To limit demands on the control system and the Earth-based operators, internal hazard-sensing devices (e.g., tilt and obstacle detectors) are provided. Operation of the vehicle during roving is intermittent in that power is first supplied to travel a short distance (approximately 2000 ft.) and then stop. Power is then supplied to perform a new visual survey and where appropriate to make a series of experiments and to transmit the information to the receiving stations. This intermittent roving and decision or experiment sequence is then repeated.

Travel Conditions. There are two possible travel conditions for the baseline design. One is the as-landed condition (Fig. V-2). Here, the descent systems are retained during roving, and could be used for emergency hops in the fashion tested on Surveyor. This results in a greater traverse weight, a smaller obstacle climbing capability, and an increase in roving power requirements as compared to the minimum weight configuration. The other configuration, having a smaller traverse weight, involves the jettisoning of the expended descent system after landing. This is accomplished by releasing the hinged and spring attached A-frame which flips off to one side. The purpose of this operation is to minimize the roving weight and reduce power requirements. The jettisoned A-frame could, of course, carry stationary experiments if desired. The current study considers the minimum weight travel condition for the baseline LRV in order to provide maximum payload capability.

2. Vehicle Performance

An estimated weight breakdown of this design concept is shown on Table V-1. This estimate indicates that the rover payload is generally comparable to that of the Surveyor.

Note: Table V-1 reflects major changes relative to Ref. V-1 as a result of: (1) increased wheel diameters, (2) revised propellant reserves, (3) revised navigation requirements, and (4) revised power requirements.

Payload Capability. It should be pointed out that the payload capability of the LRV is a critical item. This is a result of adapting the Surveyor descent propulsion, which in effect limits the landed weight to that of the Surveyor (approximately 700 pounds). This means that the weights required for the new roving systems (wheels and drive, steering, navigation and power) have to be obtained by modification and improvement of the Surveyor spacecraft and subsystems. The sizable performance achieved to date is a result of the following:

(1) Compact configuration of LRV (i.e., a single equipment compartment)

(2) Multiple use of equipment (i.e., integral roving and landing gear)

(3) Reduced landing velocity (5 to 6 ft/sec as compared to a maximum of 18 ft/sec on Surveyor)

(4) Jettisoning of cold gas attitude control system

(5) Reduced propulsion and guidance reserves

(6) Efficient roving systems (i.e., low power, slow speed, simple navigation, light suspension)

In keeping with the philosophy of using as much Surveyor hardware as possible, the baseline design has a "Dry Landed Weight" of 705 pounds for:

90 hour nominal flight

15 meter per second midcourse

25 degrees or less approach angle

2540 meters per second approach velocity

1300 pound retro propellant

127 pounds usable vernier fuel

Table V-1. Weight Breakdown for LRV

Characteristics	*	Flight configuration	Descent and land configuration	Travel configuration
Navigation		25 00	25 00	25.00
Flight Control		57 33	17 00	
Data Link		23 96	23 96	23 96
Central Command Decoder		5 87	5 87	5 87
Central Signal Processor		5 81	5 81	5 81
RADVS		34 06	34 06	
Engineering Signal Processor		6 22	6 22	6 22
Engineering Mechanisms Auxiliary		4 70	4 70	
Electrical Power		100 00	100 00	100 00
Battery	40 00			
Solar Panel	42 00			
Conversion Electronics	20 00			
Mechanisms		23 05	23 05	23 05
Pin Pullers	2 00			
Separate Sensor and Arming	1 05			
Positioners	20 00			
Basic Vehicle		479 46		
Basic Structure	50 00		50 00	50 00
Equipment Attach Hardware	20 00		18 00	15 00
Mast	10 00		10 00	10 00
Paint	1 00		1 00	0 60
Landing and Traverse Gear	100 00		100 00	100 00
Wiring	25 00		23 00	20 00
A/C Lines	1 00		1 00	
TV Boom and Platform	10 00		10 00	10 00
Retro Release Mechanism	1 00		1 80	
Centaur/Spacecraft Latch	0 66		0 66	
Vernier Propellant System	75 88		75 88	
Vernier Propellants	137 00		127 00	
Unusable Vernier Propellants	2 12		2 12	
"A" Frame	20 00		20 00	
Thermal Controls	25 00		25 00	25 00
Contingency		35 00	35 00	35 00
Retro-Rocket		1442 94	1442 94	
Case, Insulation, Release, Wiring	142 94			
Propellant	1300 00			
Altitude Marking Radar		11 74	11 74	
Buoyancy		1 00	0 90	0 50
Total Weight Less Payload (90 hr trajectory)		2254 14	2199 91	454 95
Expendables			1585 91	
Altitude Marking Radar	11 74			
Helium Gas	2 41			
Usable Vernier Fuel	127 00			
Unusable Vernier Fuel	2 12			
Retro Case	142 94			
Retro Propellant	1300 00			
Buoyancy				
Dry Landed Weight Less Payload	0 30		614 00	
Maximum Dry Landed Weight (90 hr trajectory)			705 00	
Maximum Payload (90 hr trajectory)		91 00	91 00	91 00
LRV Traverse Gross Weight (90 hr trajectory)				546 01
Total Separated Weight at Injection (90 hr trajectory)		2345 14		

*Weights are preliminary, decimals are carried in table merely to permit entry of actual Surveyor item weights where appropriate

To provide a gross performance perspective of this class of roving vehicles, rough performance estimates were also made of larger integrated rovers. This result is shown in Fig. V-1 which presents roving payload as a function of injected or roving weight capability of the launch vehicle.

3. Sequence of Events

Although this concept is considerably different from the Surveyor in configuration, the sequence of events during flight and lunar descent is essentially the same. The various phases of operation are discussed in the following paragraphs.

Space Transport Phase. During launch, the spacecraft is contained within the Atlas-Centaur shroud and supported on the Centaur tank dome in the normal Surveyor manner. In this phase the solar panel, antennae and wheels are in their stowed position. After standard shroud ejection and just prior to spacecraft separation, the solar panels and antennae are erected and the wheels spring to their roving position. Events after separation through midcourse and to lunar arrival are then identical to the Surveyor with the configuration as shown in Figure V-2 and V-48.

Descent Phase. The descent phase is essentially the same as for the Surveyor (Appendix D) in that the main retro and vernier motor plus the AMR and RADVS descent systems provide the standard controlled descent to a soft landing on the lunar surface (Fig. V-48, Cruise and Landed Configuration). However, a variation is introduced into the final touchdown phase just prior to surface contact for the purpose of softening the landing impact. This is accomplished by continuing the constant 5 ft/sec final Surveyor descent velocity (controlled by the vernier engines) to contact. Engine cutoff is then actuated by a surface contact switch (similar to that previously considered for both Apollo and Surveyor). This variation, which eliminates the 18 ft. (maximum) free fall of the Surveyor, minimizes the rover wheel and carriage weight penalties due to landing impact loads. At the same time this eliminates the need for the cold gas attitude control system for the free-fall descent and permits its early jettisoning along with the AMR. It should be noted that the high free fall distance adopted for Surveyor was a result of concern about dust transport due to surface impingement of the vernier engine exhaust. However, Surveyor flight test results have generally reduced this concern.

Roving Phase. The sequence of events being developed for the Roving Phase of the LRV has been divided into a standard sequence of events and a non-standard sequence of events. The standard sequence of events is intended to cover all operations needed to satisfy the mission requirements under expected conditions of vehicle performance and lunar environment. The intent of the non-standard sequence of events is to identify possible problems that the LRV will accommodate.

Standard Sequence of Events. The standard sequence of events for the Roving Phase has been subdivided into sub-phases consisting of Post Landing Events, Site Identification Events, Commanded Traverse Events, Science Sampling Events, Science Sample Handling Events, and Lunar Night Events. A short description of each sub-phase follows: (Refer to Appendix C.)

(1) Post Landing Sequence. (Table C-1) The general purpose of the post landing sequence is to assess the status of the LRV and the immediate lunar terrain. Based on this assessment, the roving preparation will be made. The sequence is described in the following paragraphs.

(a) Telemetry engineering assessment. The flight telemetry system is commanded through all its modes immediately after touchdown.

(b) Imaging assessment. A local area survey is performed to assess any possible physical damage to the LRV and to verify that articulated items may be safely deployed.

(c) Roving preparation. Roving preparation is completed by jettisoning the A-frame, unlocking and positioning the high-gain antenna and solar panel, and deploying articulated items such as the obstacle detectors. Exceptions to the sequence such as not jettisoning the A-frame may be elected on the basis of the telemetry and imaging assessments.

(2) Site Identification Sequence. (Table C-2) The purpose of the site identification sequence is to establish the location of the LRV on the lunar surface within the area established by radio tracking. The location is to be established by determining the direction and range from the LRV to known landmarks on the lunar surface. The sequence is as follows:

(a) Wide angle TV scan. A 360° horizontal scan is performed using ground based facilities to perform the computations required for camera pointing and operation.

(b) Landmark identification. From the imaging data provided by the 360° scan, the operation personnel must identify sufficient landmarks to perform the navigation function. The optimum performance of landmark identification personnel will depend heavily on the adequacy of the displays and other aids developed for use in the Space Flight Operations Facility (SFOF).

(c) Narrow angle survey. After a landmark has been identified in the 360° scan, a narrow-angle survey of the landmark is performed. The narrow-angle survey provides precise direction and range data to be used for determining the exact location of the LRV.

(d) Locate on map. Using the data from the wide-angle and the narrow-angle survey, the operation team pinpoints the location of the LRV on available lunar maps.

(3) Commanded Traverse Sequence. (Table C-3) The commanded traverse sequence is used to prepare the LRV for the next increment of traverse, execute the traverse and then prepare the LRV for another site identification sequence. The sequence is as follows·

(a) Select bearing and step distance. Based on the LRV condition, the immediate lunar terrain, and the desired destination, the operations personnel must determine the next short term destination. After the destination has been selected, a new bearing and a new traverse distance are selected.

(b) Orient LRV on new bearing. In order to align the LRV with a new bearing, a fixed radius turn is performed. With the turn radius known, ground computation is performed to determine the distances the LRV must move in order to be aligned with the new bearing. The LRV is then commanded to move the desired distance and stop.

(c) Verify new bearing. Verification that the LRV is aligned with the new bearing is accomplished by performing an imaging survey of the previously identified landmarks. From the new landmark bearing and range data, operations personnel determine the acceptability of the new bearing.

(d) Traverse. After traverse distance parameters have been transmitted to the LRV and stored, the initiation of traverse is commanded by ground command. Due to the power requirements of the mobility subsystem, real time

imaging cannot be accomplished, but real time telemetry is available. The traverse is normally stopped when the commanded traverse distance has been completed. An emergency stop may occur at any time during the traverse and would result in a non-standard sequence of operations. After a normal stop, the neces sary operations to place the LRV in the site identification mode are completed.

(4) Science Sampling Sequence (Table C-4). Science samples are to be obtained at various locations in the lunar traverse. When a desirable sampling location has been identified, the science sampling sequence is used to obtain the sample. A nominal science sampling sequence is as follows.

(a) Identify desirable sampling spot. In addition to the general sampling spots determined prior to the LRV landing, desirable sampling spots may be identified from the LRV data. One of the functions of the operations personnel will be to evaluate the LRV data in near real time in anticipation of locating desirable sampling spots.

(b) Traverse to sample spot and photograph. After a desired sample spot has been identified, the LRV is commanded to the location. Site identification surveys are performed to locate on a lunar map a sample spot identified from LRV data, and in the case where the sample spot was identified from other than LRV data, to certify that the desired sampling location has been reached. Narrow-angle photographs are also made of the surface material where the sample is to be obtained.

(c) Select sampler type. The operation personnel will be required to select one of the three sampler types (cf. Section V-H.) based on the type of sample desired (i.e., surface particulate, subsurface particulate, a small rock, or drilled sample from large rock)

(d) Acquire sample. Using ground commands the selected sampler is commanded through a sequence of operations that will obtain the desired sample.

(e) Determine sample disposition. From the real time LRV data, operations personnel must decide if the sample is to be stored, analyzed or dumped.

(5) Science Sample Handling Sequence (Table C-5). After the sample has been acquired and a decision relative to its disposition has been made, the science sample handling sequence is used to implement the disposition as follows:

(a) Store sample. To store a sample, a sample storage position is selected and a sample cup (cf. Section V-H.) retrieved from the storage position and placed in the sample transfer position. With the cup in place, the sampler is commanded to the transfer mode and the sample is transferred to the cup. The filled cup is then returned to the selected storage position.

(b) Dump sample. A sample may be dumped from the sampler simply by not having a sample cup in place when transfer is commanded. A sample may be dumped from a sample cup by inverting the sample cup.

(c) Analyze sample. The sample is handled the same as if it were to be stored except the cup is transferred to one of the science instruments instead of being returned to the storage position. After completion of analysis the sample may be stored or dumped.

(6) Lunar Night Sequence (Tables C-6 and C-7). The purpose of the lunar night sequence is to prepare the LRV to survive the night and at the end of the night to prepare the LRV for the next day's operation.

(a) Position solar panel. Using thermal control predictions based on LRV data, operations personnel determine the initial position for the solar panel at the start of the next lunar day. The solar panel is commanded to this position.

(b) Electronic subsystems shutdown. The selection of electronic subsystems to be de-energized will be on the basis of available power. With a battery as the only source of energy storage, all electronics will be de-energized during the night.

(c) Next day preparation. With the known shutdown status of the LRV, and predicted survival characteristics, a plan for the next day's operation is generated.

(d) Electronic subsystem reactivation. Reactivation of the electronic subsystems is started when power becomes available. During the process of reactivation, engineering telemetry and imaging assessments are made of the LRV operational status.

(e) Science operation. Assuming that the battery is not completely charged at the end of the lunar night, some time will be required for battery charging prior to the start of traverse operations. During this time in-situ science experiments may be performed.

(7) Nonstandard Sequence of Events (Table C-8). In the event that the end of the commanded traverse places the LRV at a location where the view of the horizon is inadequate to identify the required navigation landmarks, the LRV must be moved to another location where an adequate view is available. After operations personnel have selected an alternate location, the sequence of events required to move the LRV to the alternate location is essentially the same as the commanded traverse sequence.

Although detailed analyses have not been performed, several hazardous situations have been tentatively identified (Table C-9). In general, the LRV response to an indicated hazardous condition is to immediately stop the traverse and position the solar panel for maximum power. Next the communications link capacity is maximized by positioning the high-gain antenna and commanding the LRV transmitter to the high power mode. An imaging assessment then provides data to substantiate or refute the actual presence of a hazard. As a function of the type of hazard, the operations personnel develop corrective procedures.

4. LRV Roving Phase Functional Block Diagram

When the performance of the Roving Phase sequence of events is considered, the need for certain subsystems becomes evident. In conjunction with the development of the Roving Phase sequence of events, a preliminary block diagram (Fig. V-3) has been developed to depict the subsystems and the functional interfaces between them. This figure is augmented by Appendix E which contains a detailed listing of interface circuits. As the analysis of the system continues such a block diagram and interface circuit list can be updated to reflect the current LRV status.

C. LUNAR GUIDANCE AND CONTROL SUBSYSTEM

1. Remote Guidance and Control

Automated LRV. Remote guidance and control of an automated LRV can be accomplished in a variety of ways. Several approaches exist, with continuous, remote, real-time, human-operator control on one end of the range

and a self-contained, autonomous system on the other. Human control is based on the continuous transmission of stereoscopic or monoscopic TV images. The autonomous vehicle must carry an inertial and/or stellar navigation system, a set of visual and tactile terrain monitors, and a high-speed, general-purpose computer. Between these extremes is an area of intermittent operator control with the frequency of intervention decreasing as full autonomy is approached.

Anticipated Power Requirements. The two extremes mentioned in paragraph C. 1. require large amounts of electrical power, 350 to 1, 000 watts (Ref. V-2 and V-3). As these extremes are abandoned, the power demand decreases. Figure V-4 illustrates this and also illustrates a baseline vehicle design constraint that limits the complexity of the navigation scheme and the guidance and control subsystem. The baseline vehicle's power generating capability is limited by size and weight to approximately 200 watts. Of this amount, about 180 watts is allocated to essential functions such as locomotion, communication, TV, etc. This leaves only about 20 watts to spare. Therefore, only the simplest low power equipment can be incorporated into the vehicle's design to aid in its safe and efficient operation.

Rationale for Choice of Guidance and Control Method. The guidance and control method decided on, based on a minimum of on-board navigation equipment, involves a sequence of short discrete commanded "steps." Each step consists of a position-determining-and-decision period and an automatic traverse period. Navigation aids will include, but are not necessarily limited to, one or more inclinometers, one or more accelerometers and an optical ranging device. In addition there will be automatic obstacle detection equipment. The total power consumed by these aids will be a little over 20 watts. The TV subsystem, a necessary requirement in any case, is a valuable adjunct to the navigation equipment.

The baseline guidance and control method is based on "piloting by landmark." Although the applicability of this approach has been discounted by Streicher (Ref. V-4), we feel it has considerable merit, especially in a power-limited automated vehicle.

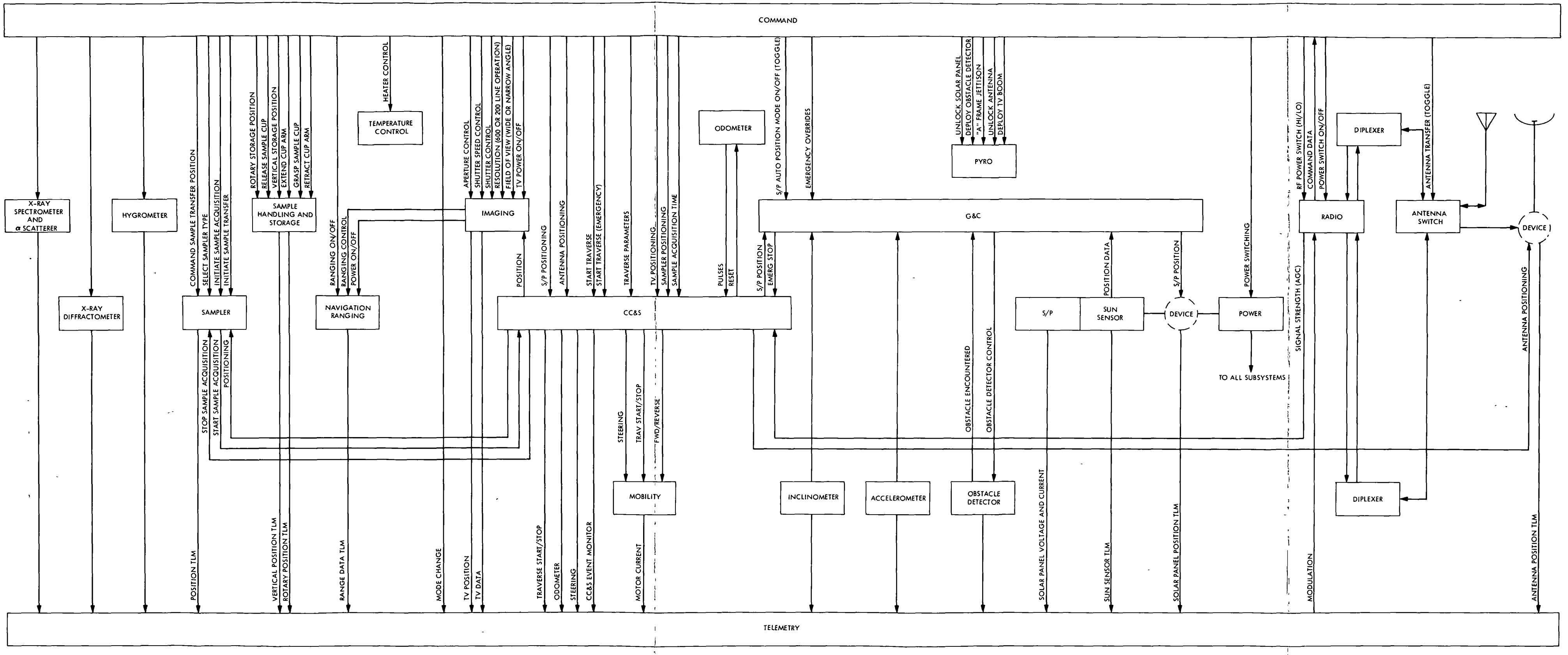

Figure V-3. LRV Functional Block Diagram

Page intentionally left blank

Page intentionally left blank

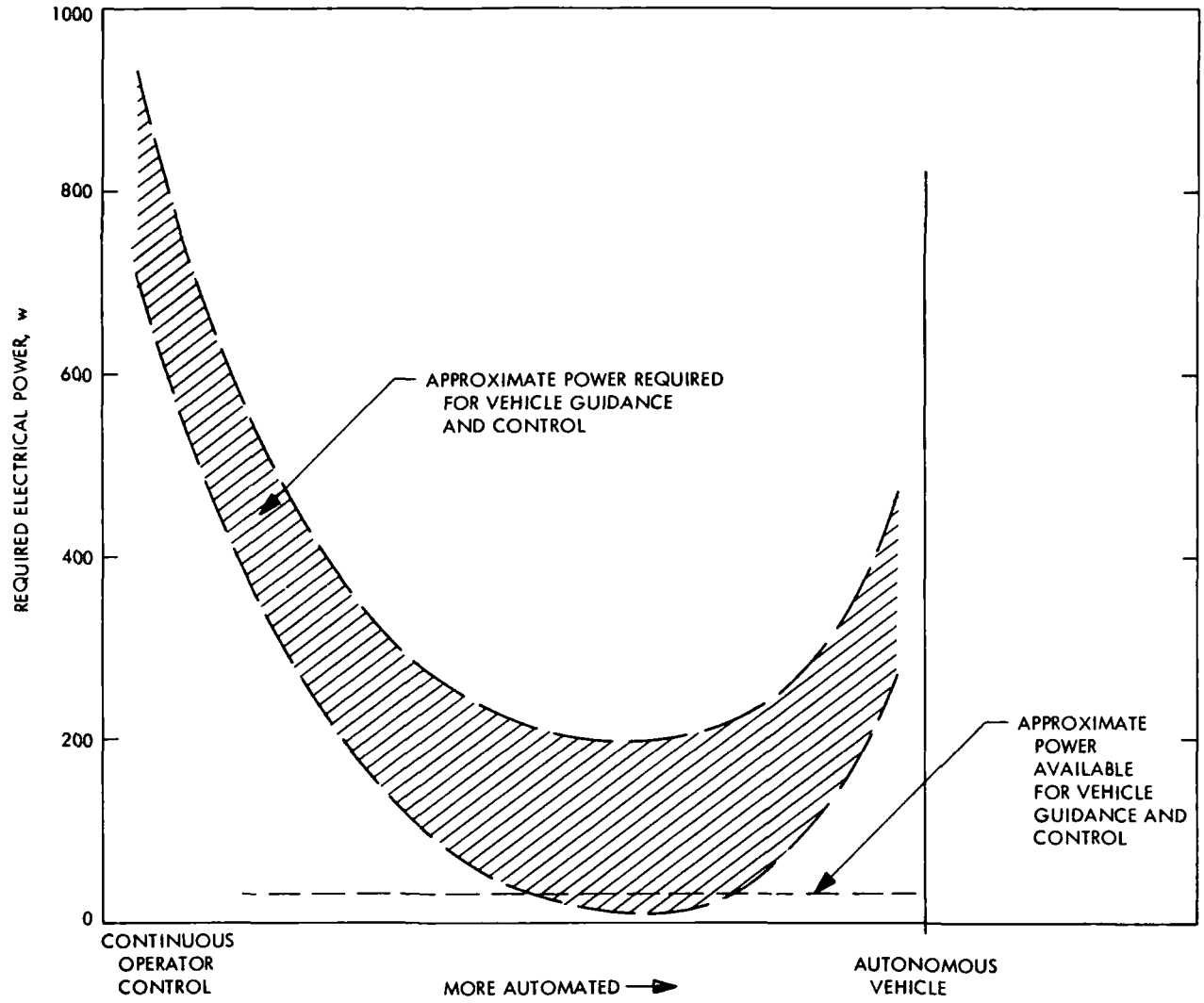

Figure V-4. Electrical Power Required for G&C of Automated LRV

Inertial or celestial navigation schemes are ruled out because of their weight, or power requirements, or inherent complexity. The navigation schemes that may use simple low-power LRV equipment are: piloting by landmark and Earth-based radio ranging and range-rate. On the grounds of accuracy, the landmark navigation scheme is the most logical choice. This conclusion is developed in subsequent paragraphs dealing with navigational studies.

Description of Guidance and Control Method. While the vehicle is stationary, an operator (or more than one) observes the landscape via TV in a 360° sweep about the vehicle. Large areas on the moon possess distinctive features

such as hills and raised crater rims. If three such features are situated within sight of the vehicle, the operator identifies these. He is then able, with the aid of accurate measurements of angles between the landmarks, to precisely locate the vehicle on a lunar map or photograph. Knowing where the vehicle is and where he wants it to head, the operator commands an automatic traverse step in the appropriate direction. He then waits for the vehicle to stop, at which time he repeats the above procedure.

Analysis of Baseline Guidance and Control Method. The feasibility of this approach is bolstered by two considerations. First, the vehicle can be made to traverse safely although blind with only simple reliable instrumentation onboard. Second, the principles of piloting by landmark on the Moon have been effectively demonstrated in the Surveyor and Lunar Orbiter programs.

(1) Blind Traverse. Every remotely operated vehicle will have to possess some minimum of automatic equipment to safeguard the vehicle. Even a 100 percent manually controlled rover must have instrumentation to inform the operator of its angle with respect to the vertical, its speed, the distance it has travelled, and the amount of slip experienced by its wheels. This information cannot be obtained from viewing a TV screen. Furthermore, because of the almost three-second roundtrip communication delay, the vehicle will need automatic emergency stopping capability. Therefore, an inclinometer, an odometer, one or more accelerometers and a wheel slip or sinkage indicator are fundamental to any vehicle. The only additional instruments needed for blind traverse are an appropriate set of above-ground feelers or bumpers and a simple slope predictor (analogous to a cane carried by a blind man). These devices are electromechanical in nature and conceptually very simple and reliable. They can be obtained at a small cost in weight, and they consume virtually no power.

(2) Piloting by Landmark. The second of the two considerations deals with the ability to relate a horizontal view of terrain features to a vertical one. That this can be done on Earth has been amply demonstrated and is further supported by the results of tests described in Section V-M. Two fundamental questions are raised concerning piloting by landmark. Are the areas on the Moon, over which it is desirable to send a rover, sufficiently covered with distinguishable features? Can location of the vehicle at the end of each step be

completed rapidly enough to accomplish the required 1835 kilometer mission (see below) at a speed that is both reasonable and consistent with the power limitations of the baseline vehicle?

(a) Response to Question 1. It appears that even in bland maria regions, the terrain variations may offer adequate opportunities for unambiguous identification. It was possible to pinpoint the location of at least one Surveyor by comparing details on Lunar Orbiter photographs with the Surveyor's view of the horizon. Although this accomplishment took several hours to complete, and verification could have taken as long as 24 hours, the fact is that it was accomplished.

(b) Response to Question 2. It can be expected that three important factors will greatly reduce the time needed for locating a moving vehicle. First, as the operator becomes more experienced he will learn the tricks of landmark identification. Second, since the vehicle's path will be known, the appropriate Lunar Orbiter photos will have been processed and studied beforehand and the operator will have some familiarity with the features he will be looking for. Last, and probably most important, the vehicle traverse steps will be short enough to allow previously identified landmarks to still be in view from one station to the next. Therefore, it may be necessary at many stops to sight on only one additional feature. It is not unreasonable to expect that these three factors will reduce the average vehicle location time to minutes.

Therefore, the response to both questions appears to be in the affirmative. It must be noted that these arguments are by no means conclusive; additional work can be done and is intended to be done to substantiate these preliminary observations.

2. Guidance and Control Subsystem Mission Requirements

Vehicle Lifetime and Distance Traveled. The vehicle lifetime will be one year and the sum of the great circle distance traveled during this lifetime will be approximately 1,500 kilometers

Operating Modes. The vehicle will be driven by operators at one location. Prime operation will be via Goldstone but limited operation through the other Deep Space Net (DSN) stations will be possible. The normal operating mode will consist of the following:

(1) Determining vehicle location and orientation by visual inspection.

(2) Orienting the rover.

(3) Commanding a traverse of distance W.

(4) Monitoring engineering telemetry until the vehicle signals that it has stopped again (refer to Appendix C for details of the Roving Phase Sequence).

Note: Procedure (4) may be altered for short periods when the traverse path contains numerous obstacles or during investigation of interesting areas.

Detection of Obstacles and Hazards. The vehicle will be capable of detecting both obstacles and hazards but will not automatically avoid them since normal operation requires the vehicle to stop and wait for operator intervention (refer to Appendix C, Table C-9).

Navigation Aids. The vehicle will carry the following navigation aids:

(1) A simple ranging device such as a laser.

(2) One or more odometers.

(3) One or more inclinometers

(4) A real-time panoramic stereo/monoscopic television.

(5) A simple, uncompensated gyroscope may also be included aboard the vehicle.

3. Factors Covering Mission Requirements

Net Traverse Time. Although the vehicle lifetime is one year, only a portion of this time will be available for traversing the lunar surface. To estimate the net traverse time during the mission, a number of factors have been

considered. The amount of time to which they decrease the available traverse time has been estimated and is included in parentheses:

(1) Lunar day travel only (45%)

(2) Goldstone operation (33%)

(3) Remainder DSN operation (50%)

(4) Feature investigation (10%)

(5) Obstacle encounters (5%)

Lunar Day Travel Only. LRV travel is assumed only during the lunar day which reduces the available travel time to 50 percent. A further assumption is that traversing will not be attempted when the sun is less than 5 degrees above the horizon. The reasoning behind these assumptions is as follows:

(1) Repose Period. A period of dormancy will be needed after sunrise to allow the vehicle to reach operating temperature. Battery charging may also be required since it would be unwise to start traversing without a fully charged battery. Therefore, the first traverse step following sunrise probably will not occur until some five to ten hours have elapsed.

(2) Hazard. Similarly, at sunset a no-traverse period may be observed since, as the sun lowers toward the horizon, the probability of the vehicle entering a shadowed area increases rapidly. This is considered a hazardous situation and extrication may be time-consuming and difficult. To compound the problem, the shadows are inexorably lengthening, making escape to a lighted area still more difficult. Obviously, in such a predicament the vehicle will not begin the lunar night in optimum fashion. Therefore, an additional 5 percent has been included in the factor limiting travel to day periods only.

Goldstone/DSN Operation. Goldstone operation is assumed for only eight hours in each 24-hour period. While this may seem somewhat pessimistic, it allows for various contingencies such as down-time of the complex, automated ground equipment. Operations through the other DSN stations are anticipated to be 50 percent less efficient than through Goldstone. A total of 15 percent has been assumed for the aggregate time spent in the investigation of unusual features and in circumventing obstacles or hazards in the vehicle's path.

Computation of Available Active Vehicle Time. With the previously discussed assumptions defined, the net time available for completing the traverse mission can now be calculated. The assumptions defined will now be combined individually to arrive at the total available active vehicle time.

(1) Total Lunar Daytime (T_D). Total daytime hours is computed as follows:

$$T_D = 0.45 \text{ (8760 hours/year)} = 3940 \text{ hours}$$

(2) Net Active Time (T_N). DSN limitations must now be accounted for. It should be noted that the 50 percent factor included for operation through other DSN stations is applicable only to the time that the vehicle is stationary and commands are being transmitted. The full period of non-Goldstone operation is 0.67 T_D. It will be assumed that the vehicle is stationary during half of this non-operative time. As described in a subsequent paragraph, a less severe ratio of stationary to total time is implied. The net active time (T_N) resulting from DSN limitations is as follows:

$$T_N = 0.33\ T_D + 0.33\ T_D + 0.5\ (0.33)\ T_D$$

$$= 2.5\ (0.33)\ T_D = 3370 \text{ hours}$$

(3) Available Active Vehicle Time. The inclusion of the remaining factors further reduces the available active vehicle time to the following:

$$T = (1\text{-}0.10\text{-}0.05)\ T_N = 0.85\ T_N$$

$$= 2870 \text{ hours}$$

Length of Traverse. With the vehicle travel time computed at 2870 hours, it is now possible to estimate the length of the prescribed traverse. While the nominal length is 1500 kilometers, degradation factors must be introduced in the same manner as those for the computation of travel time. The factors affecting traverse distance (the assumed magnitude of each is included in parentheses) are discussed in paragraphs (1) through (5).

Non-Spherical Surface (1%). While the Moon is nominally a sphere, mountains, valleys and large craters represent a departure from the spherical shape. As the vehicle traverses these surface features, the distance it travels is more than the great circle distance between two points. The increase

in the distance of 1 percent was estimated by assuming average terrain slopes in the direction of vehicle travel of 2 degrees for 40 percent of the distance, 4 degrees for 30 percent, 6 degrees for 20 percent, and 10 degrees for the remaining 10 percent. This is illustrated conceptually in Figure V-5.

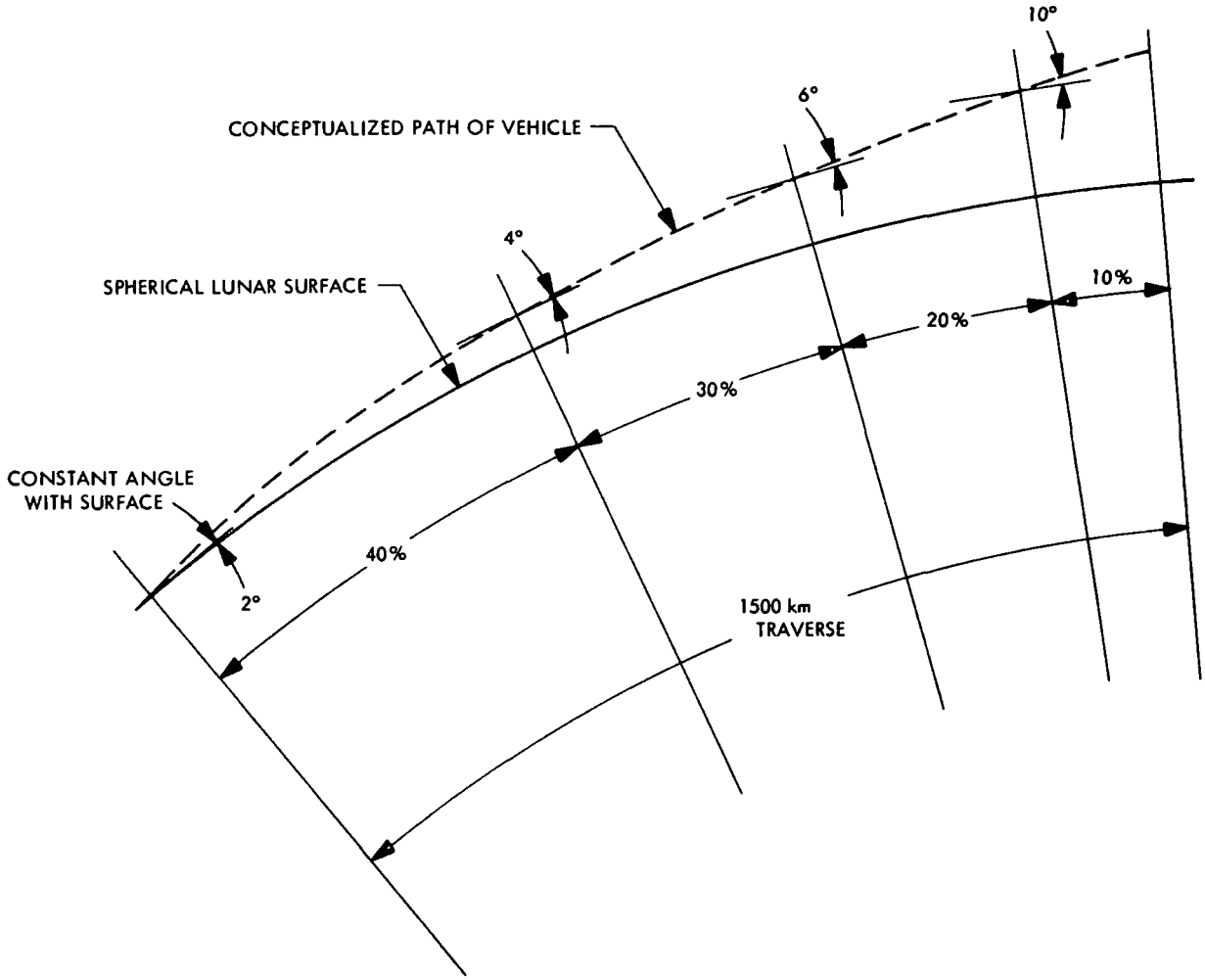

Figure V-5. Conceptual View of Vehicle Path Due to Non-spherical Lunar Surface

Terrain Ruggedness (2.5%). Terrain ruggedness refers to rocks and surface unevenness due to small craters and rises. Whereas non-spherical surface involves large surface irregularities, terrain ruggedness involves features of a size comparable to the vehicle. It is safe to assume that the wheels will be rolling into and out of small craters almost continually. Rocks and minor rises (in the order of one-third of the wheel size) may be encountered occasionally (in the order of 15 percent of the time). Further assumptions that the craters and rises are conical in shape with an apex angle of 160 degrees and that the effect of small rocks is negligible resulted in the assumed magnitude factor of 2.5 percent.

Navigation and Guidance Errors (15%). Navigation and guidance errors arise because the vehicle will depart from its intended traverse path. The vehicle will not have a real-time heading reference as it travels. Furthermore, it will travel with the steering locked in the straight-ahead position. Whenever the wheels slip on a slope, a heading change may result. Of greater significance is the deflection in azimuth that occurs when the vehicle moves along the walls of a large crater. In general, the vehicle's tracks in a circular crater of conic cross-section will appear as in Fig. V-6. If no slipping takes place the angle of deflection δ is a function of the distance, a, from the center of the crater to a projection of the vehicle's initial path. If slipping occurs, δ is not readily predictable. Since some wheel slippage (as well as soil deformation) will certainly occur, δ can be predicted on a statistical basis only. While extensive experiments to determine δ have not been conducted, a preliminary investigation has been undertaken. The results (described in Section V-N.) so far indicate that δ will generally be smaller than 20 degrees. The progress of the vehicle through a crater field can be characterized as a Markov process. The vehicle's movements can therefore be simulated by a random walk. If many of these random walks are combined in a Monte Carlo process, the expected value of δ can be found. This will be attempted when more statistical data on δ have been accumulated. For now, a conservative expected value for total deflection in one step $E(\delta)$ is assumed. The 15 percent value for navigation and guidance errors reflects an estimated $E(\delta)$ of 25 degrees. This is based on the premise that an attempt is made to fully correct any deviation from the intended path at each step. This premise results in a pessimistic estimate for the total error. Therefore, the 15 percent magnitude factor includes a pad in case $E(\delta)$ turns out to be more than 25 degrees.

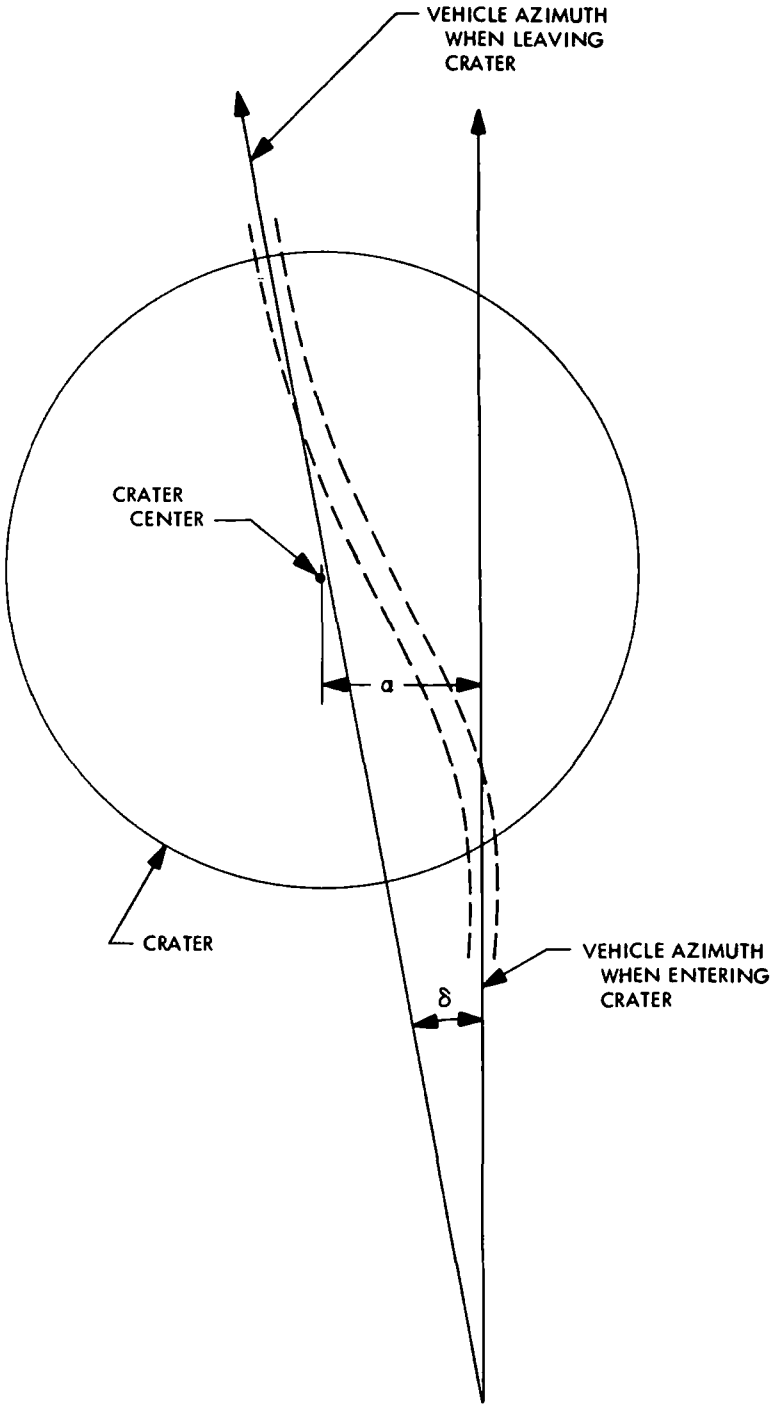

Figure V-6. Example of Vehicle Azimuth Deflection Due to Passing Over Conical Crater

(4) Feature Investigation (5%). Although an allowance in the available mission time T was made for feature investigation and obstacle avoidance, it is necessary also to include the additional distance that may have to be travelled. It will probably be necessary to move closer to features that warrant investigation. A 5 percent magnitude factor represents an allowance of 75 kilometers for this travel. Obviously, this allowance is meant to accommodate only those features which are unexpectedly encountered in the traverse. If a feature of interest is known of in advance, the distance to reach it will be included in the nominal traverse distance of 1500 kilometers. If we surmise that the majority of the interesting features encountered accidentally are within one-half kilometer of the nominal traverse path, since they must be observable via TV, the allowance permits about 75 such investigations.

(5) Obstacle Avoidance (3%). Obstacle avoidance accounts for additional distance travelled to navigate around and among obstacles and hazards. It includes allowances for avoiding boulders, entire boulder fields, and steep-walled craters. A total of about 45 kilometers is allotted for this.

Computation of Net Traverse Distance. With the various factors affecting traverse distance clearly defined, the net anticipated traverse distance can now be computed.

(1) Topographical Factors. Topographical factors are accounted for as follows:

$$D_p = (1 + 0.01 + 0.025 + 0.15)\ 1500$$

$$= 1.185\ (1500) = 1780 \text{ kilometers}$$

(2) Investigation and Safety Factors. The net traverse distance is obtained by adding those factors involving investigation and safety:

$$D = (1 + 0.05 + 0.03)\ D_p$$

$$= 1.08\ D_p = 1835 \text{ kilometers}$$

The values for D and T are updated from those reported in Ref. V-6. The new values are more realistic and reflect increased confidence in the concepts discussed.

D. LRV POWER SUBSYSTEM

The LRV power subsystem is required to provide electrical power during both the flight and lunar traverse phases.

The standard transit operations power profile (Fig. V-7) shows that the peak loads are as much as eight times the cruise power loads. Since these peak loads are short in duration it is wasteful to meet them except by a storage device such as a battery. The LRV is therefore constrained to carry a battery as a portion of its power subsystem.

1. Transit Operations Power Requirements

Since the LRV is utilizing as much Surveyor equipment as possible and its transit operations are the same as that for Surveyor, we can assume the standard transit operations power profile (Fig. V-7) to be that of Surveyor.

Traverse Power Requirements. In Ref. V-6 the average power required to move the vehicle across the lunar surface was estimated to be 96 watts. This estimate was based on empirical data compiled by General Motors Corporation during studies with the SLRV. The estimate was contingent on a vehicle net roving weight of 480 pounds on Earth and an assumed average terrain slope of 10 degrees. These factors have changed in the past year. Also, an error in converting one of the earlier numerical results was uncovered. A more realistic estimate of vehicle locomotion power has since been derived. The overall result is a small increase in the power requirements.

(1) Terrain Slope. The value for average terrain slope has been readjusted to 5 degrees and the vehicle weight has increased to 540 pounds as described in Table V-1. This adjustment in average terrain slope is consistent with Surveyor findings. Slopes generally appear to be from 1 degree to 5 degrees. Surveyor VII photos indicate that even in the highlands, extended slopes of 10 degrees or more are rare. Therefore, it can be anticipated that a majority of the traverse will be on slopes of 3 degrees or less. An average value of 5 degrees allows for such effects as local roughness and additional energy absorbed by the vehicle suspension system (cf. Sec. V-N)

(2) Rolling Friction, Soil Deformation, and Nonhorizontal Terrain. New values are now calculated for rolling friction (R_r), soil deformation (R_m) and nonhorizontal terrain (R_s). The weight on each wheel is now 22.9 pounds

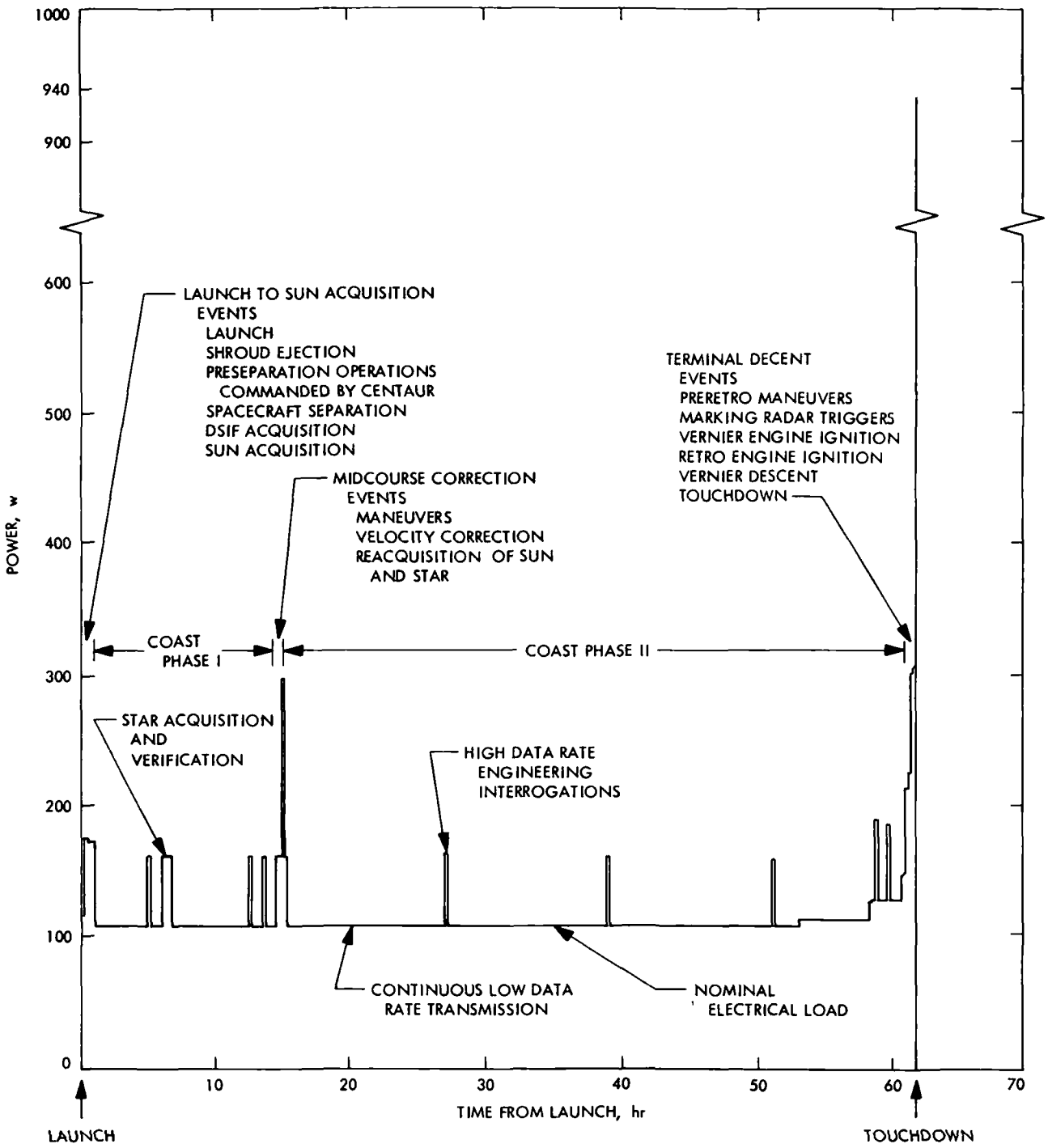

Figure V-7. Cruise Power Profile

(20.4 lb in Reference V-6). The value for R_r is assumed to be 7 percent of the weight at the wheel, R_m is taken to be 2 R_r, and R_s is the component of weight along the slope.

$$R_r = 0.07\ (22.9) = 1.6 \text{ lb/wheel}$$

$$R_m = 2\ (1.6) = 3.2 \text{ lb/wheel}$$

$$R_s = 0.087\ (22.9) = 2.0 \text{ lb/wheel}$$

The total force per wheel is the sum:

$$R_r + R_m + R_s = 6.8 \text{ lb/wheel}$$

The electrical power required for locomotion is proportional to this sum and to the vehicle speed. Figure V-8 is a plot of average locomotion power required as a function of average vehicle speed.

It has been assumed that the overall electrical/mechanical efficiency of the wheel drive circuits and mechanisms is 30 percent.

(3) Stall and Normal Power Requirements. It is necessary to know the power required under stall conditions and the normal maximum power demand when the vehicle is moving. This is necessary to determine the amount of electrical energy to be stored in batteries. The latter power demand is needed when the vehicle is traversing up a slope at its maximum safe angle. This angle is approximately 30 degrees. The values for R_r and R_m are assumed unchanged (although, in reality they may vary considerably) and R_s increases to 11.5 pounds. Maximum roving power is also shown in Fig. V-8. Stall power is estimated as two and one-half times the average power or 308 watts. If vehicle speed on the maximum slope is also 1.0 ft/sec the maximum required locomotion power is 295 watts. Since this is very near stall conditions, vehicle speed must be lower than 1.0 ft/sec. We will assume this speed to be 0.75 ft/sec and the maximum power is then 220 watts.

The variables R_r and R_m have been estimated from empirical data as previously mentioned. Those data were compiled when little was known of the lunar soil characteristics. Much has been learned since then (Ref. V-7). It should now be possible to improve our confidence in the earlier measurements by theoretical analysis. A preliminary attempt at this has been started and, to date, the numbers assumed in previous paragraphs are still the best estimate.

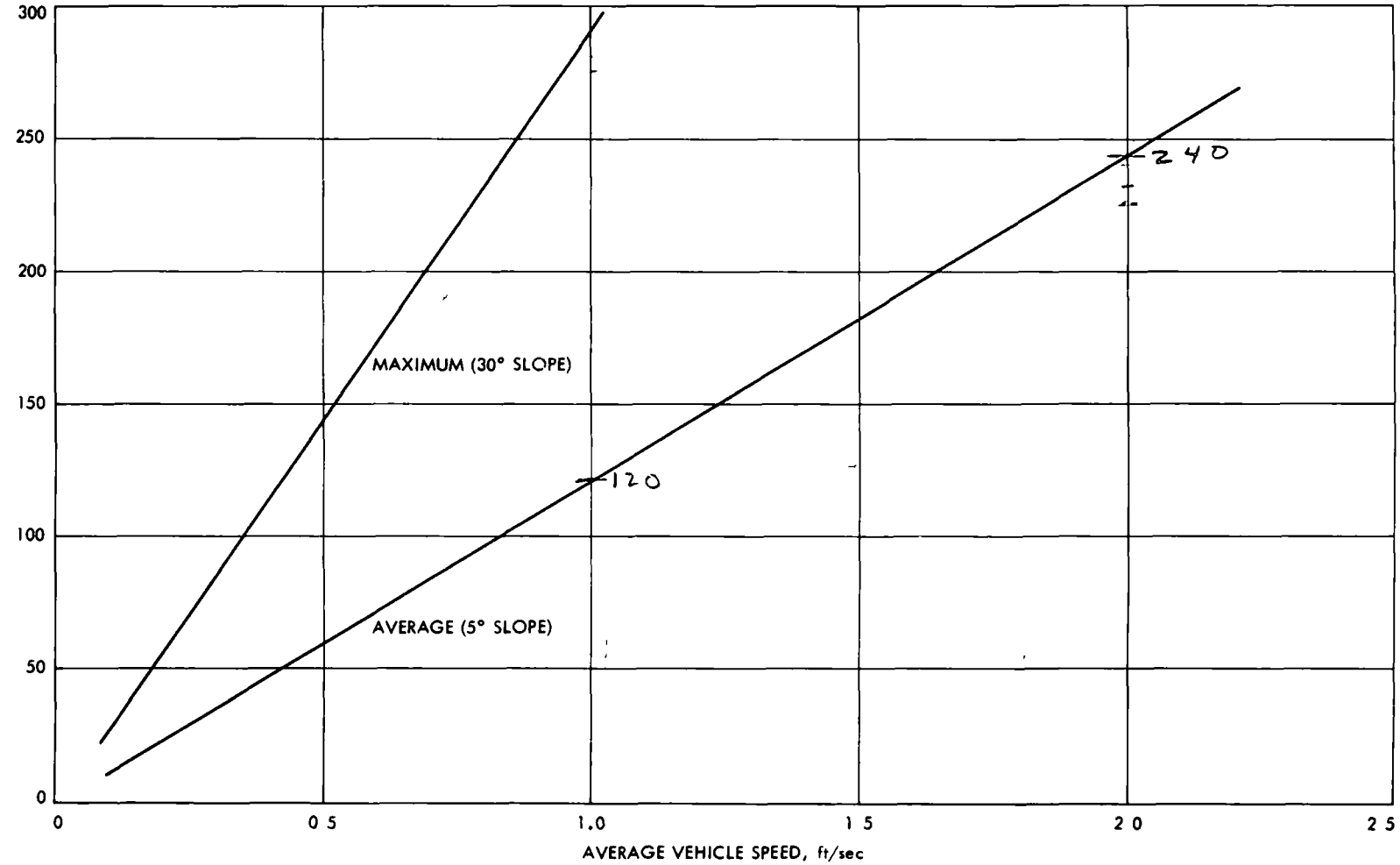

Figure V-8. Average and Maximum Locomotion Power Versus Average Vehicle Speed

(4) Estimated Total Power Requirements. In order to estimate total power requirements, it has been assumed that the average vehicle speed will be 1.0 ft/sec. Although this speed is slow, the limited power available makes much higher speeds impractical. (The faster the vehicle travels, the more time there is for investigations at stops.) However, Ref. V-6 indicates that 1.0 ft/sec should be fast enough to allow completion of the mission with adequate opportunity for investigations. The power consumed in vehicle locomotion at a speed of 1.0 ft/sec is 123 watts (see Fig. V-8). Table V-2 summarizes the estimates of total vehicle power demand. The power to many subsystems will be switched on and off as required while the locomotion subsystem will be turned off whenever the vehicle stops. The power to the transmitter power amplifier will be removed when the vehicle is moving. The TV, obstacle detection, ranging, and science equipment also share power. Aside from the advantage of reducing the peak power, this also equalizes the load profile resulting in a smaller power subsystem.

Power Subsystem Configuration. In Ref. V-6 three power subsystem configurations were mentioned as typical examples. The main difference between these was the power source. One subsystem derived power from a solar panel (either fixed with respect to the vehicle or movable and pointed to the sun). The second configuration utilized a radioisotope thermoelectric generator (RTG). The third was a combination of a panel and an RTG, each supplying half the average power. From a weight standpoint, all three approaches were competitive, with the last configuration holding the edge. However, RTG design factors have changed in the past year. Intact reentry of the radioisotope fuel appears to be a more difficult problem than earlier anticipated. This is reflected as increased RTG weight. Therefore, from a weight standpoint, the solar panel configuration now holds a decided advantage (Fig. V-9). The revised weight estimates are shown in Table V-3.

Table V-2. Estimated Raw Power Demand from Power Source

Power Demand	Vehicle Roving	Vehicle Stationary
Locomotion	123 w	–
Telecommunications		
Low power transmitter	18	–
High power transmitter	–	80 w
TV	–	12
Obstacle detection	10	–
Ranging	–	8
Control		
Articulation	3	3
Attitude sensing	5	5
Electronics	5	5
Power conditioning and battery charging	28	28
Science	–	50
Totals	192 w	191 w

Table V-3. Weight Summary for Power Subsystems

Subsystem	Solar	RTG	Solar + RTG
Panel (includes chargeable mast weight)	50 lb	–	25 lb
Battery	40	40 lb	40
RTG	–	222	111
Power conditioning and battery charging	20	23	23
Totals	110 lb	285 lb	198 lb

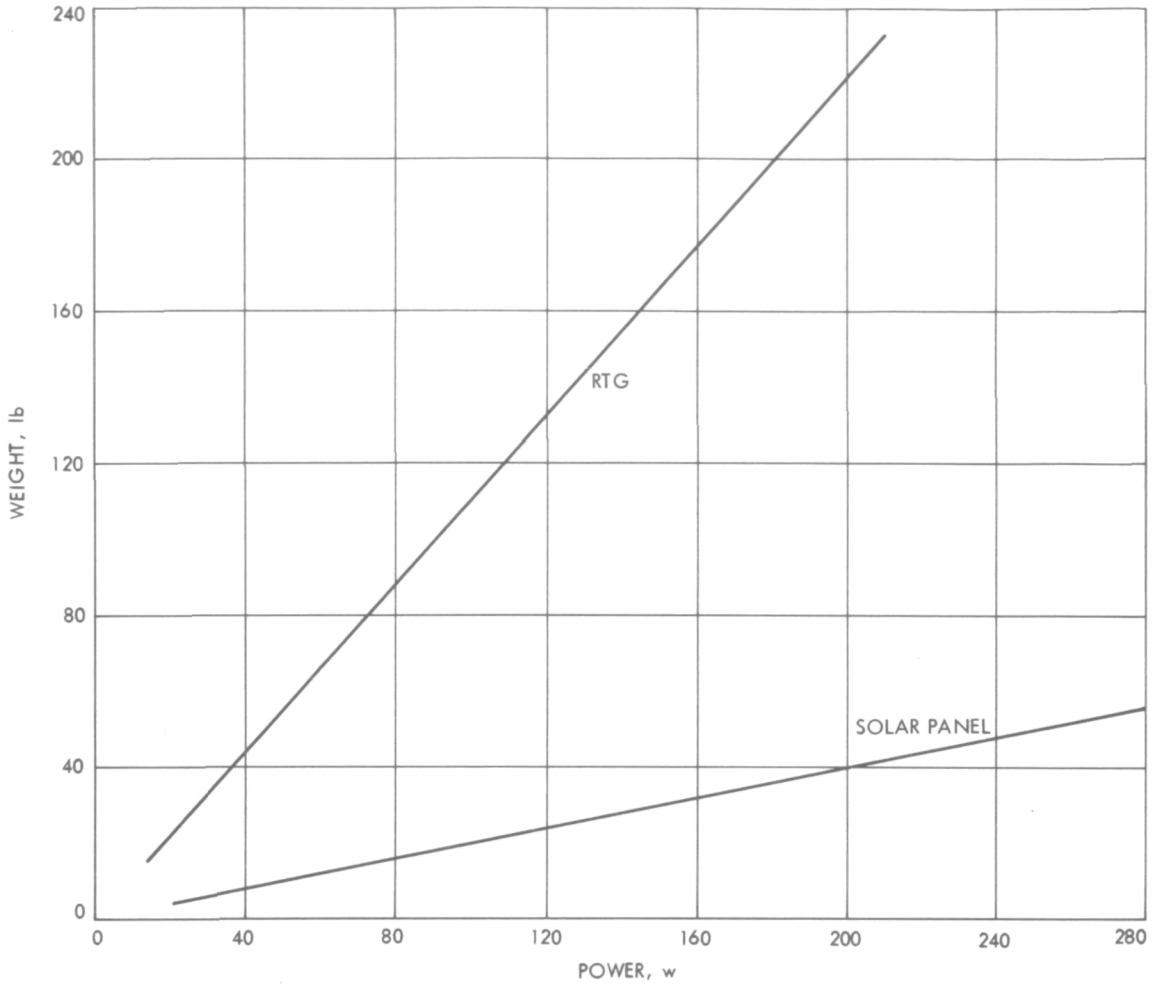

Figure V-9. Weight Versus Power for RTG and Solar Panel

Battery Size. The size of the battery is dictated by roving power requirements. Although peak power is demanded during terminal descent to the lunar surface, the time for which it is required is short. The terminal descent energy requirement is 300 w-hr and the roving requirement is 336 w-hr. The latter figure allows for one hour and thirty-five minutes of the following operations with the solar panel completely off the sun:

60 minutes of average operation	=	200 w-hr
30 minutes roving on a 30 degree slope	=	110
5 minutes in stall	=	26
Total	=	336 w-hr

Assuming a depth of discharge of 50 percent for the above condition and a Ni-Cd battery at 17 w-hr/lb, the battery weight is 40 pounds.

Although an allowance of 95 minutes of off-sun operation seems excessive it is justified, on the basis of two conditions that may be expected to arise on the lunar surface.

(1) Unusual or Hazardous Condition. First, if the LRV finds itself in shadow, it will probably be indicative of an unusual and hazardous situation. On the one hand, at high latitudes or when the sun is near the horizon, the LRV can easily get into shadow. The lunar slopes on which this can happen may be shallow and therefore not present a hazard to the vehicle. Moving out of such regions should not be difficult or time-consuming. On the other hand, in the lower latitudes and near the middle of the lunar day, if the LRV finds itself in shadow, it will have to be on a relatively severe slope away from the sun.

At these times, return of the LRV to a safe, lighted area may be a difficult dangerous, time-consuming task. Allotting one and one-half hours for this provides for a period of roving during which the rover should be able to cover about twice the distance of an average step. This should be sufficient if a sunlit area is within the view of the TV camera. As an added safety factor, the battery is sized for a 50 percent depth of discharge. If the situation warrants, most of the remaining energy can also be removed from the battery without serious harm to it.

(2) Solar Panel in Fixed Position During Steps. The second condition for estimating the energy storage capacity is based on the assumption that the solar panel will be fixed in position during each step. This is in the interests of reduced weight, power and complexity. As a result, over extensive portions of the traverse, the panel will not be optimally pointed toward the sun. Therefore, the battery will be subjected to repeated discharging and charging often throughout the mission. Battery life expressed as the number of charge-discharge cycles is a function of the depth of discharge (Ref. V-8). Therefore, it is desirable to limit the depth of discharge and to keep the charging current small (this also improves battery life expectancy). If, during a typical traverse step, the solar panel is 60 degrees off the sunline for 20 minutes, the battery will have to supply 33 watt/hr of energy. At a 10 percent depth of discharge the battery can be designed to survive approximately 7000-20000 cycles. Since the total traverse

will consist of 1000-5000 steps, increasing the depth of discharge much beyond 10 percent would degrade the reliability of the battery. This leads to the conclusion that the battery should have a capacity of at least 330 w-hr. The estimated capacity indicated earlier is very close to this value.

In summary, it can be anticipated that the battery will be discharged to about 90 percent of its capacity during each step. Whenever the solar panel is delivering peak or near peak power, the battery will be recharged. In a few unusual circumstances, the battery can be deeply discharged, if necessary, without appreciably shortening its life.

E. TELECOMMUNICATIONS SUBSYSTEM

The telecommunications consist of three interconnected subsystems (Fig. V-10) which provide command reception and decoding, telemetry signal processing, RF transmission, two-way coherent doppler tracking and LRV-to-Earth base range determination. These subsystems are:

(1) Radio Frequency Subsystem that provides RF transmission and reception.

(2) Flight Command Subsystem that provides decoding logic functions for all Earth commands.

(3) Flight Telemetry Subsystem that provides commutation, analog-to-digital conversion, and modulation functions for processing of analog, digital, and video (TV) data channels.

1. Radio Frequency Subsystem (RFS)

The RFS provides a two-way communication link between the LRV and DSN tracking stations throughout the mission. RFS receives command signals transmitted from DSN stations to the LRV and transmits signal data from the LRV to DSN tracking stations during launch, injection, transit, landing and lunar operations. The RFS consists of a transponder (RF receiver and RF transmitter), power amplifiers, telecommunications antennas, and appropriate switching.

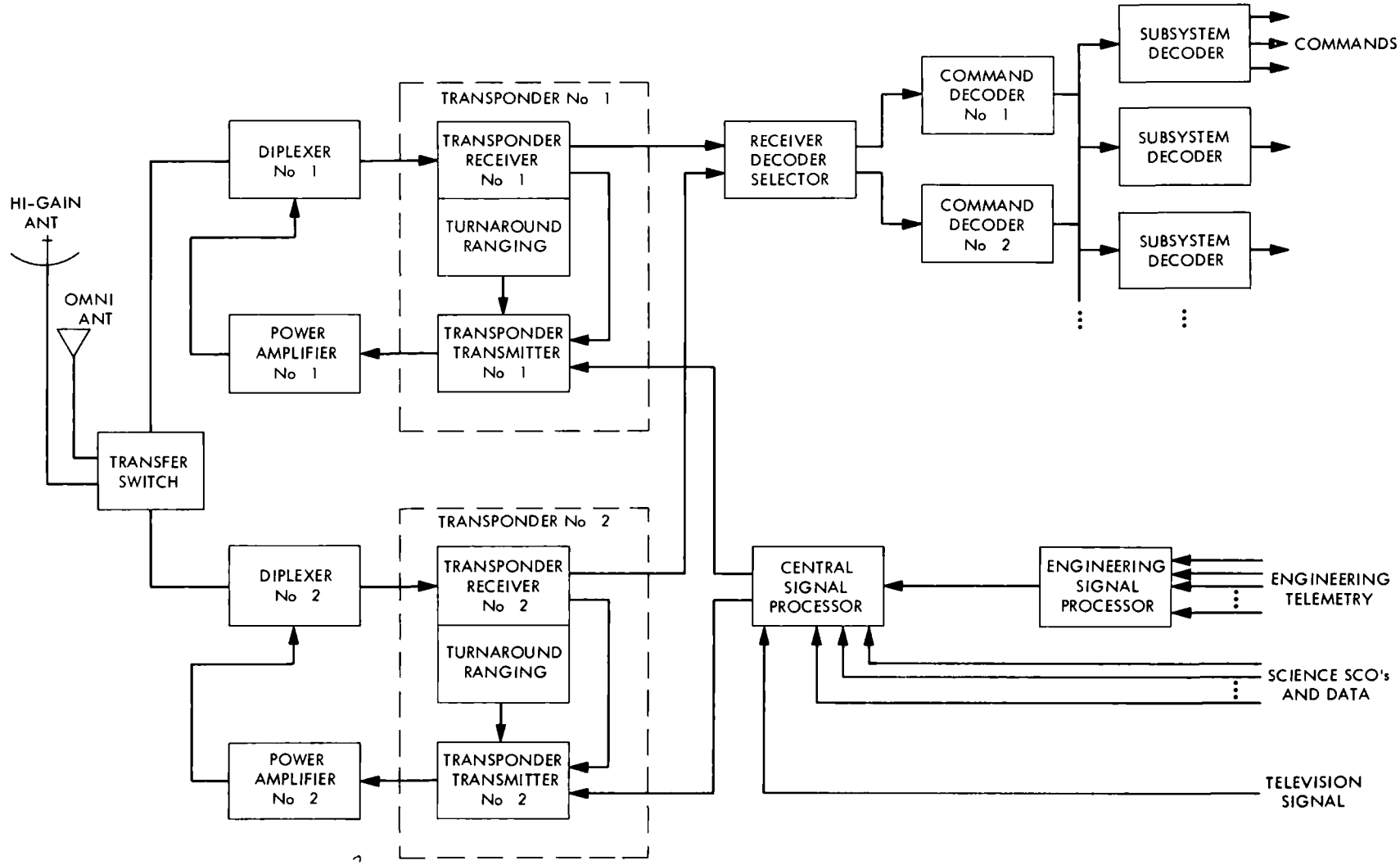

Figure V-10. LRV Telecommunications Block Diagram

Transponder. The S-band transponder provides the functions of a double superheterodyne command receiver, a phase-coherent transponder, a turnaround ranging transponder, and a telemetry transmitter. It employs three loops as shown on the block diagram of Fig. V-11. These loops are the ranging, automatic gain control (AGC), and automatic phase control (APC) loops. In the absence of a received signal from the DSN, the spacecraft telemetry information is modulated on an RF signal whose frequency is controlled by an auxiliary oscillator. When a signal from the DSN is present in the transponder receiver, the APC loop will lock to it, and AGC voltage is developed in the AGC loop. This voltage, besides controlling the receiver gain for proper operation, also produces a command voltage which turns off the auxiliary oscillator and causes the VCO to be switched to the transmitter input in its place. In this manner, closing the APC loop provides an exact ratio of 240/221 between the transmitted and received frequencies. In addition, the AGC voltage is telemetered to provide received signal strength information. The signal received from the DSN may have either ranging information or command information phase modulated on it. The second mixer provides two outputs, one to the broad-band ranging channel. The ranging code is demodulated, filtered, limited, and remodulated onto the transmitted signal along with the telemetry. The command information is demodulated by the phase detector in the narrow-band channel.

The transponder considered above is of a unique class in that it provides for a turnaround ranging capability that is compatible with the NASA-DSN tracking stations. This type of ranging transponder has been used previously on such programs as Mariner, Lunar Orbiter, and Apollo. The Surveyor transponder was not considered for the LRV since it does not have ranging capabilities.

Telecommunications Antennas. At this time it appears that the LRV requirements can be met with the use of two telecommunications antennas (single and dual omnidirectional antenna are being considered); one omnidirectional antenna system for command reception, transmission of low data rate telemetry, and turnaround ranging, and one high gain directional antenna for transmission of high-speed telemetry and video data.

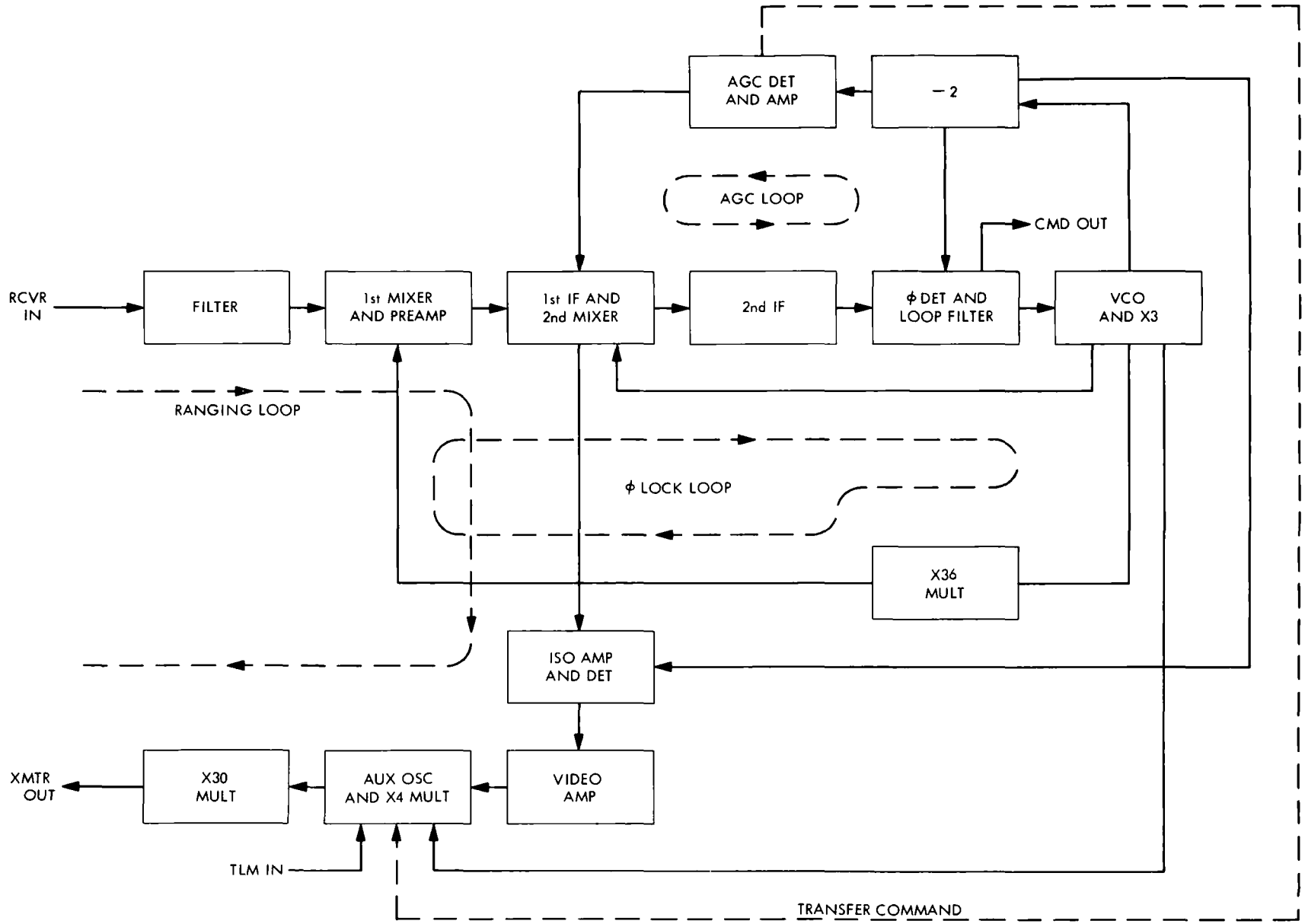

Figure V-11. S-band Ranging Transponder Block Diagram

(1) Low-Gain Antenna. The single low-gain antenna would be located at the top of the solar panel supporting mast with its axis coincident with the positive Z axis of the spacecraft. Therefore the beam axis will be displaced from the local vertical by an angle equal to the slope on which the vehicle is resting. Figure V-12 is a typical low-gain antenna pattern based on a modified Mariner 69 antenna. Since a mission requirement is for the vehicle to operate anywhere on the visible face of the moon, hemispheric coverage is required. It is also required that the vehicle operate on slopes of up to 20 degrees. These two requirements coupled with the antenna pattern of Fig. V-12 produce an antenna gain for the low-gain antenna of never less than -8 db. It should be noted this is worst case and a nominal mission would allow about 10 db additional gain.

(2) High-Gain Antenna. The high-gain antenna is a parabolic reflector mounted on one edge of the solar panel and providing a nominal gain of 12 db and a 1 db beamwidth of 22 degrees.

An automatic pointing scheme is suggested that requires no ground commands. When the vehicle comes to rest the solar panel is accurately positioned with the aid of sun sensors. Since the earth-probe-sun angle is known the antenna is positioned relative to the solar panel so that this angle is the displacement of the antenna beam from the sun line. The solar panel antenna assembly is then rotated about the sun line until the antenna is pointing at the Earth. Earth sensing is derived from the AGC voltage of the receiver that is connected to the high-gain antenna.

Ranging Link Analysis. Table V-4 presents a telecommunication design control table summarizing the performance of the transponder ranging mode. The analysis is based on an uplink configuration including an 85-foot antenna and 10-kilowatt transmitter on the ground to the low-gain receiving antenna on the LRV. The downlink is composed of the low gain transmitting antenna and a 20-watt RF power amplifier on the LRV, and an 85-foot ground receiving antenna. The nominal performance margin at lunar distance was found to be about 25 db.

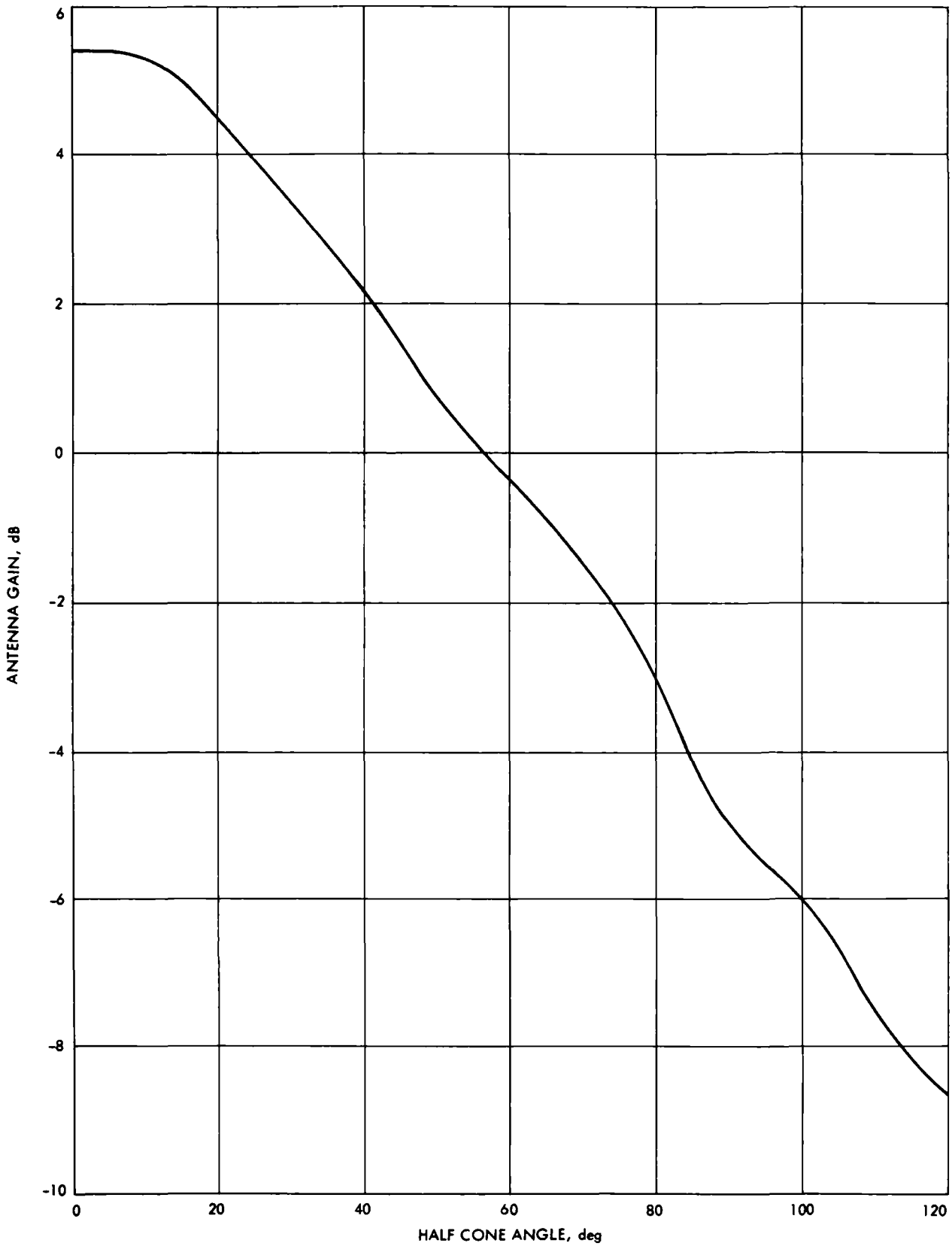

Figure V-12. Low-Gain Antenna Pattern

Table V-4. Telecommunication Design Control Table (Ranging Mode) (Sheet 1 of 3)

CHANNEL: Ranging Link
MODE: N/A

Item No.	Parameter	Value	Tolerance
A.	Earth-to-spacecraft channel:		
1	Transmitter RF power output	70.00 dbm	+0.50 -0.00 db
2	Transmitting system circuit loss	-0.40 db	+0.1 -0.1 db
3	Transmitting antenna gain	51.00 db	+1.0 -0.5 db
4	Transmitting antenna pointing loss	0.0 db	+0.0 -0.0 db
5	Space loss	-211.138 db	+0.0 -0.2 db
	Frequency = 2.113×10^3 mc		
	Range = 0.407×10^6 km		
6	Polarization loss	0.0 db	+0.0 -0.0 db
7	Receiving antenna gain	-5.0 db	+3.0 -3.0 db
8	Receiving antenna pointing loss	0.0 db	+0.0 -0.0 db
9	Receiving system circuit loss	-3.3 db	+0.0 -0.7 db
10	Received signal power	-98.84 dbm	+4.6 -4.5 db
11	Receiving system noise spectral density	-164.29 dbm/cps	+2.12 -1.11 db
	Receiving system noise temp	2700°K	+1700 -610 °K
12	Received signal power/ receiving system noise spectral density	65.45 db-cps	+5.71 -6.62 db

Table V-4. Telecommunication Design Control Table (Ranging Mode) (Sheet 2 of 3)

CHANNEL: Ranging Link MODE:			
Item No.	Parameter	Value	Tolerance
Carrier			
13	P(carrier)/P(transmitted)	9.0 db	+1.26 -1.51 db
14	APC loop noise bandwidth	13.0 db-cps	–
15	Required SNR (for ranging)	6.0	–
16	Carrier performance margin	37.45 db	+6.97 -8.13 db
Ranging channel			
17	P(ranging)/P(transmitted)	-0.59 db	+0.18 -0.22 db
18	Noise bandwidth (2 mc 3 db BW)	63.46 db-cps	+0.70 -0.58 db
19	SNR (at video limiter input)	1.40 db	+6.47 -7.54 db
B. Spacecraft-to-Earth channel:			
1	Transmitting RF power output	43.00 dbm	+1.0 -0.4 db
2	Transmitting system circuit loss	-2.3 db	+0.0 -0.22 db
3	Transmitting antenna gain	-5.0 db	+3.0 -3.0 db
4	Transmitting antenna pointing loss	0.0 db	+0.0 -0.0 db
5	Space loss Frequency = 2.295×10^3 mc Range = 0.407×10^6 km	-211.856 db	+0.0 -0.2 db
6	Polarization loss	0.0 db	+0.0 -0.0 db
7	Receiving antenna gain	53.0 db	+1.0 -0.5 db

Table V-4. Telecommunication Design Control Table (Ranging Mode) (Sheet 3 of 3)

CHANNEL: Ranging Link
MODE:

Item No.	Parameter	Value	Tolerance
8	Receiving antenna pointing loss	0.0 db	+0.0 -0.0 db
9	Receiving system circuit loss	-0.18 db	+0.05 -0.05 db
10	Received signal power	-123.34 dbm	+5.05 -4.17 db
11	Receiving system noise spectral density	-176.43 dbm/cps	+0.84 -1.04 db
	Receiving system noise temp	165°K	+35 -35°K
12	Received signal power/ receiving system noise spectral density	53.09 db-cps	+6.09 -5.01 db
Carrier			
13	P(carrier/P(transmitted)	-10.00 db	+1.0 -1.0 db
14	APC loop noise bandwidth	10.79 db-cps	
15	APC loop required SNR (for ranging)	6.0 db	—
16	Performance margin	26.3 db	+7.59 -6.01 db
Ranging channel			
17	P(limiter output)/ P(transmitted)	-11.02 db	+0.93 -1.03 db
18	P(ranging)/P(limiter output)	-1.30 db	+1.28 -5.30 db
19	P(clock)/P(ranging)	-11.96 db	
20	Clock APC loop noise bandwidth 0.8 Hz	-0.97 db-cps	+0.0 -0.97 db
21	Clock APC loop required SNR	6.0 db	—
22	Performance margin	+23.78 db	+9.27 -11.34 db

2. Flight Command Subsystem (FCS)

The basic functions of the LRV FCS are:

(1) Accept a command subcarrier from the LRV receiver.

(2) Demodulate the command subcarrier and receive the digital command information.

(3) Provide timing, decoding of the digital command information and perform error detection.

(4) Issue commands in a form suitable for execution by the appropriate LRV subsystems.

Command Control. The nature of the mission to be performed by the LRV is such that it requires initial control of each step by command from Earth. The LRV command subsystem will be exercised to a great extent throughout the vehicle lifetime. In choosing a command subsystem it is therefore important to make sure that its operation will not place any limitations on the performance of the mission. The command parameters that are most important to the LRV operation are the command word time, the command word error rate, and the operational complexity involved in sending a command.

Command Time. Since the mission consists of many discrete steps and each step may require several commands, it is important to keep the command time short to minimize mission time. It is anticipated that no provisions will be made for the verification of correct command reception through the telemetry system prior to command execution. Because of Earth-Moon propagation times and decommutation delays such verification would add significantly to mission time. It is therefore important that a command be received correctly on the first try, both to minimize mission time and to increase operation confidence. Finally, because the command function is to be exercised so often the procedure for sending commands must be made as simple as possible.

Command Link Analysis. Table V-5 contains a design control table for a representative LRV command link. The table is based on a noncoherent FSD link such as that used for Surveyor. It has been shown that a coherent PSK command channel such as that used for Mariner could provide an improvement of about 15 db.

Table V-5. Telecommunication Design Control Table
(Command Link)

CHANNEL: Command Link
MODE: Uplink, DSN 10 kw, 85 ft

Item No.	Parameter	Value	Tolerance, db
1	Total transmitter power 10 kw	70.0 dbm	+0.5 -0.0
2	Transmitting circuit loss	-0.4 db	+0.1 -0.1
3	Transmitting antenna gain 85 ft	51.0 db	+1.0 -0.5
4	Transmitting antenna pointing loss	0.0 db	+0.0 -0.0
5	Space loss at 2113 mc, R = 407000 km	-211.138 db	+0.0 -0.2
6	Polarization loss	0.0 db	+0.0 -0.0
7	Receiving antenna gain	-5.0 db	+3.0 -3.0
8	Receiving antenna pointing loss	0.0 db	+0.0 -0.0
9	Receiving circuit loss	-3.3 db	+0.0 -0.7
10	Net circuit loss	-168.84 db	+4.1 -4.5
11	Total received power	-96.84 dbm	+4.6 -4.5
12	Receiver noise spectral density (N/B) T system = 2700°K	-164.29 dbm/Hz	+2.12 -1.11
13	Carrier modulation loss	-6.83 db	+1.56 -1.96
14	Received carrier power	-105.67 dbm	+8.28 -7.57
Data channel			
15	Modulation loss	-1.1 db	+1.0 -1.0
16	Received data subcarrier power	-99.94 dbm	+5.6 -5.5
17	Bit rate (1/T) 100 bps	20 db	—
18	Required ST/N/B	29.9 db	+1.0 -1.0
19	Threshold subcarrier power	-114.39 dbm	+3.12 -2.11
20	Performance margin	14.45 db	+8.72 -7.61

Design Control Table is based on Surveyor Link Parameters

3. Flight Telemetry Subsystem (FTS)

The FTS gathers engineering and science instrumentation signals from various subsystems and provides the appropriate signal conditioning. The FTS comprises the engineering signal processor and a central signal processor.

Engineering Signal Processor. The engineering signal processor processes data from the LRV and in conjunction with the central signal processor, converts it to a suitable form preparatory to being transmitted to Earth. This processor handles all data required to assess the performance of the basic bus (engineering data).

The engineering signal processor is comprised of the following major components: commutators, current sources (thermal measurements), a command enable and reject channel, accelerometer channel (if required), and a gyro speed channel for the inertial reference subsystem that is required during transit between the Earth and the lunar surface.

The engineering signal processor contains a commutator capable of several modes of operation for priority type engineering data as a function of mission phase (i.e., launch, transit maneuvers and cruising, and lunar roving).

Central Signal Processor. The central signal processor combines the outputs of the engineering signal processor and other units. These signals are processed and sent to the frequency or phase modulation inputs of the transmitter. The subsystem has the capacity for handling analog data and converting it to digital data for subsequent transmission. Synchronizing patterns, parity digits, and timing signals for controlling commutators are generated in the central signal processor.

Telemetry Link Analysis. Four basic telemetry modes result from use of the four antenna-power amplifier combinations. These combinations are high-power and high-gain, low-power and high-gain, high-power and low-gain, and low-power and low-gain.

(1) High-power and High-gain Telemetry Mode. This mode provides the highest available gain-power product at the cost of a high raw-power requirement and a requirement for antenna pointing. This mode will be used

for transmission of high resolution television pictures and high speed science data while the vehicle is stationary. As can be seen in Table V-6 and Figure V-13, this mode can provide data transmission at 400 kbps or transmission of a 600 line high resolution television picture in about 5 seconds.

(2) Low-power and High-gain Telemetry Mode. This mode provides a moderately high data rate for transmission of science and engineering telemetry when the vehicle is stationary and power limited, such as during operation of some of the science experiments. The design control table of Table V-7 demonstrates the feasibility of a 10 kbps data rate for this mode.

(3) High-power and Low-gain Telemetry Mode. This mode, as does the preceding one, provides a moderately high data rate. The main purpose of this mode is to provide low-resolution television transmission when it is inconvenient to position the high-gain antenna. Table V-8 demonstrates that a bit rate of 10 kbps is feasible. From Figure V-13 one can see that a 200 line low-resolution television picture can be transmitted in about 20 seconds.

(4) Low-power and Low-gain Telemetry Mode. While the vehicle is in motion a low-data rate telemetry mode is provided by a 500-milliwatt transmitter and an omnidirectional antenna. A telecommunications design control table that summarizes the link parameters and approximate capabilities is presented in Table V-9.

As with the high-data rate mode, coherent PSK modulation is assumed. The approximate upper bound link capability for this mode is 300 bps with an error probability of 10^{-3}.

Telecommunications Weight and Power Estimates. An example of telecommunications weight and power estimates, as derived from a typical Surveyor spacecraft and the subsystem block diagram of Figure V-10, is given in Table V-10.

Table V-6. Telecommunication Design Control Table
(High-power and High-gain) (Sheet 1 of 2)

CHANNEL: Telemetry Link, 400K bps
MODE: Downlink, High Gain Antenna, 20 watt Transmitter

Item No.	Parameter	Value	Tolerance, db
1	Total transmitter power 20 watts	43 dbm	+1.0 -0.4
2	Transmitting circuit loss	-2.3 db	+0.0 -0.22
3	Transmitting antenna gain	12 db	+0.5 -0.5
4	Transmitting antenna pointing loss	0.0 db	+0.0 -0.0
5	Space loss at 2295 mc, $r = 40.7 \times 10^4$ km	-211.856 db	+0.0 -0.2
6	Polarization loss	0.0 db	+0.0 -0.0
7	Receiving antenna gain	53.0 db	+1.0 -0.5
8	Receiving antenna pointing loss	0.0 db	+0.0 -0.0
9	Receiving circuit loss	-0.18 db	+0.05 -0.05
10	Net circuit loss	-149.34 db	+1.55 -1.97
11	Total received power	-106.34 dbm	+2.55 -1.67
12	Receiver noise spectral density (N/B) T System = 165 ±35°K	-176.43 dbm/Hz	+0.84 -1.04
13	Carrier modulation loss	-10 db	+1.0 -1.0
14	Received carrier power	-116.34 dbm	+3.55 -2.67
15	Carrier APC noise BW ($2B_{LO}$ = 12 cps)	10.79 db	+0.0 -0.5

Table V-6. Telecommunication Design Control Table
(High-power and High-gain) (Sheet 2 of 2)

CHANNEL: Telemetry Link, 400K bps
MODE: Downlink, High Gain Antenna, 20 watt Transmitter

Item No.	Parameter	Value	Tolerance, db
Carrier performance			
16	Threshold SNR in $2B_{LO}$	43.30 db	+0.0 -0.0
17	Threshold carrier power	-122.34 dbm	+0.84 -1.54
18	Performance margin	+6.0 db	+5.09 -3.51
Data channel			
19	Modulation loss	-0.9 db	+0.0 -1.0
20	Received data subcarrier power	-107.24 dbm	+2.55 -2.67
21	Bit rate (1/T)	400 KB/S	—
22	Required ST/N/B	7.0 db	+0.2 -0.2
23	Threshold subcarrier power	-113.24 dbm	+1.04 -1.24
24	Performance margin	+6.0 db	+3.79 -3.71
Sync channel			
25	Modulation loss	-20 db	+1.0 -1.0
26	Receiver SYNC subcarrier power	-126.34 dbm	+3.55 -2.67
27	SYNC APC noise BW ($2B_{LO}$ = 0.5)	-3 db	+0.4 -0.4
28	Threshold SNR in $2B_{LO}$	+13.5 db	+0.5 -0.5
29	Threshold subcarrier power	-167.93 db	+1.74 -1.94
30	Performance margin	+41.59 db	+4.41 -5.49

Design Control Table is based on Surveyor Link Parameters.

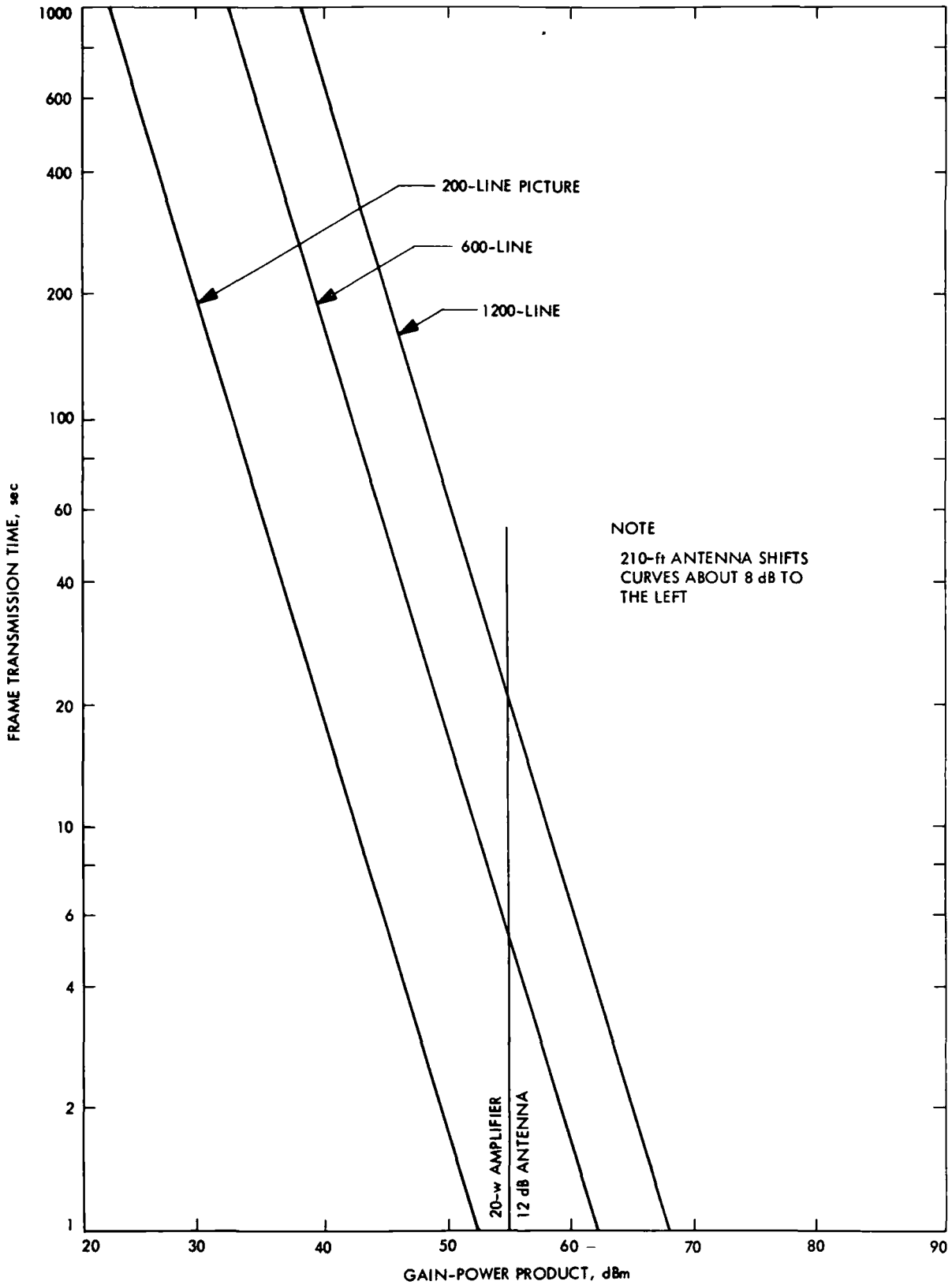

Figure V-13. Frame Transmission Time Versus Gain Power Product

Table V-7. Telecommunication Design Control Table
(Low-power and High-gain) (Sheet 1 of 2)

CHANNEL: Telemetry Link, 10K bps
MODE: Downlink, High Gain Antenna, 0.5 watt Transmitter

Item No.	Parameter	Value	Tolerance, db
1	Total transmitter power 0.5 watt	27 dbm	+1.0 -0.4
2	Transmitting circuit loss	-2.3 db	+0.0 -0.22
3	Transmitting antenna gain	12.0 db	+0.5 -0.5
4	Transmitting antenna pointing loss	0.0 db	+0.0 -0.0
5	Space loss at 2295 mc, $r = 40.7 \times 10^4$ km	-211.856 db	+0.0 -0.2
6	Polarization loss	0.0 db	+0.0 -0.0
7	Receiving antenna gain	53.0 db	+1.0 -0.5
8	Receiving antenna pointing loss	0.0 db	+0.0 -0.0
9	Receiving circuit loss	-0.18 db	+0.05 -0.05
10	Net circuit loss	-149.34 db	+1.55 -1.97
11	Total received power	-122.34 dbm	+2.55 -1.67
12	Received noise spectral density (N/B) T system = 165 ±35°K	-176.43 dbm/Hz	+0.84 -1.04
13	Carrier modulation loss	-10.0 db	+1.0 -1.0
14	Received carrier power	-132.34 dbm	+3.55 -2.67
15	Carrier APC noise BW ($2B_{LO}$ 12 cps)	10.79 db	+0.0 -0.5

Table V-7. Telecommunication Design Control Table
(Low-power and High-gain) (Sheet 2 of 2)

CHANNEL: Telemetry Link, 10K bps
MODE: Downlink, High Gain Antenna, 0.5 watt Transmitter

Item No.	Parameter	Value	Tolerance, db
Carrier performance			
16	Threshold SNR in $2B_{LO}$	27.30 db	+0.0 -0.0
17	Threshold carrier power	-138.34 dbm	+0.84 -1.54
18	Performance margin	+6.0 db	+5.09 -3.51
Data channel			
19	Modulation loss	-0.9 db	+0.0 -1.0
20	Received data subcarrier power	-123.24 dbm	+2.55 -2.67
21	Bit rate (1/T)	10 KB/S	—
22	Required ST/N/B	7.0 db	+0.2 -0.2
23	Threshold subcarrier power	-129.43 dbm	+1.04 -1.24
24	Performance margin	+6.19 db	+3.79 -3.71
Sync channel			
25	Modulation loss	-20 db	+1.0 -1.0
26	Receiver SYNC subcarrier power	-142.34 db	+3.55 -2.67
27	SYNC APC noise BW ($2B_{LO}$ = 0.5)	-3.0 db	+0.4 -0.4
28	Threshold SNR in $2B_{LO}$	+13.5 db	+0.5 -0.5
29	Threshold subcarrier power	-167.93 db	+1.74 -1.94
30	Performance margin	+25.59 db	+4.41 -5.49

Design Control Table is based on Surveyor Link Parameters.

Table V-8. Telecommunication Design Control Table
(High-power and Low-gain) (Sheet 1 of 2)

CHANNEL: Telemetry Link, 10K bps
MODE: Downlink, Low Gain Antenna, 20 watt Transmitter

Item No.	Parameter	Value	Tolerance, db
1	Total transmitter power 20 watt	43 dbm	+1.0 -0.4
2	Transmitting circuit loss	-2.3 dbm	+0.0 -0.22
3	Transmitting antenna gain	-3.0 db	+3.0 -3.0
4	Transmitting antenna pointing loss	0.0 db	+0.0 -0.0
5	Space loss at 2295 mc, R = 40.7 x 10^4 km	-211.856 db	+0.0 -0.2
6	Polarization loss	0.0 db	+0.0 -0.0
7	Receiving antenna gain	53.0 db	+1.0 -0.5
8	Receiving antenna pointing loss	0.0 db	+0.0 -0.0
9	Receiving circuit loss	-0.18 db	+0.05 -0.05
10	Net circuit loss	-164.34 db	+4.05 -3.97
11	Total received power	-121.34 dbm	+5.05 -4.37
12	Receiver noise spectral density (N/B) T system = 165 ±35°K	-176.43 dbm/Hz	+0.84 -1.04
13	Carrier modulation loss	-10.0 db	+1.0 -1.0
14	Received carrier power	-131.34 dbm	+6.05 -5.37
15	Carrier APC noise BW ($2B_{LO}$ = 12 cps)	10.79 db	+0.0 -0.5

Table V-8. Telecommunication Design Control Table
(High-power and Low-gain) (Sheet 2 of 2)

CHANNEL: Telemetry Link, 10K bps
MODE: Downlink, Low Gain Antenna, 20 watt Transmitter

Item No.	Parameter	Value	Tolerance, db
Carrier performance			
16	Threshold SNR in $2B_{LO}$	27.30 db	–
17	Threshold carrier power	-138.34 db	+0.84 -1.54
18	Performance margin	+7.0 db	+7.59 -6.21
Data channel			
19	Modulation loss	-0.9 db	+0.0 -1.0
20	Received data subcarrier power	-122.24 db	+5.05 -5.37
21	Bit rate (1/T)	10 K bps	–
22	Required ST/N/B	7.0 db	+0.2 -0.2
23	Threshold subcarrier power	-129.43 db	+1.04 -1.24
24	Performance margin	+7.19 db	+6.29 -6.41
Sync channel			
25	Modulation loss	-20 db	+1.0 -1.0
26	Receiver SYNC subcarrier power	-141.34 dbm	+6.05 -5.37
27	SYNC APC noise BW ($2B_{LO}$ = 0.5 Hz)	-3.0 db	+0.4 -0.4
28	Threshold SNR in $2B_{LO}$	+13.5 db	+0.5 -0.5
29	Threshold subcarrier power	-167.93 db	+1.74 -1.94
30	Performance margin	+26.59 db	+7.79 -7.31

Design Control Table is based on Surveyor Link Parameters.

Table V-9. Telecommunication Design Control Table
(Low-power and Low-gain) (Sheet 1 of 2)

CHANNEL: Telemetry Link, 300 bps
MODE: Downlink, Low Gain Antenna, 0.5-watt Transmitter

Item No.	Parameter	Value	Tolerance, db
1	Total transmitter power 0.5 watt	27 dbm	+1.0 -0.4
2	Transmitting circuit loss	-2.3 dbm	+0.0 -0.22
3	Transmitting antenna gain	-3.0 db	+3.0 -3.0
4	Transmitting antenna pointing loss	0.0 db	+0.0 -0.0
5	Space loss at 2295 mc, $R = 4.07 \times 10^4$ km	-211.856 db	+0.0 -0.2
6	Polarization loss	0.0 db	+0.0 -0.0
7	Receiving antenna gain	53.0 db	+1.0 -0.5
8	Receiving antenna pointing loss	0.0 db	+0.0 -0.0
9	Receiving circuit loss	-0.18 db	+0.05 -0.05
10	Net circuit loss	-164.34 db	+4.05 -3.07
11	Total received power	-137.38 dbm	+5.05 -4.37
12	Receiver noise spectral density (N/B) T system = 165 ±35°K	-176.43 dbm/Hz	+0.84 -1.04
13	Carrier modulation loss	-10 db	+1.0 -1.0
14	Received carrier power	-147.38 dbm	+6.05 -5.37
15	Carrier APC noise BW ($2B_{LO}$ = 12 cps)	10.79 db	+0.0 -0.5

Table V-9. Telecommunication Design Control Table
(Low-power and Low-gain) (Sheet 2 of 2)

CHANNEL: Telemetry Link, 300 bps
MODE: Downlink, Low Gain Antenna, 0.5-watt Transmitter

Item No.	Parameter	Value	Tolerance, db
Carrier performance			
16	Threshold SNR in $2B_{LO}$	12.47 db	—
17	Threshold carrier power	-153.59 db	+0.84 -1.54
18	Performance margin	+6.21 db	+7.59 -6.21
Data channel			
19	Modulation loss	-0.9 db	+0.0 -1.0
20	Received data subcarrier power	-138.28 db	+5.05 -5.37
21	Bit rate (1/T)	300 bps	—
22	Required ST/N/B	7.0 db	+0.2 -0.2
23	Threshold subcarrier power	-144.69 db	+1.04 -1.24
24	Performance margin	+6.41 db	+6.29 -6.41
Sync channel			
25	Modulation loss	-20 db	+1.0 -1.0
26	Receiver SYNC subcarrier power	-157.38 dbm	+6.05 -5.37
27	SYNC APC noise BW ($2B_{LO}$ = 0.5 Hz)	-3.0 db	+0.4 -0.4
28	Threshold SNR in $2B_{LO}$	+13.5 db	+0.5 -0.5
29	Threshold subcarrier power	-167.93 db	+1.74 -1.94
30	Performance margin	+9.55 db	+7.79 -7.31

Design Control Table is based on Surveyor Link Parameters.

Table V-10. Telecommunications Weight and Power Estimates

	Estimated Weight, lb	Required Power, watts
Radio frequency subsystem		
Transponder No. 1	3.88	1.41
Transponder No. 2	3.88	1.41
Power amplifier No. 1	5.00	63/5
Power amplifier No. 2	5.00	–
Transfer switch	0.88	–
Low-gain antenna	0.32	–
High-gain antenna	5.0	–
Flight command subsystem		
Central command decoder	5.87	1.83
Flight telemetry		
Central signal processor	5.81	1.53
Engineering signal processor	6.22	3.07
Totals	41.86	72.25/14.25

Note: Antenna positioning mechanisms are not included in the estimates.

F. MOBILITY

1. Mobility Requirements

In order to establish preliminary LRV mobility requirements, a review was first made of similar efforts on previous roving studies. It was found that these early studies (SLRV, LSSM, MOLAB) were all designed to operate over what was considered to be a conservative range of terrain requirements based on the then limited knowledge of lunar surface topography and physical characteristics. Recent data obtained by Lunar Orbiters and particularly Surveyors have greatly improved this knowledge. One can now classify the majority of the lunar surface as a desert of fairly compact fine sand (similar to beach sand) which is pocked generously with craters of all sizes and has rocks and debris sparsely strewn over the surface, mainly in the highlands and in the vicinity of the larger craters (cf. Section IV).

Roving Deficiencies. These data have served to refine the original roving requirements and to point out some of their deficiencies.

(1) Mobility in Soft Soil Original SLRV requirements for soft soil mobility have changed considerably. (The minimum friction soil modulus values, which were assumed as low as $K_\phi = 0.08$, have been found to have values approaching $K_\phi = 2.0$ to 3.0.)

(2) Soil Hardness and Slope. The relationship between soil hardness and slope indicated in the ELMS Lunar model for the LSSM studies is unconservative for slope climbing capability and power requirements and is being revised.

(3) Cohesion. Cohesion, originally neglected, is sufficient to be of major importance to roving vehicle design. ($C = 0.06$ to 0.26 psi)

(4) Obstacle and Crevasse Crossing. Obstacle and particularly crevasse crossing requirements are less severe than originally considered. (Exceptions may exist in the rough terrain of some of the highlands.)

These refinements have served to emphasize the need for desert-type mobility and, in particular, the ability to traverse sandy slopes of the order of 35 degrees (near angle of repose) formed by crater walls and to traverse intersecting craters.

With this perspective in mind, the preliminary mobility characteristics being considered for the LRV are defined in Table V-11.

Table V-11. Mobility Characteristic Estimates

Criteria	Estimates
1. Maximum slope capability (Affects. wheels, drive, wheelbase and tread)	30 to 35 degrees soft soil
2. Ground clearance (Affects· suspension, wheels, wheelbase, tread)	Straddle a 35 degree wedge formed by two intersecting crater walls
3. Maneuverability (Affects: wheels, suspension, steering, tread, wheelbase)	(a) Standard type turning radius 15 to 20 feet (b) Zero turn radius if possible by individual wheel steering to a 45 degree position (c) Front and rear steering (d) Reverse drive
4. Stability (Affects: wheel suspension, tread, wheelbase)	Approximately 40 to 45 degrees for traversing crater walls of soft soil and providing for some wheel sinkage
5. Obstacle capability (Affects: wheel, suspension, wheelbase, tread)*	8 to 10 inches (one wheel) 5 to 6 inches (two wheels)
6. Crevasse capability	12 to 15 inches (not critical)
7. Roving route capability** (drag, torque, power)	
(a) General slopes	5 to 10 degrees continuous over route
(b) Local slopes	20 percent of route assumed to be 30 degree crater walls
(c) Other: (Local roughness, obstacles, steering, tire, shock absorber)	35 percent of (7. (a) + 7. (b))

*A preliminary review of lunar topography indicates that the single and two-wheel obstacles should have separate criteria.
**These are initial estimates for typical roving mission studies. Refined requirements will consider a statistical approach to a spectrum of roving missions on the lunar surface.

2. Mobility Performance

The following paragraphs present the preliminary analysis of the ability of the LRV design to meet the requirements previously discussed. It should be emphasized that these initial mobility studies pointed out the inadequacy or lack of analytical tools for off-road mobility design. This seems particularly true in the desert type of mobility required for the Moon. For example, no generally accepted analytical methods seem available for determining maximum slope climbing capability on sandy slopes. Here, we even lack the information to adequately define the depth of penetration of a loaded wheel on highly-sloped sandy surfaces, which probably should be amenable to straightforward analytical solution.

Off-road Mobility Review. In order to understand this limited analytical development in this field, a review was made of the major industrial and military efforts concerned with off-road mobility. It was found that there has been considerable effort in this area, mainly sponsored by the Army. However, these efforts started with rough analytical methods and then depended heavily on experimental testing for new developments (which is quite simple on Earth).

The early lunar studies thus merely extended this Earth approach to lunar vehicles using the same limited analytical tools available. These studies also depended heavily on Earth tests for the lunar vehicle development. This dependence on testing has probably been economical for the development of Earth vehicles. However, for the Moon, it presents a costly and complicated test program involving simulation which usually has undesirable technical limitations, such as those attending tests in airplanes simulating lunar gravity. As has been proven in many engineering development and particularly aerospace programs, analytical tools are of primary importance to assure adequate design and maximize benefits, from difficult and costly testing programs.

Mobility Problems. To alliviate this technology gap, desert mobility problems are being investigated for the LRV in a combined analytical and experimental approach. The purpose of this effort is to develop reliable analytical mentods for use in the design of lunar and planetary roving vehicles. Problems to be investigated are as follows

(1) Wheel-soil interaction (loaded flexible wheel on sandy soil).

(2) Slope climbing capability of (1).

(3) Obstacle capability on slopes with flexible suspension and wheels.

(4) Steering on sandy slopes.

(5) Stability on sandy slopes.

Exploratory Analytical Tests. For the purposes of this study, some exploratory analytical approaches have been developed based on fundamental soil mechanics as presented in paragraph 3. To evaluate this method a few preliminary wheel-soil load-penetration tests are in progress. These tests apply wheel loads to representative lunar soils varying as follows:

(1) Wheel footprint shape and aspect ratio

(2) Slope of soil surface

(3) Orientation of the wheel relative to the surface slope. This testing program is discussed in Section V-O.

3. Analytical Approach

The evaluation of the mobility performance characteristics of the LRV design involves analytical methods to develop:

(1) Energy and power requirements

(2) Max slope climbing capability

(3) Obstacle climbing capability

(4) Crevasse crossing capability

(5) Wheel-drive torque and drag requirements

Wheel-soil Interaction. Fundamental to most of these performance characteristics is the wheel-soil interaction problem or model. This model determines the wheel sinkage into the soil and the corresponding permissible thrust at the wheel-soil surface interface. On rigid soils sinkage is eliminated and there is no problem. However, in soft soils similar to the lunar desert conditions, the sinkage and thrust are critical to the entire performance analyses; particularly on sloped surfaces where the soil is near its angle of repose (similar to sand dune or crater slopes on Earth).

(1) Review of SLRV, LSSM, and MOLAB Analytical Methods. For this reason, a review was made of the analytical methods of previous wheeled lunar rover studies (SLRV, LSSM, MOLAB). It was found that they were generally based on adaptations of the Bekker (Land Locomotion Lab) approach. This approach assumes a combined frictional-cohesive soil (which seems appropriate for the lunar conditions) as a basis for the following wheel-soil equations·

Wheel Sinkage Equation

$$P = \left(\frac{K_c}{b} + K_\phi\right) z^n = (K)\, zn$$

where

K_c = cohesion mod of deformation
K_ϕ = friction mod of deformation
P = pressure
z = sinkage
n = soil exponential coefficient
b = width of wheelprint

Tractive Force Equation (soil thrust)

$$H = (AC + W \tan \phi)\left[1 - \frac{K}{sl}\left\{-\exp\left(1 - \frac{sl}{K}\right)\right\}\right]$$

where

H = soil thrust
A = area of cohesion
C = coefficient of cohesion
W = weight
ϕ = friction angle of soil
s = slip
l = length of wheelprint

It should be noted that these equations were developed for horizontal surfaces only. Slope effects on the soil properties which affect the sinkage and soil thrust results considerably are not considered.

These earlier studies then based their mobility analysis upon Bekker's equations and designed their vehicles to meet the NASA ELMS lunar model specifications. This preliminary ELMS model assumed the soil as a purely frictional material with zero cohesion (K_c = O, C = O) which was considered conservative. This simplified the use of the Bekker equations, since it removed the cohesive term which presented some questions regarding analytical scaling from earth measurements and left the frictional term for which scaling from earth measurement to lunar "g" conditions is reasonably straightforward. At the same time, the ELMS model requirements presented an increasing soil hardness versus slope criterion which greatly minimized the problem of slope climbing on soft soil. The studies reviewed went one step further in this direction by completely omitting the slope effect on the soil properties of the soft soil performance analyses.

(2) Changes to LRV Analytical Methods. Conditions for the LRV study are considerably changed from the earlier conditions due, in some degree, to new lunar surface data available from various flight tests. Revised criteria of major importance which limit the applicability of the Bekker equations on the LRV as compared to previous studies are:

(a) Although the lunar surface is generally a frictional type soil packed with crater slopes approaching 35 degrees, it has a low but very important cohesive character (0.06 to 0.26 psi) which should not be neglected in mobility design.

(b) The LRV is expected to rove in, out, and along the side of small and large craters which have side slopes approaching 30 to 35 degrees.

The effect of these changes has been to make the slope climbing in soft soil a major design problem of the LRV. This, of course, emphasizes the necessity of considering slope effects on wheel sinkage and thrust which Bekker's approach did not include.

It should be pointed out that this emphasis on slope effects increases the importance of cohesion since at high slope angles (approaching the angle of repose) the soil's strength and rigidity due to its frictional character tends to disappear leaving mainly the cohesive component for load support.

In view of these limitations of Bekker's sinkage expression, a modified approach is being investigated analytically and experimentally for the LRV study which

(a) Uses analytical methods based on fundamental soil mechanics concepts

(b) Considers the effect of soil slope

(c) Will be experimentally developed for various frictional type soils similar to lunar conditions and extended analytically to account for the cohesive soil properties

(d) Is dimensionally correct

This method (which is used to provide early rough performance estimates) applies the limit load analysis of the theory of plasticity to determine the failure strength of the soil at various depths below the soil surface. These are then combined to provide a load-sinkage expression.

The strength at depth is based on an infinite strip type loading analysis applied at or below the surface of the soil. Specifically, an upper bound ultimate bearing pressure is obtained using the following energy approach. A velocity field compatible with the failure pattern is adopted for a horizontal and sloping terrain respectively (Fig. V-14 and V-15). In the case of a horizontal surface, it is also considered that a side failure similar to Fig. V-14 is possible so that two failure modes and their corresponding ultimate loads are considered. The energy dissipated along the slipping regions ACDE (Fig. V-14) and CDE (Fig. V-15) as well as zone BCD is equated to the work done by the applied loads and the body force (soil weight) from which an expression of the ultimate pressure is obtained.

$$p = F(c, \phi, \alpha, \psi, \theta, B, z_o, \gamma) \qquad (1)$$

where

c = soil cohesion

ϕ = soil angle of internal friction

α = slope angle

ψ, θ = geometric parameters of failure pattern (Fig. V-14 and V-15)

B = strip width

z_o = initial depth below surface

γ = soil density

Minimizing p with respect to ψ defines the upper bound pressure load as a function of the depth z below the surface.

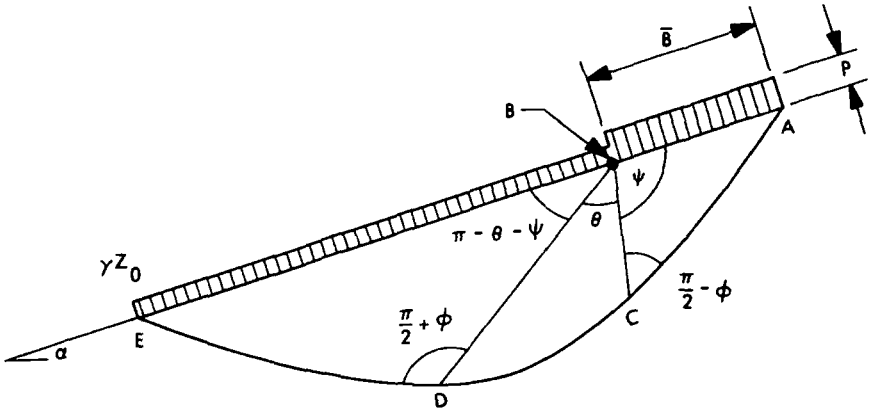

Figure V-14. Failure Mode on a Slope

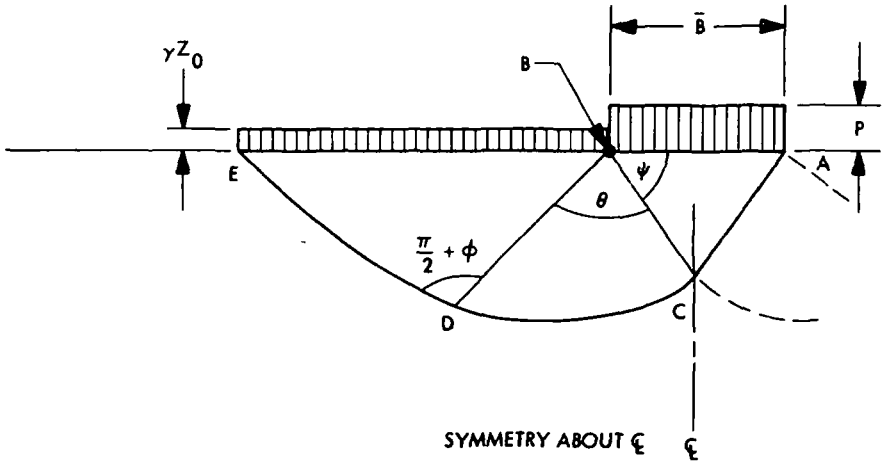

Figure V-15. Failure Mode Over Horizontal Terrain

The postulated solution assumes that the lunar soil behaves as a rigid plastic material which obeys the Coulomb-Mohr failure condition for soils and its associated flow rule. This criterion satisfies reasonably well the expected failure modes and the character of the lunar soil as described by its mechanical properties based on Surveyor lunar experiments; the angle of internal friction ϕ = 37 degrees ±2 degrees, Cohesion C = 0.06 psi and unit weight in the lunar gravitational field, 15.0 lb/cft ±2.0 lb/cft. A computer program was developed from which the following semi-empirical expression of the pressure sinkage resulted.

$$p' = \left[0.60 + (3.55 + 0.582B)\left(1 - \frac{\alpha+\beta}{\phi'}\right)^{1.64}\right]\left(\frac{Z}{B}\right)^{0.204} \qquad (2)$$

where

$$\phi' = \tan^{-1}\left(\frac{C \cos\beta}{p\ ws\ (\alpha+\beta)} + \tan\phi\right) \qquad (3)$$

where

p' = the bearing capacity of the soil in pounds per square inch

B = the width of the footing in inches

Z = the depth of the footing, which is parallel with the surface in inches

α = is the angle of the surface with respect to the horizontal in radians

β = the angle, positive towards the up slope of the load vector with respect to the vertical, radians

B, Z, α, and β are shown in Fig. V-14

Development of Performance Characteristics

(1) Energy Requirements. In the past, the wheel-soil interaction models were based on two widely different approaches· some assume the wheel to be rigid with the further assumption that the contact-area is rectangular in plan

form and has no contact behind the axle, and the other approach simulates the elastic tire or track by assuming that the entire contact area has uniform penetration.

It is clear that the intermediate stiffness tire will be somewhat deformed and that none of the existing approaches is satisfactory. Due to this deformation, there will be contact behind the axle even without elastic rebound of the soil. To bridge the gap between the above two extreme models, the deformed tire shape has been assumed and the variation in sinkage depth has been accounted for, consistent with the basic assumption of soil properties, namely that the load at any point is due to the sinkage at that point and is not influenced by adjacent points.

The geometry of the model used is shown in Fig. V-16. The shape assumed is parabolic in section, both lateral and longitudinal, and compatible with an elliptical horizontal section (approximately the contact area on a hard surface) at maximum depth expanded to a half elliptical section compatible with a toroidal wheel at the soil surface. Such a surface has uniform distribution of area with depth for depth less than the maximum.

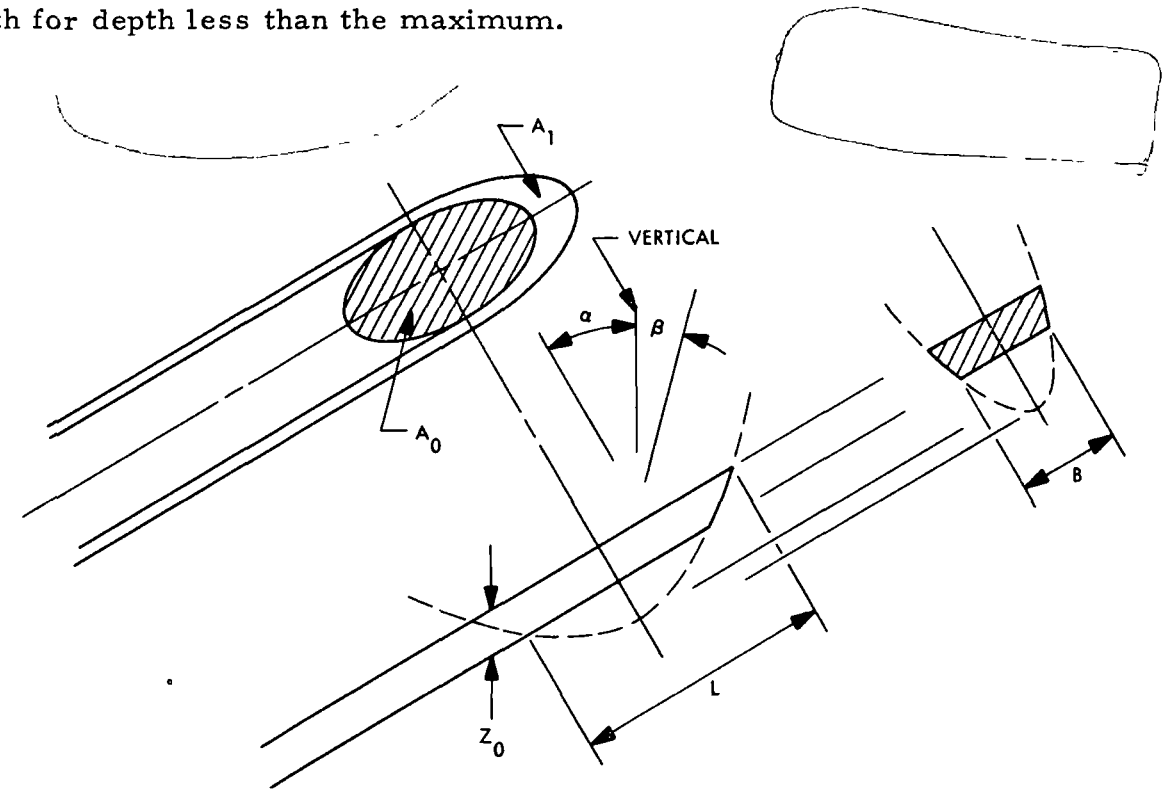

Figure V-16. Geometry of Assumed Wheel Penetration Model

The analytic model of the soil allows the sinkage to be calculated, based on the assumed wheel shape.

The model is based on the fundamental sinkage equation and has the following advantages·

(a) The area behind the axle is accounted for

(b) The added area due to sinkage is accounted for

(c) The approximation of the plan form has been improved

Simple integration gives the total load as

$$P = \left[A_o + \frac{A1}{(n+1)}\right] K \; z_o^{\,n} \tag{4}$$

where

P = the total load in pounds

A_o = the hard surface contact area in inches^2

A_1 = the area with intermediate depth in front of the axle in inches^2

z_o = the maximum sinkage in inches

K = is a coefficient dependent on α, the local soil slope β, the angle of the load vector with respect to the vertical and B, the width of the footing

n = the exponent of sinkage equal to 0.204

The solution is iterative since A_1 is dependent on z_o

The angle β between the resultant load and vertical is 0 for equilibrium of a non-accelerating vehicle (with all wheels powered) but the surface tractions are not uniformly vertical. For calculation of both soil properties and required tractive force tangent β is assumed to be the rolling resistance plus the compaction resistance, with the sum divided by the weight of the vehicle.

Compaction resistance is evaluated by assuming that soil particles move vertically and equating the energy of displacing the soil to the compaction resistance for a unit forward progress

$$R_c = \frac{BK}{n+1} Z^{n+1} \tag{5}$$

where R_c is the compaction resistance in pounds.

The rolling resistance (due to tire deformation) was assumed equal to 0.02 of the weight based on SLRV experience. Slip (S) between the tire and the soil mass is based on

$$F_t = (cA + F_n \tan \phi)\left\{1 - \frac{K'}{SL}\left[1 - e^{-\frac{SL}{K'}}\right]\right\} \tag{6}$$

where

F_t = the force along the surface in pounds

F_n = the force normal to the surface in pounds

$A = A_o + A_1$, the total area in inches^2

K' = was assumed to be 0.5

S = the slip

Equation (6) is basically for a cohesionless soil, which is considered to be adequate for preliminary analysis but may require modification.

All resistances are multiplied by 1 + S even though this may be incorrect for the compaction resistance, due to the energy method of calculation. No recovery of energy on downslopes is allowed.

No bulldozing resistance has been included, as the proposed methods of evaluation assume no friction between the soil and the wheel and it is clear that had it been included the resulting resistance would be negative at least for low sinkages.

No power-train losses or surface irregularity losses have been included and no transfer of weight due to vehicle tilt is included.

The performance of a vehicle based on the analytic model of the soil is measured by the resistance to motion, when traversing a specified distribution of slopes, and maximum slope capability.

Preliminary estimates of the average energy requirements of the LRV were established as a function of the terrain. The preliminary terrain requirements were defined in terms of slope distribution. Two slope distributions along a path were considered. The first (Fig. V-17) is described as having 80 percent of the terrain at a 10 degree slope, 10 percent at a 30 degree slope and 10 percent at a -30 degree slope. The second (Fig. V-18) has 80 percent at a 5 degree slope, 10 percent at a 30 degree slope, and 10 percent at a 30 degree slope. (Note that these are more severe slopes than the average slopes assumed in Section V D.; the question is further discussed in Section V.N.)

The average energy dissipated, per foot of travel, was estimated by considering the forces associated with the rolling resistance, slope resistance, and compaction resistance, modifying the results for the losses due to slip.

The results for the two slope distributions are presented in Fig. V-17 and V-18. These two figures show average energy dissipated as a function of wheel diameter for constant hard surface pressures. The dependent variables are ζ and w.

Where,

ζ = the ratio of tire section to tire diameter

w = the total Earth weight of the four tires

Figure V-17 shows that the baseline vehicle with a wheel diameter of 28 inches would require a $\zeta = 0.25$ for a hard surface pressure of 0.7 psi. The wheel assembly would weigh 21.1 pounds and the energy required would be 32 ft lbs/ft. For a hard surface pressure of 0.8 psi ζ is approximately 0.225 and the weight would be approximately 19.2 pounds. The values of ζ and w are interpolated linearly between two adjacent points.

The tire weights are based on the elastic type LSSM type tire, using the 10 x 40 1.11 psi test tire as a reference.

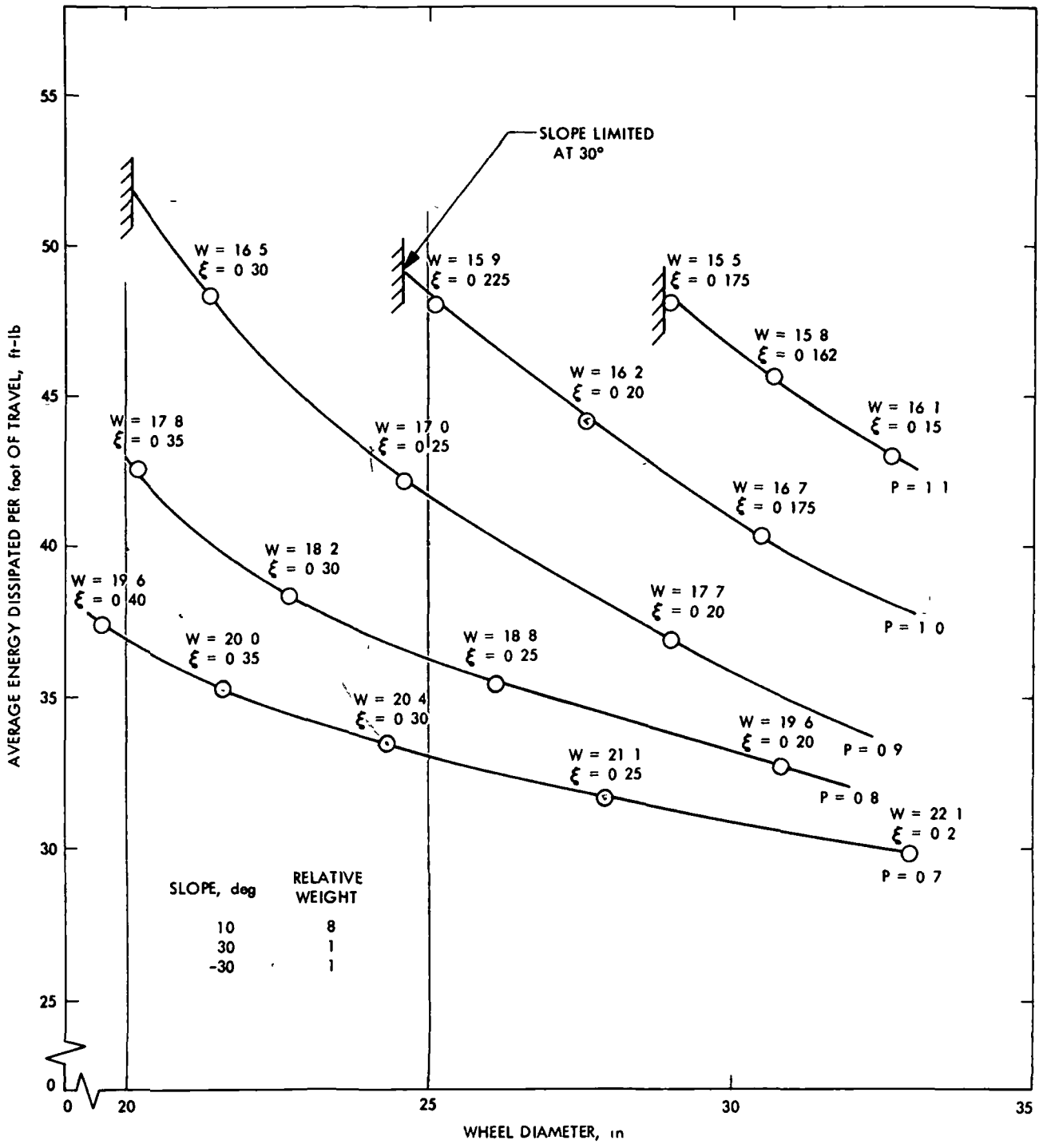

Figure V-17. Energy, Slope Distribution at 10, 30, and -30 Degrees

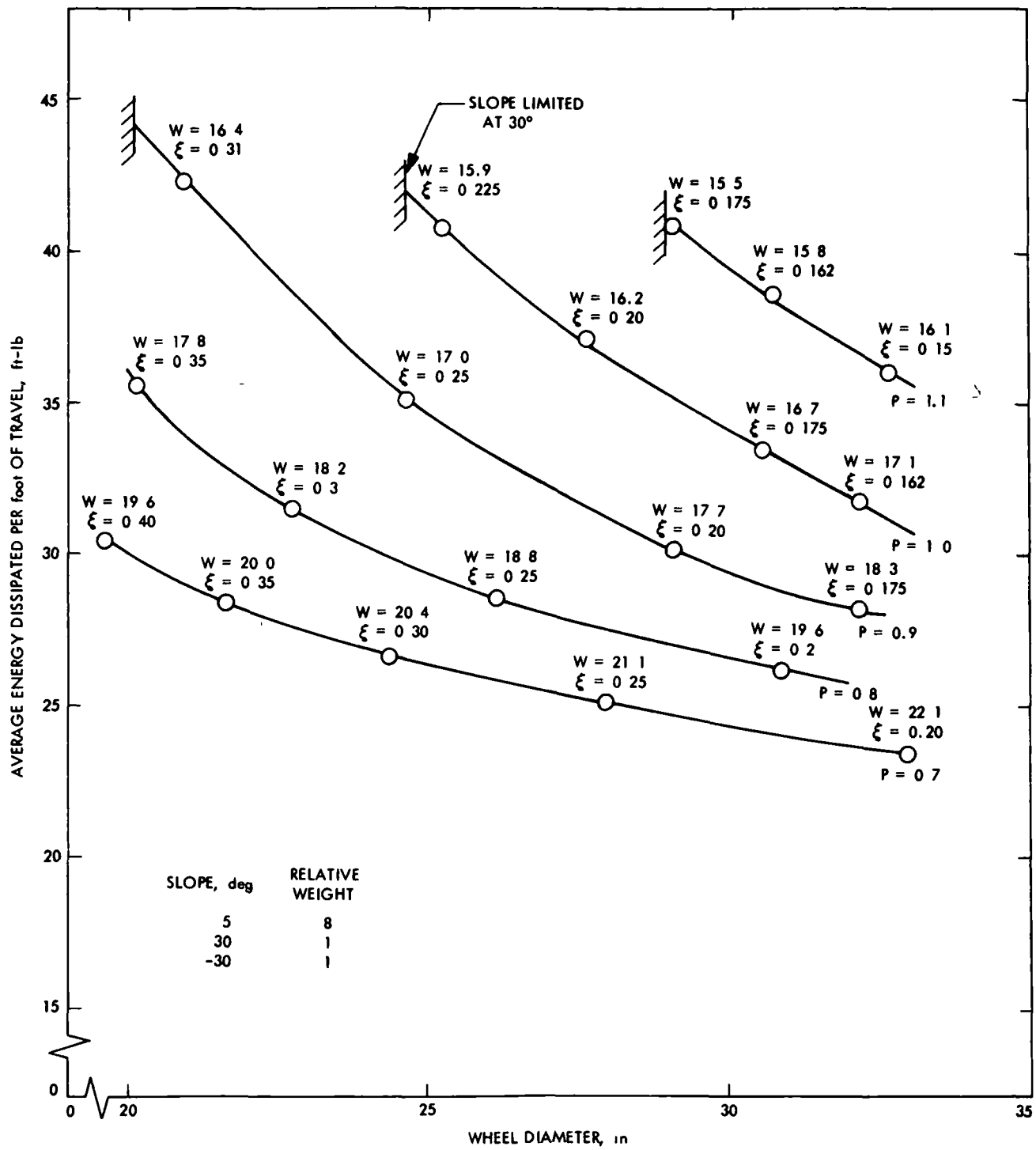

Figure V-18. Energy, Slope Distribution at 5, 30, and -30 Degrees

By appropriate use of these estimates in combination with allowances for soil roughness and other secondary energy absorbing mechanisms, it will be possible to develop an optimum weight of combined mobility mechanical (wheels and drive) system and electrical power system for specific missions.

However, it should be pointed out that these are preliminary results based on upper-bound wheel-sinkage analysis. Lower-bound requirements which are being analyzed may be more critical.

(2) Maximum Slope Capability. Preliminary estimates of the maximum slope capability have been calculated based on the preceding eqs. 1 and 3. The solutions are iterative. The critical slope is established when the vehicle no longer progresses up slope for which:

$$\frac{\alpha + \beta}{\phi'} = 1$$

Figure V-19 shows the critical slope as a function of wheel diameter for constant hard surface pressures (P). For a 28-inch diameter tire, the critical slope is 35 degrees for P = 0.7 and 32.4 degrees for P = 0.9 psi.

These preliminary results indicate that the baseline design will meet the required soft-soil slope capability of 30 to 35 degrees with tires having a design such that ζ ranges from 0.20 to 0.25 and a hard surface pressure, P, ranging from 0.7 to 1.1 psi.

(3) Obstacle Climbing Capability

(a) Rigid Surface – Obstacle climbing performance of a four-wheel vehicle has been studied by Bekker[3]. In his treatment, the vehicle is assumed to be rigid, hence the performance can be evaluated only for two wheels negotiating rigid blocks.

Since the LRV has an elastic suspension system, it was desirable to extend the analysis to an elastic frame and then study the LRV obstacle climbing performance for both one wheel and two wheels negotiating an obstacle.

The approach taken was to first establish the critical suspension spring constant, then analyze the obstacle performance assuming the suspension spring constraint has been met.

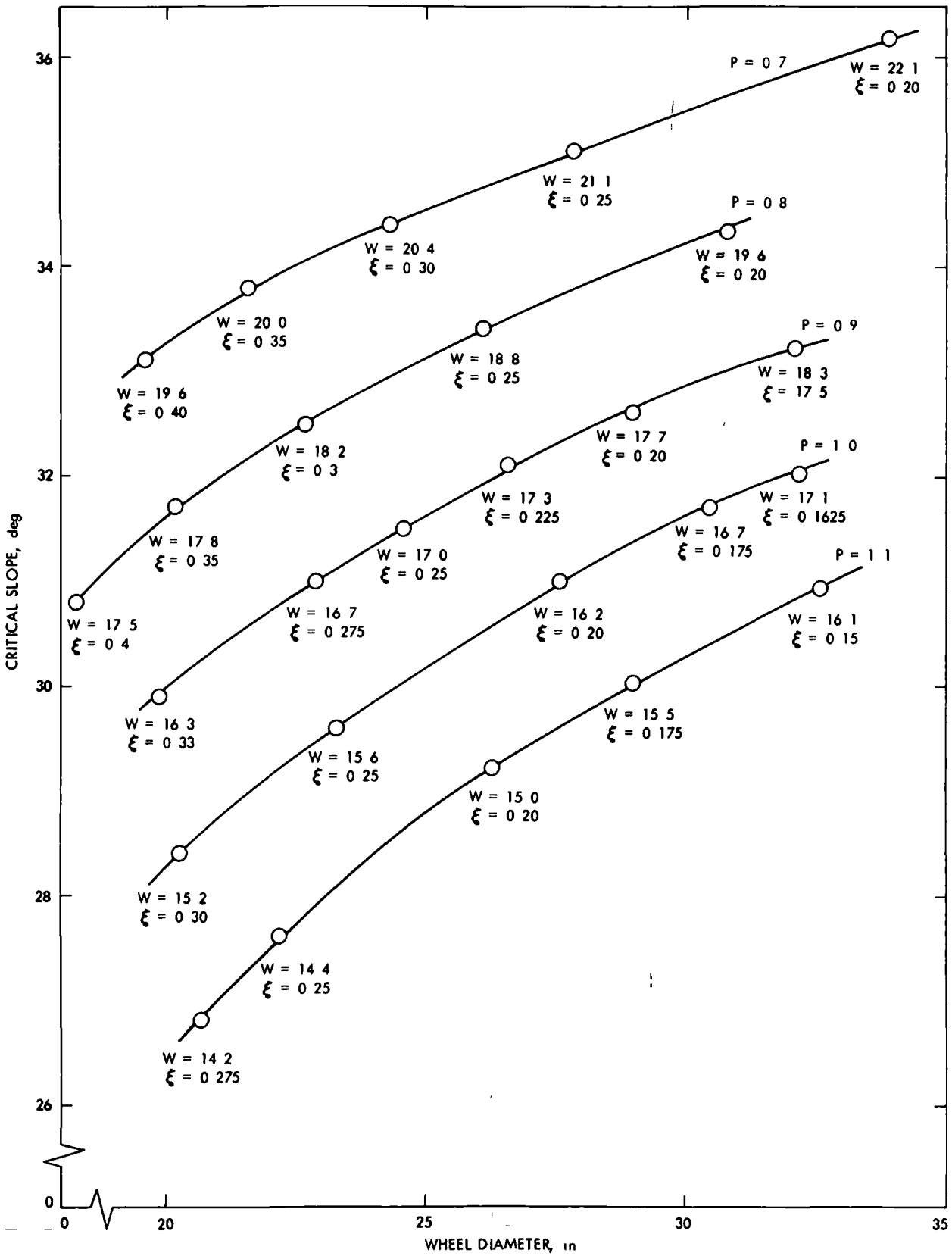

Figure V-19. Maximum Slope Capability

The critical suspension spring constant as a function of the coefficient of friction and the wheel diameter is shown in Fig. V-20. There is no mobility advantage to be gained by reducing the spring constant below the critical value, which is the value for which the required friction coefficient reduces as the wheel lifts.

A preliminary investigation of the vehicle climbing performance showed that the rear wheel on an obstacle was limiting in all cases.

In the derivation of an analytic tool for the evaluation of the obstacle performance, a force system must be assumed which assures the equilibrium of the vehicle. Such a force system is shown in Fig. V-21. In the derivation of the equilibrium equations, the wheel geometry was neglected. It was further assumed that the vertical reactions at the four wheels are equal. Vertical force and roll moment equilibrium are satisfied if there is no lateral force, T, at the wheel negotiating the obstacle. While this condition was originally an assumption, the analysis showed this condition maximizes obstacle climbing performance. The edge of the block is assumed normal to the direction of travel in all cases.

The equilibrium equations of the force system shown in Fig. V-21 are functions of the α's. In evaluating the obstacle climbing capability, a set of α's was selected resulting in a force equilibrium system maximizing the obstacle height to wheel diameter ratio, h/D. Lagrange multipliers were used in the maximization. Finally the formulation is corrected for the effect of wheel geometry, which requires the establishment of equilibrium about the pitch axis of the vehicle. Interpolation between solutions for various wheel sizes and loading angles is used to obtain the results shown in Fig. V-22.

Figure V-22 indicates that the baseline design will meet the requirements of negotiating a 10 inch obstacle with one wheel and a 6 inch obstacle with two wheels provided the friction coefficient is approximately 0.7 and the suspension spring constant does not exceed 13 lb/in.

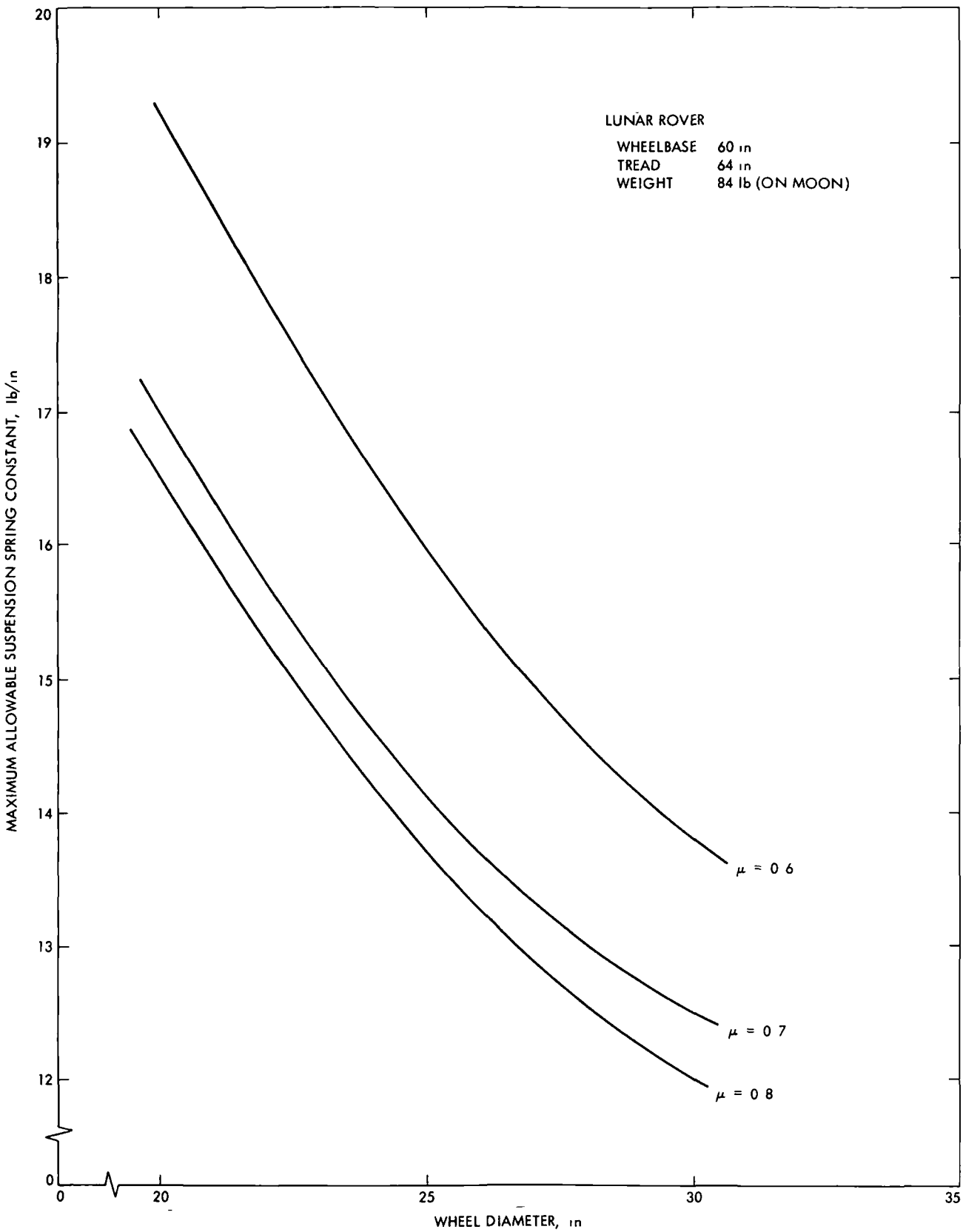

Figure V-20. LRV Suspension Spring Requirements

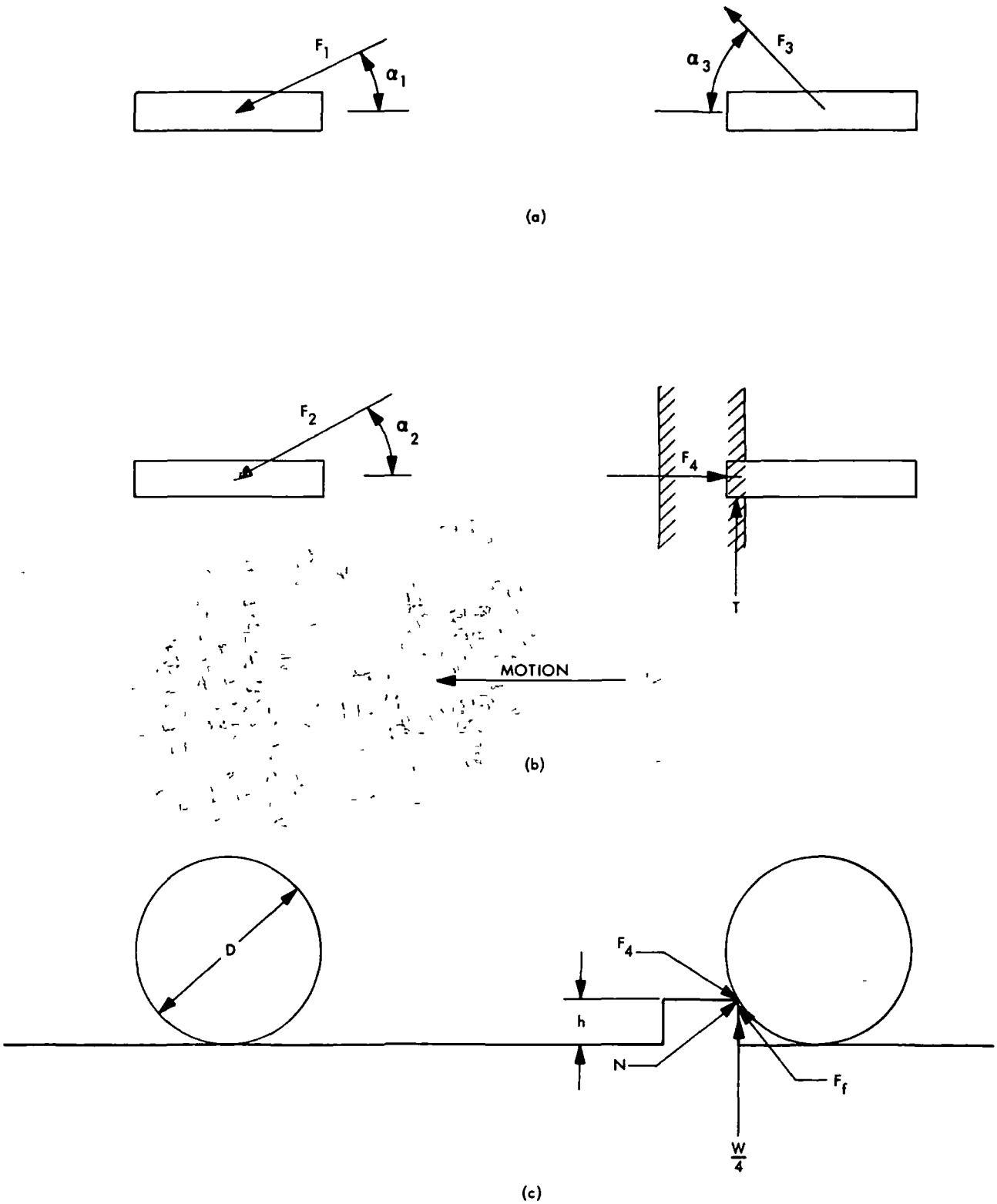

Figure V-21. Assumed Force System

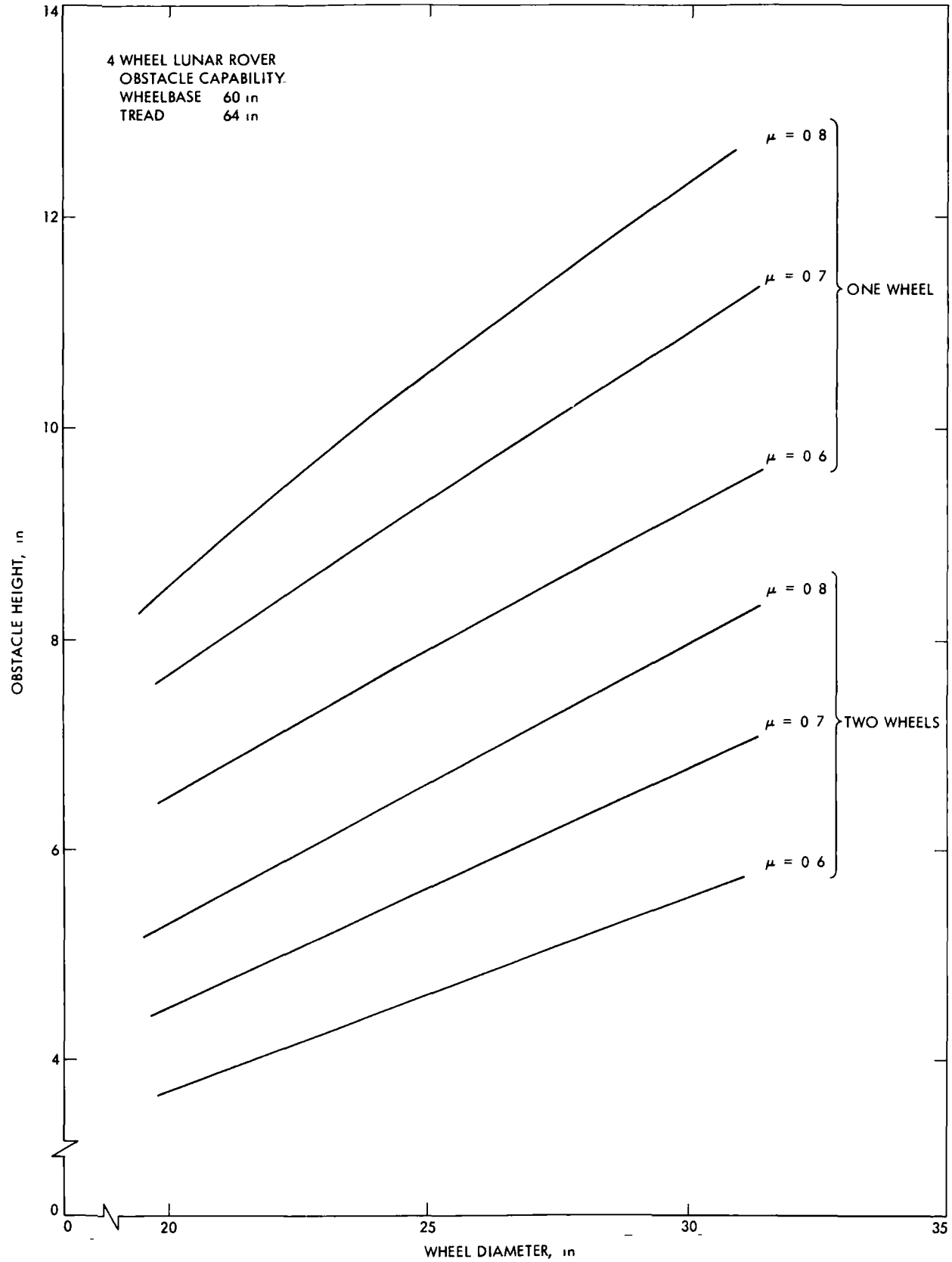

Figure V-22. Vehicle Obstacle Capability

It should be pointed out that these results are conservative in that:

(a) The obstacle is considered to be a sharp step where lunar obstacles will probably be rounded or shaped to a considerable degree.

(b) Effects of the flexible tire on climbing geometry are completely neglected.

(b) Soft Soil (Horizontal). Since the vehicle may traverse soft soils strewn with blocks, some measure of the degradation relative to obstacle performance on a rigid surface is required. It is assumed that the angle of the resultant force to the vertical at each wheel is constant and the sinkage associated with that angle is evaluated using the analytic soil model; the tire deflection is subtracted from the obstacle height on a rigid surface. The results are shown in Fig. V-23 for various wheel configurations. The curves are plotted for constant hard surface pressures.

It is seen that the obstacle climbing capability on a soft horizontal surface is reduced by approximately one inch, which is still within the range of the stated requirements for the vehicle.

(4) Crevasse Crossing Capability. The crevasse negotiation performance of a four wheel vehicle on a rigid surface has been studied by Bekker. Bekker illustrates that the maximum crevasse capability is related to the maximum obstacle climbing capability by:

$$\frac{l_c}{D} = 2\sqrt{\frac{h}{D} - \left(\frac{h}{D}\right)^2}$$

where,

l_c = the crevasse width in inches

h = the obstacle height in inches

D = the wheel diameter in inches

Applying the above relationship to the baseline design requirements with $h = 10$ inches and $D = 28$ inches gives $l_c = 27$ inches and therefore, shows that the crevasse capability is less critical than the obstacle performance.

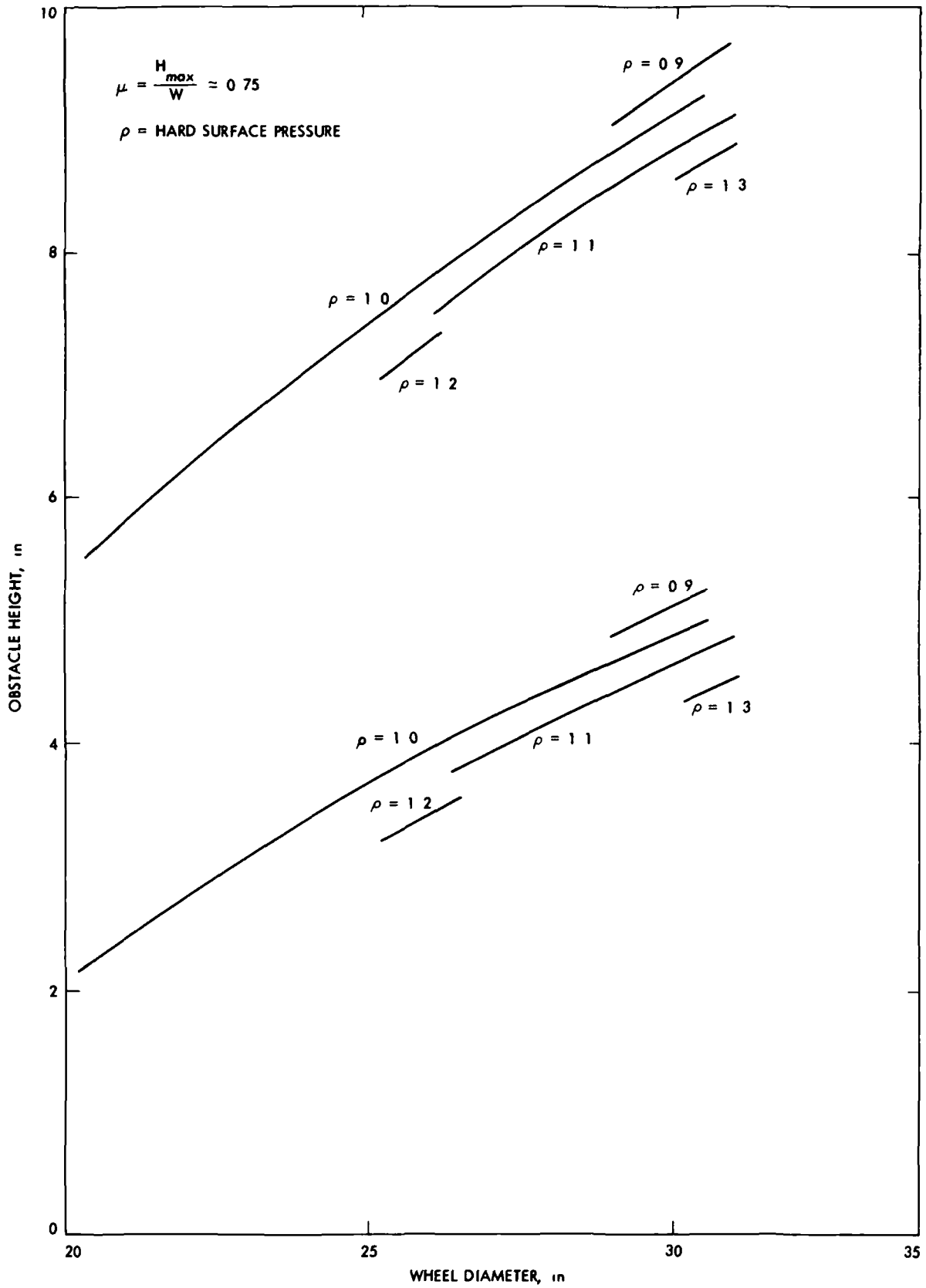

Figure V-23. Obstacle Capability in Soft Soil

As indicated on Figure V-24, the undercarriage clearance is adequate to rove across a 37 degree wedge formed by two intersecting craters. It is only capable of clearing a 32 degree wedge traveling along the crest of such a wedge which is marginal but may be adequate for this unusual roving condition.

G. THERMAL CONTROL

1. Thermal Control Requirements

The major operational phases for the thermal control requirements of the baseline LRV are flight, lunar day roving, and lunar night hibernation. During the course of the investigation it was ascertained that the flight condition presented in the baseline sequence of events was less critical than the lunar operational phases of Appendix C. The lunar day temperature can reach a maximum of +260 degrees Fahrenheit and the lunar night can reach a minimum of -260 degrees Fahrenheit. Discussed in this section are the lunar day and night thermal control requirements.

Thermal requirements for lunar day operations and lunar night hibernation consist of the operational and survival temperature limits for the subsystems of the baseline LRV which are shown in Table V-12. These LRV requirements are based on Surveyor experience. Thermal design then employs the appropriate type of temperature control (passive, active, and semi-active) to ensure that temperatures will be within the desired operational and survival temperature limits throughout all phases of the mission.

Types of Thermal Control. The three types of temperature control being considered for the LRV are passive, semi-active, and active.

(1) Passive Control. Passive temperature control consists of controlling a component to a desired temperature level through the use of insulation, reflectors, second surface mirrors, shades and surface finishes. Passive temperature control may be applied to internal components as well as external components. Surface finishes include paints, polished surfaces, vapor deposited metals, platings and aluminized plastic films.

(2) Semi-Active Control. Semi-active temperature control consists of employing a number of temperature actuated switches in the thermal compartment.

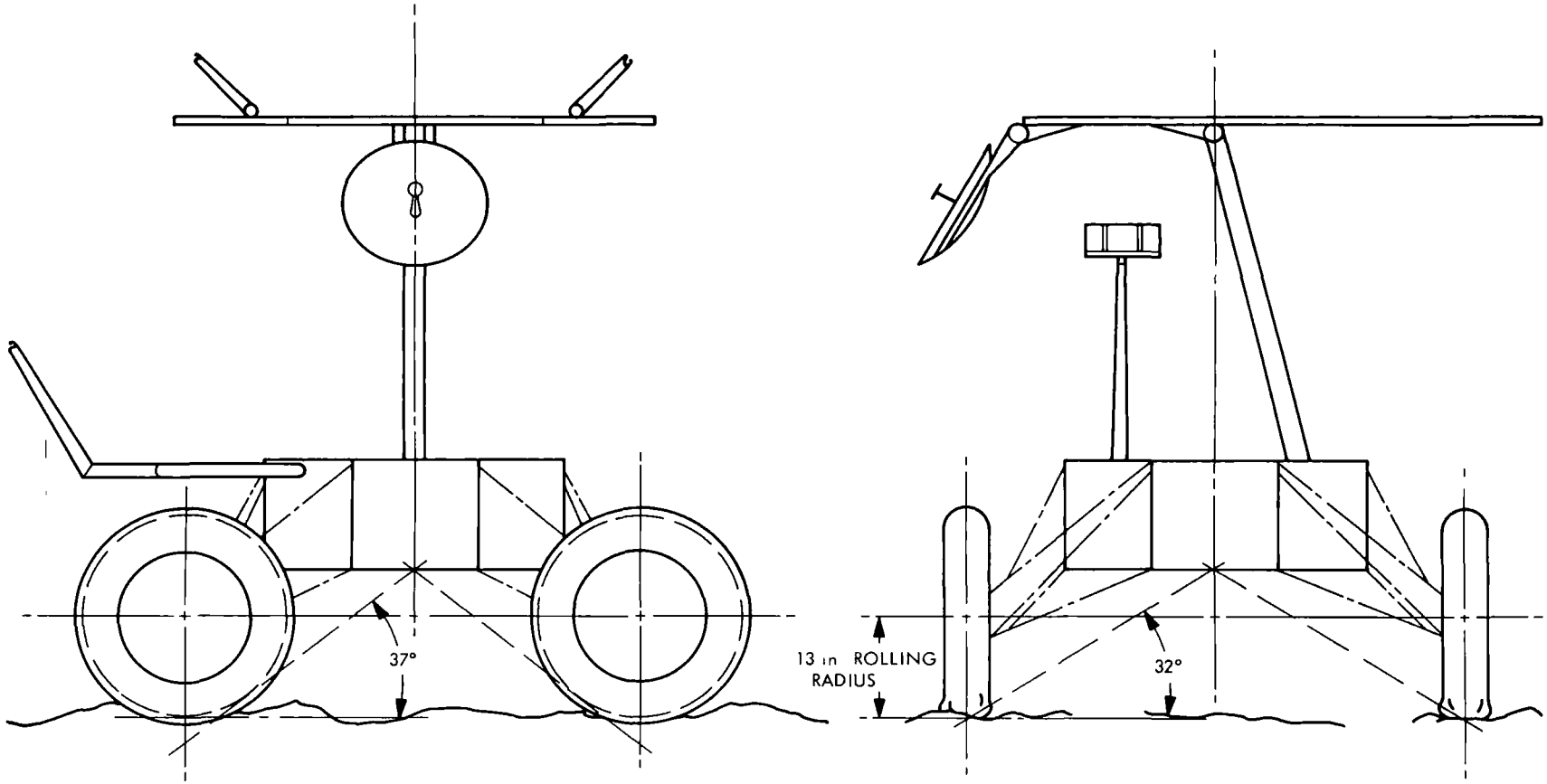

Figure V-24. LRV Undercarriage Clearance

Table V-12. Baseline LRV Thermal Requirements for Lunar Operations

Subsystem	Type of Temperature Control	Operational Temperature Limits ~ °F	Survival Temperature Limits ~ °F
Thermal compartment	Passive, semi-active and active	20 to 100	-20 to 125
Battery	Passive	20 to 125	20 to 125
Solar panel	Passive	-240 to 180	-240 to 260
High gain antenna	Passive	-225 to 275	-255 to 280
TV camera	Passive and active	-50 to 165	-250 to 185
Wheel-drive mechanism	Passive	-50 to 150	-250 to 185

(3) Active Control. Active temperature control consists of radioisotope heaters (continuous heat dissipation) or electrical resistance heaters which may be operated by thermostatic actuation or external command or both. Active temperature control would be used for those components whose survival cannot be achieved by passive control. In several instances, it is desirable to combine active and passive methods of temperature control. This optimizes the effectiveness of the heaters by minimizing heat losses from the equipment being temperature controlled.

2. Thermal Control Design

The following paragraphs present the thermal control system being considered for the central compartment of the LRV which contains most of the sensitive electronics and the battery. Passive, semi-active and active thermal control techniques are utilized to maintain the compartment internal equipment within operational and survival limits during the lunar day and night. Some of these techniques also are used to temperature control the other subsystems listed in Table V-12.

Central Equipment Compartment. The thermal control design of this compartment is considered to be similar to that of the Surveyor equipment (Reference V-9) compartments with modifications as necessary to assure night survival

The compartment consists of an external octagonal box, the bottom and sides of which provide a thermal shell to isolate the internal equipment from the lunar environment. An insulating blanket composed of 75 layers of one-quarter mil thick aluminized Mylar is installed within the outside structural shell to provide the thermal insulation. The internal electronic equipment is mounted on thermal trays whose purpose is to distribute the heat uniformly throughout the compartment. As in the Surveyor compartment design, thermal control is obtained by the use of Vycor mirror radiators which are installed on the top of the compartment. Thermal switches are then used to vary the conductance path to these external radiators thereby maintaining the compartment at a desired temperature. For daytime operations these switches are opened or closed in accordance with the heat absorbed or generated internally during the roving operations. However, during the lunar night the switches are open to minimize heat loss from the compartment. Radioisotope heaters (as recommended for later Surveyors, Ref. V-10) are included to maintain an appropriate minimum nighttime temperature for the battery (20 degrees Fahrenheit) and other sensitive equipment within the compartment.

(1) Radiator Requirement. Second surface Vycor glass mirrors (similar to Surveyor) were selected for radiators since they afford a low absorptance-to-emittance ratio and have a good stability under ultraviolet solar radiation. The Vycor radiator surface area required, is dependent upon the maximum amount of heat to be ejected from the central compartment. This condition occurs at lunar noon where the lunar surface temperature reaches 260 degrees Fahrenheit and the solar input is 442 btu/hr ft^2. Maintaining the central compartment interior at 100 degrees Fahrenheit, the heat dissipated during a traverse mode would be 66.6 watts and during a decision mode would be 108.6 watts. These heat dissipations include 17.5 watts from the radioisotopes required for lunar night survival.

Although a firm duty cycle has not been established, it is considered that 20 minutes out of every hour should be available for decision making. For this situation the duty cycle would consist of one third decision mode and two thirds traverse mode. To maintain the compartment at 100 degrees Fahrenheit during the lunar noon, assuming no shading benefit, a radiator surface of 5 foot^2 is required along with 16 thermal switches of the Surveyor type. This corresponds to an average heat dissipation capability of 83.5 watts.

A standby mode is being considered for TV operation during lunar noon periods with power requirements defined in Table V-13. It may be pointed out that the LRV may remain in this standby mode as long as necessary to cool the camera and the thermal compartment to within the thermal design limits.

Table V-13. Proposed Standby Mode

Item	Traverse Standby	Decision
Telecommunications – high low	18	60*
Control sensing	5	5
Control electronics	5	5
Power conditioning and battery charging	10	10
Heat leaks	11.1	11.1
Subtotal	49.1 watts	91.1 watts
Radioisotopes fixed in compartment	17.5	17.5
Total	66.6 watts	108.6 watts

*Total communications power = 80 watts; assumes 20 watts radiated as RF.

(2) Thermal Switch Design. The thermal design requirement imposed on the LRV had to provide for high thermal isolation during the lunar night. It also had to be capable of dissipating the heat generated by the spacecraft electronics during the hot lunar day environment without exceeding the electronic and battery temperature limits.

In order to satisfy these requirements, it was necessary to use a thermal switch developed for and successfully used on the Surveyor program. The thermal switch shown in Fig. V-25 and V-26 is capable of providing a conductance ratio of approximately 300 to 1 between the fully closed position and the open position. The conductance across the switch for the closed position is shown in Fig. V-27 as a function of the temperature above the closure temperature. The thermal switch closure point is set at 35 degrees Fahrenheit ± 10 degrees Fahrenheit. Then as the mounting surface temperature of the thermal tray rises above the switch closure temperature, the contact load increases linearly with the temperature and, in turn, the contact conductance increases as illustrated. Therefore, as the demand for energy dissipation increases, the switch conductance capability increases and provides a measure of self-compensation for varying rates of internal power dissipation within the thermal compartment.

Sticking of thermal switches in the closed position was encountered on the Surveyor program. This sticking was found to be caused by a migration of the intended interface material molybdenum disulfide (MoS_2) into the RTV-11 coating on the contacts. It was found that curing the RTV-11 contacts at 300 degrees Fahrenheit for 48 hours and recharging the contacts with MoS_2 greatly reduced the tendency of the thermal switches to stick closed. It is believed that a further development effort in this area would produce an extremely reliable thermal switch.

Thermal Coatings. The LRV will require many types of surface finishes to achieve proper temperature control. These finishes include paints, polished aluminum, vapor-deposited aluminum, platings and aluminized plastic films. These have been described in Ref. V-9 for the Surveyor application.

Most critical to this mission will be the selection of a white coating (having a low solar absorptance and a high infrared emittance) in which the degradation in solar absorptance from solar exposure is a minimum. For this reason an inorganic white Z-93 is recommended.

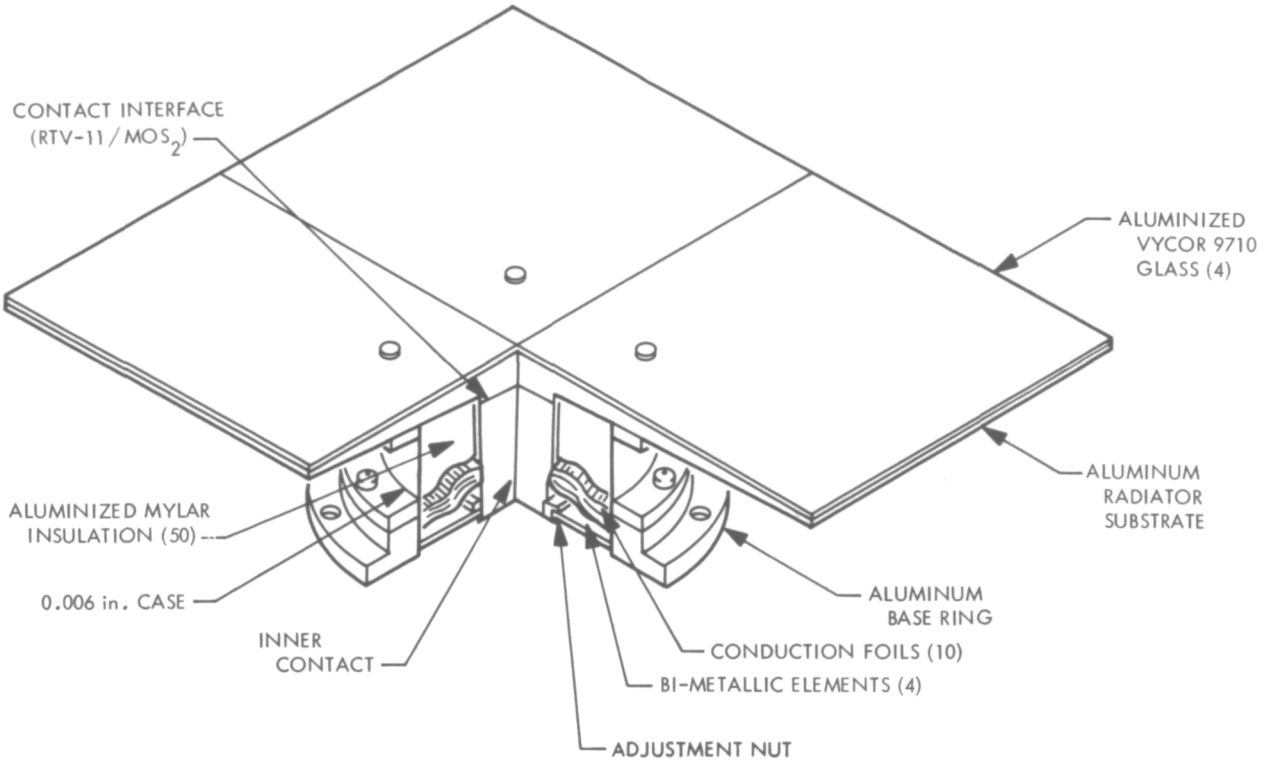

Figure V-25. Surveyor Thermal Switch

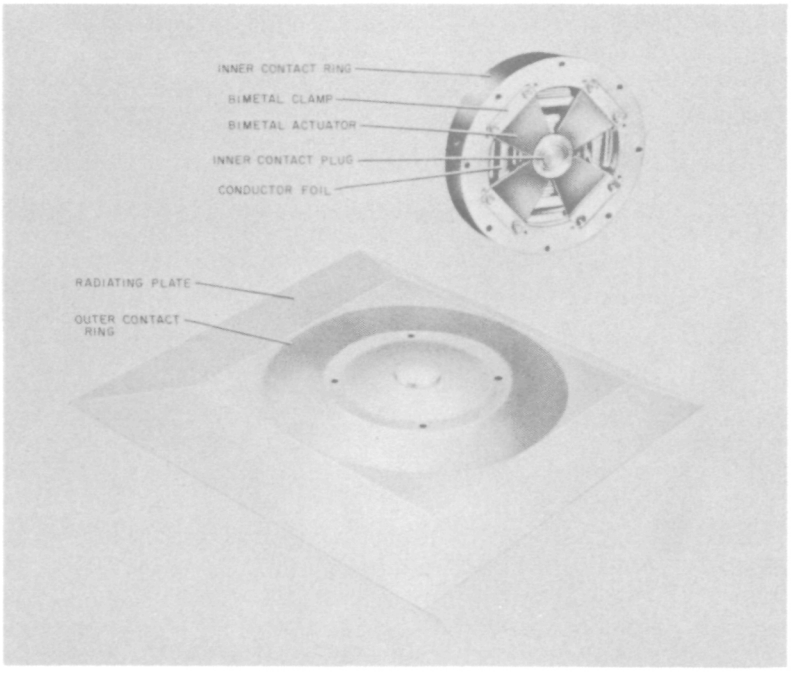

Figure V-26. Thermal Switch on Surveyor Compartment

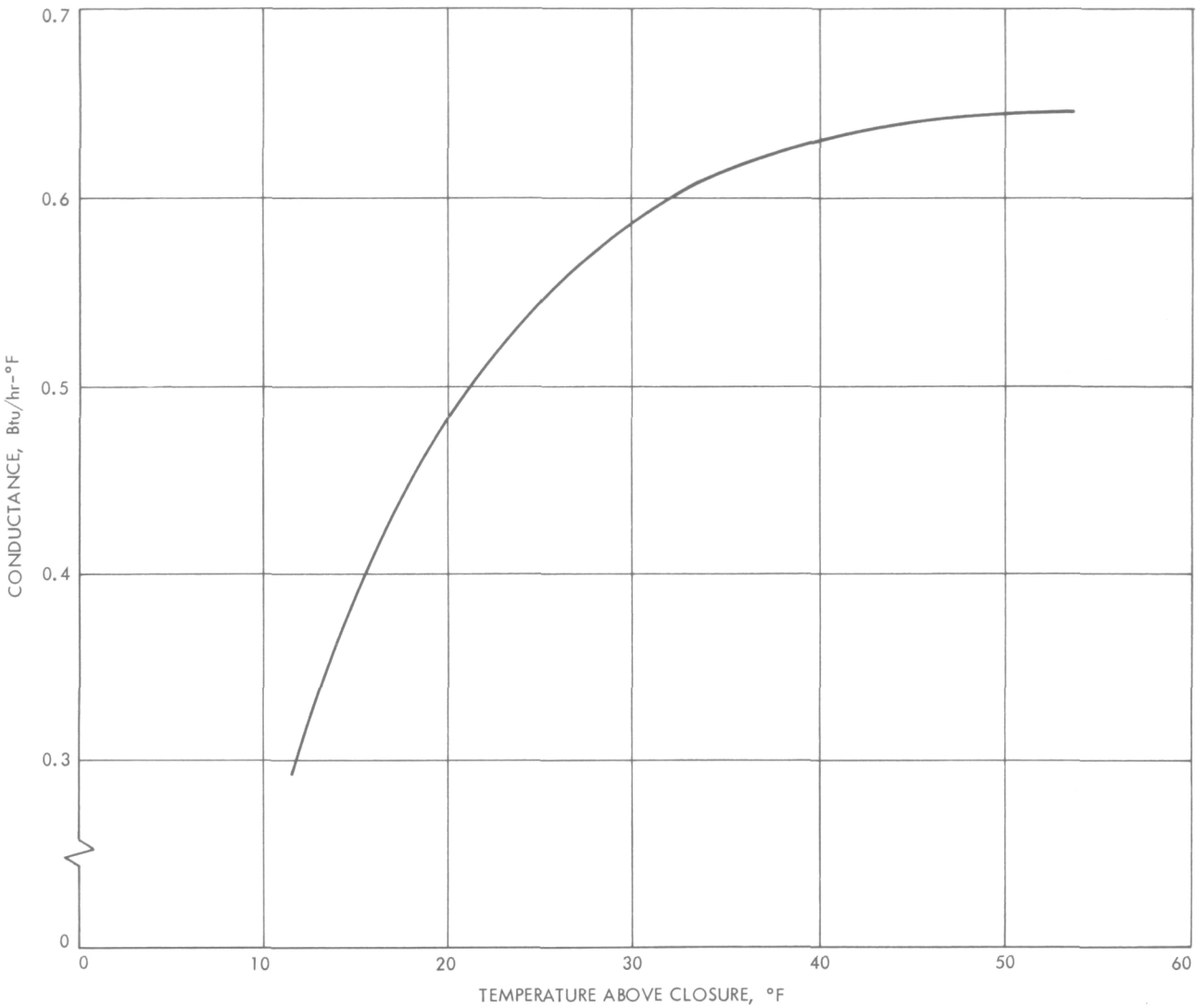

Figure V-27. Typical Surveyor Switch Conductance

For the LRV, the general thermal coating philosophy will be to use polished surfaces on the underside to achieve isolation from the lunar surface in the infrared range of radiation. For those surfaces which are directly exposed to solar radiation or to an appreciable amount of back-scattered solar radiation via the lunar surface, a white coating is recommended. Black paint may be used in isolated cases where a heat input may be desired (e.g., early morning revival).

In certain instances, a good thermal conduction path may be required, such as dissipating internally hot spots. This conduction path can be enhanced by using indium foil where equipment is attached.

Dust Problem. Although dust was not found to be a problem on the Surveyor missions, it should be considered in the case of the LRV. The LRV will be encountering a variation in soil types and has an extended mission duration; thus it is quite likely to accumulate dust on its surfaces.

Dust accumulation on the top of the Vycor mirrors can reduce their effectiveness by increasing the solar absorptance and causing the central compartment to run at higher temperatures. White surfaces covered with dust will be similarly affected. Dust erosion of polished underside surfaces also can reduce their thermal isolation from the warmer lunar surface. Dust penetration of seals such as in the wheel hubs can create a wear problem.

The dust problem does require further study but is felt to be solvable. If found to be significant, it can be anticipated through overdesign of the thermal control capability. Alternatively, dust removal or shielding techniques could be incorporated. For example, dirt dropped by the Surveyor 7 Surface Sampler on top of the Alpha-scattering instrument slid off when the instrument was moved, leaving a very small residue (Fig. V-28). However, dirt blown up by the vernier engines did adhere to a nearly vertical surface on one of the Surveyor omni-antennas (Fig. V-29).

Lunar Night Survival. Lunar night survival of the LRV is dependent upon the use of active temperature control in the compartment to provide sufficient heat to maintain the compartment and its internal components at 20 degrees Fahrenheit. During lunar night the thermal switches are set to open at 35 degrees Fahrenheit ± 10 degrees Fahrenheit. Consequently any heat leak out of the compartment must be across the superinsulation. The total area of superinsulation has been estimated to be 30 feet^2. Based upon Surveyor experience as applied to the LRV, it has been estimated that a heating requirement of 6300 watt hours (17.5 watts continuously) will be required to maintain the compartment at 20 degrees Fahrenheit throughout the lunar night which lasts for approximately 15 Earth days or 360 hours.

Use of Radioisotope Heaters. The primary purpose of adding radioisotope heaters to the thermal compartment is to maintain components in the compartments at a safe survival level during night and thus to allow the spacecraft to operate on subsequent lunar days.

Figure V-28. Dirt on Surveyor VII Alpha Scattering Instrument

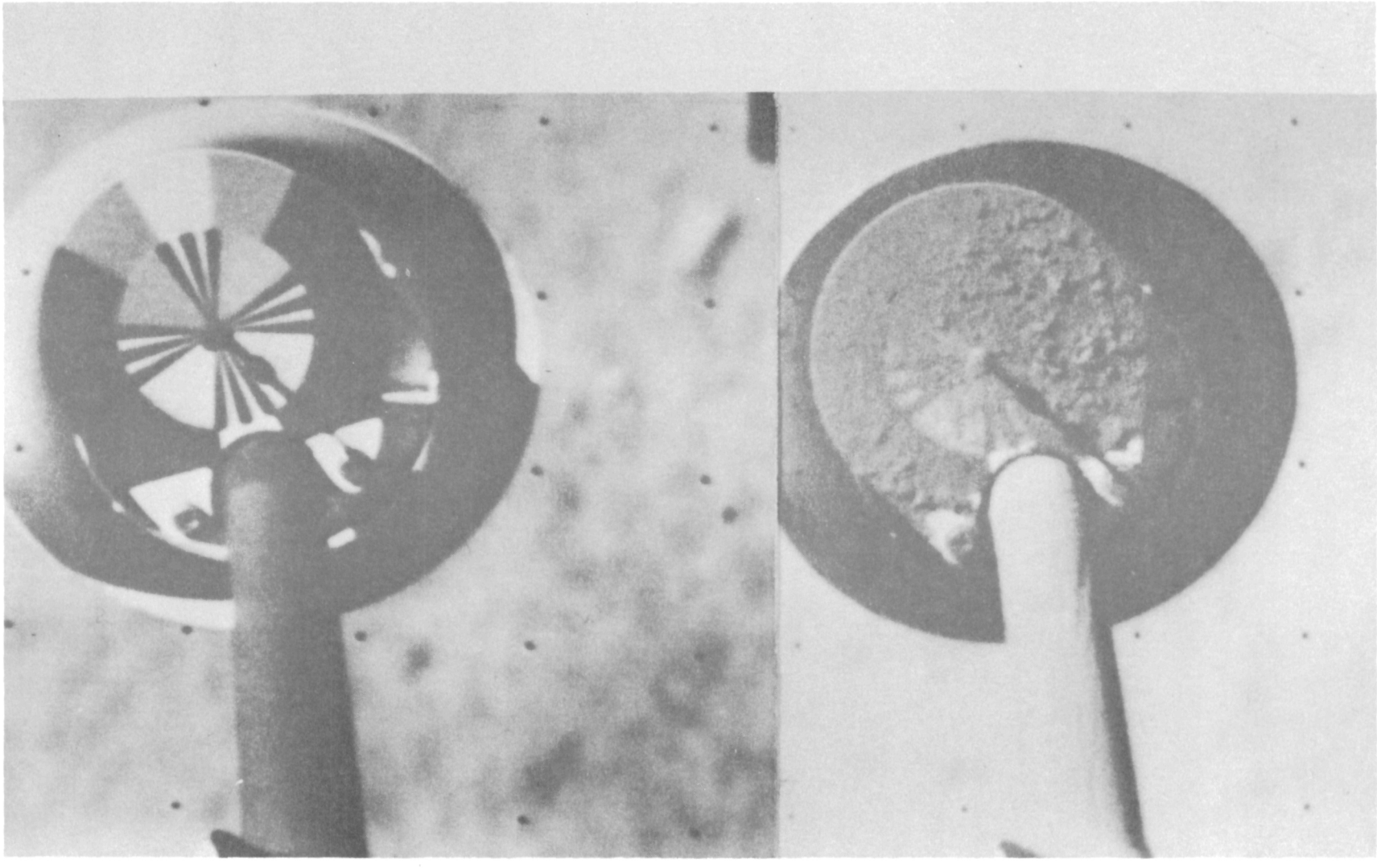

Figure V-29. Dirt on Surveyor Omni

Because of the limitations involved in using a much heavier battery to provide electrical power to resistance heaters, it was decided to employ radioisotope heaters to provide the heat required for nighttime survival (similar to those considered for Surveyor).

The use of radioisotope heaters will require minimal special handling procedures and will require approval for lunar usage by the appropriate Government agency. However, the approved usage of radioactive material was granted for the Alpha-scattering instrument used on the Surveyor program. Therefore approval of radioisotope heaters for the lunar rover should not be a major constraint.

Data have been obtained on a radioisotope capsule which has the heating characteristics required for night survival:

(1) Fuel – Promethium (Pm^{147})

(2) Weight – 0.5 pounds per capsule

(3) Half life – 2.62 years

(4) Heat generation – 2.5 watts (continuous) per capsule

Seven of these radioisotope capsules will provide the 6300 watt-hours required for night survival and have a total weight of 3.5 pounds. The half life of 2.62 years is more than sufficient in relation to the one year operational life of the LRV.

According to Atomics International, the radiation dose rate per capsule (1.82 milliroentgens per hour) is so low that special handling requirements are minimal and the usage area would not be required to be posted as a radiation area. This is the result of each radioisotope capsule having its own radiation shield. Promethium -147 is an emitter of beta radiation with subsequent creation of X-rays; these bremsstrahlung emissions are completely absorbed in the shielding of the capsule walls.

Battery Performance during Lunar Night. The rechargeable battery located in the thermal compartment provides stored electrical energy to handle

peak electrical loads as required by the mission. The capacity of the battery when fully charged is 336 watt-hours. Performance of the battery (output voltage and power) can be maintained from no load to full load providing the battery temperature does not exceed the operational limits of 20 degrees Fahrenheit to 125 degrees Fahrenheit.

For nighttime survival, the use of the stored electrical energy in the battery as a boot-strap system to maintain the thermal compartment at 20 degrees Fahrenheit is insufficient. The nighttime heater requirement of 6300 watt-hours far exceeds the 300 watt-hour capacity of the battery.

The use of radioisotope heaters can maintain the thermal compartment and the battery at 20 degrees Fahrenheit throughout lunar night. Consequently, at sunrise of the next lunar day the battery would be within operating temperature limits.

Thermal Control of Wheels. The electrical power dissipated in each of the four wheel drives is 30 watts during normal driving and 70 watts during a stall (limited to less than five minutes). The mechanical efficiency of a wheel-drive motor is estimated to be 50-60 percent. Therefore, as much as one-half the power could be dissipated in the form of heat which would be generated in the bearings and the electrical wiring.

Solar energy is absorbed by the wheels through direct illumination and from the albedo (reflected off the lunar surface). Further, infrared heat radiates from the lunar surface due to its temperature, from shaded portions and from the nearby central electronics compartment outer shell.

The wheel can get quite hot near lunar noon and would be about 300 degrees Fahrenheit at the lunar equator. The electrical drive motor in the wheel-hub must be kept much cooler than this; 150 degrees Fahrenheit under normal driving conditions. This appears feasible provided some care is taken in the design and choice of materials and thermal finishes.

The thermal design approach proposed is similar to that taken on Surveyor for several subsystems limited by their upper temperature operational limits. Internal to the hub, high thermal conduction is required to distribute the internal heat more uniformly and to conduct it to a radiator located on top. This radiator

is a highly polished mirror surface which is aluminized or silvered to reduce the direct solar input (low α, high ϵ). The undersurface of the wheel-hub compartment also should be polished to isolate it from the lunar surface radiation. The sides of the hub compartment should be painted white to reduce the solar input.

The hot-wheel (near lunar noon) should be thermally isolated from the hub to reduce heat conduction into the hub. This wheel is in contact with the hot lunar surface but gets most of its thermal energy from the radiating lunar surface adjacent to it, as well as some direct solar heating. Painting the sides of the wheel white (inside and outside) will minimize the heat input from the direct sun and the albedo. However, the infrared heat from the lunar surface cannot be reduced significantly without reducing the capability of the wheel to re-radiate its heat away. This results in a "hot" tire.

One way to isolate the tire from the hub would be to use spokes. A compromise is use a solid conical disk for support but have sizable holes in the disk. Partial reduction in thermal conductive paths from tire to hub is accomplished and two other improvements are made by this design: (1) there is less surface to collect heat from either the lunar surface or from the direct sun, and (2) this provides more surface to re-radiate heat, compared to heat collecting surfaces.

Estimated temperatures determined from the near-noon equatorial location were: 300 degrees Fahrenheit for tires, 150 degrees Fahrenheit for 75 percent cutout disks, and 150 degrees Fahrenheit for the hubs during normal driving. This requires a 0.25 foot^2 radiator on top of each hub with clearance from the wheel movement and clearance when packaged under the shroud.

The materials considered were: aluminum hub housings, titanium cutout disks and bare (outer) metal tires. Fiberglas might be considered as an alternate for the disks, since it has quite a low thermal conductivity. The sides of the hubs, disks and tire (not the treading surface) were considered painted with a white paint having a low UV degradation (Z93 inorganic white paint is recommended). At the end of the 12-month mission, the heat input to the degraded surfaces would be about double the initially non-degraded surfaces. The undersides of the hubs should start out as highly polished aluminum surfaces. The radiators considered were similar to the Vycor mirrors used on Surveyor, and also recommended for the top of the electronics compartment. Lubricants, electrical wiring and connections should be able to withstand -260 degrees to +200 degrees Fahrenheit.

Solar Panel, Baseline LRV. The solar panel temperature is very responsive to changes in thermal environment, reaching +250 degrees Fahrenheit during the lunar day and -260 degrees Fahrenheit during the lunar night. Surveyor experience has proven that a solar panel and its positioning mechanism can be designed to withstand these thermal environments. The application of Surveyor experience to a lunar rover also must consider the extended lifetime where degradation is significant.

The solar panel is oriented toward the sun. Some variation in the sun orientation will result during tracking of the sun, which would be increased by the motion of the rover over the rough lunar surface. The backside of the solar panel can be painted black since it sees very little solar illumination.

Thermal shock from rapid heating at sunrise (also after Earth shadowing during transit and eclipse) and mechanical movements caused cells to crack on the earlier Surveyors. A redesign of the solar panel for the later Surveyors, with less flexibility, led to an alternate source of failure, namely the breaking of electrical contacts. These problems are considered surmountable. Another problem which also can occur at sunrise is an over-voltage condition on the unregulated bus. This can be solved by using Zener diodes to clamp the voltage until the battery properly functions.

Figure V-30 shows the Surveyor solar panel degradation and that which could be anticipated for a new design considering conservative estimates for long lifetime. The dashed line is the high temperature UV degradation during the lunar days and a high solar flare degradation which depends upon the cover glass thickness. Dust also can obscure the sun and raise the cell temperature. Total degradation will need to be determined from the mission requirements (year, probability of flare, solar panel/sun orientation, etc.).

Television Camera. Temperature control for the TV camera is provided by both passive and active modes. Internally a passive thermal radiator is used to control temperature of the vidicon face plate. Also small resistance heaters for active temperature control are located on the electronic chassis within the camera. External temperature control consists of coating the surfaces with white paint. For a normal camera duty cycle, operational temperature limits are -50 to 165 degrees Fahrenheit.

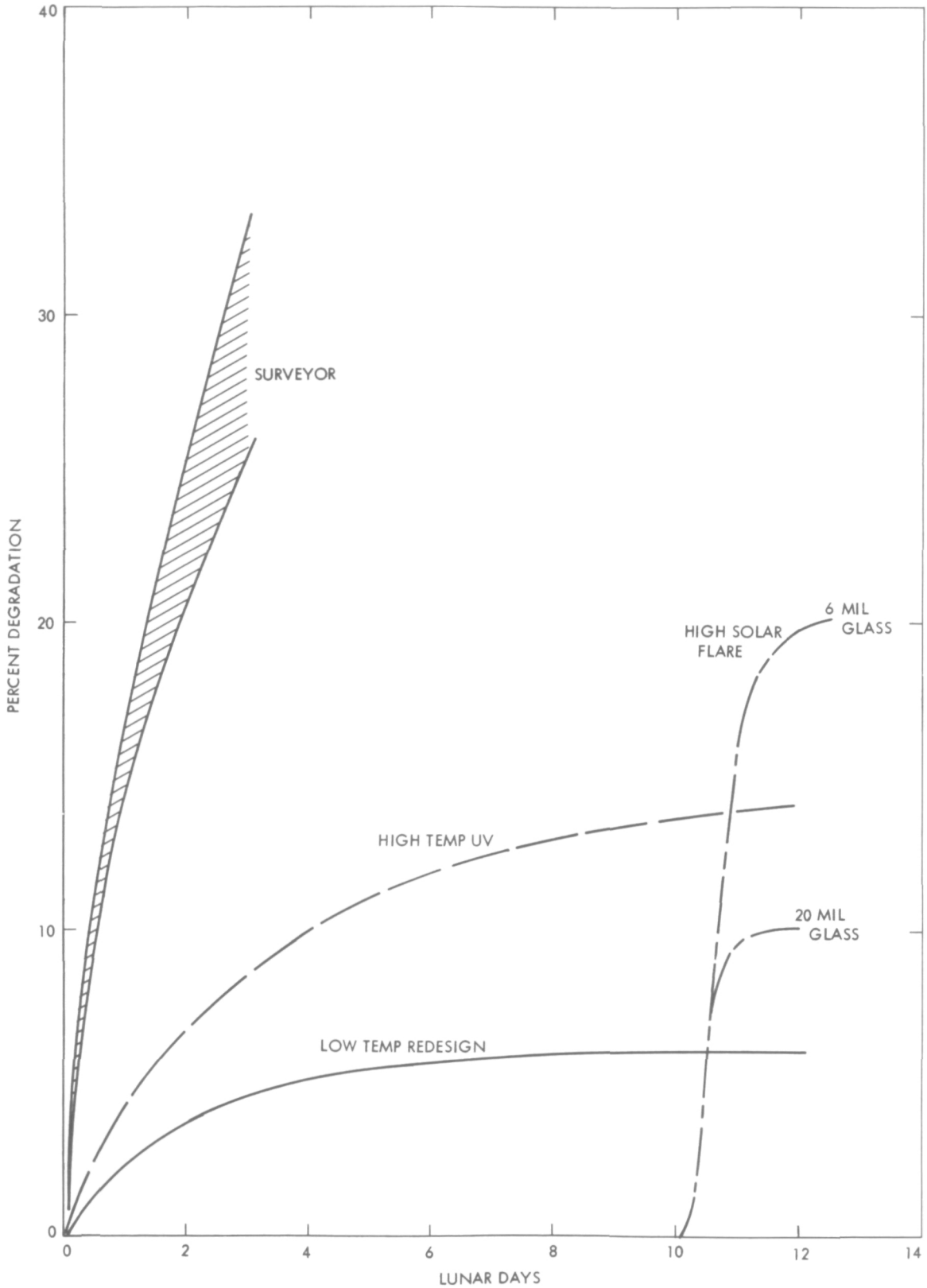

Figure V-30. Solar Panel Degradation

Because the TV camera is located outboard from the thermal compartment, it cannot be shaded by the solar panel when the sun is in the near noon position. Consequently, as with Surveyor, combinations of high camera duty cycle, high sun angle and no shading may result in temperatures exceeding operational limits. For this case camera operations must be terminated until the camera cools to within operational temperature at which time normal operations may proceed. An alternative approach would be to design a camera sun shade which would be attached to but thermally isolated from the camera.

Lunar night survival can be achieved without use of active heaters. However, for immediate camera usage in the morning of the following lunar day, the active resistance heaters in the camera electronics can be used to increase the warm-up rate of the camera.

H. SCIENCE SUBSYSTEMS

1. Instrument Payload

The LRV instrument payload selected from Table III-1 is defined in Table V-14 and illustrated in Fig. V-31. Items 1 through 5 include photo-imaging (required for navigation), sampling, and sample handling equipment. Items 6 and 7 are discriminatory science instruments required to aid in the selection of desirable samples and sampling regions (stratigraphic units). These instruments provide mineral phase and elemental analysis (Z=4 to 92). Item 8 was included as an example of a simple, light-weight means of finding water on the Moon.

The X-ray spectrometer can be combined with either the X-ray diffractometer or the alpha-scattering instrument, since it can use the radioactive sources of either instrument. Combination with the alpha-scatterer is proposed because of the resulting low power consumption. The X-ray diffractometer will probably use an X-ray tube source requiring about 40 watts while the alpha-scatterer will probably use a radioisotope source requiring no power.

2. Description of Instrument Payload

Photo-imaging. A survey TV imaging system of resolution equal to or better than that used on Surveyor will be required for navigation as well as for supplying surface morphological and rock-fabric information. This will include both small scale and gross structural features of the lunar surface. Observation of rock-fabric such as bedding planes in depositional rocks, preferred

Table V-14. Example Instrument Payload for LRV Sample Return Mission with Geological and Compositional Discriminatory Instrumentation

Instrument/Experiment	Weight in Pounds	Objectives
1. Photo-imaging	8	Provide images for guidance and displaying the surface topographic form, structure, stratification and texture. Provide high resolution images of sampling sites before and after sampling, and of acquired samples.
2. Bulk sampler	9	Acquire whole particulate, whole rock, and rock chip samples.
3. Hard-rock drill and particulate sampler	11	Acquire fine particulates, drill and acquire rock samples, and break-off rock chips for acquisition by bulk sampler.
4. Subsurface soil auger	9	Bring up subsurface material to one meter depth, for water analysis by hygrometer, and acquisition by bulk sampler.
5. Sample handling and storage system	18 (Empty Weight)	
6. X-ray diffractometer	15	Identify the types and relative abundance of crystalline phases present in lunar samples.
7. Alpha scattering/ X-ray spectrometer	20	Provide information on the elemental composition of lunar material. Z = 4 to 92
8. Hygrometer	1	Detect presence of water in material brought up by the one meter drill.
Total Weight	91	

① SCOOP SAMPLER
AZIMUTH: ± 90 deg
ELEV: +45 deg, -90 deg
EXTEND: 4 ft
SCOOP: OPEN/CLOSE

② HARD ROCK DRILL
AZIMUTH: ± 15 deg
ELEV: ± 90 deg
EXTEND: 4 ft

③ SUBSURFACE SOIL AUGER (1 in. DIA)
ELEV: 0 deg OR -90 deg
EXTEND: 1 METER DEPTH
FEED: DOWN OR UP
ROTATE: START OR STOP

④ HYGROMETER DEPLOYS TO GROUND AFTER AUGER IS SEATED

⑤ SAMPLE STORAGE SYSTEM
20 ROTARY x 6 VERTICAL POSITIONS
CAPACITY: 119 SAMPLE CUPS

⑥ X-RAY DIFFRACTOMETER

⑦ ALPHA-SCATTERER/X-RAY SPECTROMETER

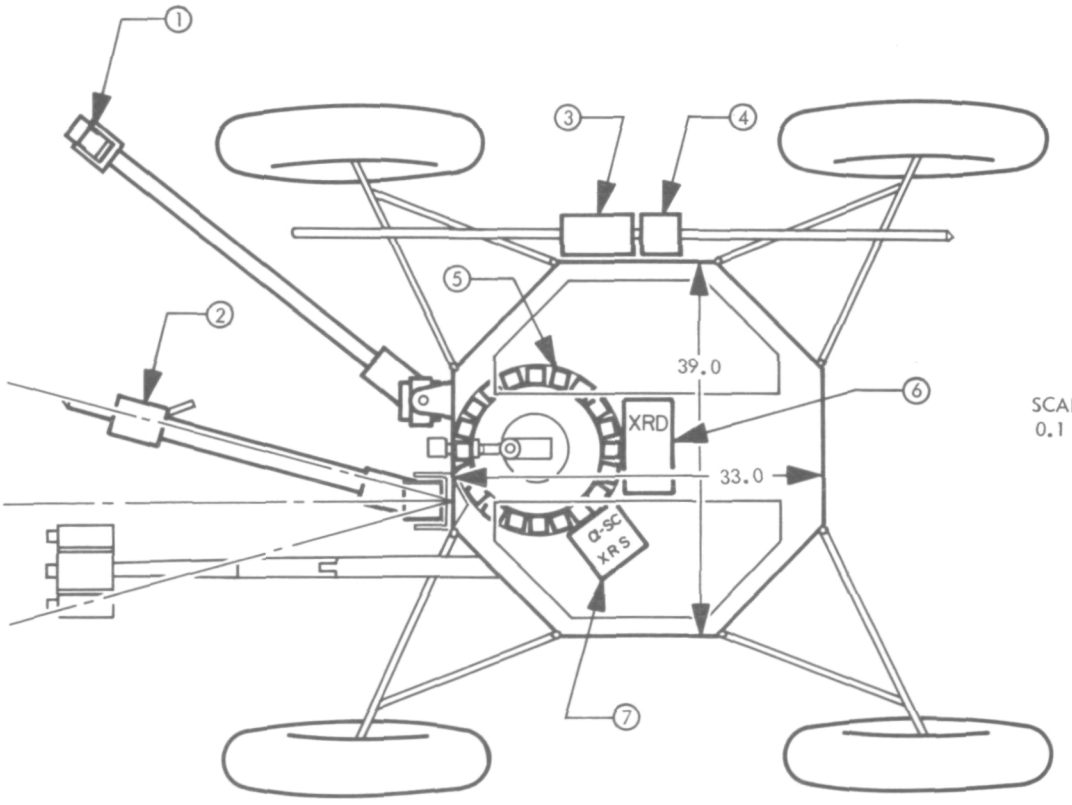

SCALE:
0.1 in. = 2 in.

SOLAR PANEL AND HIGH GAIN ANTENNA
OMITTED IN THIS VIEW

Figure V-31. LRV Instrument Payload

orientation of vesicles and/or crystals in lava flows, and foliations and lineations in deformed rocks, requires a down-looking TV, preferably with stereo and color filters for spectral reflectivity measurements.

Studies are currently being made on the spectral reflectances and absorption bands in the visible, near-infrared and at 8-14μ. Observation in these ranges may be useful for mineralogical and petrological interpretations of planetary surfaces (Ref. III-8 and III-9). A photo-imaging system is under development which will cover these ranges.

(1) Television System. Once a sampling site has been selected, TV coverage will be required for proper emplacement of the sampler, for close observation of the site before and after taking samples, and observation of the placement of the samples in the sample cups by the sampling devices.

For navigational purposes landmarks identifiable on Orbiter photos will be used. The smallest identifiable landmarks are about 80-meters across and 10-meters high (when they cast an 80-meter shadow). In its narrow angle TV mode LRV should be able to detect such landmarks from a distance of 10 kilometers. Assuming that four picture elements (pixels) on each axis will resolve an object, the minimum angle of resolution will be 10 m/4 x 10 km = 1/4 milliradian or 0.0143 degrees per pixel in the vertical direction, and 80 m/4 x 10 km = 2 milliradians or 0.115 degrees per pixel in the horizontal direction. The system should provide for a 360 degree panoramic coverage or a selected sector thereof, from 40 meters to infinity with a pointing accuracy of one-half degree in azimuth. This will separate objects 80 meters apart at a range of 10 kilometers. The luminescence handling capability should range from about 1 ft-lambert to 2,500 ft-lamberts, and the light level latitude for each frame should be telemetered in at least eight shades of grey.

In the wide-angle mode, the camera should have a vertical field of view of 26 degrees. (With the camera at the foot of selected landmarks, the whole feature should be viewable from level ground to its top), and a horizontal field of view of 60 degrees (for the camera standing 40 meters from an object 80 meters in diameter, it should see the whole object in one picture), with a resolution of 0.1 degree per pixel both horizontally and vertically.

The camera should provide the ground display with a direct indication of the pointing direction relative to LRV. (Operators must have instant access to the relative bearing of interesting features on the display imagery. This will enable them to command the camera to obtain additional imagery at different elevation angles and/or with telephoto lens.) Refer to Table V-15 for system requirements.

The band-width or data bit-rate requirements for telemetry will be essentially the same for any photo-imaging system, being proportional to the frame transmission rate, frame size, image point density, and shades of grey required. For example, a 10 degrees by 360 degrees panorama frame at a resolution of 0.01 deg/pixel totals 3.6×10^7 pixels. If 32 shades of grey are required this requires 5 data bits per pixel for a total of 1.8×10^8 data bits. At 400kb/sec the time required for transmission would be 450 seconds.

There is also the problem of exposure and latitude control adjustments which must continually be made in order to match the photo-sensor response to the variations of the scene luminescence. These adjustments may have a fully automatic mode of operation and may also be partially compensated by transmitting additional grey levels to cover the widest expected range of scene luminescence. Therefore, for an average scene, many of the levels would be all black or all white; the remainder of the light levels would contain the picture.

Except for the wide-angle frame sizes desired for navigational purposes, a vidicon system similar to that used on Surveyor (Fig. V-32) will meet the LRV requirements. With improvements and a lighter weight mechanization the weight can probably be reduced to the eight-pound target goal. See Ref. V-13 for a full description of the Surveyor TV camera system.

(2) Facsimile Camera System. A variable-parameter facsimile camera system for lunar surface operation is currently under development (Fig. V-33 and V-34) and should also meet LRV requirements. The system can be designed to scan, within one frame, a 360 degree panoramic view with a 100-degree included vertical-angle, or any portions thereof, at any desired resolution within some practical limits, e.g., 0.01 to 0.60 deg/pixel to pixel. In addition it can be made to readjust its gain level continuously so that closely spaced bright and dark areas can be scanned without loss of detail. Its spectral

Table V-15. Photo-imaging System Requirements

Parameter	Navigational Requirement	Science Requirement
Stereographic baseline, horizontal or vertical (dual-imaging is desirable but not essential since the vehicle can be moved to produce stereo).	3/4 to 3 feet	3/4 to 3 feet
Horizontal pointing capability	360 degrees	360 degrees
Vertical pointing capability with reference to LRV axes	+35 to -65 degrees (which provides +10 degrees on a -25 degree slope)	+35 degrees to -65 degrees (depends on location of the camera, the operating area of the sampling devices must be viewable)
Pointing accuracy	±1/2 degree	±1/2 degree
High resolution mode	Vertical = 0.0143 deg/pixel Horizontal = 0.115 deg/pixel	0.0143 deg/pixel (both axes)
Low resolution mode	0.1 deg/pixel	0.1 deg/pixel
Frame sizes	See discussion	No special requirement
Light level range	1 to 2500 ft-Lamberts	1 to 2500 ft-Lamberts
Focus or depth of field	4 feet to infinity	4 feet to infinity
Grey level	8 shades	32 shades
Wide spectral response and high spectral fidelity	Not required	Required with color and polarizing filters
Weight	8 pounds	8 pounds

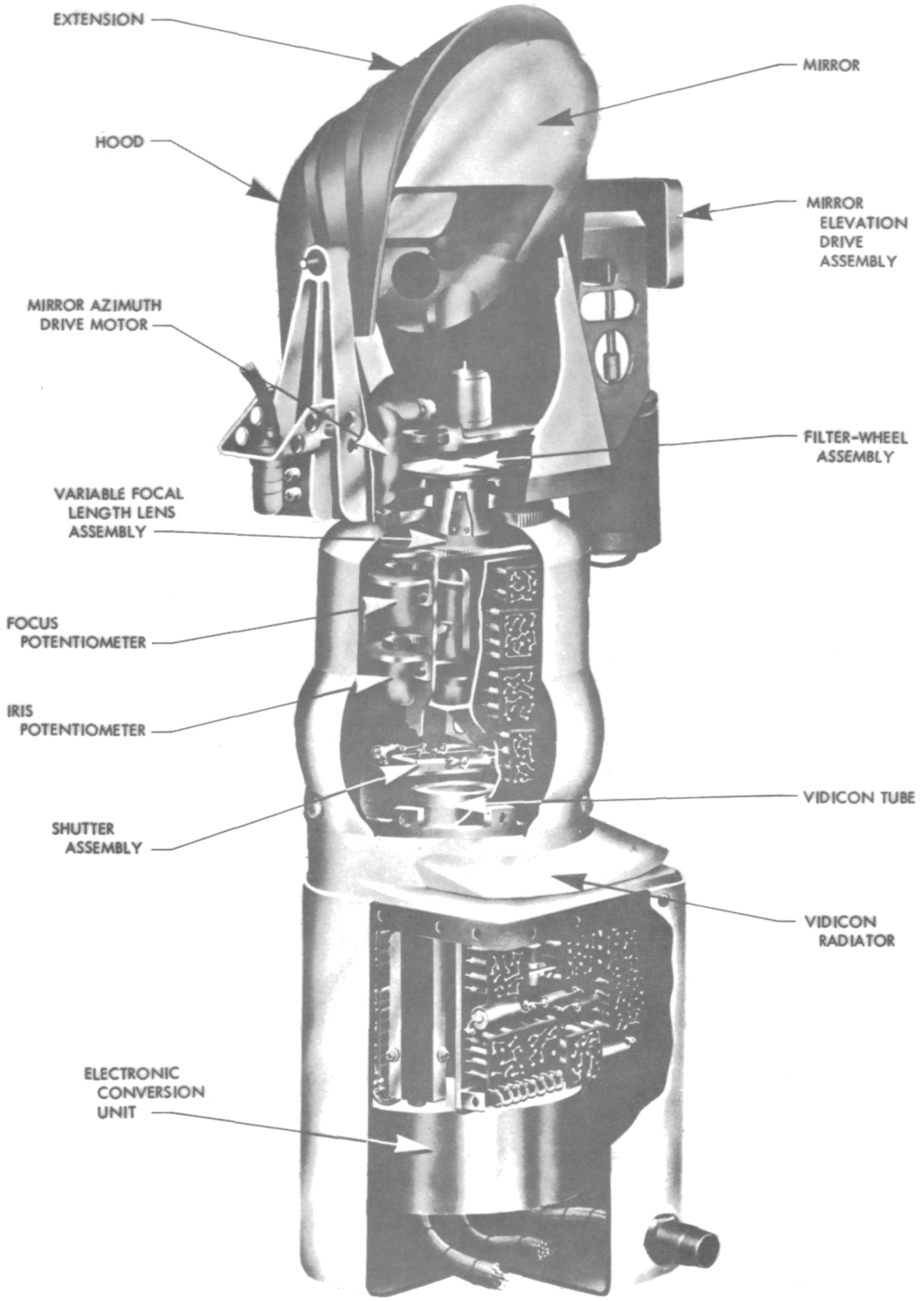

Figure V-32. Surveyor TV Camera

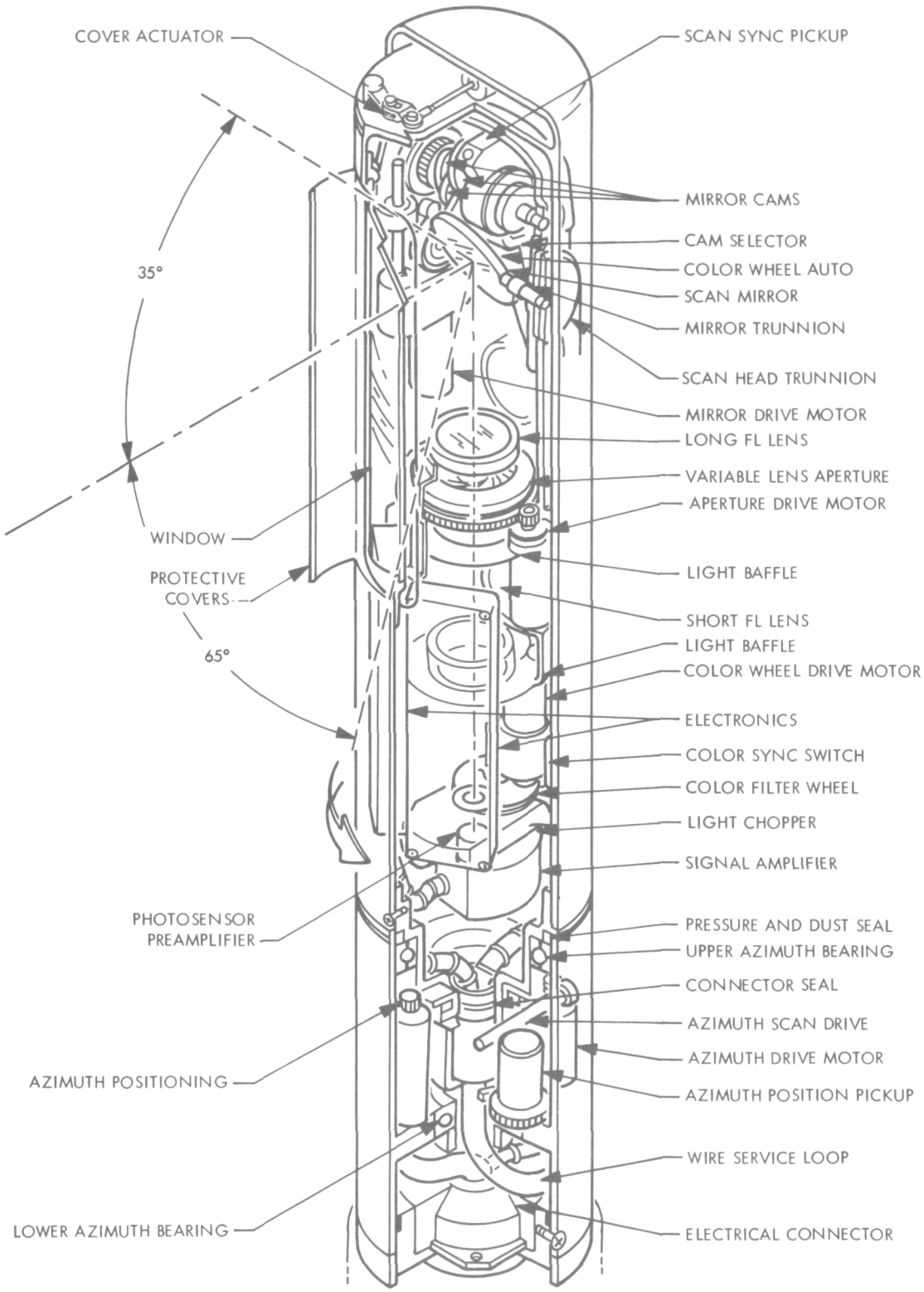

Figure V-33. Variable Parameter Facsimile Camera

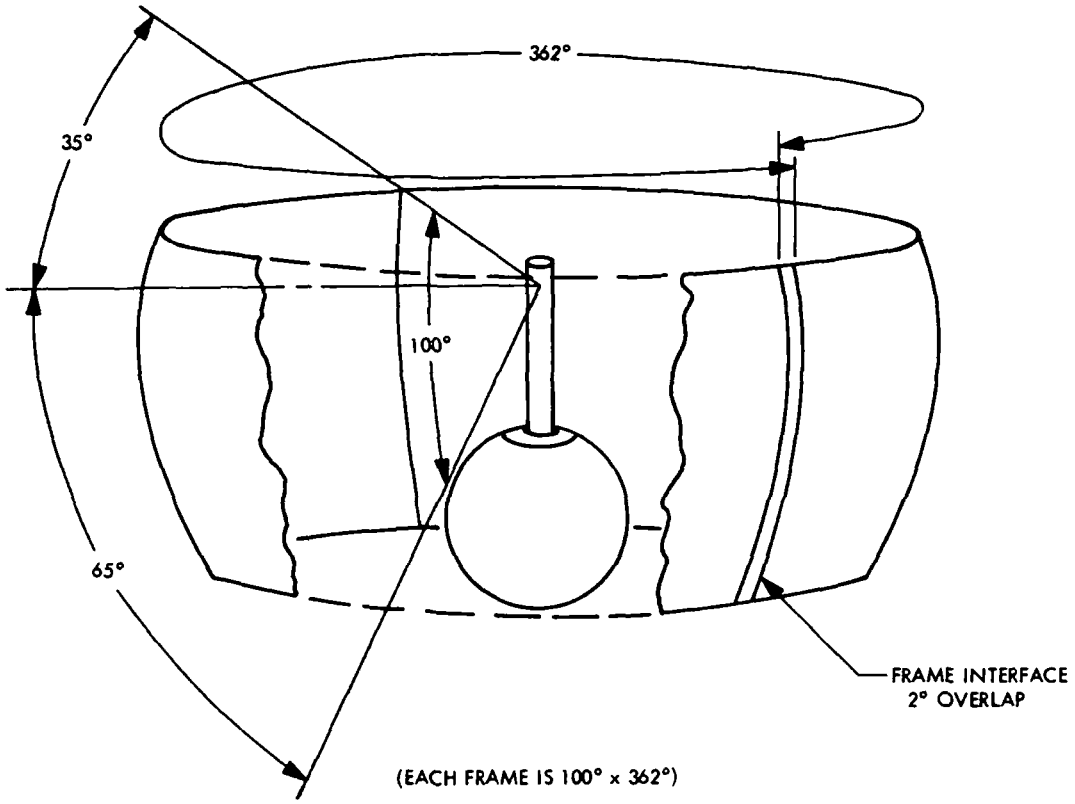

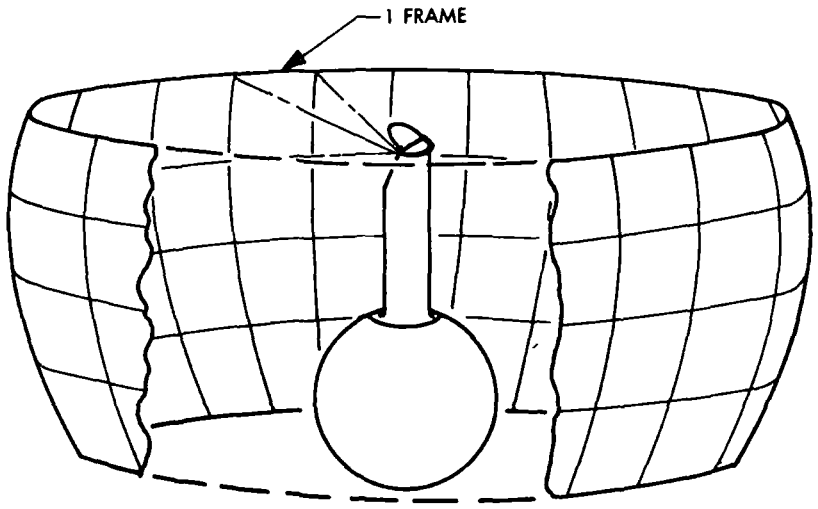

FIGURE V-34. FACSIMILE FRAME FORMAT AND VIDICON FRAME FORMAT

Figure V-34. Facsimile Frame Format and Vidicon Frame Format

response can vary depending on the sensor used, from 0.2 to 0.9 microns with a photomultiplier, 0.4 to 1.4 microns with a silicon-sensor, 0.8 to 3.3 microns with an uncooled PbS sensor, and longer wavelengths as in the 8 to 14 micron range by cooling the detector and the optics.

The major element of the camera is a top tubular section which contains the optical viewing subassembly, plus vertical drive, and scanning mechanisms. These elements provide one degree of motion to the optical system by "nods" in the vertical plane. The top section also houses the photoelectric transducers and the first stage of signal amplification. The lower section contains an azimuth drive mechanism, which provides the necessary second degree of motion to the optics for rotation in the horizontal plane; motor drive electronics, which provide the power to both the vertical and horizontal drive motors; signal electronics; and synchronization electronics, which provide accurate timing signals to ensure proper playback of the data. The assembly is a 3.0-inch diameter cylinder approximately 18 inches long. A viewing port in the wall of the top section is sealed with a glass window. Inside the housing and behind the window, is a flat distortionless mirror which is pivoted so that it may swing 50 degrees in a vertical plane, thereby generating a 100-degree scan. By this action, the mirror reflects light down the tube into an image-forming lens, through filters if desired, and onto the surface of a photosensitive transducer. The complete device including an extension mast for vertical stereographic pictures would weigh less than 10 pounds.

Refer to Table V-16 for performance capabilities of vidicon and facsimile systems.

A facsimile camera system was developed as an experiment for the Ranger Capsule scientific payload. This device proved to be extremely rugged, light in weight, reliable, and in subsequent field tests by the Astrogeology Branch of U.S. Geological Survey at the Bonito lava flows, it produced high quality, geometrically stable images that were well suited to stereographic viewing and reduction techniques. Similar cameras were delivered to the lunar surface in 1966 by the Soviet spacecraft Luna 9 and 13 and produced good images. (Ref. V-11 describes details of the Soviet facsimile system.)

Table V-16. Performance Capabilities of Vidicon and Facsimile Systems

Parameter	Vidicon System	Facsimile System
Stereo	Repositioning or dual cameras	Repositioning (vertical base)
Frame size		
Narrow angle	6.4 degrees by 6.4 degrees	10 degrees by 10 degrees (from +35 degrees to -60 degrees vertically and 360 degrees horizontally
Wide angle	25 degrees by 25 degrees	100 degrees by 360 degrees
Frames per 360 degree pan		
Narrow angle	60	36
Wide angle	15	1
Resolution		
Narrow angle	0.01 deg/pixel (600 line)	0.01 deg/pixel
	0.30 deg/pixel (200 line)	
Wide angle	0.04 deg/pixel (600 line)	0.60 deg/pixel
	0.12 deg/pixel (200 line)	
Light level range	10 to 2500 ft-Lamberts (0.15 second exposure) to 0.008 ft-Lamberts (time exposure)	0.5 to 5000 ft-Lamberts
Focus requirement	1.23 meters to infinity	Not required
Depth of field	Varies	1 meter to infinity
Spectral sensitivity	0.4 to 0.6 microns (visible spectrum)	0.4 to 1.2 microns (visible and near IR, silicon sensor)
Size	6 1/2 inches deep by 22 1/2 inches long or 800 inches^3 (can be reduced)	3 inches deep by 18 inches long or 127 inches^3
Power	25 watts (can be reduced)	15 watts

Bulk Sampler. The desire to pick up 3 centimeter diameter rocks as well as particulate material in their indigenous forms (i.e., without size or density sorting) eliminates the prospect of using several types of samplers currently under development, and indicates the use of a shovel, bucket, clam-shell or other bulk type sampler similar to the Surveyor Surface Sampler The Surveyor Surface Sampler itself could be used, however, for the sake of greater compactness, versatility and adaptability to the LRV configuration and requirements a new design is preferred. The bulk sampler shown in Fig. V-35 is a shovel or clamshell type similar to the Surveyor Surface Sampler but is deployed with a furlable boom rather than with a pantograph linkage Some of its characteristics are defined in Table V-17.

Several types of furlable booms are under development, two of which look promising for this application. One is made by DeHavilland (the Bi-stem) and the other by Ryan (Fig V-36). In either case they will have approximately the features defined in Table V-18.

DeHavilland's Bi-stem extensible structures are composed of two or more partially open slit-tubes, co-axially nested in a front-to-front configuration The tubes are formed from thin-strip metal, which can be opened, flattened and rolled onto a drum for compact storage.

Table V-17. Bulk Sampler Characteristics

Requirement	Parameter
Space (stowed)	5 inches by 5 inches by 12 inches
Weight	9 pounds
Power	5 to 10 watts
Motions	Boom: 110 degrees left, 90 degrees right, 45 degrees up, 90 degrees down, and extend 3 feet
	Scoop: Forward and reverse
	Blade: Forward and reverse
Total reach	Approximately 4 feet
Scoop capacity	Approximately 100 cubic-centimeters

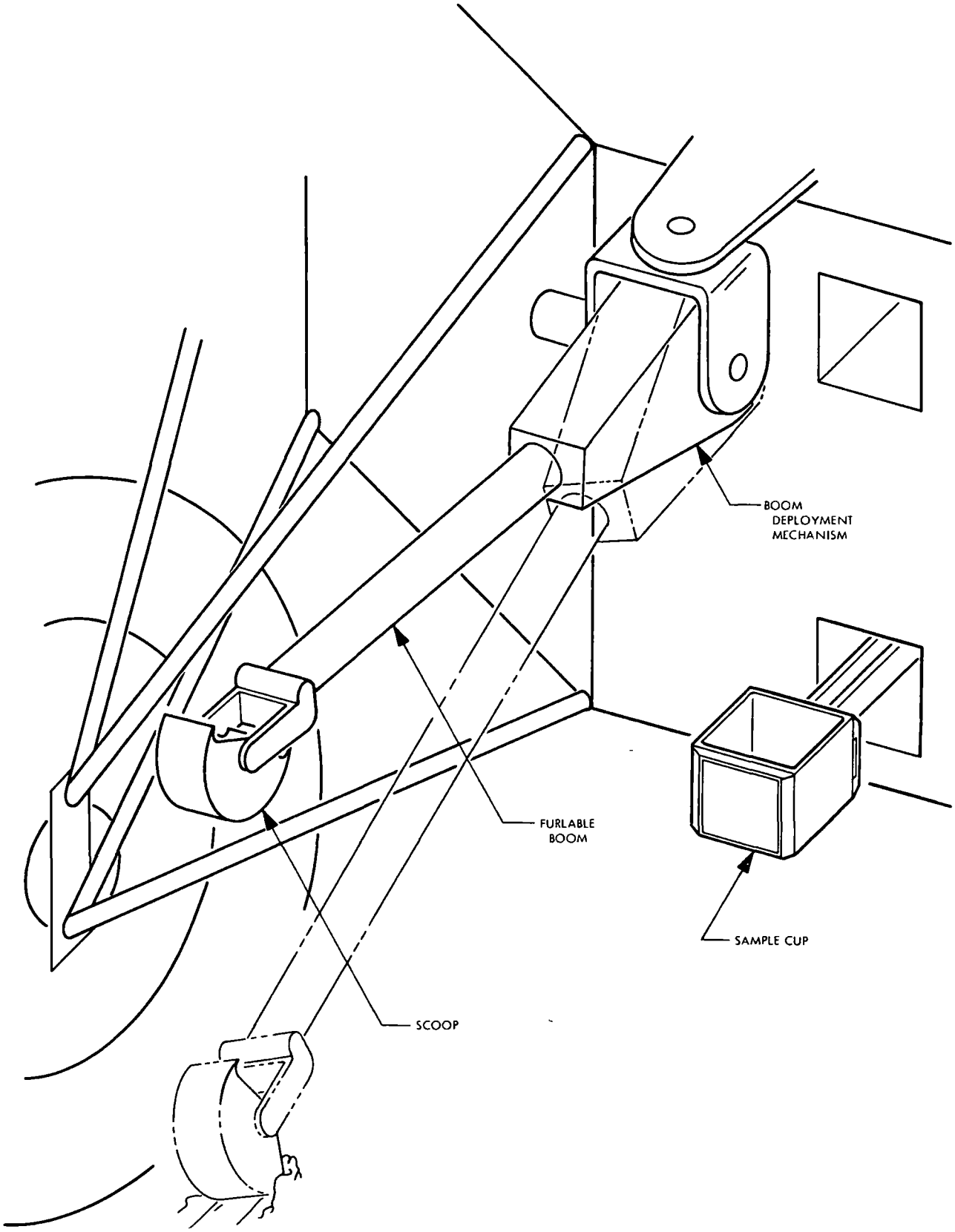

Figure V-35. Bulk Sampler

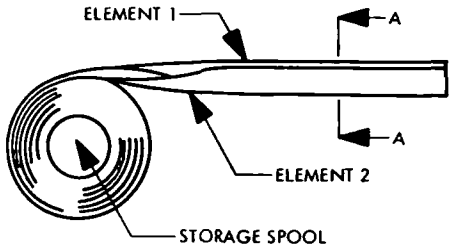

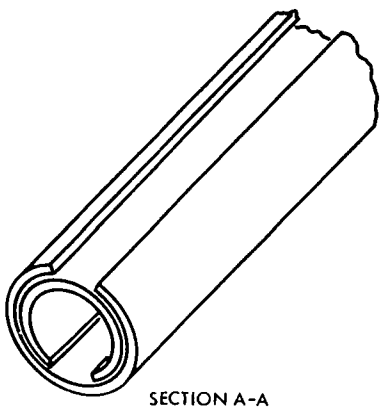

DE HAVILAND'S BI-STEM BOOM PRINCIPLE

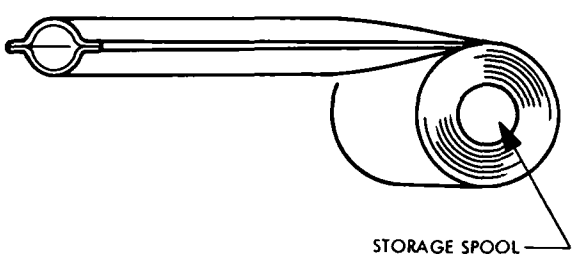

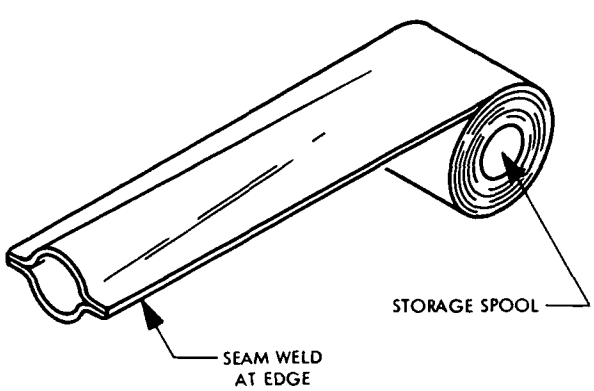

RYAN BOOM

Figure V-36. Booms

Table V-18. Furlable Boom Characteristics

Requirement	Parameter
Boom diameter	1 1/2 inches
Length	3 in. (provides 4 foot reach)
Package size	4 inches by 4 inches by 8 inches
Weight	3 to 5 pounds
Bending strength	30 to 40 ft-lbs
Extension and retracting force	20 pounds

Ryan's boom consists of two thin metal sheets, seam-welded along the edges and formed into a tubular cross-section, which can be compressed flat and rolled on to a storage drum.

Figure V-37 shows a scoop design which enables the sample to be dumped into the sample cup, when the sampler is in its fully retracted (down 80 degrees and left 110 degree) position.

Hard Rock Drill and Particulate Sampler. A boom-deployed, rotary-impact, hard rock drill is suggested as a second and backup sampler Should the bulk sampler be unusable, the drill sampler can also acquire particulate material near the surface (that is, the finer material, rejecting sizes over one to two millimeters). It can obtain samples from large rocks and outcrops, whereas the bulk sampler cannot. Drilled samples from outcrops will be pulverized, and though less desirable than chunks, are useful; they may be the only kind of samples obtainable from larger bodies of rock. Also, pulverized samples can be examined by the onboard science instruments whereas the whole rock samples or rock chips cannot. The hard rock drill may also, on occasion, be able to function as a rock chipper by breaking off corners or edges of rocks for retrieval by the bulk sampler.

The hard rock drill and particulate sampler shown in Fig. V-38 and V-39 would use the same type of boom deployment system as the bulk sampler. Table V-19 defines characteristics of the sampler.

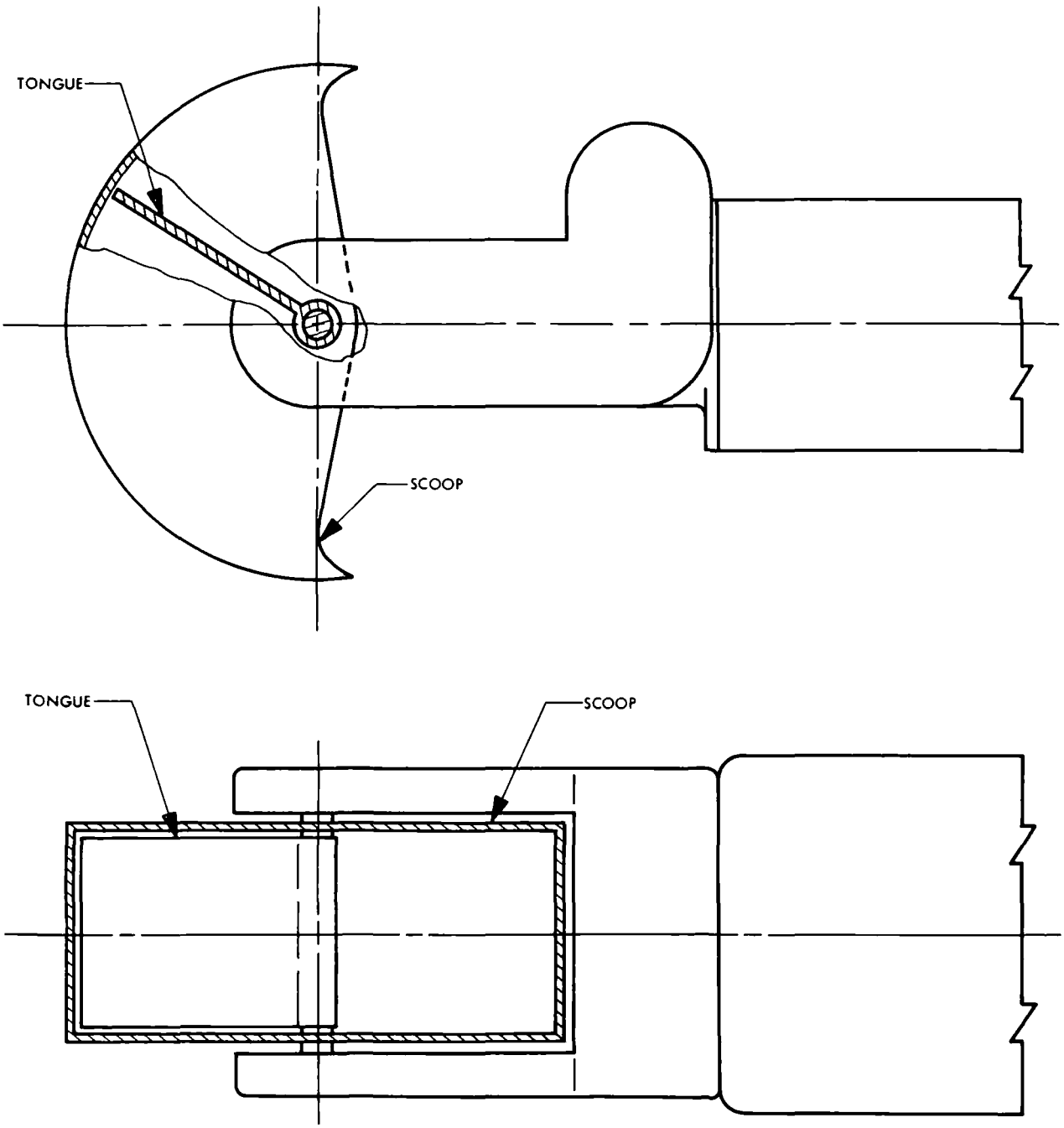

Figure V-37. Scoop Design

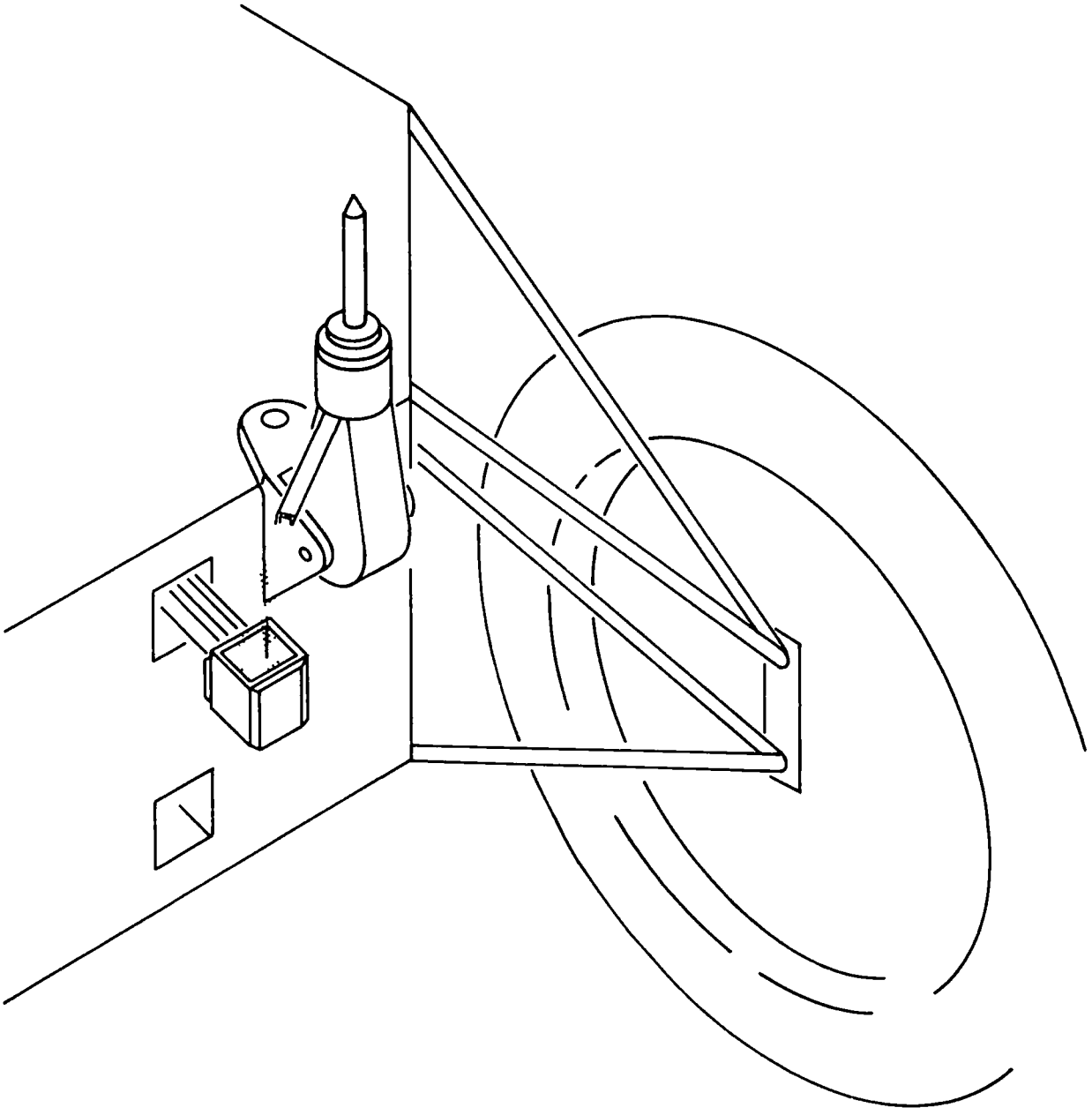

Figure V-38. Hard-rock Drill Dump Position

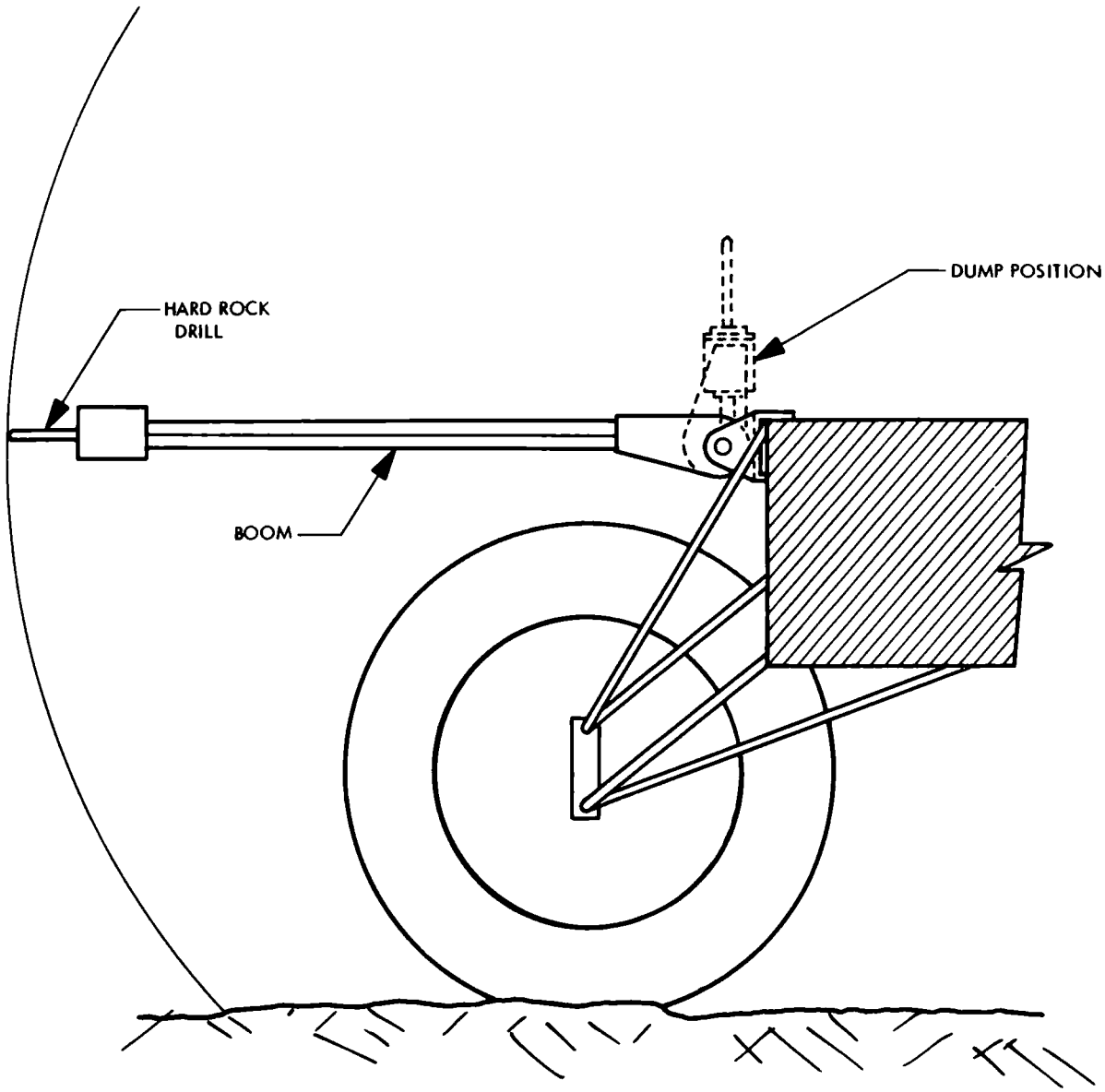

Figure V-39. Hard-rock Drill Operating Position

Table V-19. Hard-rock Drill and Particulate Sampler Characteristics

Requirement	Parameter
Space (stowed)	5 inches by 5 inches by 16 inches
Weight	11 pounds
Power	5 to 10 watts for positioning and 10 to 50 watts for drilling
Motions	Boom: 15 degrees left, 15 degrees right, 90 degrees up, 90 degrees down, and extend 3 feet Impactor: Start and stop Screw conveyor: Start and stop
Total reach	Approximately 4 feet
Drill diameter	5/8 inch
Drill length	4 inches (longer if desired)
Sampling capability	20 to 40 cubic-centimeters per hole (pulverized)
Sampling time	10 to 20 minutes depending on the hardness of the rock

Subsurface Soil Auger. A one-meter auger is suggested as a third part of the sampling system. It will bring subsurface samples to the surface from a depth of one meter (Fig. V-40). The auger flights will transport the subsurface material to the surface where it can then be picked up by the bulk sampler. The auger will not penetrate rock but will indicate if rock is present below the surface. The power required to penetrate the soil will give an indication of the mechanical characteristics of the soil. The auger also provides the subsurface drillings, and a one-meter vent hole, to be analyzed by the hygrometer for the presence of water.

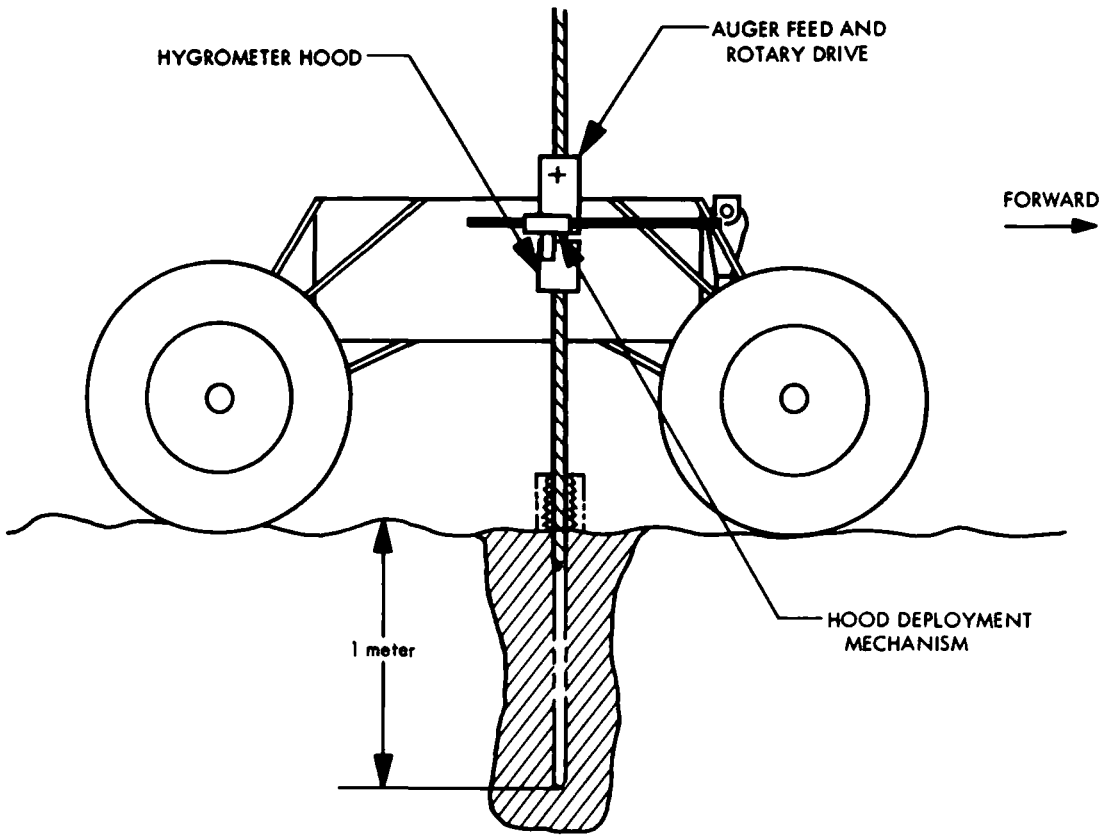

Figure V-40. Auger Operating Position

In Fig. V-41 the auger is shown mounted on the side of the LRV in the stowed position. The auger is both rotated and fed by a drive system through which it passes, similar to a well-drilling rotary or Kelly. The auger would be pivoted to a vertical position for the drilling operation. After the drilling operation, the LRV must back up so that the drillings will be within reach of the bulk sampler. Provisions must be made for release of the auger from the LRV should the auger get stuck or become inoperative during the drilling operation. Table V-20 defines the soil auger characteristics.

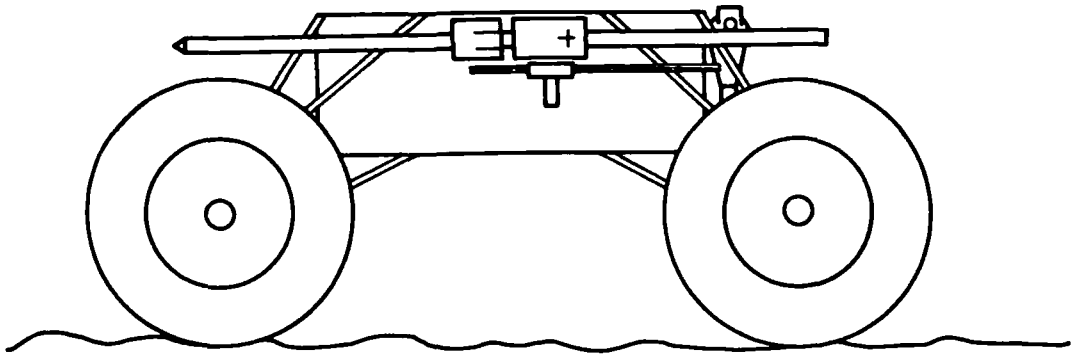

Figure V-41. Auger Stowed Position

Table V-20. Soil Auger Characteristics

Requirement	Parameter
Size	3/4 inches or 1 inch diameter by 72 inches long by 45 degree flights
Weight	9 pounds
Drive size	4 inches in diameter by 7 inches long
Power	30 watts (can be reduced)
Time (one meter depth)	20 minutes depending on soil drillability

Sample Handling and Storage System. In order to handle 3-centimeter diameter rocks, the sample cups proposed for the baseline design have inside dimensions of 4 centimeters on a side so as to easily contain 3-centimeter diameter rock fragments. This gives each cup a capacity of 64 cubic centimeters or about 70 to 80 grams (2-1/2 ounce) of sample. The storage system, as tentatively designed, will hold 116 sample cups giving it a net capacity of 7424 cubic centimeters or about 8 kilograms (about 18 pounds) of sample. It may be permissible or even desirable to add sufficient particulate material along with a rock sample to completely fill the sample cup. This will keep the rock from rattling around and being damaged, as well as allowing two samples to share one cup. Thus, the total possible number of samples is 232. (See Table V-21.)

Table V-21. Sample Handling and Storage System Characteristics

Requirement	Parameter
Weight:	
Cups (0.802 each)	6 pounds
Sample handling storage racks	12 pounds
Space requirement	17 inches in diameter by 12 inches high
Power	3 watts
Cup size (inside)	1 5/8 inches by 1 5/8 inches by 1 5/8 inches.
Stack size (six cups)	2 inches by 2 inches by 12 inches
Number of stacks	20
Number of sample cups	116
Total sample capacity	7400 cubic-centimeters (approximately 9 kilograms)
Arm functions	Rotate about a vertical axis to any of 20 positions
	Raise or lower to any of six positions
	Extend to any of three positions
	Grasp or release cup
	Rotate 90 degrees about its longitudinal to dump samples

Provision will be made to dump any sample either at the time it was put in the cup or at a later time if the sample is not wanted; for example, if all cups have been filled and the LRV comes across a higher priority sampling area, or if an acquired rock were too large it would have to be dumped because it could not be stored. As the cup is retracted from the sample receiving position it will pass under a scraper which will level the top surface of an overfilled cup and provide a dump signal if a rock extends above the top and the top cannot be leveled. Also if such a rock becomes stuck in the sample cup and will not dump, provisions will be made to drop the whole cup.

The sample handling system will be able to transport any cup at any time to and from the following positions:

(1) Storage

(2) Sample receiving position

(3) Any of the onboard analytical instruments

Figure V-42 shows a layout of the sample storage system. In the center is a sample cup handling device (arm) which can index to any of 20 rotary positions and 6 vertical positions, on command, and take a sample cup from any one of the 20 stacks of cups which surround it. Four of the positions are for sample loading and dumping, and for placing the sample in the science instruments. The arm may be positioned at three different radii from the center: an inner position where it can move radially or vertically with a cup attached, a second position for taking or replacing sample cups from storage, and a third position for holding cups in sample receiving position or for placing them in the science instruments. The arm has one additional motion, invert the cup for dumping. Of course, the functions of the arm, or any other such mechanism, are vital to the success of the sampling, so this component would be subject to extensive detail development and test. The sample cup stacks would be designed for easy removal from the LRV by an astronaut.

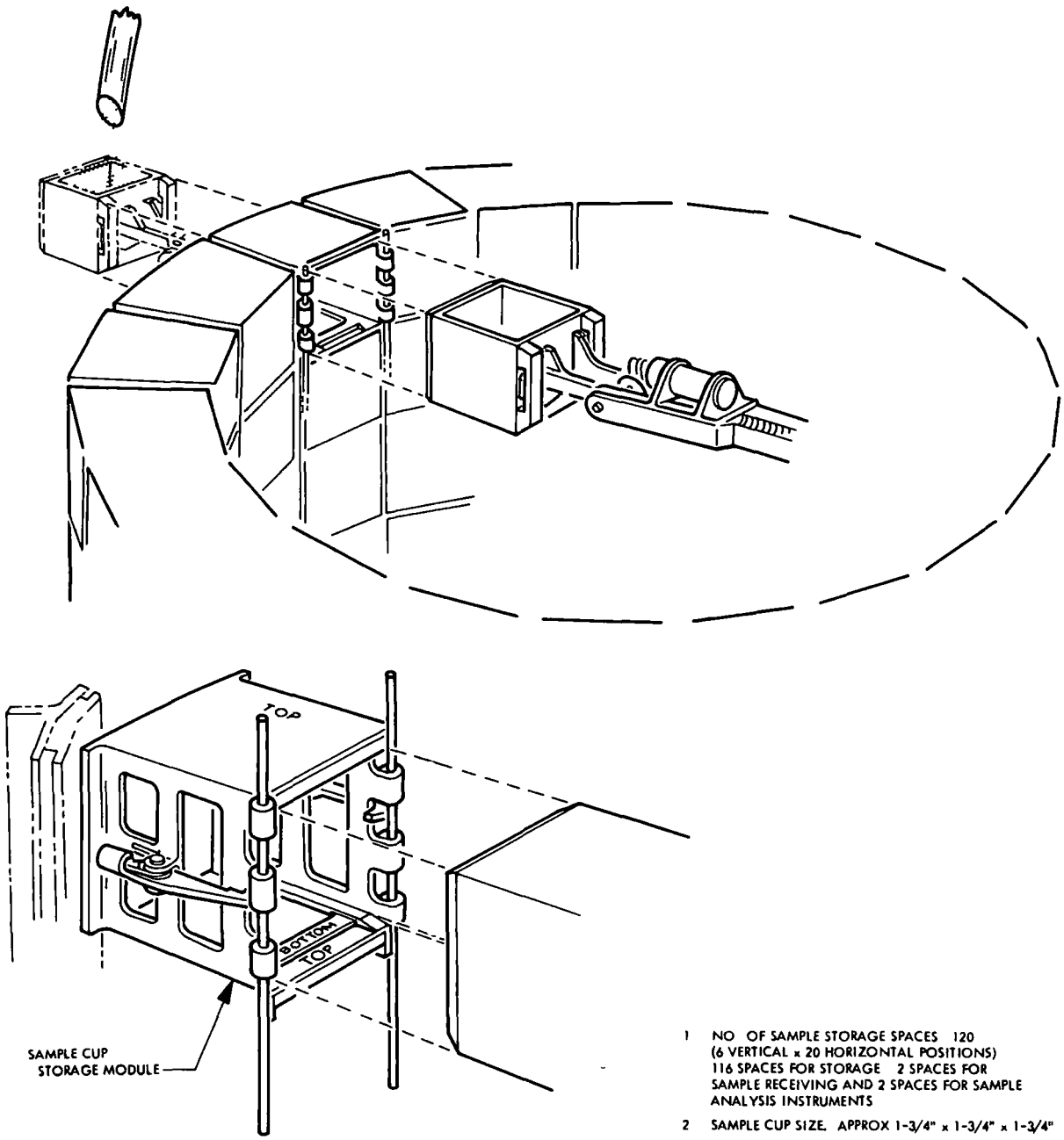

Figure V-42. Sample Storage System

X-Ray Diffractometer. The X-ray diffractometer has been fully described in Refs. V-14 and V-15, so only a few summary remarks will be given here. The primary objective of this instrument is to aid in determining whether to store or discard given samples. It can determine the types and relative abundances of crystalline phases present and identify most major rock forming and accessory minerals. (See Table V-22.)

Table V-22. X-ray Diffractometer Characteristics

Requirement	Parameter
Approximate size	12 inches long by 6 inches wide by 10 inches high
Weight	15 pounds
Power	45 watts
Time per analysis	8 to 60 minutes

This instrument will be fixed, (Fig. V-43) requiring a sample from the sample handling system. An analysis can be performed in from eight minutes to one hour depending on the resolution desired. This is with an X-ray tube source which makes the total power required 45 watts. A radioisotope source could be used to bring the power down to 5 watts but the time for an analysis would go up to 12 to 18 hours requiring a total power consumption of 90 watt hours as compared to 45 watt hours using an X-ray tube.

Alpha-scattering X-ray Spectrometer. The alpha-scattering mode of the instrument is capable of analyzing all elements between boron and calcium (except Ne and Ar) with a sensitivity of at least three atomic percent. The sensitivity for carbon is better than one percent. The elements between titanium and zinc can be identified only to within an atomic number of about ±1, those between zinc and silver to within an atomic number of ±3, etc.

The useful range of response for the X-ray mode extends from sodium through uranium. Only those elements from sodium through nickel are expected to be present as major constituents. Since the energy of the characteristic X-radiation decreases with atomic number, the sensitivity of the method becomes poorer for the lighter elements. Experimental data indicates the following sensitivities for accuracies of ±10 - 20 percent: down to Z = 24, better than 1 percent, to Z = 13, 2 - 5 percent.

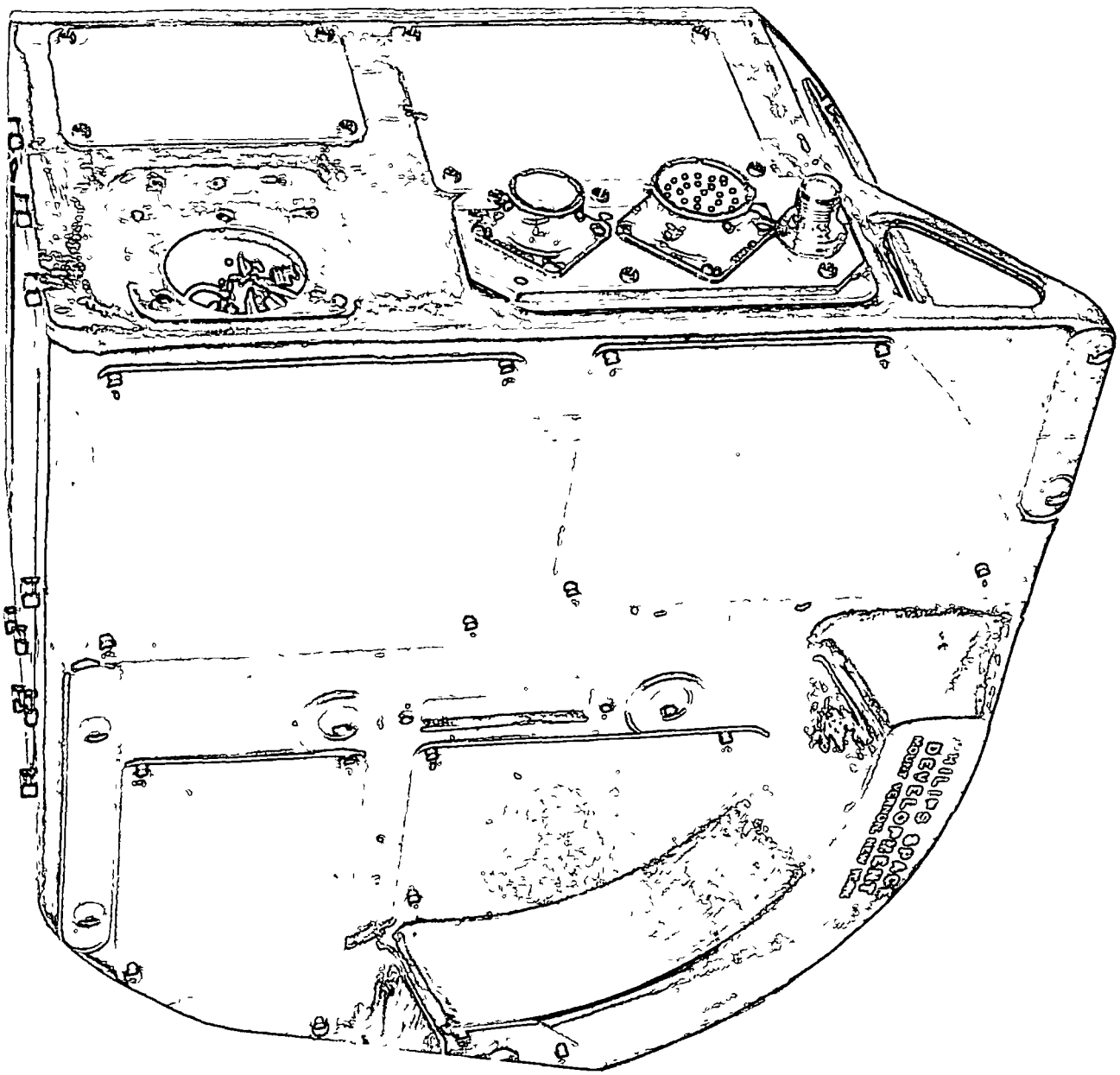

Figure V-43. X-ray Diffractometer

In the X-ray analysis, as a result of the inherent resolution limitation of the detector, it is exceedingly difficult to resolve adjacent atomic-numbered elements, such as Mg and Al. The use of one to three selected absorption filters or optically dispersing channels may be required to overcome this problem.

Measurement characteristics for both scattering and X-ray mode are as follows: Atomic number range = 4 to 92 (scattering mode) and 11 to 92 (X-ray

mode). Event rate = 1 to 10 events/second (scattering mode) and 10 to 3000 (X-ray mode). Detector resolution = 2 percent (scattering mode) and 16 to 20 percent at 7 KeV (X-ray mode).

The remaining paragraphs describe the various elements of the alpha-scattering X-ray spectrometer.

(1) Source. For both modes of the instrument, a method of sample excitation is needed. A radioactive alpha source that would be common to both modes of analysis is 163 d Cm^{242}. ($T\alpha$ = 6.11 MeV). The decay of this species during an approximately half-year voyage is tolerable. A source with an intensity of 100 to 200 millicuries will be suitable.

(2) Detectors (Sensors). For the alpha-scattering mode, the detectors will consist of silicon semi-conductors, probably of the diffused-junction type. Solid-state detectors are used because of their high energy resolution and efficiency for charged-particle spectroscopy.

The requirements of the X-ray mode also call for a pulse-amplitude energy-dependent detector. A gas-filled proportional counter(s) is currently the most suitable device for this. By varying the gas, pressure of fill, effective path length, and mass absorption in the window, a proportional counter can be made to respond preferentially over portions of the energy range. Within the next 12 to 18 months, the state-of-the-art in solid-state detectors may advance sufficiently for them to replace the proportional counter in this application.

(3) Electronics.

(a) Power Supply

1) Alpha-scattering system: Capable of supplying dc voltages of about 24 volts for electronics, and about 7 and 50 volts for detector bias

2) X-ray system: High voltage supply capable of operating the proportional counter(s) at 1600 to 2000 volts, and having regulation of 0.02% over 40°C temperature range

3) X-ray detector amplifier: A low-voltage supply needed to operate the X-ray detector amplifier

4) Memory and programmer: A low-voltage supply needed to operate the memory and programmer.

(b) Amplifiers

1) Alpha-scattering system: Approximately 6 amplifiers will be used in association with the alpha, proton, and guard detectors

2) X-ray system: One linear amplifier will be required for each of the X-ray detectors.

(c) Analog-to-Digital Converters. Two analog-to-digital converters of 128 or 256 channels each will be shared by the alpha, proton, and X-ray systems.

(d) Memory. The memory will contain 256 or 512 words of a maximum capacity of 16 bits per word.

(e) Programmer. The programmer will provide logic circuitry for interfacing with the Science Data System (SDS) so that the operational sequence can be programmed with either an on-board sequencer or via Earth-command.

(f) Mechanical System. For calibrating the instrument, a standard sample of known composition will be transported along on the mission with the instrument. A means of mounting this sample and a method for presentation to the detector assembly must be considered.

Functional Operation

(1) Sequence of Operations. A tentative mission profile would be as follows (starting after positioning of the Lunar Rover Vehicle):

(a) Power turn on in the combined instrument

(b) Stabilization period (10 min)

(c) Calibration readings

1) Alpha-scattering mode (15 min)

2) X-ray mode (5 min)

(d) Background measurement

1) Alpha-scattering mode (60 min)

2) X-ray mode (15 min)

(e) Preliminary analysis of prepared samples (4)

1) X-ray mode (5 min/sample) total of 20 min

2) Alpha-scattering mode (20 min/sample) total of 80 min

(f) Calibration readings

1) Alpha-scattering mode (15 min)

2) X-ray mode (5 min)

(g) Extended analysis of prepared samples (selection based on preliminary analyses)

1) X-ray mode (15 min/sample)

2) Alpha-scattering mode (1 - 2 hours/sample)

(h) Analysis of acquired lunar samples

1) X-ray mode (15 min to 2 hours)

2) Alpha-scattering mode (2 to 8 hours)

(2) Intra-Instrument Logic. The instrument would be designed so as to have the capability of switching from one detector to another upon command from the SDS.

Operating Temperature Range

(1) Alpha-scattering mode: the temperature should be in the range -30°C to +30°C.

(2) X-ray mode: The proportional counter(s) will operate from -50°C to +125°C, but the temperature variation during the counting mode should be limited in order to maintain maximum gain stability.

Functional Interface Requirements

(1) Sample Access. For the analysis of a prepared sample, the alpha-scattering mode requires a flat sample, approximately 1 to 2 inches in diameter (or on a side) at least 0.5 mm thick. The X-ray mode does not require as

much sample as the alpha-mode, a 2 gram sample, approximately 1 mm thick, would suffice. If the larger sample were available, the analysis would be enhanced in the sense that a "more representative composition" might be presented.

(2) Data Format. For the alpha-scattering mode, a maximum of 512 channels (energy intervals) is required. The X-ray mode requires a maximum of 256 channels. Thus, for one complete analysis involving both modes consecutively, a total of 768 channels is required. Associated with each channel will be a number representing the frequency of events in that energy interval. This number will require up to a maximum of 16 binary digits per channel. Some bits will be required for synchronization and parity checks.

The application of data compression techniques may reduce the total number of bits by a factor of two or more.

(3) Programming Requirements

On-Board Commands:

(a) Power on/off

(b) High voltage on/off

(c) Alpha mode/X-ray mode

(d) PHA store/readout

(e) Calibrate

(f) Heater (override by Earth command)

Commands from Earth·

(a) Failure mode (instrument off)

(b) High-voltage control (desirable from Earth)

(c) Detector on/off (e.g., 3 lines, 3-bit word).

Hardware Interface Requirements

(1) Mechanical

(a) Weight: The weight estimate of the combined alpha-scattering X-ray instrument is 14 lb, ±2 lb

(b) Dimensions: The volume estimate of the combined alpha-scattering X-ray instrument is 0.4 to 0.5 cubic foot.

(2) Power. The power requirement of the combined alpha-scattering X-ray instrument is 2.2 watts, ±0.5 watts.

(3) Science Data System (SDS). In addition to the science data already described, it would be desirable to have certain engineering data, such as:

(a) Temperature of the sensor head

(b) Power supply voltages.

Experiment Constraints. If a radioisotopic-thermal generator power system were used on the LRV, the alpha-scattering X-ray spectrometer instrument would have to be shielded from on-board sources. There appear to be no excessive constraints that this instrument should place on other instruments in the spacecraft or in the capsule. Low-energy, low-intensity gamma rays associated with the alpha source may have to be shielded if radiation sensitive instruments are used.

Hygrometer. The hygrometer would be used in conjunction with the one meter soil auger and would measure the equilibrium vapor pressure of water in the drillings brought to the surface by the auger or of vapors outgassing from the hole. The hygrometer detector would be installed in a hood which would be deployed to the ground, and through which the auger would pass while drilling. The hood would have sufficient volume to cover the drillings which would form a mound around the top of the hole.

(1) Functional Requirements

(a) Purpose: To detect the water content of lunar subsurface material.

(b) Range of Instrument. The sensor can measure dew/frost points from +30°C to -110°C. This represents a measurement of partial pressure from 40 millibars to 10^{-6} millibars.

(c) Sensitivity and Accuracy. The accuracy of a sensor used in balloon flights is approximately ±2°C in the lower frost point region. This is

equivalent to an accuracy of about ±30 percent of the amount present at a partial pressure of 10^{-4} millibars. The limit of sensitivity appears to be below 10^{-7} millibars, or a frost point of -125°C.

(2) Functional Elements

(a) Aluminum Oxide Detector. The aluminum oxide element consists of a thin sheet of aluminum which is anodized by a special procedure to provide a porous oxide coating. A gold layer is evaporated on the oxide to form the outer electrode. The element senses absolute vapor concentration. At a fixed frequency, the element changes impedance as water is adsorbed onto the pores of the oxide. Element impedance is an inverse function of the applied frequency. The sensor measures the partial pressure of water vapor in contact with the element, and is not affected by total pressure or temperature. (See Fig. V-44 and Table V-23.)

(b) Instrumentation. The system consists of six basic elements:

1) Bridge Circuit. The bridge circuit has, as one of its four arms, the aluminum oxide sensor. The other three arms are resistors. By driving the bridge circuit at the appropriate frequency, the difference of the absolute values of the voltage between two reference points can be maintained at zero (nulled) as the capacitance of the sensor changes.

2) Transistorized Rectifier and Filter. Because the absolute value of the difference in voltage between two reference points is a constant, it is necessary to compare only their magnitudes. To accomplish this, the reference point voltages are individually rectified and filtered.

3) Differential Amplifier. The differential amplifier in this instrument operates on the difference in dc voltages from the rectifier-filters.

4) Voltage-Controlled Oscillator (VCO). The VCO uses the current-variable dynamic resistance of forward-conducting silicon diodes to provide the means of varying the frequency of a Wien-bridge oscillator. The VCO is designed to operate between 800 and 4500 cycles per second. The frequency of the VCO is controlled by imbalance in the bridge circuit caused by changes in the capacitance of the sensor.

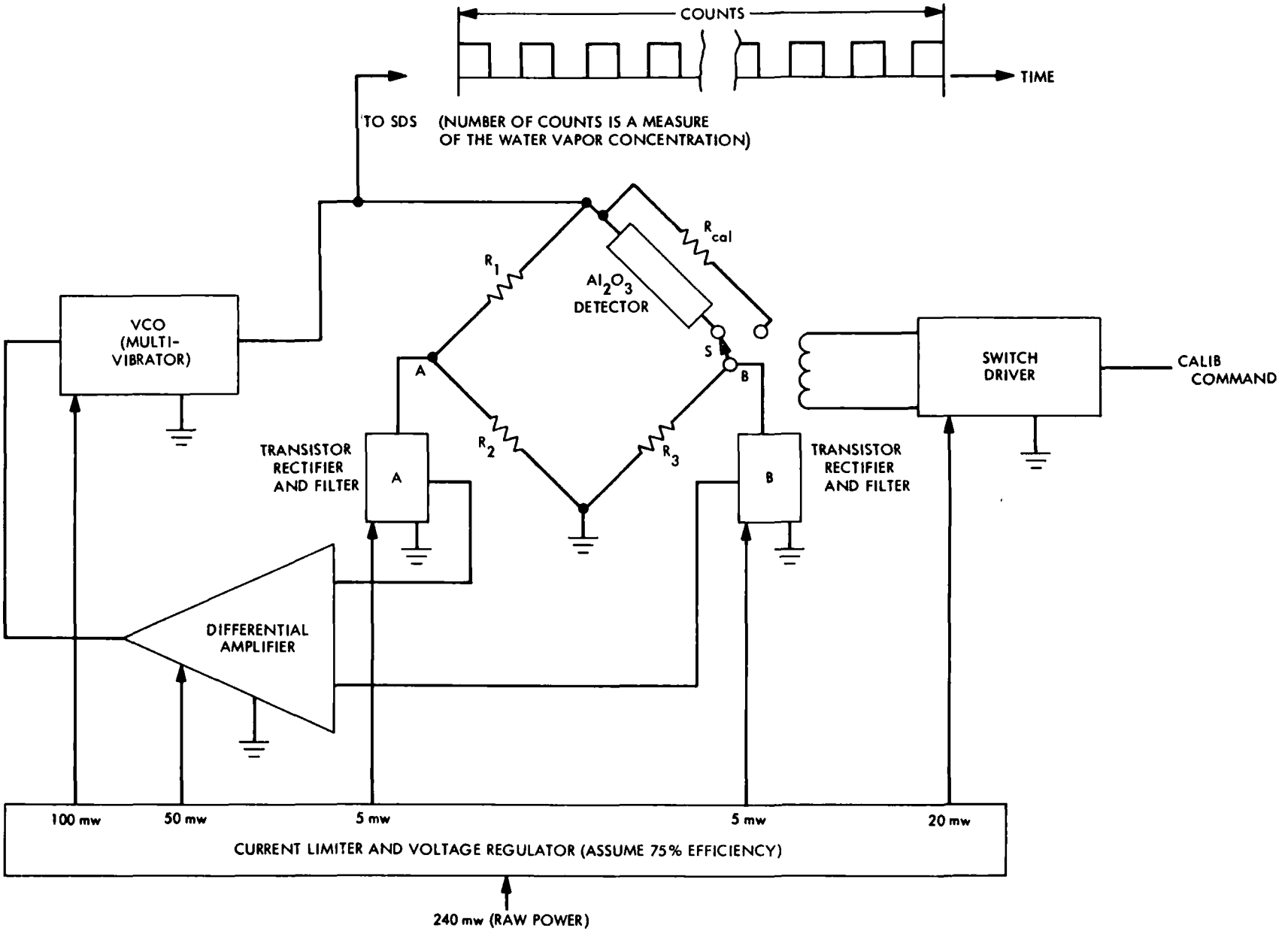

Figure V-44. Aluminum Oxide Detector

Table V-23. Aluminum Oxide Detector Weight Requirements

Element	Weight (grams)
VCO and bridge circuit	50
Rectifier-filter and differential amplifier	50
Sensor, switch and switch driver	20
Regulator with limiter	80
Mount circuit boards on one side of a standard 6 x 6 x 1 in. blivet	150
Total	350

5) Switch Driver. The switch driver is essentially an inverter that allows current to energize a coil upon receipt of a calibrate command, switching the calibrate-element into the bridge circuit.

6) Voltage Regulator with Current Limiter. The voltage regulator is used to provide power at the several voltages needed in the instrument electronics. Assuming a conversion efficiency of 75 percent, 240 milliwatts of raw power are required for operation.

(3) Functional Operation

(a) Sequence of Operation for One Experiment

1) A calibration of the electronics can be accomplished upon command just prior to deployment to lunar surface

2) Auger is deployed to surface

3) Hood is deployed to surface

4) Water content of subsurface material is measured as auger brings material to the surface.

(b) Intra-Instrument Logic. When the instrument is turned on, operation is automatic, except for the ability to receive an external "calibrate" command. If several sensors are used, they could be switched upon command.

(c) Operating Temperature Range. The circuitry (in an engineering-breadboard model) has been operated over the temperature range of -60°C to +100°C with frequency deviations from room temperature values of less than 1 percent. The aluminum oxide sensor located outside the LRV, can operate well below -100°C and up to 75°C.

(4) Functional Interface Requirements

(a) Sample Access/Acquisition. The sensor will be employed to measure the water content of lunar subsurface materials by bringing a sample of subsurface material to the vicinity of the sensor. The equilibrium vapor pressure of water in the solids will be determined at the ambient temperature; more information would be obtained by heating the material during the measurement, as could be done for example by placing the shroud in sunlight.

(b) Data Format and Programming. The data output will be a digital signal representing the frequency of the variable oscillator, a measurement of the frequency by counting the pulses for a fixed period of time. At one kilocycle, a one-second sampling time would give more than sufficient accuracy. Each such measurement could be represented by a 6- to 10-bit word.

(5) Hardware Interface Requirements

(a) Mechanical.

1) Weight. The weight of the instrument will be 0.8 ±0.2 lb (Table V-23).

Each additional sensor, together with switch and switch driver, would add only 20 g to the system. A surface probe is not included in the estimate of weight, power, and volume.

2) Dimensions. The circuitry can be packaged compactly within 15 to 20 cubic inches. The sensor(s) will be mounted separately; each sensor is 0.5 x 0.25 x 0.04 in.

3) Power. The instrument draws current only when operating. The power dissipated is 0.40 watts.

4) Data to Telemetry. The data to telemetry would be a digital signal representing the frequency of the variable oscillator (which is a function of the partial pressure of water vapor in contact with the sensor).

(b) Control from Command System. Several commands would be necessary:

1) On/off

2) Calibrate

3) Sensor switch (if more than one sensor is used).

I. ALTERNATE LRV DESIGN (6-wheel)

Exploratory investigations of various roving concepts (3, 4, and 6 wheeled) indicated that the 4 wheeled baseline vehicle was the most appropriate choice for the initial Atlas-Centaur sized LRV study, because it gave maximum payload with adequate mobility. However, recent improvements in the payload capability indicate that a sufficient margin may exist to permit a more mobile configuration. For this reason, the study effort has been broadened to include a six wheeled LRV approach. This concept is still in early development phase; however, some preliminary results are sufficiently complete to present at this time.

1. Design Concept

Six-Wheel Rover. The six-wheel rover being considered for the Atlas-Centaur sized LRV is shown in Fig. V-45. This design utilizes the same approach as the four wheeled baseline vehicle for the lunar delivery, descent, and landing systems. It uses the same Surveyor descent radar and propulsion

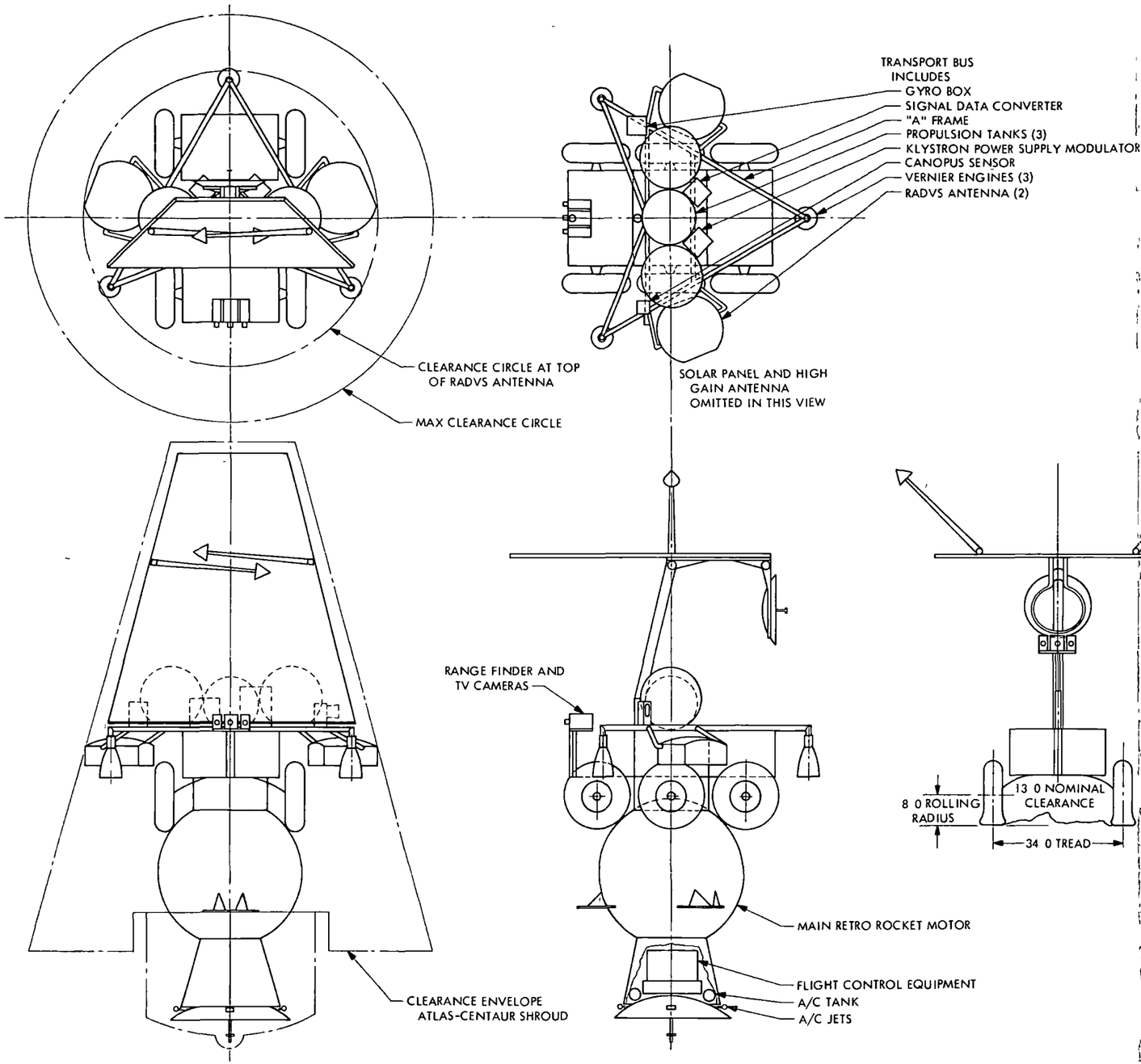

Figure V-45. Six-wheel LRV for Atlas-Centaur

Page intentionally left blank

Page intentionally left blank

systems and performs the same sequence of events. However, it lands on its six wheels with the three equipment compartments in the compressed and interlocked condition as shown on Fig. V-45. After landing, the jettisoning of the descent stage (A-frame equipment) unlocks these compartments from each other and they extend to their normal roving position as shown on Fig. V-45. This roving configuration is then a scaled-up 500 to 600 pound version of the 100 to 200 pound SLRV designed and built for the Surveyor program. This concept has a number of major design problems still being resolved including:

(1) Acceptable landing energy absorption concepts

(2) Appropriate solar panel and high gain antenna support concepts which avoid the effects of high center-of-gravity and extreme displacements during large obstacle climbing

(3) Distribution of weight and spring stiffness between the three compartments for desired mobility

(4) Marginal payload capability (compared to the 4 wheeled LRV).

The following paragraphs discuss some of the problems.

(a) Payload Performance. Exploratory estimates indicate a 25 to 45 pound (approx.) payload reduction of the six wheeled concept as compared to the four wheeled baseline LRV. This estimated reduction is mainly due to:

(1) Increased motor drive weight (5 to 10 pounds)

(2) Increased equipment compartment weight (15 to 25 pounds)

(3) Miscellaneous weights associated with: increased support structure for high gain antenna and solar panels, decreased packaging efficiency, etc. (5 to 10 pounds)

The payload capability of this size of six wheeled LRV is, therefore, in the 46 to 66 pound range as compared to the 91 pound baseline performance previously discussed. This capability may be somewhat limiting from a science viewpoint as indicated in Section III. However, the advantages of the increased mobility may provide access to lunar sites of special interest with sufficient science capability to make this approach desirable.

(b) Mobility. Mobility investigations for this LRV are still in an early phase. However, it is clear that the six wheeled design presents certain improved characteristics over the four wheeled baseline design which offset its reduced payload capability. Some of these are·

(1) Increased obstacle climbing and crevasse crossing capability which improves with increasing wheel, soil friction coefficient

(2) Increased redundancy in event of failure of individual wheel drive

(3) Increased redundancy for soft soil hazards

In general the other mobility characteristics of the six wheeled LRV design are the same as the baseline (4-wheel) design (slope climbing, ground clearance, energy, etc.). However, descent system restraints (due to the vernier motor locations) restricts the wheel tread of this vehicle so that its stability and maneuverability are somewhat limited. The preliminary evaluation of these limitations as well as the obstacle capability are briefly discussed in the following paragraphs.

(c) Landing Stability. The landing stability estimates for the six wheeled LRV have been obtained using the same assumptions as outlined for the four wheeled LRV. Results of the stability analysis are shown on Fig. V-46 which indicates a limiting slope of 20 degrees for landing with the impact velocity conditions of the LRV. It is evident that the reduction in stability from the 30 degree capability on the four wheeled design is due to the less favorable ratio of center-of-gravity height to minimum overturning radius. This is the result of the narrow wheel tread forced by the wheel clearance requirements to avoid the vernier exhaust gas plume.

(d) Maneuverability. On reviewing the maneuvering criteria of the LRVs with regard to· minimum turning radius, reverse drive, and rear steering, it was evident that both the four and six wheeled vehicle were comparable. However, the zero turn radius possible in the four wheeled design does not seem achievable with the six wheeled LRV. This limitation is again mainly the result of the narrow tread forced by the descent system.

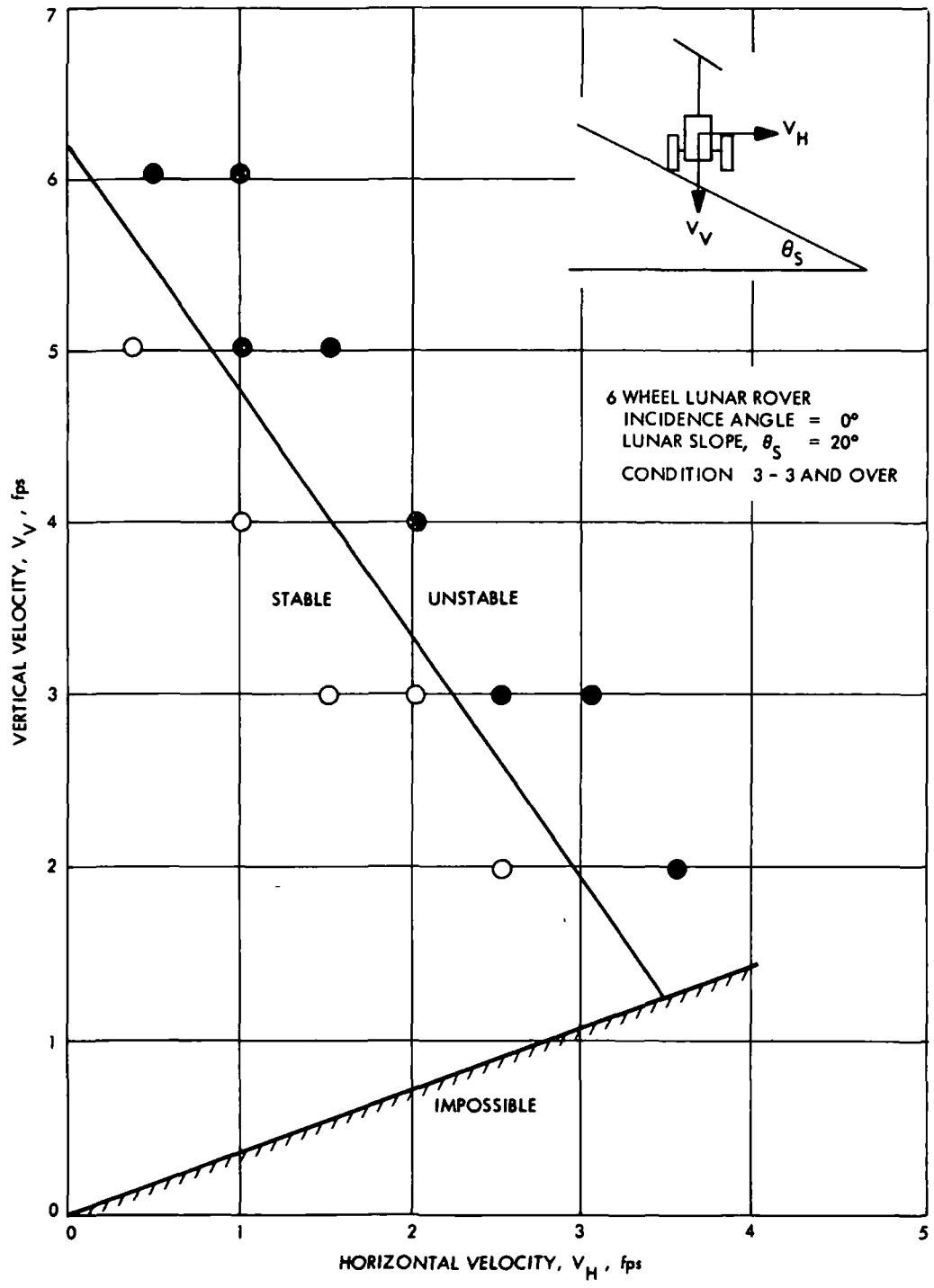

Figure V-46. Six-wheel Landing Stability Boundary Estimate

(e) Obstacle Capability. The general character of the obstacle capability of the four and six wheeled LRV's is shown on Fig. V-47 as a function of the wheel to surface friction coefficient. This preliminary information is similar to that obtained in the study of the six wheeled SLRV rover of Surveyor. Considering equal weight distribution to each of the three axles, preliminary results indicate the obstacle performance of the six wheeled rover is approximately 20 to 30 percent higher than the equivalent four wheeled vehicle in the $\mu = 0.5$ to 0.7 range. This includes the effect of the smaller wheels used on the six wheeled vehicle to maintain an equivalent ground pressure for slope climbing and other performance characteristics. Above $\mu = 0.7$ to $\mu = 1.0$ there is considerably larger advantage of the six wheeled concept (in the SLRV this was approximately a factor of 2 to 3). As indicated, an unequal weight distribution causes the large improvement in obstacle performance to occur above $\mu = 0.45$ rather than $\mu = 0.7$. However, this is at the expense of reduced reverse obstacle capability, as well as other soft soil performance characteristics. Investigations are continuing in this problem area.

J. BASELINE DELIVERY SYSTEM

This study has emphasized the Atlas-Centaur self-landed delivery mode of the LRV, since this appeared to be the most economical approach. Delivery by the manned lunar module is presented in paragraph K as an alternate concept which can accommodate the LRV as a strap-on payload.

1. Delivery System. As illustrated in Fig. V-48 and described in paragraph A, the delivery system of the self-landed concept is essentially the same as that of Surveyor with specific effort being made to adapt Surveyor hardware where possible. In this approach both the Surveyor descent radar hardware (AMR and RADVS) as well as descent propulsion hardware (main retro and vernier motors) have been incorporated into the LRV concept. As a result, the sequence of flight,

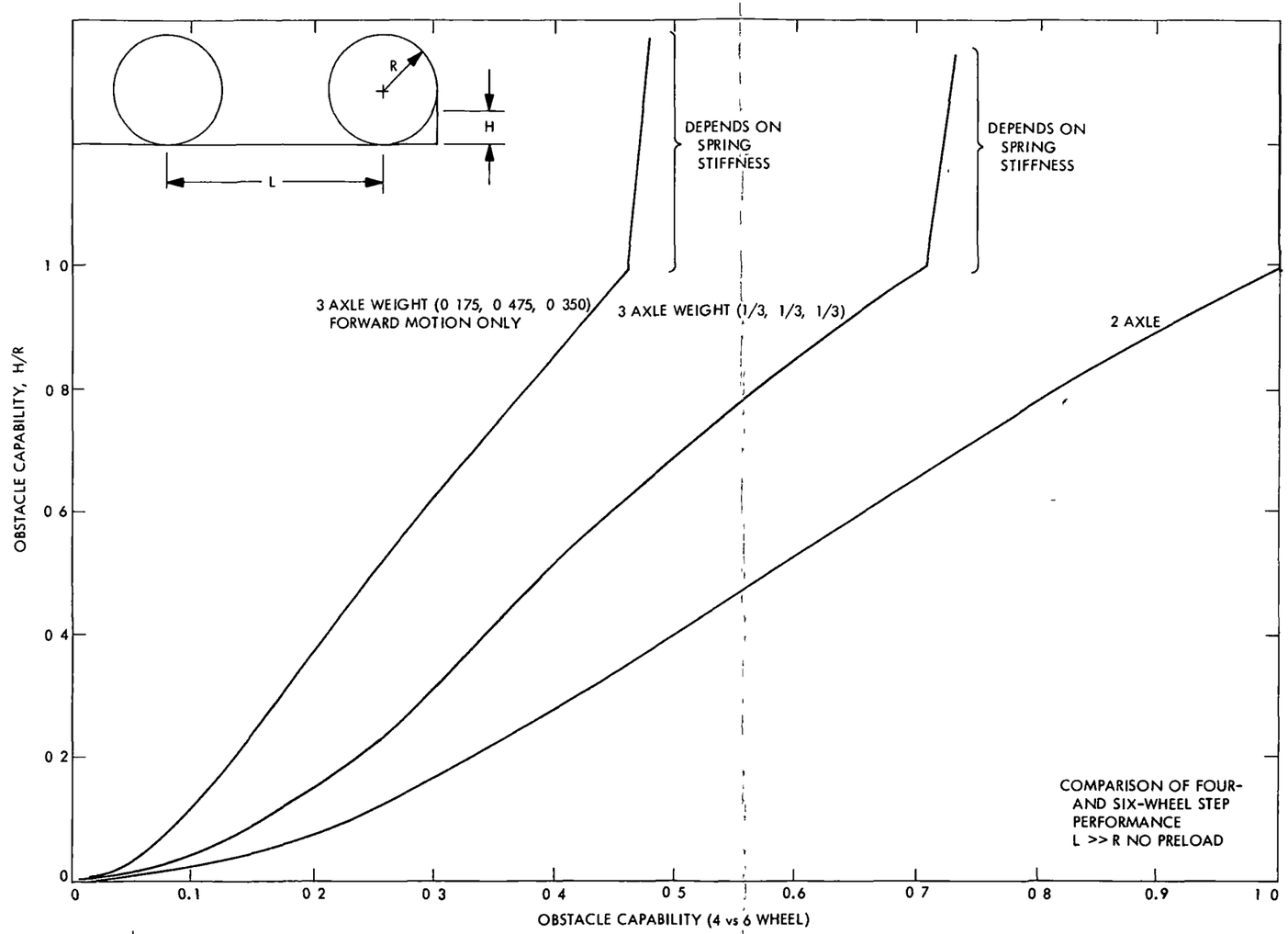

Figure V-47. Comparison of Four and Six-wheel Step Performance

Page intentionally left blank

Page intentionally left blank

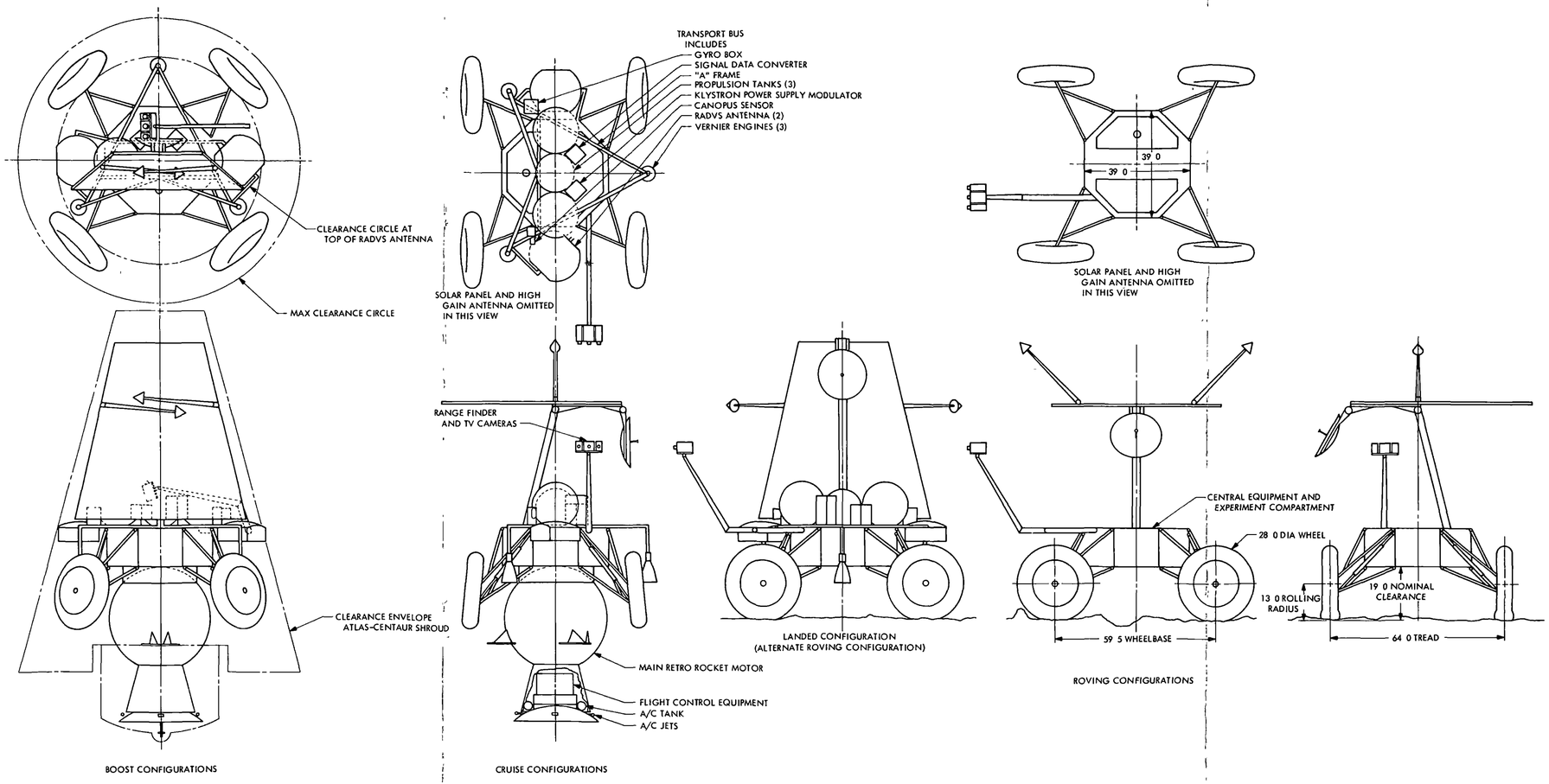

Figure V-48. Four-wheel LRV for Atlas-Centaur

Page intentionally left blank

Page intentionally left blank

descent, and landing events are essentially identical to that of Surveyor as presented in Appendix D There are two relatively minor but important changes incorporated into the LRV system·

(1) The cold-gas attitude control system is relocated inside the main retro nozzle and ejected along with the AMR.

(2) The vertical landing impact velocity is reduced from approximately 18 feet/sec (max) to approximately 5 to 6 fps by allowing the vernier cutoff to occur at near contact conditions.

These changes plus the changes in total weight and configuration gave rise to questions regarding: propulsion system soft landing payload capability, control stability during descent, landing stability, and landing energy absorption requirements.

The following paragraphs explore these questions and, in addition, briefly consider the problem of flight thermal control (for both delivery modes).

Propulsion System Soft Landing Capability. Since the LRV would weigh approximately 50 pounds more than Surveyor VII, a study was made to determine if it would be feasible to use hardware from the Surveyor propulsion and guidance systems on a spacecraft designed to land the LRV on the Moon

The study concentrated on the capability of Surveyor to operate under increased payloads. Efforts were first made to maximize Surveyor payload without any change in hardware or spacecraft design To accomplish this the midcourse and terminal maneuvers of Surveyor were optimized and excess propellant replaced by payload The optimized payload would represent the maximum capability of the Surveyor propulsion system if used on the LRV spacecraft.

In this study it was assumed that no midcourse propellant remained during the Surveyor terminal descent and that approximately 10 pounds of propellant was reserved for variations in the specific impulse and mixture ratio of the vernier engines and for thrust vector misalignment of the retro rocket. The remaining propellant included 2 pounds of unusable propellant trapped in the lines, bladder and standpipe and 132 pounds of usable propellant available for the terminal descent

Propellant consumption was calculated and plotted as a function of burnout slant range and velocity (Fig. V-49) To minimize the propellant requirement and still land safely on the Moon, burnout velocity and slant range were designed to occur above, but as close as possible, to the line segments Figure V-49 indicates that if the nominal burnout is designed to occur at approximately 27,000 feet and at a velocity of 375 feet per second, the propellant requirement would be 132 pounds Figure V-49 also indicates that if the nominal burnout velocity were reduced to 200 feet per second (a minimum imposed by radar constraints) and if the nominal burnout altitude were reduced to accommodate the 200 fps velocity, the propellant consumption would be decreased by 10 pounds. If, in addition, the expected error in predicting burnout slant range is recalculated from flight data, it is found to be significantly less than the conservative values which were used during the Surveyor missions. (The values were determined by combining estimates of all interfacing systems errors through the Monte Carlo technique.) The 3σ dispersion on burnout slant range was reduced from ±9000 feet to approximately ±2700 feet. Because of the small sample size (Table V-24), this was increased to ±4000 feet.

If the error ellipse is reduced to ±4000 feet of dispersion in burnout slant range and ±100 feet per second of dispersion in burnout velocity, the propellant requirement is reduced to only 105 pounds. A total savings of 27 pounds in propellant could be realized Since this propellant would have remained with the Surveyor spacecraft until touchdown, it can be replaced by payload on 1-to-1 ratio

In addition to this 27 pounds, analysis indicates that the propellant reserved for variations in specific impulse, mixture ratio and thrust vector misalignment can be reduced 5 pounds and payload increased 5 pounds. Also, by flying a 90-hour mission instead of the Surveyor 66-hour mission, less energy would be required during terminal descent and an increase in payload of 13 pounds could be realized Finally, because the LRV mission is to translate across the Moon's surface, accuracy in landing close to a preselected target will not be as important as it was for Surveyor The midcourse maneuver capability could be reduced from 50 meters per second to 15 meters per second, payload increased by 10 pounds and the Atlas-Centaur injected weight maintained constant. Without significantly reducing the probability of success, Surveyor's trajectory, midcourse

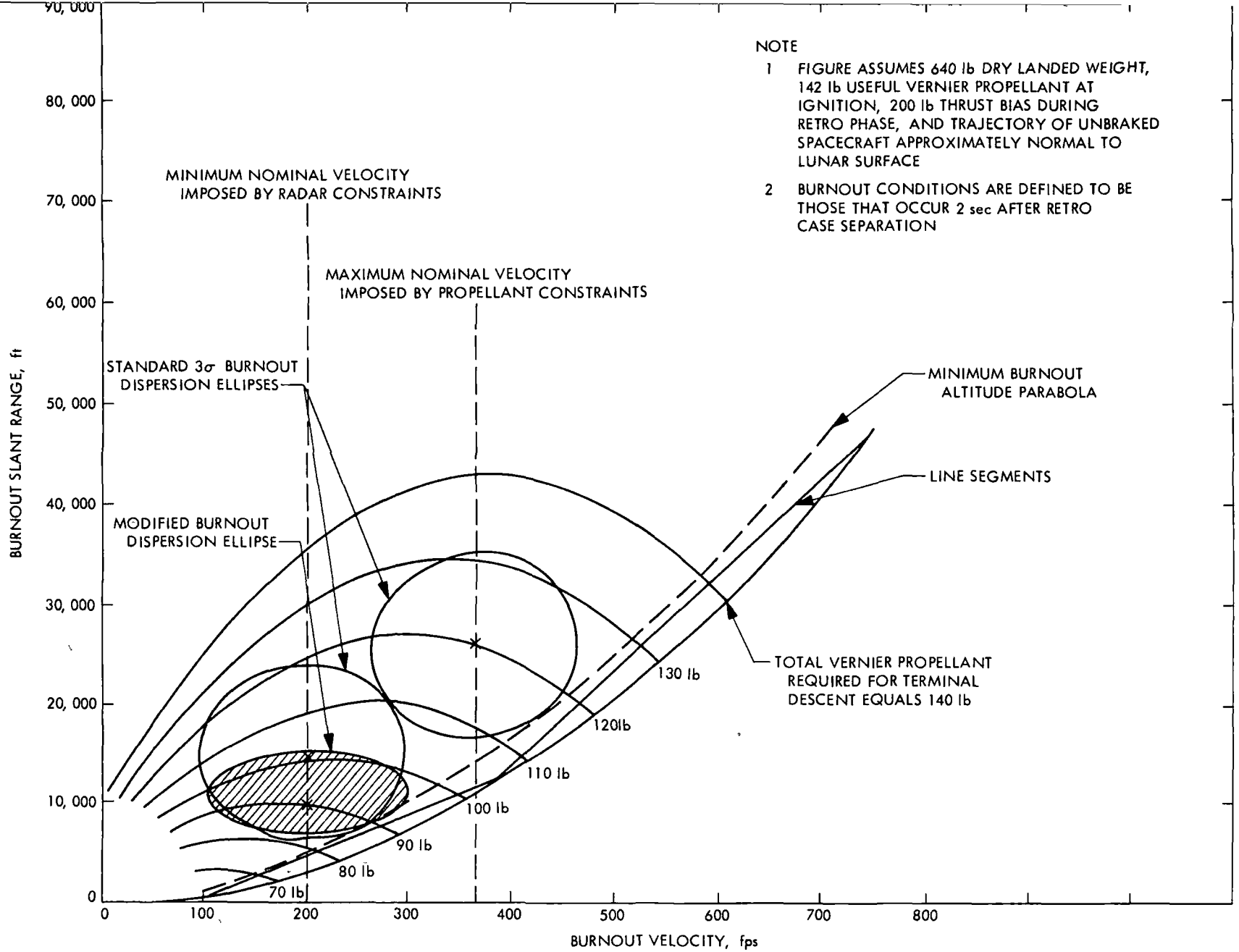

Figure V-49. Surveyor Descent Parameters

Table V-24. Surveyor Spacecraft Burnout Dispersions

Spacecraft	Predicted Burnout Range (feet)	Actual Burnout Range (feet)	Predicted Burnout Velocity (feet per second)	Actual Burnout Velocity (feet per second)
Surveyor I	28,415	27,850	394	431
Surveyor III	34,734	36,158	460	493
Surveyor V	6,600	6,300	94	88
Surveyor VI	40,800	40,645	482	515
Surveyor VII	48,000	51,259	477	447

and terminal maneuvers can be optimized and the payload increased by approximately 55 pounds. Without any change in hardware, the Surveyor propulsion subsystem could be used to land approximately 705 pounds of dry weight and 10 pounds of residual propellant on the Moon. This is sufficient capability to make it feasible to incorporate the Surveyor propulsion system on a 700-pound integrated LRV. Table V-25 summarizes the possible means of increasing Surveyor payload. Included are alternatives which require no hardware change, little expense and no new technology, to alternatives requiring major redesign with costly and time consuming development programs.

Terminal Descent Stability Investigation As illustrated in Fig. V-48 the self-landing LRV has a center of gravity which is approximately twice as far from the center of the retro rocket nozzle as was the center of gravity on Surveyor (28 inches for Surveyor versus 60 inches for the LRV). A preliminary analysis was made to determine if the resulting offset between the retrorocket thrust vector and spacecraft c.g. was within the capability of the attitude control system.

On Surveyor, the pitch and yaw torques exerted on the spacecraft during the retro engine firing were controlled through the selective throttling of the three vernier engines. The roll torque was controlled by a roll actuator on Vernier Engine 1 which pivoted the engine ±5 degrees around an axis in the x-y plane. The pitch and yaw torques exerted on Surveyor were proportional to the

Table V-25. Increase in Capability of Surveyor Propulsion System

Change	Comments	Increase in Payload	Total Landed Weight
Reduce burnout altitude.		27	687
Reduce propellant allowance for variations in the specific impulse and mixture ratio of the vernier engines and thrust misalignment of retro engines.	Current allowance ~ 10 pounds.	5	692
Fly a 90 hour mission instead of a 66 hour mission.	Depending on launch period, trajectories are possible which would allow a total increase in payload of 33 pounds.	13	705
Reduce midcourse capability from 50 meters per second to 15 meters per second.	Launch vehicle injected weight maintained constant. Because of mission contingencies, it is not recommended that midcourse capability be reduced below this level.	10	715
With Minimum Hardware Changes			
Replace retro rocket with Burner II (1440) rocket motor with lighter nozzle.	Launch vehicle injected weight would have to be increased. Further analysis is necessary to assess secondary effects.	44	759
Approximately 1 Year's Development and Redesign Costing $1 Million			
Replace steel retro case with titanium retro case.		13	772
Approximately 2 Years' Development and Redesign Costing $5 Million			
Replace conventional retro propellant with higher energy propellant containing beryllium additive.	Development program is costly and dangerous.	25	797

offset between the center of gravity and retrorocket thrust vector. These offsets were due to an angular misalignment of the retrorocket, a lateral error in positioning the retrorocket and a migration of the thrust vector about the centerline of the retrorocket nozzle. For the torques exerted about the pitch and yaw axes of the LRV spacecraft, a worst case is studied if it is assumed that the total offset on Surveyor was due to an angular misalignment and, therefore, proportional to the distance between the center of the retro nozzle and the center of gravity of the spacecraft. Table V-26 summarizes the maximum distance between the Surveyor retro thrust vector and total spacecraft center of gravity and the maximum pitch, yaw and roll torques experienced during the retro engine firing.

Due to the thrust, throttling range, response and location of the vernier engines, the offset between the retrorocket thrust vector and spacecraft center of gravity was limited to 0.2 inches. However, as noted in Table V-26, the maximum observed was 0.027 inches. Because the margin is more than a factor of 7, there is no doubt that the Surveyor attitude control system could control the pitch and yaw torques which would be exerted on the self-landing LRV.

Roll torques result from swirl in the retro exhaust gases acting on the retro nozzle and from a combined lateral and angular displacement of the thrust vector from an axis passing through the center of the retro nozzle and the center of gravity of the spacecraft. If either the lateral or angular displacement is zero, the only roll torque exerted on the spacecraft will be that from swirl in the nozzle. The component resulting from thrust vector misalignment will be zero.

The roll torque which could be tolerated by Surveyor was a function of the thrust commanded of Engine 1. The engines could be throttled from 104 to 30 pounds thrust but during the retro firing the nominal thrust of Engine 1 was 67 pounds ±10. The resultant roll torque capability was approximately 220 inch pounds ±33. This is significantly above the maximum roll torque which would result by approximately doubling the distance between the center of the nozzle and the center of gravity of the spacecraft (60/28 x 62 inch pounds = 133 inch pounds).

Table V-26. Surveyor Retro- thrust Misalignment Data

	Requirement	Surveyor Spacecraft				
		S/C I	S/C III	S/C V	S/C VI	S/C VII
Maximum distance between retro thrust vector and total spacecraft center of gravity (inches)	Less than 0.200	0.008	0.017	0.013	0.027	0.010
Maximum S/C pitch/yaw torque at retro ignition (inch-pounds)	Less than 2000	80	390	100	350	340
Maximum S/C steady state pitch/yaw torque during retro firing (inch-pounds)	Less than 2000	75	175	125	275	200
Maximum S/C roll torque at retro ignition (inch-pounds)	Less than 187 (nominal) Less than 90 (minimum)	47	20	25	28	20
Maximum S/C steady state roll torque during retro firing (inch-pounds)	Less than 187 (nominal) Less than 90 (minimum)	62	35	60	60	40

In addition, because much of the roll torque resulted from swirl in retro exhaust gas and since the lateral misalignment would not vary between Surveyor and the self-landing LRV, the only element which would tend to increase the roll torque from Surveyor would be the extended length between the center of the nozzle and the spacecraft center of gravity. A conservative estimate would be that the roll torque would be less than 90 inch pounds and well within the capability of the system.

Landing Stability. In order to establish the landing velocity requirements of the LRV on surface contact a review was first made of the Surveyor landing performance. Flight data obtained from four of the five successful Surveyor landings indicate that the landing system performed well within the impact 3σ velocity predictions. Figure V-50 shows the performance of SC-1, SC-5, SC-6 and SC-7 relative to the 3σ predictions.

Three other important parameters not shown in Fig. V-50 are the spacecraft incidence angle at touchdown, the horizontal velocity at touchdown, and the touchdown rate. The first two of these parameters are interrelated. Surveyor data shows that the vehicle was kept nearly level at touchdown resulting in a low horizontal velocity. Table V-27 shows the horizontal velocity and incidence angle for the Surveyor landings.

The 3σ prediction for the horizontal velocity at touchdown was less than 5 fps and for the incidence angle was less than 7 degrees.

Since Surveyor experience has shown no intolerable dust effect from the vernier motors, a lower engine cutoff altitude resulting in a lower vertical velocity at touchdown seems feasible for the LRV. Figure V-51 is an extension of Fig. V-50 showing the engine cutoff altitude versus the descent velocity for constant velocities at touchdown.

Stability estimates for the four wheel rover have been obtained using the following assumptions:

(1) The most critical condition is a downhill landing with a vehicle orientation such that the ratio of the center of gravity height to overturning radius is maximum. Past Surveyor experience has shown this to be the case. This assumption neglects possible degradation due to three-dimensional effects as found for the Lunar Module.

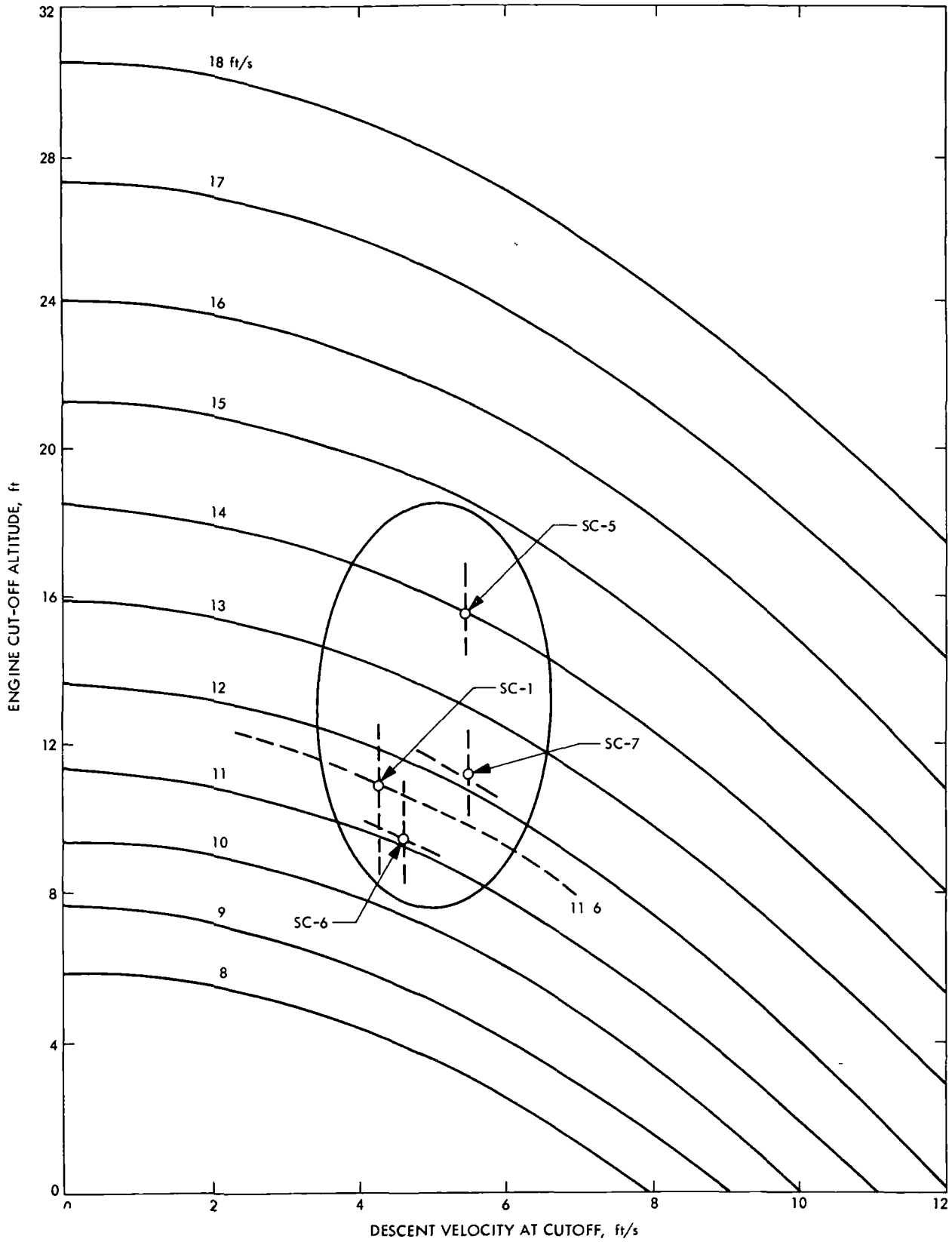

Figure V-50. Three-sigma Ellipse Showing Prediction in Descent Velocities and Engine Cutoff Height

Table V-27. Horizontal Velocity and Incidence Angle for Surveyor Landings (SC-1, SC-5, SC-6, and SC-7)

	SC-1	SC-5	SC-6	SC-7
Horizontal velocity at touchdown (fps)	0.8	< 1.2	1.0	< 0.2
Incidence angle at touchdown (degrees)	1.8	< 3.2	2.3	< 0.5

(2) The vehicle acts as a rigid body during the landing maneuver. This assumption is generally conservative since the deflection of the landing gear tends to reduce the ratio of center of gravity height to overturning radius. It is not conservative in the sense that no rebound is allowed.

(3) In calculating the stability profiles it is assumed that the linear momentum along the line connecting the vehicle center of gravity to the contact point is reduced to zero instantaneously. The remaining linear momentum is converted to rotational momentum. This assumption implies an infinite coefficient of friction and leads to a linear relationship between the vertical touchdown velocity and the horizontal touchdown velocity for a neutrally stable condition. Thus, the stability boundary is a straight line.

The stability profiles for the four wheel rover landing on lunar slopes of 20 degrees and 30 degrees are given in Fig. V-52 and V-53. These two figures in conjunction with Fig. V-51 establish the preliminary requirements for the descent system.

Energy and Strength Requirements. As a result of the Surveyor experience and the stability estimates presented in the previous section, the preliminary landing system requirements being considered are: Vertical velocity, 5 to 6 fps and Horizontal velocity, 1 to 2 fps. The performance of the baseline design is examined using the above requirements. It is desirable to meet these requirements within the stroke and load capability available from the roving mechanism, otherwise additional weight will be required and the roving performance will be

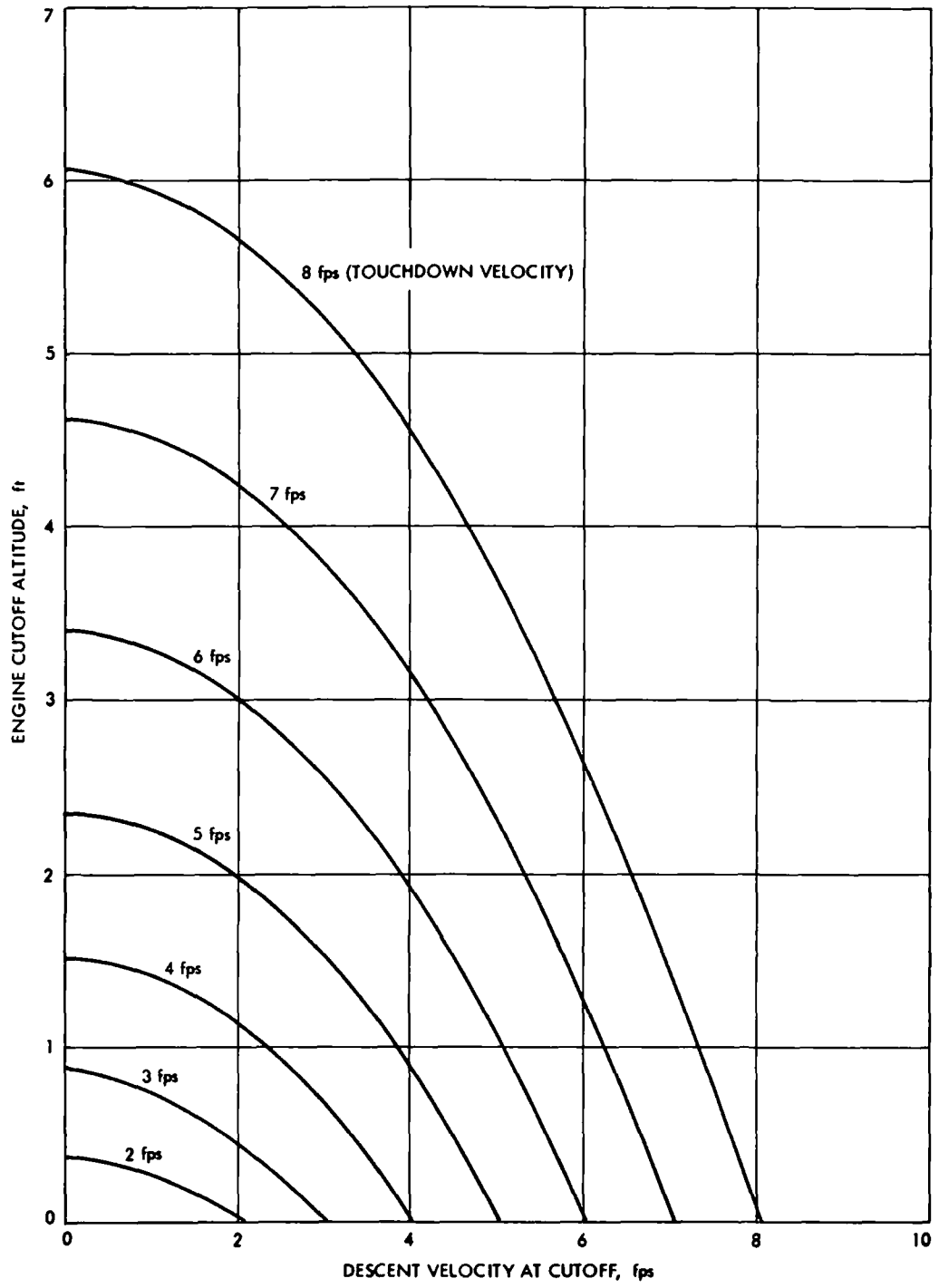

Figure V-51. Engine Cutoff Altitude Versus Descent Velocity

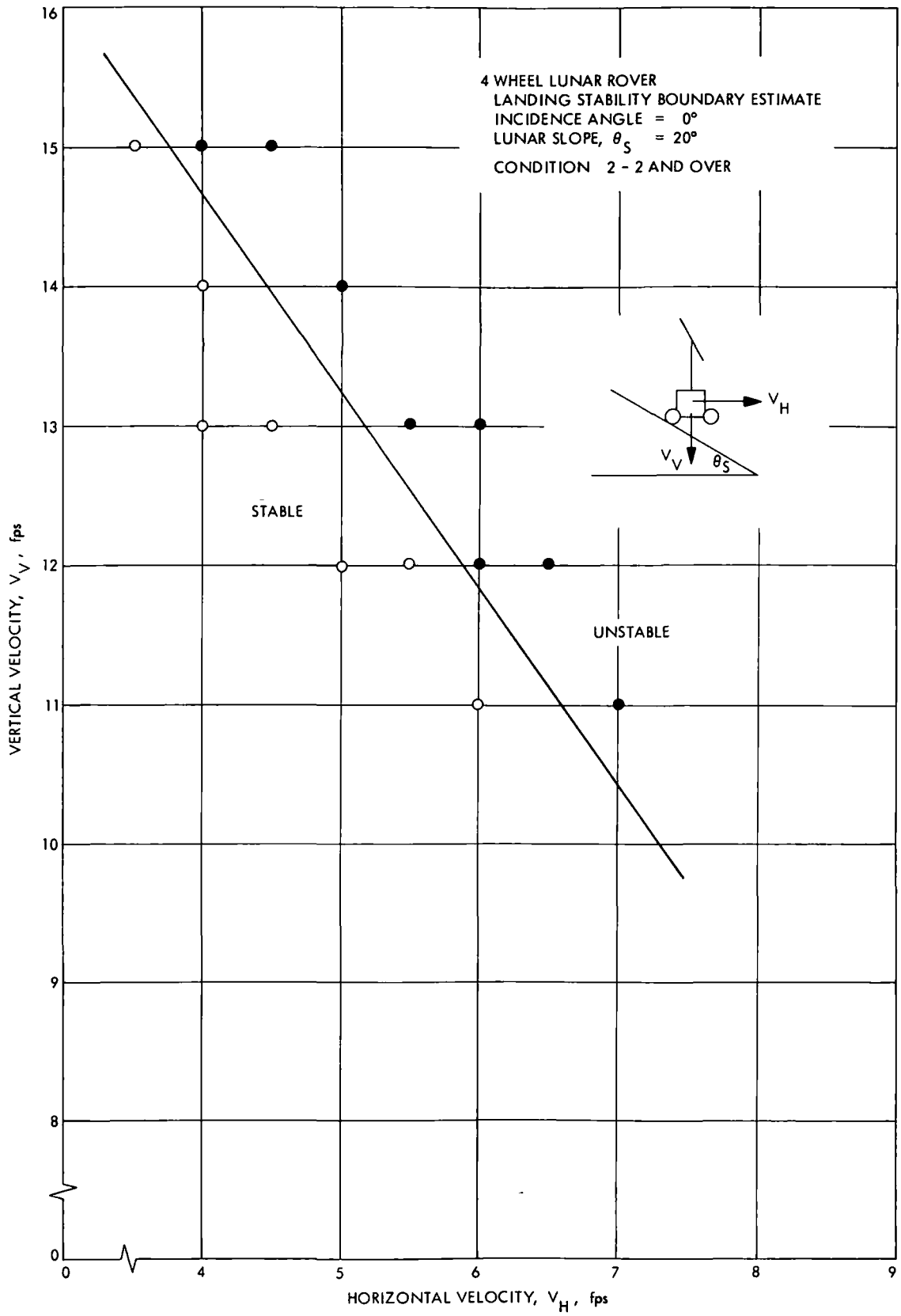

Figure V-52. Four-wheel Landing Stability Boundary Estimate (20-degree Slope)

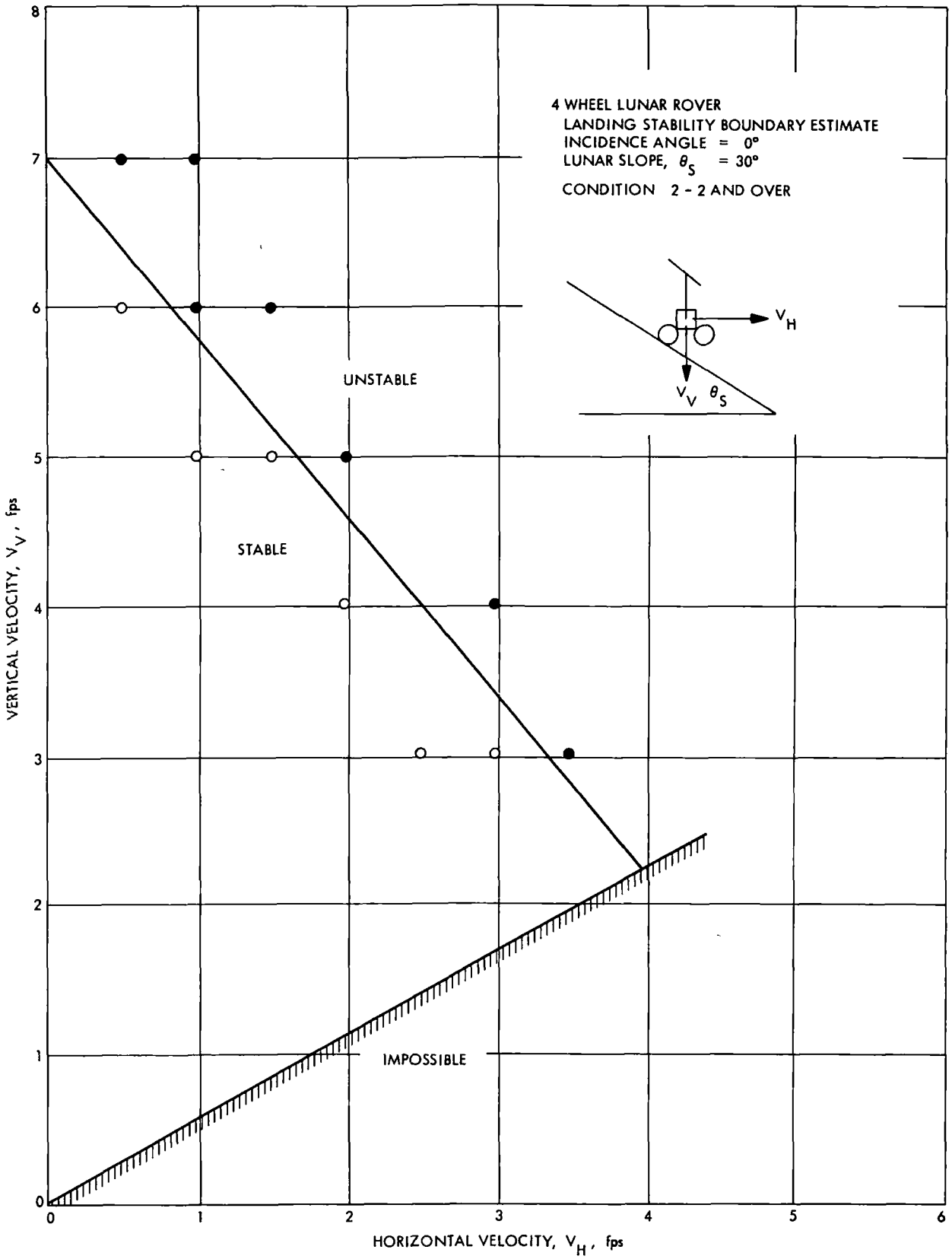

Figure V-53. Four-wheel Landing Stability Boundary Estimate (30-degree Slope)

degraded to provide the additional capability. For conservatism, the energy dissipated in the soil and in the tire is neglected. The landing velocity, load applied, and stroke required can be related if four simplifying assumptions can be made:

(1) The velocity is parallel with the landing mechanism motion

(2) The landing mechanism is a constant force device to minimize stroke

(3) The landing mechanism is weightless

The derived relationships, based on the above assumptions, should be used as an order of magnitude estimate only, since the assumptions are not valid in all cases.

A preliminary investigation of the vehicle landing dynamics has shown that upon touchdown the rotational rates induced due to a nonsymmetric landing are high. Hence, the time delay between the first and second impact is very small and for preliminary analysis it will be assumed that all the kinetic energy will be absorbed by two wheel assemblies.

A simple balance of kinetic and potential energies gives

$$\frac{Wv^2}{2g} = Nsf$$

where

W = Earth landing weight, in pounds

v = velocity at touchdown, fps

g = Earth acceleration of gravity ft/sec^2

N = number of active energy absorbing devices

s = stroke of contact relative to center of gravity, in feet

f = force at contact, in pounds

For the baseline design, with

$W = 700$ pounds

$g = 32.2$ ft/sec^2

$N = 2$

The above relationship simplifies to

$$v = 0.43 \sqrt{fs}$$

The radial strength of a lunar wire tire, scaled from the 40 inch x 10 inch LSSM wheel, maintaining a rigid contact pressure of 1.11 psi for a 500 pound roving vehicle with $\zeta = d/D = 0.25$, is 365 pounds.

The maximum stroke available is approximately 9 inches; however, to account for the desire for low lateral motion due to the suspension linkage the preliminary analysis is limited to 6 inches.

The maximum total velocity without exceeding the roving wheel capability can now be estimated.

Thus,

$$V_{maximum} = 0.43 \sqrt{\frac{(365)(6)}{12}} = 5.7 \text{ fps}$$

The allowable velocity combinations, due to the limitations of the tire are simply given by

$$V_H^2 + V_V^2 \leq 5.7$$

where

V_H = horizontal touchdown velocity, fps

V_V = vertical touchdown velocity, fps

The above relationship is shown graphically in Fig. V-54.

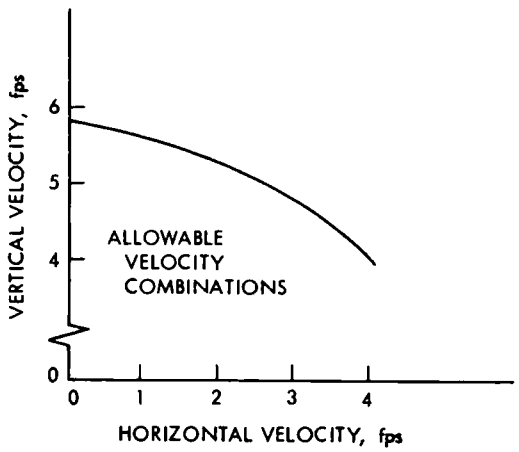

Figure V-54. Tire-limited Touchdown Velocity Combinations

Several considerations should be mentioned in conjunction with the above results:

(1) The distribution of loading is partly equalized by rigid body rotations if contact is on a flat surface. The effect of high contact velocity at the second point of impact due to induced rotations is minimized by using near constant force devices.

(2) The effect of initial velocity not being parallel to mechanism motion (assuming the mechanism has only 1 degree of freedom) is the generation of very large forces normal to the mechanism motion unless the forces are relieved by secondary motions of the mechanism, such as wheel rotation and lateral displacement of a tire if the motion is within the permissible displacements, or slipping relative to the surface which may result from low soil strength when loaded parallel to the surface.

(3) If the lateral tire displacement is the primary method of relief, long strokes are not possible because the permissible lateral displacements of the tire are exceeded.

(4) The above approach assumes all kinetic energy is absorbed by the landing gear. An appreciable amount of the energy is expected to be absorbed by the soil, making the above approach conservative.

The average translational load factor, L_f, can now be calculated

$$L_f = \frac{(365)\,(4)}{700} = 2.1 \text{ g (Earth)}$$

Although the analysis is still in progress preliminary results indicate that the baseline design is capable of meeting the requirement of a vertical landing velocity of 5 to 6 fps and a horizontal landing velocity of 1 to 2 fps.

2. Flight Thermal Requirements

Thermal flight requirements for the baseline LRV as delivered by Atlas-Centaur and by Lunar Module are shown in Tables V-28 and V-29 respectively. These requirements are essentially identical to those developed for the Surveyor flight and descent system. Thermal design employs the proper method of temperature control (passive, active, semi-active) to insure that temperatures will be within the desired operational temperature limits. Only operational temperature limits have been listed because, as stated earlier, those systems that are required to operate during the flight portion of the mission are jettisoned shortly after landing on the Moon and need not be thermally designed for post-landing survival. In addition, those subsystems that are required to operate on the lunar surface need only to survive transit (flight) whose thermal environment and corresponding survival limits are less severe than those presently specified for lunar day operations and lunar night survival.

It is important to note that from Surveyor thermal design experience and a preliminary analytical review, each component in Tables V-28 and V-29 can be designed to operate within the temperature limits shown without imposing undue weight penalties under either delivery system.

K. LRV ADAPTATION TO APOLLO LM

1. Review of Manned LSSM Rover

In order to provide the LRV design with the capability for delivery by the Apollo system a review was first made of the manned LSSM rover and its adptation to the Apollo LM. This 2000 pound class of rover was designed for the dual

Table V-28. LRV Flight Thermal Requirements
(Delivered by Atlas-Centaur) (Sheet 1 of 3)

Item	Type of Temp. Control	Estimated Oper. Temp. Limits ~ °F	Remarks
TV camera	Passive-active	-140 to 85	
Solar panel	Passive	-120 to 140	
High gain antenna	Passive	-60 to 95	
Antenna and solar panel drive mechanism	Passive	-30 to 100	
Antenna and solar panel mast	Passive	-84 to 100	
Flight control elect.	Passive	50 to 95	Located in nozzle of retro rocket
Canopus sensor	Passive	60 to 100	Located on A-frame
Pitch, yaw and roll gyros	Active	173 to 187	Located on A-frame
Nitrogen tank	Passive	40 to 100	Located in nozzle of retro rocket
Attitude control jets	Passive	40 to 100	Located in nozzle of retro rocket
Roll actuator	Passive	85 to 95	Located near vernier Engine 1
Radars			
Klystron power supply	Passive	10 to 85	Located on A-frame
Signal data converter	Passive	30 to 88	
Doppler preamp.	Passive	10 to 85	
Alt. velocity preamp.	Passive	18 to 85	
Alt. marking radar elec.	Active	-10 to 83	Located in retro rocket nozzle
AMR antenna	Active	20 to 83	Located in retro rocket nozzle

Table V-28. LRV Flight Thermal Requirements
(Delivered by Atlas-Centaur) (Sheet 2 of 3)

Item	Type of Temp. Control	Estimated Oper. Temp. Limits ~ °F	Remarks
Thermal compartment	Passive; semi-active and active	20 to 100	Represents average temperature of equipment inside compartment. Individual temperature may be higher depending on duty cycle.
Upper tray	Passive	45 to 110	
Lower tray	Passive	55 to 100	
Transmitter A	Passive	40 to 100	
Transmitter B	Passive	50 to 125	
Battery	Passive	55 to 85	
Battery charge regulator	Passive	65 to 105	
Boost regulator	Passive	70 to 115	
Thermal switch	Semi-active	20 to 86	
Base ring			
Second surface radiators	Passive	-5 to 85	
Thermal shell			
inside	Passive	22 to 92	
outside	Passive	120 to 90	
Wire harness	Passive	65 to 85	
Radioisotopes	Active	100	
Super insulation blanket	Passive	-120	

Table V-28. LRV Flight Thermal Requirements
(Delivered by Atlas-Centaur) (Sheet 3 of 3)

Item	Type of Temp. Control	Estimated Oper. Temp. Limits ~°F	Remarks
Propulsion			
Oxidizer tank	Passive-active	15 to 76	Located on A-frame
Fuel tank	Passive-active	25 to 75	Located on A-frame
Helium tank	Passive	46 to 98	Located on A-frame
Vernier engines	Passive	30 to 380	Located on A-frame
Fuel lines	Active-passive	24 to 81	Located on A-frame
Oxidizer lines	Active-passive	20 to 83	Located on A-frame
Main retro rocket	Passive	64 to 72	Main retro is actively temp. controlled prior to launch
Main retro lower case	Passive	42 to 77	
Main retro rocket nozzle	Passive	-130 to 80	
Retro attach. points	Passive		
A-frame	Passive		
Support rods to wheels	Passive		
Shock absorbers	Passive		
Wheels	Passive		
Wheel drive mechanism	Passive		

Table V-29. LRV Flight Thermal Requirements
(Delivered by Lunar Module)

Item	Type of Temperature Control	Estimated Operating Temperature Limits ~°F	Remarks
TV camera	Passive-active	-140 to 85	
Solar panel	Passive	-120 to 140	
High gain antenna	Passive	-60 to 95	
Antenna and solar panel drive mechanism	Passive	-30 to 100	
Antenna and solar panel mast	Passive	-84 to 100	
Support rods to wheels	Passive		
Shock absorbers	Passive		
Wheels	Passive		
Wheel drive mechanism	Passive		
Thermal compartment	Passive; semi-active and active		Represents average temperature of equipment inside compartment. Individual temperature may be higher depending on duty cycle.
Upper tray	Passive	45 to 110	
Lower tray	Passive	55 to 100	
Transmitter A	Passive	40 to 100	
Transmitter B	Passive	50 to 125	
Battery	Passive	55 to 85	
Battery charge regulator	Passive	65 to 105	
Boost regulator	Passive	70 to 115	
Thermal switch	Semi-active	20 to 86	
Base ring			
Second surface radiators	Passive	-5 to 85	
Thermal shell inside	Passive	22 to 92	
outside	Passive	120 to 90	
Wire harness	Passive	65 to 85	
Radioisotopes	Active	100	
Super insulation blanket	Passive	-120 to 92	

launch mode using two Saturn 5 boosters and two Apollo spacecraft; one to deliver it to the lunar surface, and one to bring the men, the purpose being to extend the exploration capability of the astronauts. Life support and safety requirements restricted this capability, and as program constraints evolved smaller LRV configurations compatible with single-launch, manned LM delivery came to be preferred.

Since recent analysis of the performance capabilities of the manned Apollo vehicle indicated a possible reserve of 500 to 1200 pounds, a design review was then made of the strap-on feasibility of the baseline LRV roving configuration (with Surveyor landing systems detached) to the LM.

Review Results. Results were satisfactory as indicated on Fig. V-2A, V-55 and V-56 which illustrate the installation of the LRV (or the alternate six wheeled design) onto the LM descent stage. The LRV equipment compartment is attached to the basic structure of the LM in one of the equipment quadrants with its wheels extending out radially. This location was chosen since it:

(1) Is compatible with the launch, separation, descent and abort systems of the manned Apollo missions

(2) Presents a minimum effect on the LM attitude control system from the center of gravity offset as well as the exhaust impingement standpoints

(3) Orients the LRV equipment compartment for convenient thermal control of its equipment during transit and descent phases

(4) Permits convenient detachment and lowering of the LRV to the lunar surface either automatically or by the astronauts (using a hoist cable to the upper LM structure).

For this adaptation the upper mast and equipment are stowed on the LM for transit and assembled to the LRV after lowering it to the lunar surface. Problems concerned with the installation include:

(1) Separation Clearances. In order to assure adequate separation of the LM from the Apollo shroud (SLA), a 10 degree clearance envelope was required for LM equipment. This LRV baseline installation was critical for clearance and required a 10 to 15 degree canted attachment (Fig. V-55) to provide clearance between the LRV wheels and the SLA.

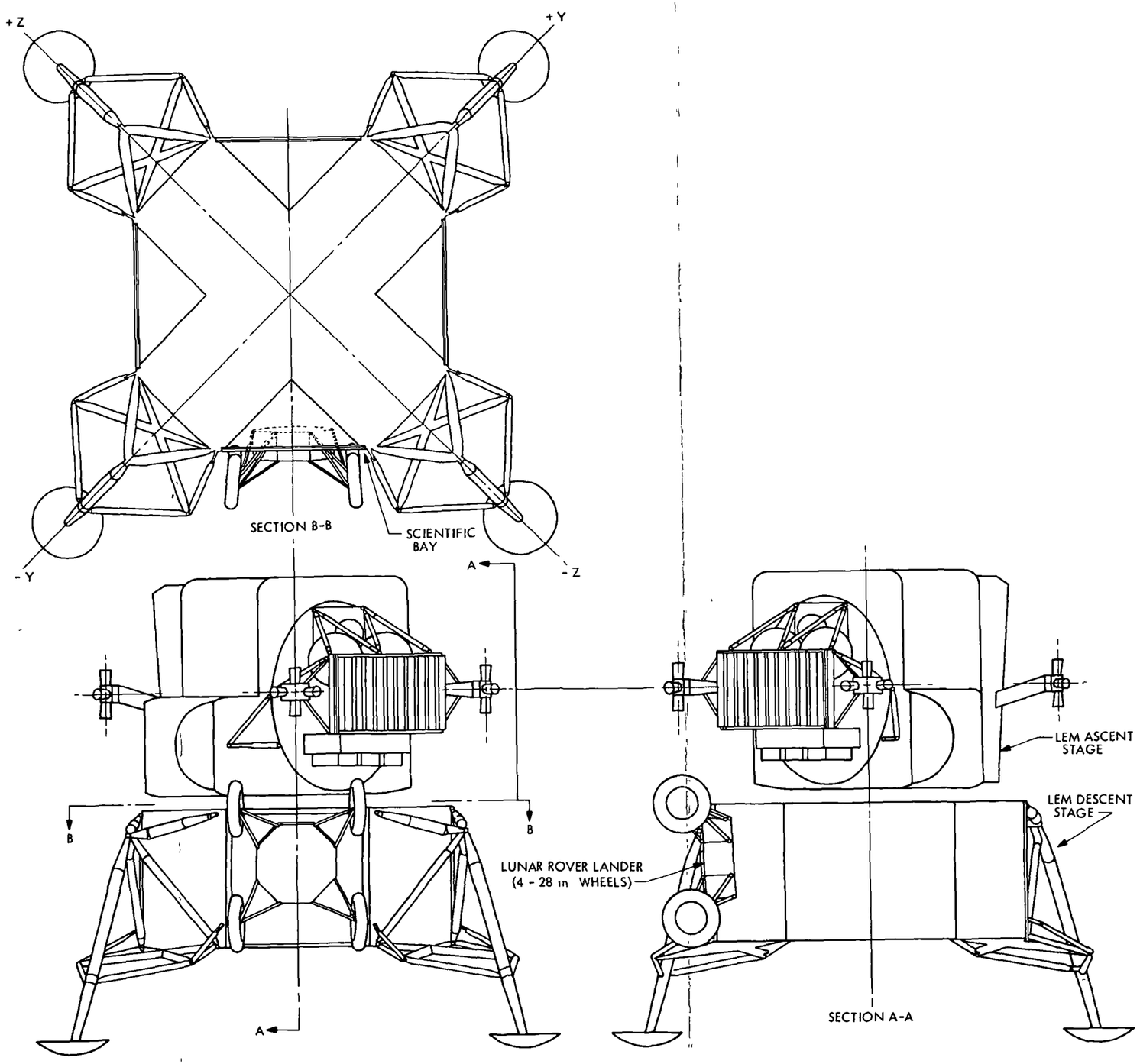

Figure V-55. Four-wheel LRV Mounted on LM

Page intentionally left blank

Page intentionally left blank

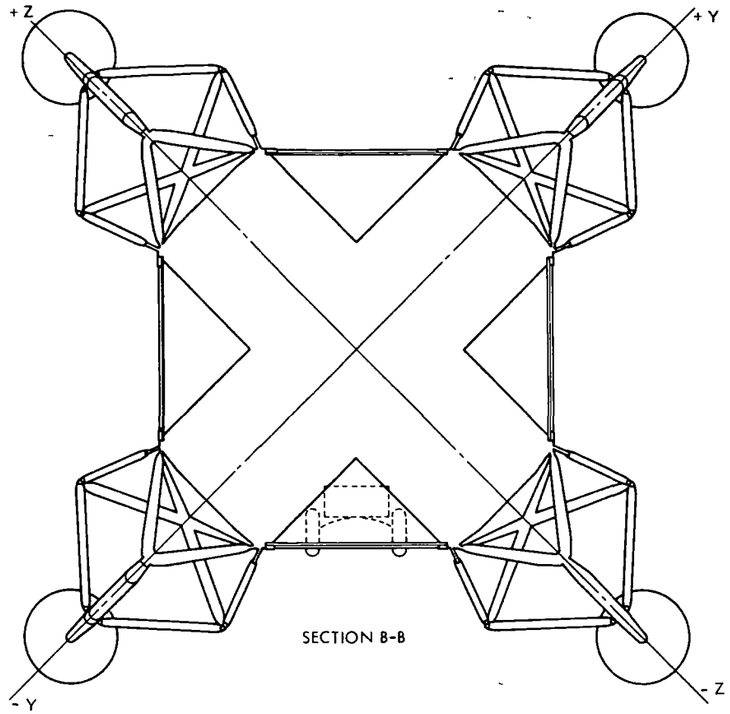

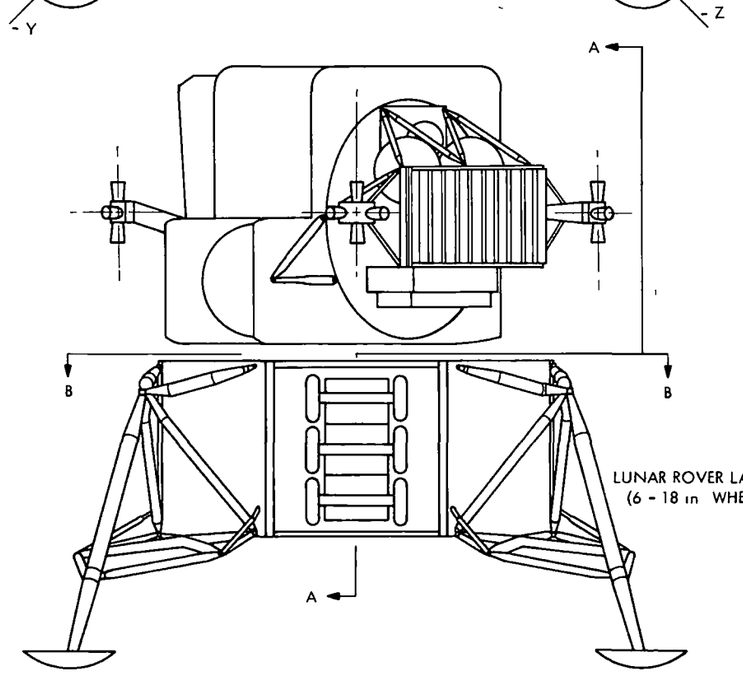

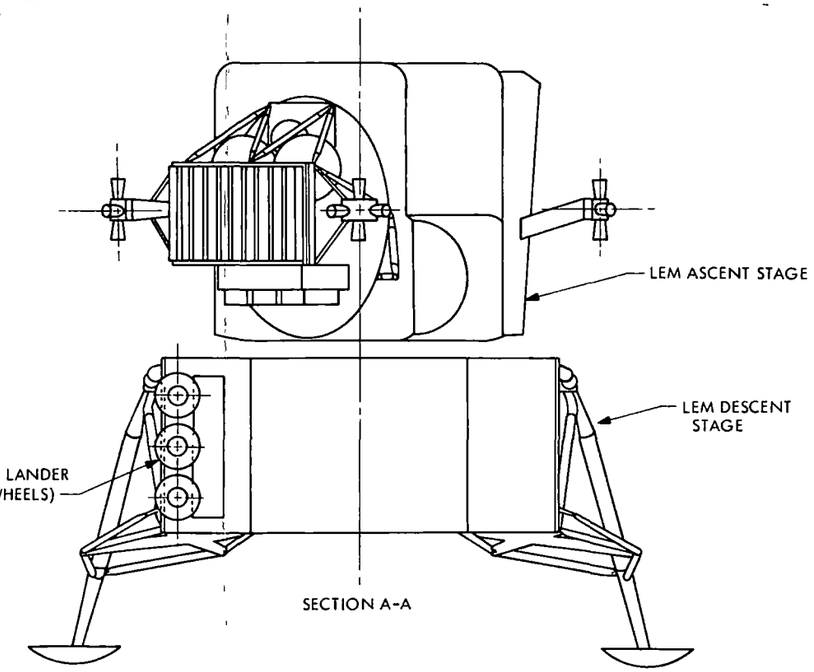

Figure V-56. Six-wheel LRV Mounted on LM

Page intentionally left blank

Page intentionally left blank

The alternate design presented no problem due to its smaller wheel diameter.

(2) Attitude Control Effects. This installation of the LRV introduces two effects on the LM attitude control system: a change in center of gravity offset due to the eccentric addition of LRV weight, and a change in the moment control capability due to partial impingement of the control motor exhaust on the LRV wheels and undercarriage.

However, the combined result of these two effects was found to be within the capability of the control system since:

(a) The LM attitude control was designed to accommodate the larger LSSM located in a similar eccentric position.

(b) Plume analysis utilizing a method of characteristics solution and an expression for calculating plume density, developed by L. Roberts (Ref. V-16), has indicated that the rocket's plume will exert a drag force of less than three pounds and a heating rate of less than 10 BTU per second per foot^2.

(3) EVA Timeline. Assembly of the LRV by astronauts would consume a part of the limited time available for extravehicular activity.

L. LARGER LRV ADAPTATION TO TITAN IIIC AND LM

1. Titan IIIC LRV

In order to broaden the study perspective and provide some parametric information for larger roving vehicles of the LRV type, an exploratory investigation was started based on the Titan IIIC booster. Since the injection capability of this booster is twice that of the Atlas Centaur, this effort involved increasing the baseline 500 pound to 600 pound LRV to the 1000 pound to 1200 pound size. The design considered for this larger rover was essentially a scaled-up version of the baseline concept. It uses the same Surveyor type of flight, descent and landing concepts to deliver a four or six wheeled rover to the lunar surface.

Review Results. Although the analysis of this rover is in its early stages, the design results (see Fig. V-57 and V-58) seem sufficiently complete and interesting to present at this time. Both the four and six wheeled 1000 pound to 1200 pound LRV's are shown here, installed in the 10 foot diameter of the Titan IIIC shroud. (The Atlas Centaur LRV (500 to 600 pounds) is contained within a 6 foot diameter of the Atlas Centaur shroud. (Fig. V-48).) Performance calculations are still in progress, however, early payload estimates are as follows·

No.	Design	Payload in pounds
1	Four wheel	200 to 300
2	Six wheel	150 to 250

These preliminary design results indicate that this scaling of the LRV concept presents no new technology developments not already contained within the smaller LRV. Flight, descent, landing and roving systems are essentially enlarged duplicates of the small version. In the case of the descent propulsion system, however, this enlargement results in two major propulsion development programs not required in the smaller LRV. Both the main retro and the vernier propulsion systems roughly require a doubling of total impulse and thrust level. This increase in propulsion size is well within the state of the art, however, it does represent a sizable development effort, either in clustering of existing engines or in making new ones. In other systems such as descent radar (AMR and RADVS), the increased LRV size has very little effect and the same Surveyor hardware can be adapted.

In order to provide the desired flexibility to various lunar delivery systems, this Titan IIIC LRV was then investigated for compatibility with the LM. Since its weight was within the possible upper limit of performance for improved LM versions, an installation on the LM was considered similar to that of the Atlas Centaur LRV design. Results are indicated on Fig. V-59 and V-60 which show the four and six wheeled Titan IIIC LRV installed onto the side of the LM descent stage. This adaptation appears satisfactory to the Apollo launch,

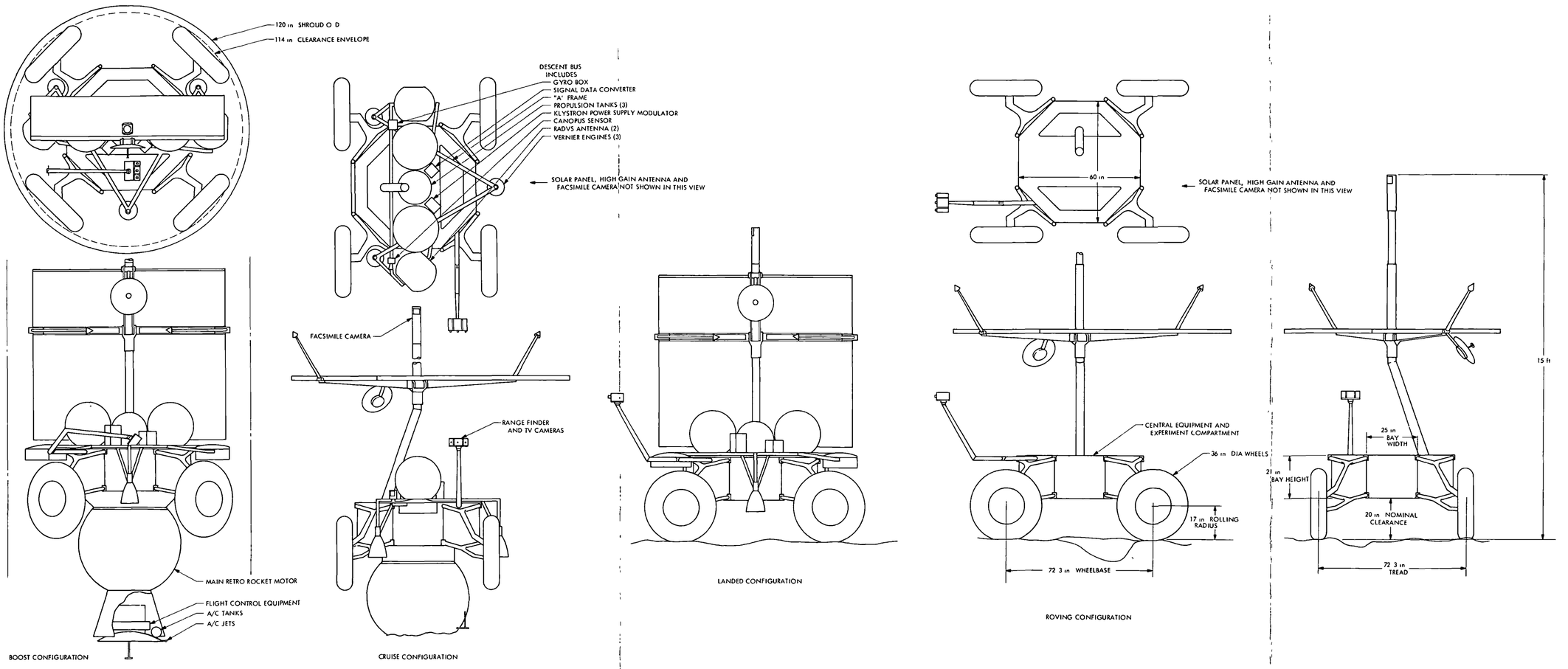

FIGURE V-57 PRELIMINARY STUDY, FOUR-WHEEL LRV MOUNTED ON TITAN IIIC

Figure V-57. Preliminary Study, Four-wheel LRV Mounted on Titan IIIC

Page intentionally left blank

Page intentionally left blank

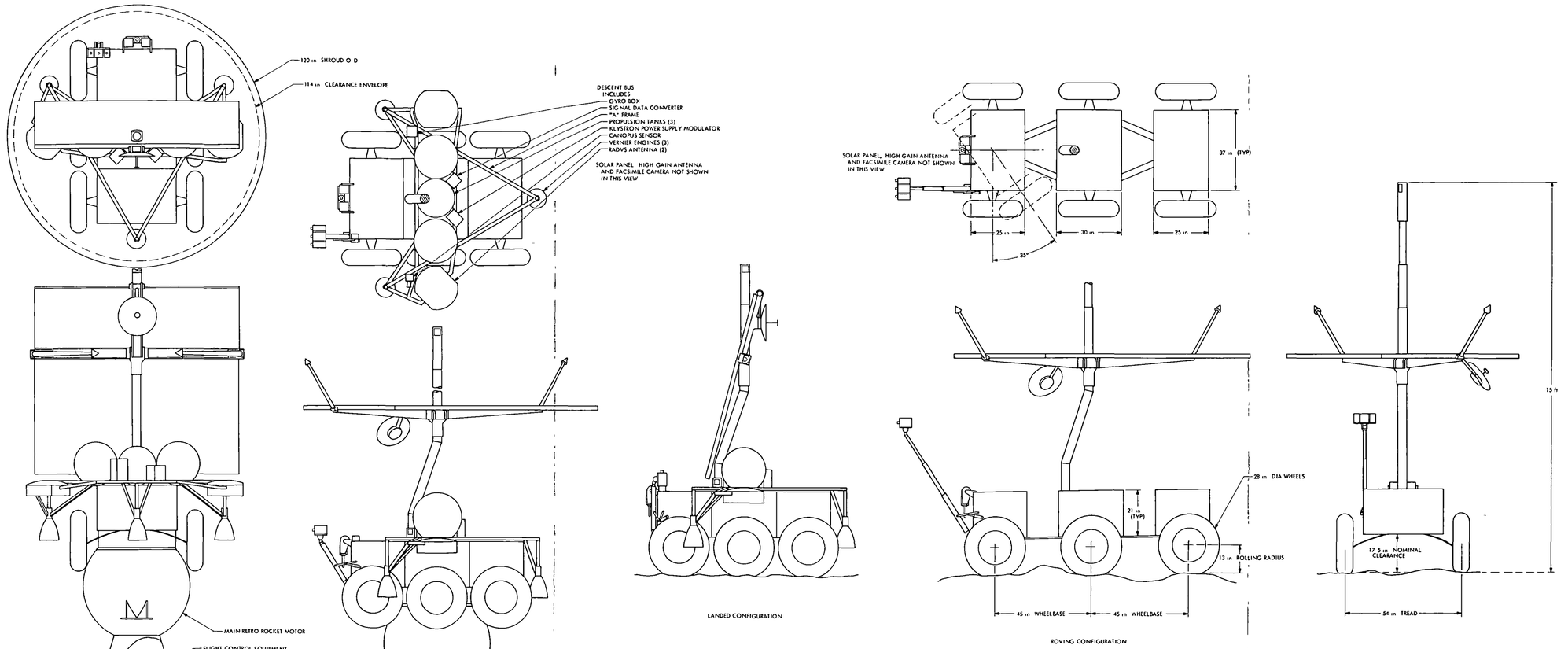

Figure V-58. Preliminary Study, Six-wheel LRV Mounted on Titan IIIC

Page intentionally left blank

Page intentionally left blank

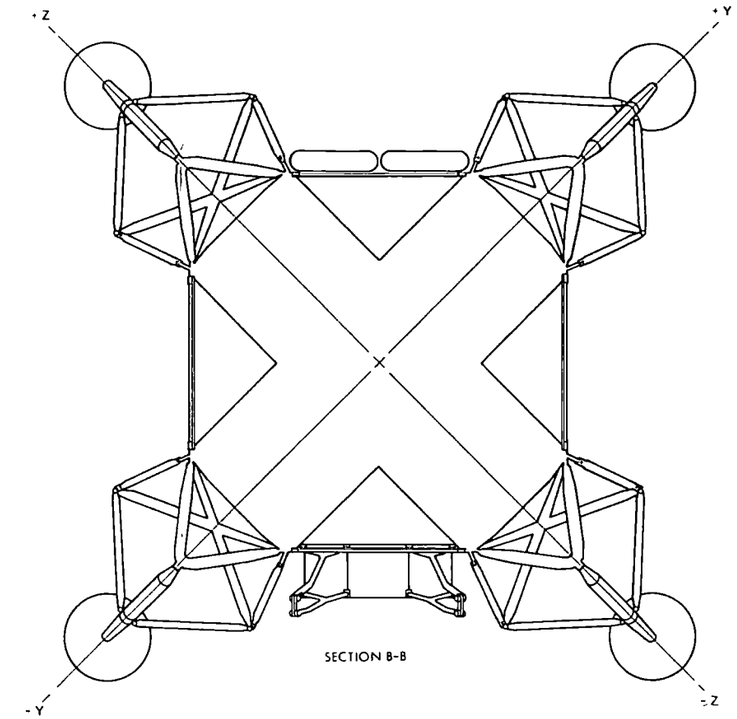

SECTION B-B

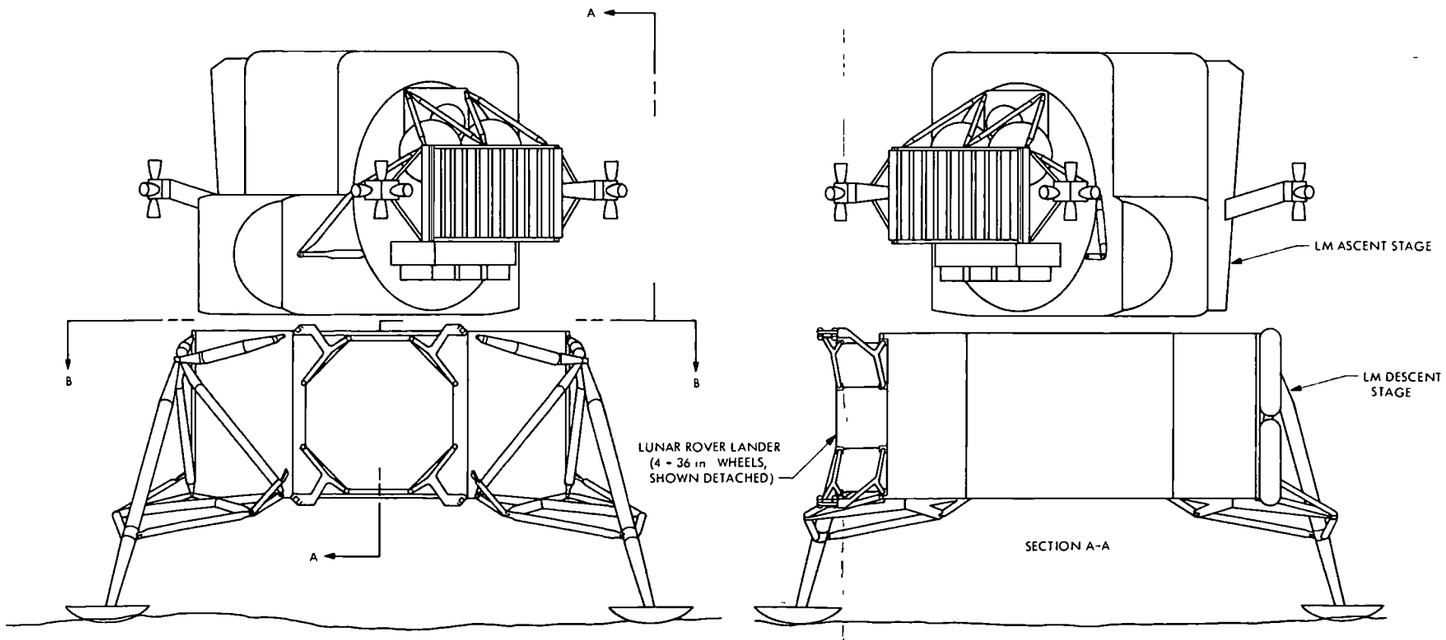

SECTION A-A

Figure V-59. Four-wheel LRV Mounted on LM (Titan IIIC)

Page intentionally left blank

Page intentionally left blank

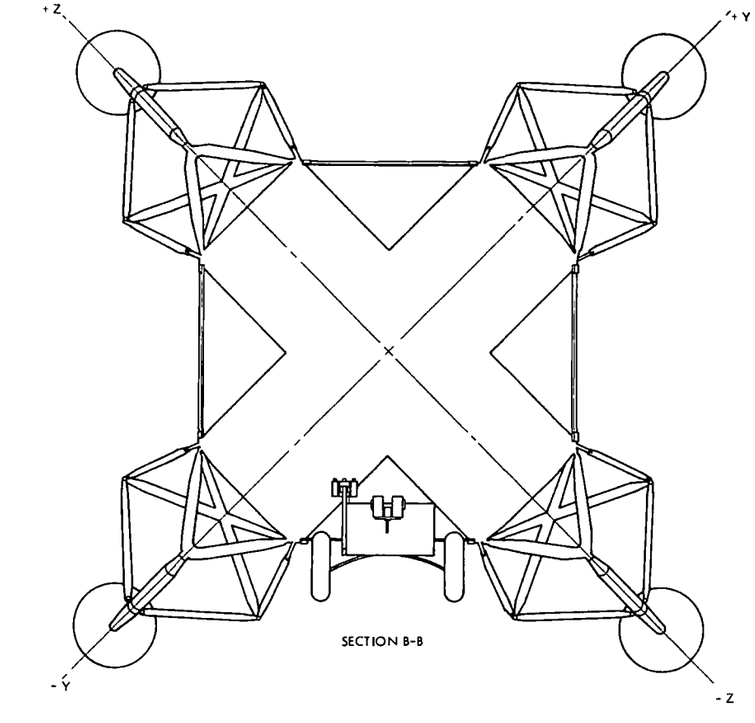

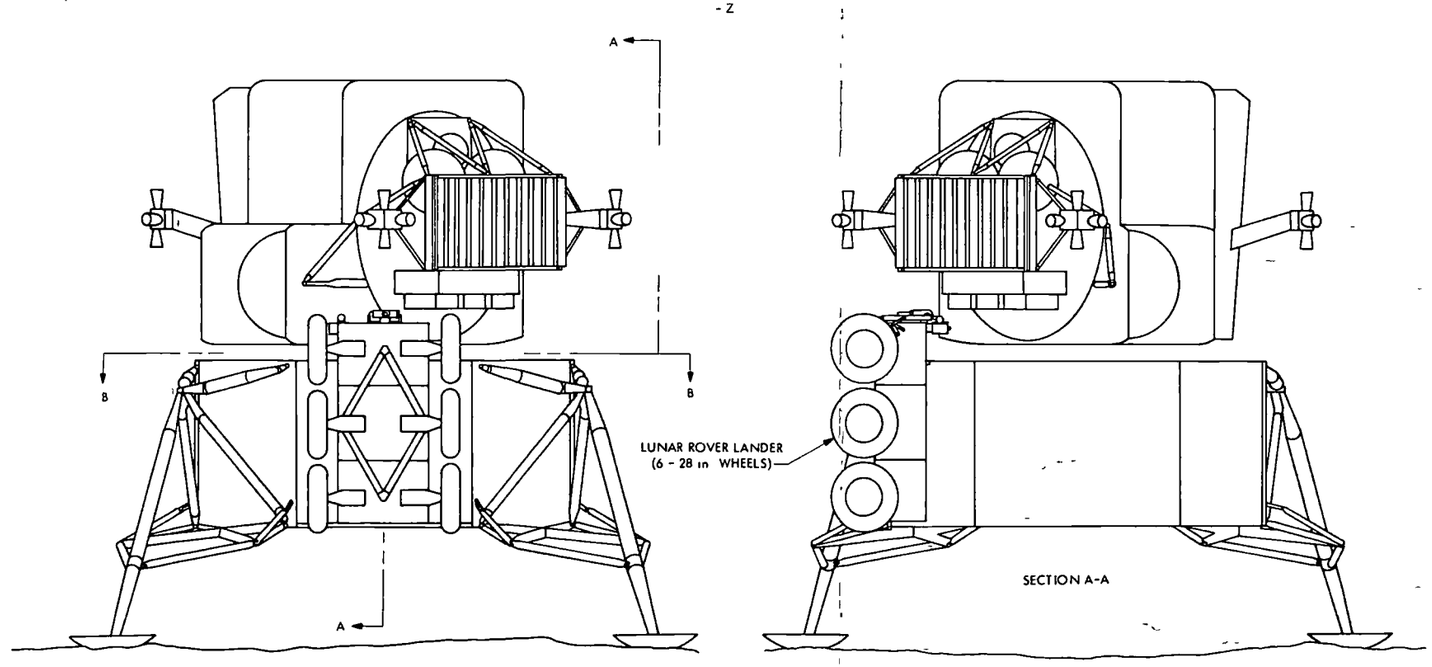

Figure V-60. Six-wheel LRV Mounted on LM (Titan IIIC)

Page intentionally left blank

Page intentionally left blank

separation, descent and abort systems as was the smaller LRV. While this does not seem to present any new major problems, it does increase some sensitive conditions as follows:

(1) Clearance for Separation. In order to provide separation clearance for the shroud (SLA), it is necessary to stow the wheels as indicated on Fig. V-59. Reassembly of these wheels onto the axles just prior to lowering the LRV to the lunar surface is considered to be an acceptable task for the astronauts but would consume additional EVA time.

(2) Attitude Control Effects. The installation of the enlarged LRV increases the center of gravity offset problem and presents a different exposed contour to the motor exhaust impingement. Drag forces would approach twenty pounds, and could tax the capability of the LM's attitude control system. Heating rates would be high but could perhaps be protected against by thermal shielding. Further analysis is required for this design alternative.

M. NAVIGATION STUDIES

The feasibility of four navigation schemes has been considered for an automated LRV: piloting by landmark, Earth-based radio ranging and range rate, celestial navigation, and inertial navigation. The first of these has been studied in a field simulation of the concept, and the other three have been analyzed critically for their utility in LRV. The landmark navigation scheme emerges as the most logical candidate with radio tracking serving for a gross initial fix after touchdown and for emergency use as a back up system. Celestial and inertial navigation are not feasible for the baseline LRV.

1. Landmark Navigation

The feasibility of the landmark navigation scheme depends on whether landmarks can be identified by TV imagery, taken from the ground, and whether measurements deduced from the imagery are adequate to direct a vehicle to a predetermined objective. It appeared that even a crude test in an earth environment would indicate the general feasibility of the scheme and also give us a feel for operating problems and techniques.

To this end four requirements were set up for validation or rejection in a field test.

Field Test Requirements. The requirements for the field test, assuming TV in use only when LRV is stationary, (1) through (3) and TV operating continuously (4) were as follows:

(1) TV sighting of landmarks, with dead-reckoning and ground contact, is capable of navigating a vehicle remotely from point-to-point.

(2) 800-line TV provides feasible resolution for locating a vehicle from landmarks.

(3) A geologically interesting site can be recognized from TV imaging at the site.

(4) Continuous TV is feasible for remote guidance of a roving vehicle.

In addition, certain questions could receive partial or tentative answers: Is self-leveling device required for TV? How much time is required for location determinations and new-bearings?

Field Test Results. For the field test, the required area had to be sufficiently devoid of signs of human habitation that operators would not be tempted to rely on such structures in the locating process. Moreover, the area had to have a reasonable density of landmarks, e.g., hills and mountain ranges, and also be within easy commuting distance of JPL by helicopter. After a reconnaissance of much of the western Mojave Desert, an area (Fig. V-61) was found in the vicinity of the Shadow Mountains north of Victorville, California. The area actually traversed was from El Mirage Dry Lake in the south, across the west and north pediment of the Shadow Mountains, and from the Kramer Hills to Buckthorn Canyon. Figure V-62 gives a view of the terrain from the air.

(1) TV Sighting of Landmarks. Equipment for the field test was borrowed from around the Laboratory and mounted on a four-wheel drive truck. As expected, a laser range finder could not be found. The TV camera finally used limited us to just 500-line images. Figure V-63 shows the test system in its field configuration.

Two controllers were seated in the rear of the truck at a table holding the TV monitor. One controller was blindfolded during his helicopter trip to the test site and the windows of the rear compartment were blacked out. His only clues to his location were an area on the map 10 miles square plus what he saw on the monitor. Figures V-64 and V-65 illustrate the type of landmarks used to locate our vehicle.

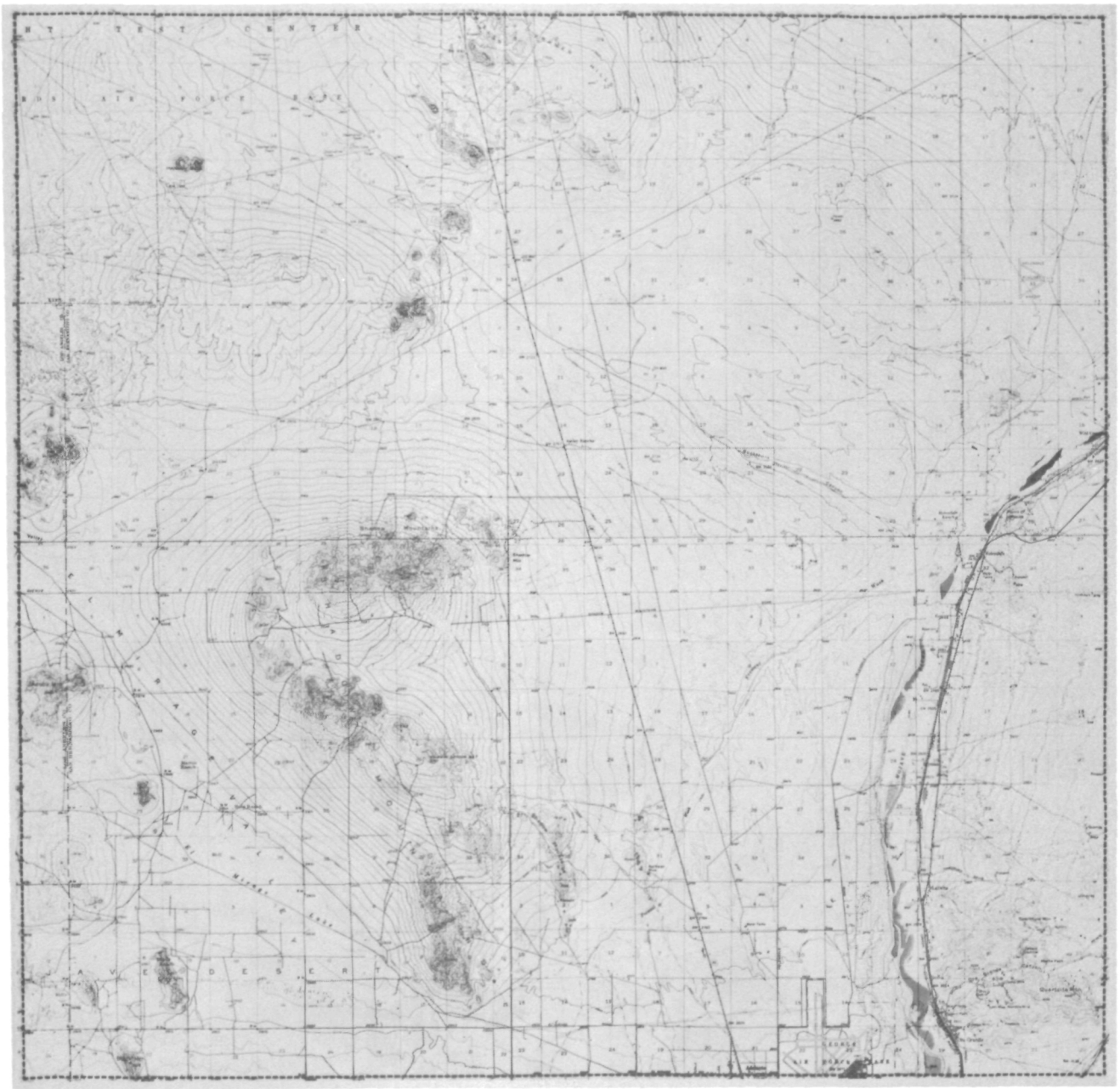

Figure V-61. Map of Mojave Desert Test Area

Figure V-62. Air View of Test Region

Figure V-63. Truck Used for Navigation Test

Figure V-64. Typical Landmark

Figure V-65. Typical Landmark

We had difficulty in making positive identification of a feature when in close to it. Identification was easier when gross character was more in evidence and when its association with surrounding terrain was clear. This was especially true of a range of hills such as the Shadow Mountains. Fields of view containing a number of landmarks, especially when their relative distance from the viewer is implied, greatly assist precise identification of those landmarks (Fig. V-65).

The results of the field experience relative to the original hypotheses are as follows: The ALS Team is confident that TV sighting of landmarks is generally feasible for navigating a vehicle remotely from point-to-point. In seven days of actual field tests five objectives were reached or successfully approached. The first objective required three and one-half days as our techniques improved. For each of the last three days the objective of that day was obtained. The accuracies attained are summarized in Table V-30.

Obviously there is a learning curve effect for operators of a TV navigation system. Another important observation from field experience is that the accurate identification of visible landmarks is essential. Without it the additional information from magnetic or inertial bearings is of little value. Even a panoramic view is of little help until at least one feature in the sequence has been definitely and reliably identified.

The Team's confidence is enhanced by recognizing the value of ranging data obtainable from an optical ranging device in the system. At this time it appears that ranging data are not absolutely necessary but that their availability will reduce the time required for a successful fix.

(2) 800-line TV. Concerning the feasibility of 800-line TV, if 500-line resolution is adequate, any higher resolution will also do the job. The experience was that the 500-line TV was adequate. However, in the interest of more rapid identification of features and detection of marginal images on the horizon, 600-line or greater resolution may yet be desirable.

(3) TV Imagery (Geological Site). The field experience does not allow an adequate comment on the problem of recognizing a geologically interesting sight from TV imagery. Small dry lakes were easily identified on the TV monitor, but no outcroppings of bedrock were encountered or sought. This hypothesis requires additional experience.

Table V-30. Accuracy in Location Determinations

	Day						
	1st	2nd	3rd	4th	5th	6th	7th
Station No. 1	2 miles (approx)	6.5 miles	5 miles (approx)	0.5 mile	0.2 mile	1.8 mile	0.25 mile
Station No. 2	0.5 mile (approx)	(1)	5 miles (approx)	0.25 mile	0.1 mile	1.9 mile	0.4 mile
Station No. 3	1 mile (approx)	(1)	—	0.1 mile(2)	0.1 mile	1.5(2) mile	0.4 mile
Station No. 4	—	(1)	—	1.8 mile	0.1(2) mile	—	—
Objective	—	—	—	0.2(3) mile	100 yds	1.4 mile	0.2(4) mile

Notes: (1) Fix not obtained for this station.

(2) Station intended to be near objective.

(3) Accuracy for first objective; second objective of day not reached.

(4) Last traverse, if completed, would have ended 0.4 mile from objective.

(4) Continuous TV Operation. Operating TV continuously while the vehicle was moving was attempted only once, and proved completely impractical because of image motion. The minimum truck speed was five miles per hour, whereas the LRV's planned speed is on the order of one mile per hour. Therefore, the dancing of the image on the test monitor may be much more severe than that to be experienced by the LRV. However, the baseline concept for obstacle detection and avoidance does not require TV imaging during a traverse.

The question of a self-leveling device for the TV camera became obvious after frequent requests from the controller to the cameraman to raise and depress the camera. Current thinking is to provide for motion of the camera in elevation and azimuth and to calculate by ground computer these pointing angles to compensate for tilt of the LRV.

The field test did not provide a fair measure of the time requirements for location determinations and new bearings. The system used in the field did approximate the level of automation required for LRV, and the daily turnover of personnel involved in the test inhibited development of a time-saving routine.

Other observations made during our field test plus a more detailed treatment of the technique for locating an LRV will be included in a test report.

2. Accuracy of Lunar Surface Position Determination Using Earth-Based Radio Ranging and Range-rate

In the standard orbit determination problem, the range and range-rate between a spacecraft and tracking station are expressed as a function of the location of the tracking station and the elements of the spacecraft orbit. A reference or nominal orbit is chosen and the partial derivatives of the range and/or range-rate with respect to each orbital element are used to determine how small changes in the elements affect the range and range-rate signals. By looking at the differences between observed range and range-rate measurements and the measurements expected from some reference orbit, the differences between the elements of the observed orbit and the elements of the reference orbit can be determined and hence the true elements of the observed orbit.

In the case of an orbit sitting on the surface of the Moon, a similar technique can be applied. The range and range-rate are expressed as functions of the location of the observing station, the position of the Moon's center and the

location of the spacecraft relative to the Moon's center. The expected range and range-rate from a reference or nominal position on the lunar surface are compared with observed range and range-rate and the differences used to determine the difference between the nominal and observed positions.

(1) Accuracy Factors. The accuracy with which such determinations can be made depends on the following factors:

(a) Accuracy with which range and range-rate measurements can be made.

(b) Accuracy of tracking station locations.

(c) Accuracy of the lunar ephemeris.

(d) Time.

(2) Accuracy Determination Assumptions. For the purpose of determining the accuracy with which lunar surface location can be determined using radar ranging and range-rate the following assumptions were made:

(a) Twelve hours of tracking data at one ranging and range-rate data point per minute.

(b) One-sigma uncertainties of 5 meters in tracking station longitude and distance off the Earth's spin axis.

(c) One-sigma uncertainties of 10 meters and 1 millimeter/sec in ranging and range-rate observations respectively.

(d) A noise model for the lunar ephemeris of the form

$$E_i = \alpha + \beta t + \frac{\gamma t^2}{2}$$

where

E_i is the noise in each component of the Moon's position and α, β, and γ are Gaussian random variables of mean zero and standard deviations respectively:

$$\sigma_\alpha = 100 \text{ m}$$

$$\sigma_\beta = 0.5 \text{ mm/sec}$$

$$\sigma_\gamma = 0.3 \text{ mm/sec/day}$$

The size and orientation of the error ellipsoid associated with either range-rate only or combined ranging and range-rate determinations were found to be fixed with respect to the Earth independent of the position of the vehicle on the lunar surface. Because the orientation of the lunar surface varies with respect to the Earth-Moon direction as the location on the Moon is changed, there is a variability in the capability to resolve surface coordinates within an error ellipsoid of fixed dimensions and orientation (Fig. V-66).

The dimensions and orientation of the error ellipsoid associated with a position determination on a particular day of the month vary strongly as a function of which day is chosen. This is largely due to relatively more or less favorable geometries between the position of the Moon and the plane of rotation of the tracking site from which data are being taken.

Figure V-67 shows the dimensions of the 1-σ error ellipsoid associated with a position determination using range-rate data as a function of day of the month. Day zero is the day on which the Moon passes through the Earth's equatorial plane. The declination of the Moon increases to a maximum of 23 degrees at day seven and returns to zero by day 14. The orientation of the error ellipsoid is such that one axis points along the direction of the Earth-Moon line and the other two axes point in what are the North-South and East-West directions on the surface of the Moon at the sub-Earth point.

Figure V-68 shows the dimensions of the error ellipsoid associated with a position determination using combined range and range-rate data.

The error ellipsoid associated with the best Earth-based determination of lunar surface position yields an error ellipse on the lunar surface of about 1.5 by 4 kilometers. Since the rover only moves about 10 kilometers per day, this accuracy would not seem sufficient for the day-to-day navigation of the rover. However it is sufficient to remove ambiguities and aid the more precise location method using landmarks, as described above.

3. Accuracy of Lunar Surface Position Determination Using Celestial References

Assuming a perfect sphere as a model for the Moon for purposes of illustration, a single observation of the angle between the vertical at a point on the surface and the direction to a star serves to confine the position to a circle on the Moon's surface (Fig. V-69). The accuracy with which the radius of the

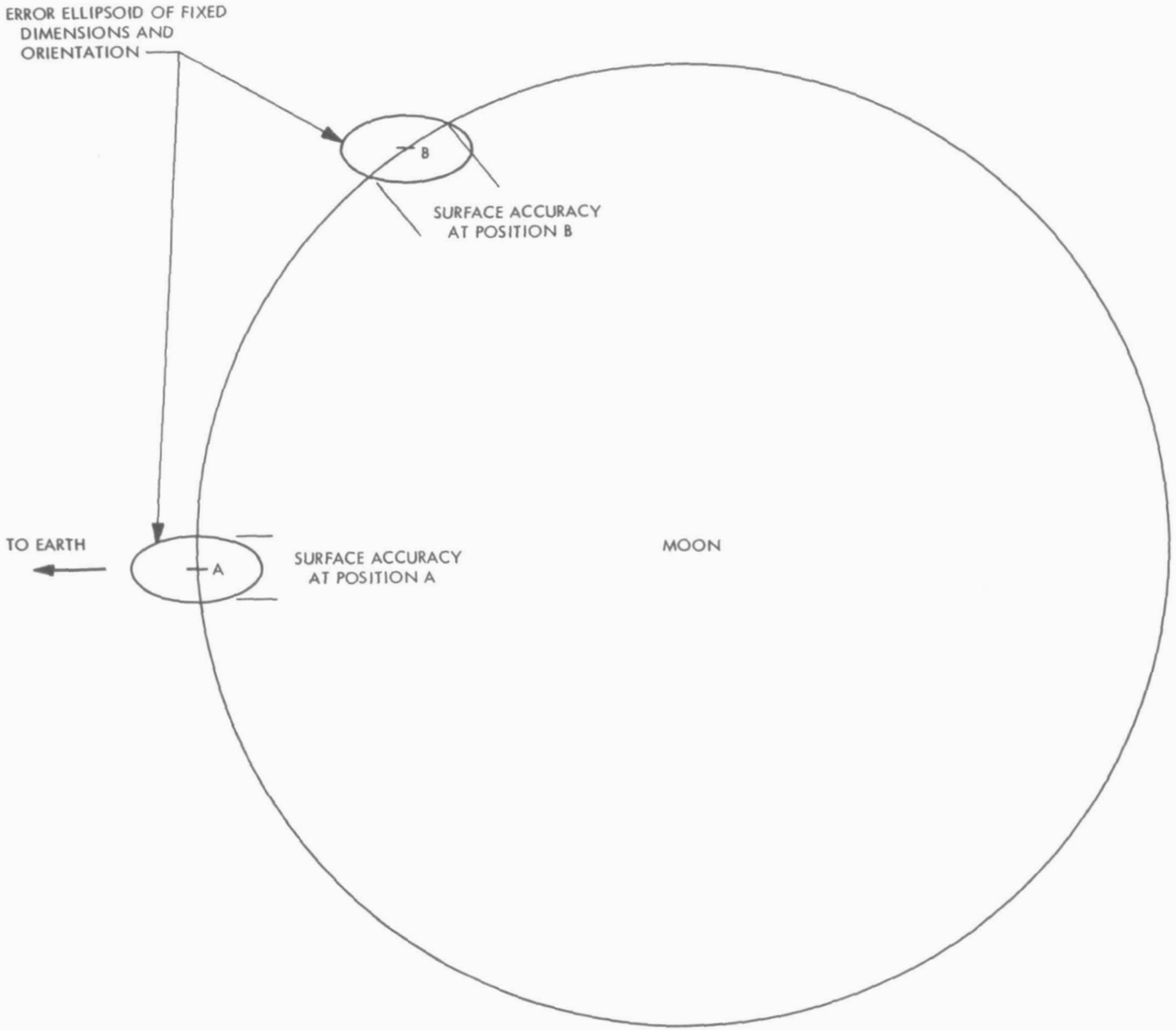

Figure V-66. Geometry of Tracking Errors

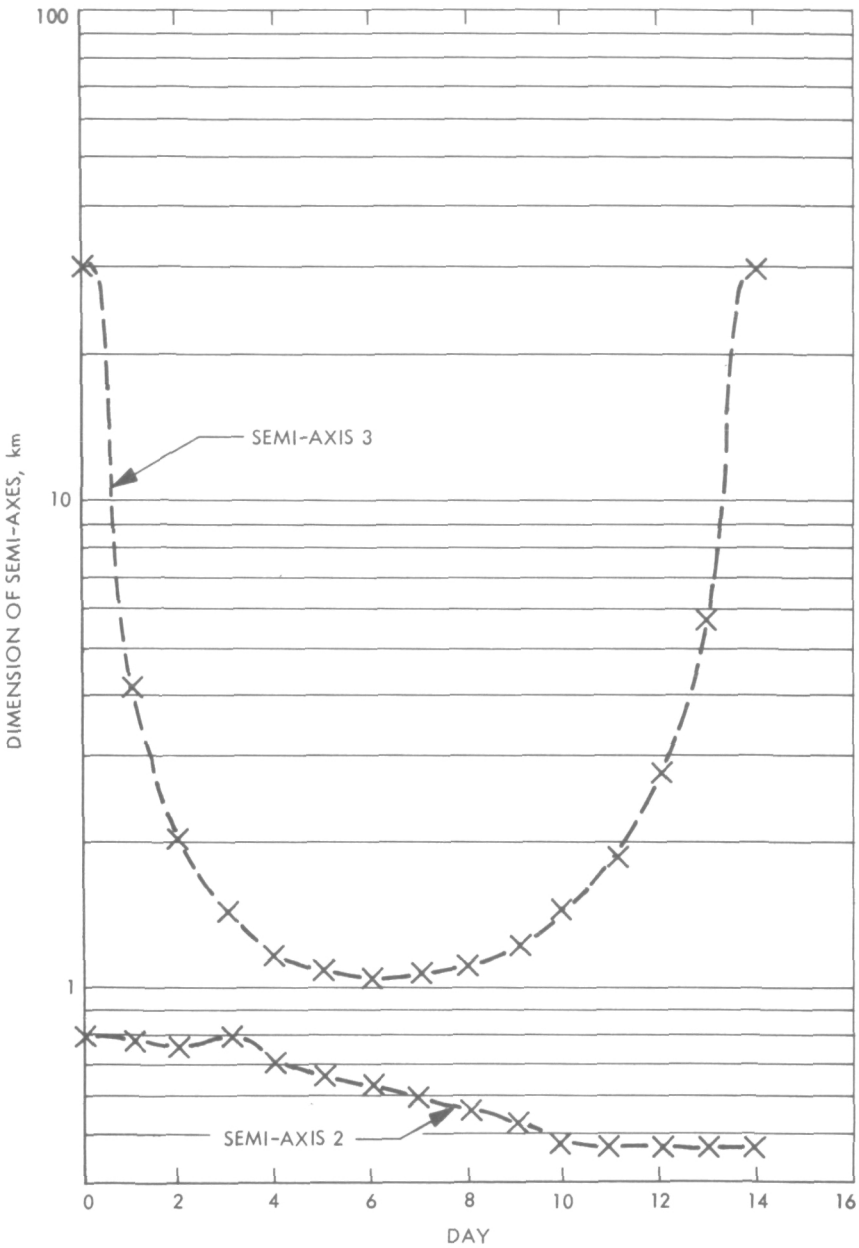

THE DIMENSIONS OF TWO OF THE THREE SEMI-AXES OF THE ERROR ELLIPSOID ASSOCIATED WITH DOPPLER ONLY TRACKING ARE SHOWN ABOVE. SEMI-AXIS TWO POINTS ALONG THE DIRECTION OF THE MOON'S ORBITAL MOTION SEMI-AXIS THREE POINTS IN APPROXIMATELY THE DIRECTION OF THE MOON'S SPIN AXIS. SEMI-AXIS ONE POINTS ALONG THE EARTH-MOON LINE AND IS NOT SHOWN, BEING OF THE ORDER 400 TO 2000 km

Figure V-67. Accuracy of Doppler Only Position Determination

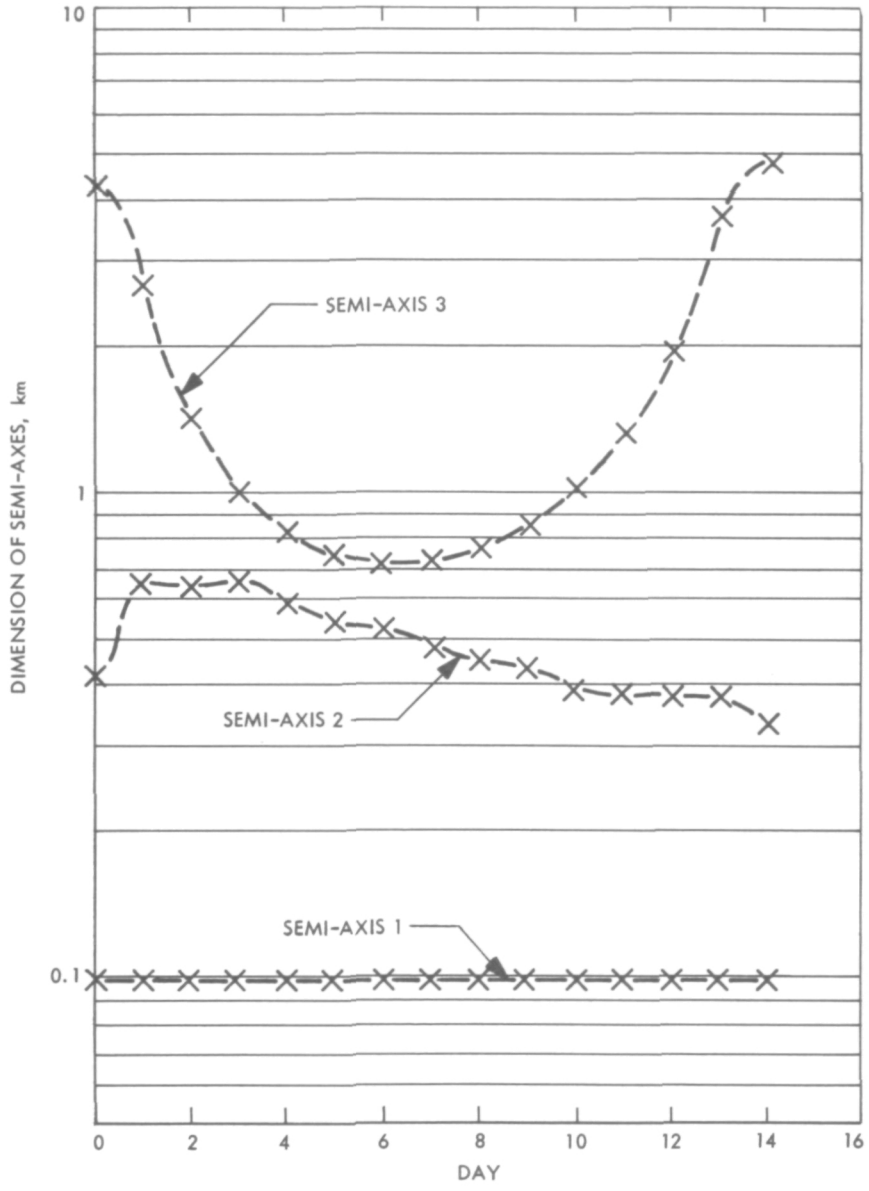

Figure V-68. Accuracy of Position Determination Using Combined Ranging and Doppler Data

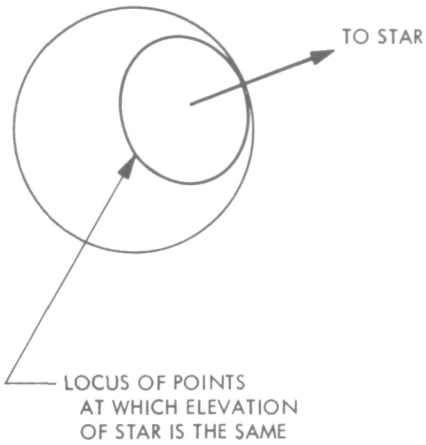

Figure V-69. Circle of Position Determined by Single Star

circle is known corresponds to the accuracy with which the angular observation can be made. An angular uncertainty of 1 degree corresponds to an uncertainty of 30 kilometers in the radius of the location circle.

By an optimum choice of the stars upon which angular measurements are made, it is possible to get the circular location patterns to intersect nearly at right angles for any lunar location (Fig. V-70). The resulting error ellipse on the lunar surface is circular or nearly so and its radius is directly proportional to the uncertainty in angular measurement.

Because of difficulties of mechanization, it is necessary for a lunar surface rover to measure the elevation of a star with two measurements. The direction

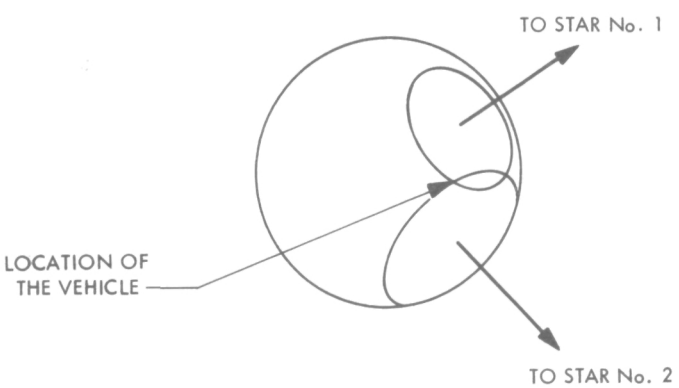

Figure V-70. Two-Star Fix

angles of the local vertical are measured with respect to a set of spacecraft-fixed coordinates, and the direction angles of the star are measured in the same coordinates. The angle between local vertical and the star can then be determined.

This process is subject to three sources of error: errors in the measurement of the local vertical, errors in the measurement of star angles, and errors due to local gravitational anomalies which cause the local vertical to point in a direction different from that which the surface position would lead one to expect. Assuming accuracies of 0.5 degrees for measurement of local vertical, 0.5 degrees for measurement of star angle and 0.1 degrees for deviation of local vertical due to gravitational anomalies yields a total uncertainty of 0.7 degrees. This corresponds to an error circle on the lunar surface 42 kilometers in diameter.

4. Accuracy of Inertial Guidance

The continual estimation of vehicle position using an inertial reference system, i.e., a stable platform, becomes more inaccurate as the vehicle moves about the surface. The inaccuracy results from platform misalignment, gyro drift, and accelerometer errors. Along with an initial position fix, subsequent period fixes to update or correct the calculated vehicle position are necessary. These fixes will be obtained by one or both of the previously mentioned methods, that is, celestial measurements for the LRV or radio ranging and range-rate from the Earth. Obviously, the navigation error will generally be at least as great as the position error inherent in these two methods.

Inertial Techniques. A variety of inertial reference techniques is available. The one best suited for the LRV is the one that utilizes the simplest on-board instrumentation and electronics, which is a gyrocompass. It employs a platform that is maintained perpendicular to the local vertical and in a fixed horizontal direction on the Moon. In this system, acceleration components in the East and North directions are directly obtained. Gyro torquing, necessary because of vehicle movement on the surface and lunar rotation, is required infrequently and

can be performed by ground command. Accelerometer compensation is accomplished with relatively simple analogue techniques. The equation to be solved is the following vector relationship:

$$\bar{A}_e = \bar{A} + \bar{G} - \bar{\Omega} \times (\bar{\Omega} \times \bar{R}) - (2\bar{\Omega} + \bar{\omega}_e) \times \bar{V}$$

where

$\bar{A}_e$ = acceleration in the local vertical frame

$\bar{A}$ = inertially sensed acceleration

$\bar{G}$ = gravity acceleration vector

$\bar{\Omega}$ = lunar spin rate

$\bar{R}$ = vehicle radius vector

$\bar{V}$ = vehicle velocity

$\bar{\omega}_e$ = angular velocity of platform relative to local vertical.

Errors on the order of 0.5 degrees in platform alignment in each direction, 0.25 deg/hr in gyro drift, and 10^{-6} Earth g's in the accelerometers can be expected. Assuming no errors due to gyro torquing, the resulting cumulative error in estimated vehicle position is about 1 km/hr. If a position fix were obtained twice each lunar day, the total error accumulated prior to each fix would be about 160 kilometer. From another point of view, if the position fixes were without error, it would be necessary to take one position fix every hour to keep the maximum error within 1 kilometer.

It becomes obvious that accurate altitude determination cannot be obtained by these means. More complex inertial techniques, however, do not greatly reduce the expected errors. Altitude information, if needed, might be obtained with other instrumentation: a gravimeter, for instance.

N. TRADE-OFF STUDY OF MISSION PARAMETERS

1. Average Vehicle Velocity

In order to develop a reasonable estimate of the average velocity V_A, one must consider the effect of the terrain as well as the vehicle's mode of operation. The LRV at a point where the slope of the gradient is θ, has a tilt angle in the vertical plane that may range from plus θ to minus θ. This tilt, called the instantaneous slope σ, is positive when LRV is climbing and negative when headed downhill.

V_A is then computed by weighting the velocity, a function of the power P and σ, by the distribution of instantaneous slopes.

$$V_A = \int_{-\theta_{max}}^{\theta_{max}} v(P, \sigma) p'(\sigma)\, d\sigma \qquad (1)$$

The integration is performed over the whole range of instantaneous slopes the LRV may encounter, i.e., θ_{max} is equal to the angle of repose.

The function $p'(\sigma)$ is obtained by first defining $p'_\theta(\sigma)$, the probability density of σ given θ. Since at a point θ ranges from $-\theta$ to $+\theta$ and if all orientations of LRV at a point are equally likely, it can be shown that p'_θ has a form shown in Fig. V-71.

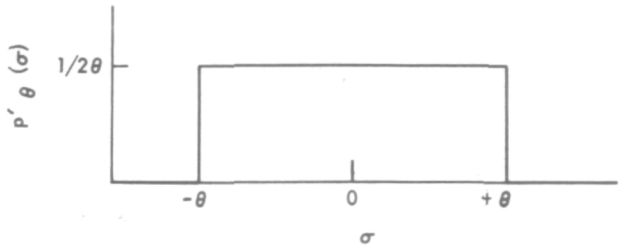

Figure V-71. Probability Density of σ Given θ

Since

$$\int_{-\theta}^{+\theta} p'_{\theta}(\sigma)\, d\sigma = 1 \tag{2}$$

and since $p'_{\theta}(\sigma)$ is assumed constant over the applicable range,

$$p'_{\theta}(\sigma) = \frac{1}{2\theta} \tag{3}$$

The probability of σ is equal to the conditional probability of σ given θ times the probability of θ. This relation also holds for the relevant probability densities, so

$$p'(\sigma) = \int_{\sigma}^{\theta_{max}} p'_{\theta}(\sigma) p(\theta)\, d\theta \tag{4}$$

The reason for integration over θ can perhaps be better seen by integrating both sides of equation (4).

$$\int_{0}^{\sigma} p'(\sigma)\, d\sigma = \int_{0}^{\sigma}\int_{\sigma}^{\theta_{max}} p'_{\theta}(\sigma) p(\theta)\, d\theta\, d\sigma \tag{5}$$

The contribution to the integral $\int p'(\sigma)\, d\sigma$ for a given σ is developed by an integration over θ, but only over the range in which $\sigma \leq \theta \leq \theta_{max}$. Therefore,

$$p'(\sigma) = \int_{\sigma}^{\theta_{max}} \frac{p(\theta)}{2\theta}\, d\theta \tag{6}$$

and

$$V_A = \int_{-\theta_{max}}^{+\theta_{max}} v(P, \sigma) \int_{\sigma}^{\theta_{max}} \frac{p(\theta)}{2\theta}\, d\theta\, d\sigma \tag{7}$$

The slope distribution function $p(\theta)$ has been estimated by various workers. Choate (Ref V-17) developed the cumulative percentages of lunar slope angles from an average of Rangers VII, VIII, and IX, cameras P_1 and P_3, last frame. The analytical expression developed for the slope angle cumulative probability P_c (in percent) is

$$P_c(\theta) = 10^{2.19} \times 10^{-0.17\theta} \tag{8}$$

for the range $\theta \geq 2°$. For the range $0° \leq \theta \leq 2°$ it can be shown that a function of the same form, meeting the boundary conditions is

$$P_c(\theta) = 10^{2.00} \times 10^{-0.74\theta} \tag{9}$$

It can also be shown that

$$p(\theta) = \frac{dPc}{d\theta} \tag{10}$$

Performing this differentiation on equations (8) and (9), one obtains

$$p_1(\theta) = 17\, e^{-0.17\theta} \qquad 0° \leq \theta \leq 2° \tag{11}$$

$$p_2(\theta) = 61\, e^{-0.39\theta} \qquad \theta \geq 2° \tag{12}$$

Using these functions in equation (6) then leads to:

$$p'(\sigma) = \int_{\sigma}^{2°} \frac{p_1(\theta)}{2\theta}\, d\theta + \int_{2°}^{\theta_{max}} \frac{p_2(\theta)}{2\theta}\, d\theta \qquad 0° \leq \theta \leq 2° \tag{13}$$

$$p'(\sigma) = \int_{\sigma}^{\theta_{max}} \frac{p_2(\theta)}{2\theta}\, d\theta \qquad \theta \geq 2° \tag{14}$$

The evaluation of integrals in equations (13) and (14) requires calculation of a sufficient number of terms for convergence in the general integral

$$\frac{e^{-ax}}{x}\,dx = \ln x - ax + \frac{(ax)^2}{2 \cdot 2!} - \frac{(ax)^3}{3 \cdot 3!} + \cdots \tag{15}$$

By use of the recurrence formula for the n^{th} term (where $T_1 = ax$),

$$T_n = (-1)^n \frac{N-1}{n^2} (ax)\, T_{n-1}, \tag{16}$$

$p_1'(\sigma)$ and $p_2'(\sigma)$ are evaluated to yield the composite curve for $p'(\sigma)$ shown in Figure V-72.

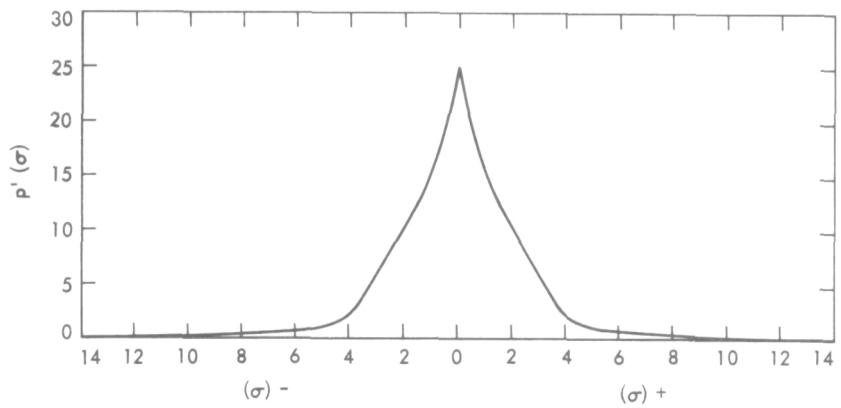

Figure V-72. Composite Curve for $p'\sigma$

From the shape of $p'(\sigma)$ it is obvious that instantaneous slopes within just a few degrees of 0° are heavily favored. This fact clearly implies otherwise higher average velocities if $v(P, \sigma)$ is a decreasing function of σ.

In order to obtain a useful velocity function $v(p, \sigma)$, certain assumptions must be made.

Landed vehicle Earth-weight is 480 lb. This is equivalent to 81.5 lunar pounds or 20.4 lb per wheel. The force transmitted to each axle is composed of three components. They result from the rolling friction at the wheels (R_r), soil deformation in and around the area of contact (R_m) and non-horizontal terrain R_s). While these components are influenced by such presently unknown factors as wheel design and terrain character, representative values have been determined empirically in studies with the SLRV. R_r is given as 7 percent of the weight at the wheel, R_M is $2R_r$, and R equals the weight on a wheel multiplied by the sine of the instantaneous slope.

$$R_r = 0.07\ (20.4) = 1.428 \text{ pound} \tag{17}$$

$$R_m = 2\ (1.428) = 2.856 \text{ pound} \tag{18}$$

$$R_s = 20.4 \sin\sigma \tag{19}$$

The instantaneous velocity v is then equal to the effective power P_e applied to each wheel divided by the total force at each wheel. For power in watts, force in pounds, and velocity in km/hr,

$$v(P_e, \sigma) = \frac{0.81 P_e}{4.284 + 20.4 \sin\sigma} \tag{20}$$

If the new forces derived in Section V—D1 for a 540-lb LRV are used, Equation (20) becomes

$$v(P_e, \sigma) = \frac{0.81\ P_e}{4.8 + 22.9 \sin\sigma} \tag{21}$$

Since freewheeling of LRV on negative slopes may increase the chances of overturning and other hazardous events, it is assumed that the wheels are always in gear and that the downhill velocity is constant and equal to that on level ground.

The velocity function $v(P_e, \sigma)$ is shown for the full range of σ in Fig. V-73. Equation (7) can now be evaluated for the functions described in Figs. V-72 and V-73. A numerical calculation produces for the 480-lb LRV

$$V_A = 0.178\ P_e \tag{22}$$

Assuming a constant mobility power of 96 watts or 24 W per wheel and a mechanical efficiency of 30 percent, the average velocity would be

$$V_A = 1.28 \text{ km/hr} \tag{23}$$

V_A for the 540-lb. LRV would be somewhat less than this.

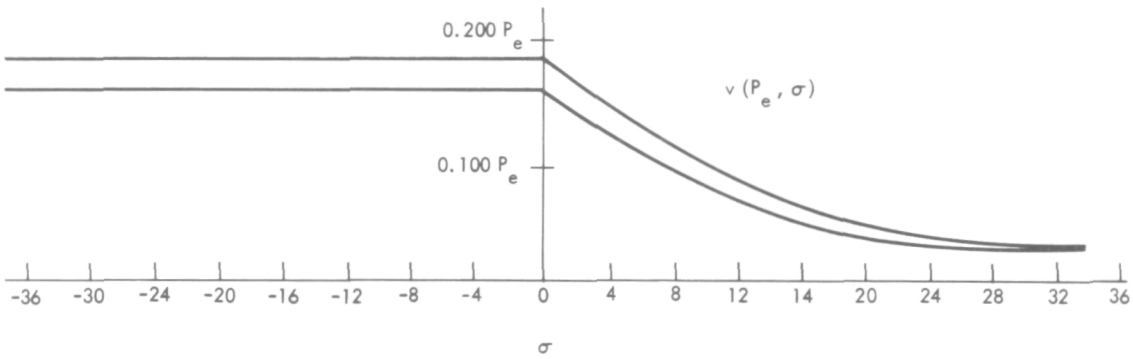

Figure V-73. Velocity Functions for $v(P_e, \sigma)$ for Full Range of Sigma

Vaughn (Ref. V-18) describes in tabular form the distribution of slopes for four types of mare. The calculation of V_A, given the smaller vehicle, for these slope distributions leads to somewhat more pessimistic values as shown in Table V-31.

Table V-31. Speed as Function of Terrain

Type	V_A
Dark Regional Mare	0.171 Pe
Regional Mare	0.165 Pe
Smooth-Rayed Mare	0.169 Pe
Rough-Rayed Mare	0.159 Pe

The average velocity V_A is plotted as a function of the effective power P_e in Fig. V-74 for each of three terrain types: Choate's model for Maria Cognitum and Tranquilitatis and the floor of Alphonsus; Vaughn's Smooth-Rayed Mare; and his Rough-Rayed Mare.

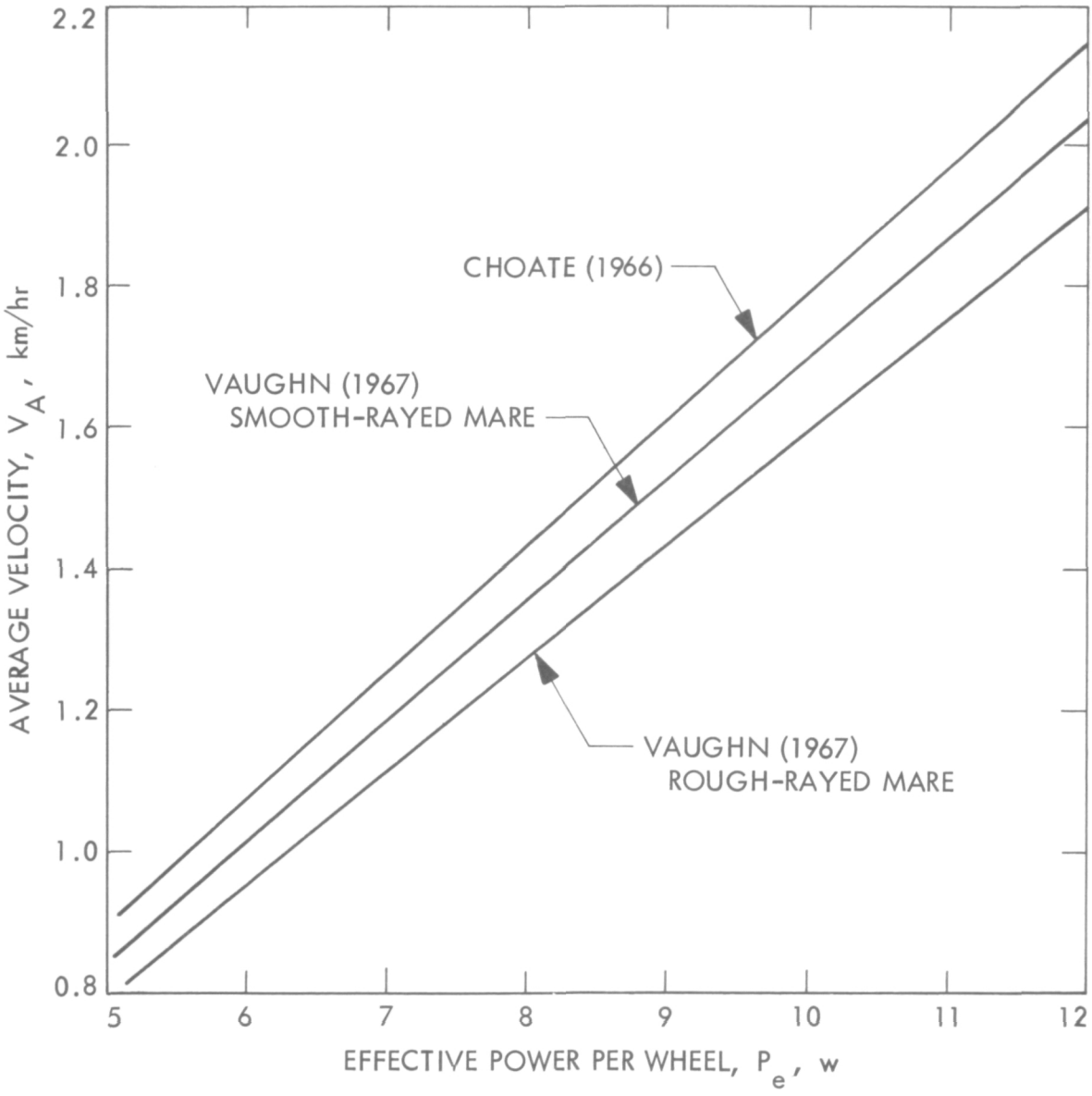

Figure V-74. Average Speed as Function of Effective Power per Wheel

The new power estimates in Section V. D1 built around a 540-lb LRV call for 125w for locomotion. This is more than enough to compensate for the heavier vehicle in the calculation of V_A.

2. Assumptions

A brief examination of the assumptions underlying these results and particularly the estimate in equation (22), may allow us to anticipate somewhat higher average velocities for LRV. The first two assumptions act against a higher V_A, the next two can be made to increase it, and the effect of the last is more uncertain.

(1) The slope distribution of Choate (1966) is clearly too mild for LRV planning purposes. Vaughn's (1967) mare models show a more severe distribution of slopes. The introduction of highland terrains would require a yet more severe $p(\theta)$. All other things being equal, this certainly means a lower V_A.

(2) The assumption that $p'_\theta(\sigma)$ is a constant for all σ may not be accurate. A tendency has been observed on a model vehicle in sand to seek the local gradient when going both uphill and downhill. If this is indeed a general effect, by equation (4) $p'(\sigma)$ will show a greater preference for the higher instantaneous slopes, and V_A decreases.

(3) The assumption of constant velocity for negative σ and constant power for positive σ is not a requirement. If the mobility system permits free wheeling on negative slopes up to a safety limit of say 5 km/hr, clearly this would produce an increased V_A. If the power system permitted more power to the wheels on positive slope, not necessarily to maintain a constant speed, the average velocity would be higher. The trade-offs involved in these variants require more study.

(4) It is felt that the assumption of 7 percent for the coefficient of rolling friction is conservative. However, more accurate information on this parameter may require a full scale engineering model and testing.

(5) The force due to soil deformation in and around the area of contact (R_m) is difficult to assess. Current studies at JPL on soil-wheel interaction problems (cf. Section V-O) should help in making a more accurate estimate of this parameter. In particular, it is important to know whether R_m is in any way a function of velocity.

Obviously, more power available at the wheels allows a greater V_A. This can be accomplished by greater power capacity, e.g., larger solar panels, and/or more efficient transmission of power to the wheels. Relying heavily on prospects of some freewheeling on negative slopes, more power on increasingly negative slopes, and greater electromechanical efficiencies one can anticipate the negative effect of other factors to be more than offset. For purposes of further discussion of mission parameters, V_A is taken to be 1.5 km/hr with the expectation that it may be as high as 2.0 km/hr.

3. Average Station Time

In addition to average vehicle speed V_A, a necessary estimate is the average time S spent at a station for purposes of navigation. The average station time S originally estimated at 13-1/4 minutes in Ref. V-3, is revised higher to reflect a more detailed analysis of the activities and commands required for a typical station at which the standard site identification sequence and commanded traverse sequence are performed. The revised value of S is

$$S = 23\text{-}1/2 \text{ min} \tag{24}$$

The detailed time estimates are summarized in Table V-32 and fully listed in Appendix C.

Table V-32. Average Station Time

Site Identification Sequence	Time in Seconds
Wide angle TV scan	269
Landmark identification	480
Narrow angle survey	164
Locate on map	300
Commanded Traverse Sequence	
Select bearing and step distance	40
Orient LRV on new bearing	20
Verify new bearing	90
Pre-traverse and post-traverse preparations	48
	1411 = 23-1/2 minutes

4. Average Step Time and Average Step Distance

This value of S is important in a consideration of which combinations of the mission parameters, average velocity V_A, average step time M, and average step distance W, are acceptable. In order for the mission to cover 1500 kilometers on the Moon in 12 months time, the LRV must traverse a total distance,

$$D = 1835 \text{ kilometers} \tag{25}$$

in a total traverse time

$$T = 2870 \text{ hours} \tag{26}$$

(These values of D and T are revisions of figures published in Ref. V-6.) The mission parameters must satisfy the equation given on page 58, Ref. V-6.

$$D = TV_A \frac{M}{M + S} \tag{27}$$

In equation (27) D, T, and S are constraints of the mission. For values of these quantities given in equations 24-26, $V_A = F(M)$ is shown in Figure V-75.

Points on this curve represent a lower limit of V_A for a given M that LRV must perform and still meet the mission constraints. Since $W = MV_A$, lines of constant step distance W are shown parametrically in Figure V-75. Since an upper limit of 1.5 km/sec has been concluded for V_A, this sets an upper bound in Figure V-75 to a region of acceptable combinations of the mission parameters.

The last bound to the region is set by either an upper limit on the average step time M or the average step distance W. The more likely limitation in practice will be on W since there are two factors involving navigation efficiencies which suggest lower step distances. One is the desire not to lose sight of all

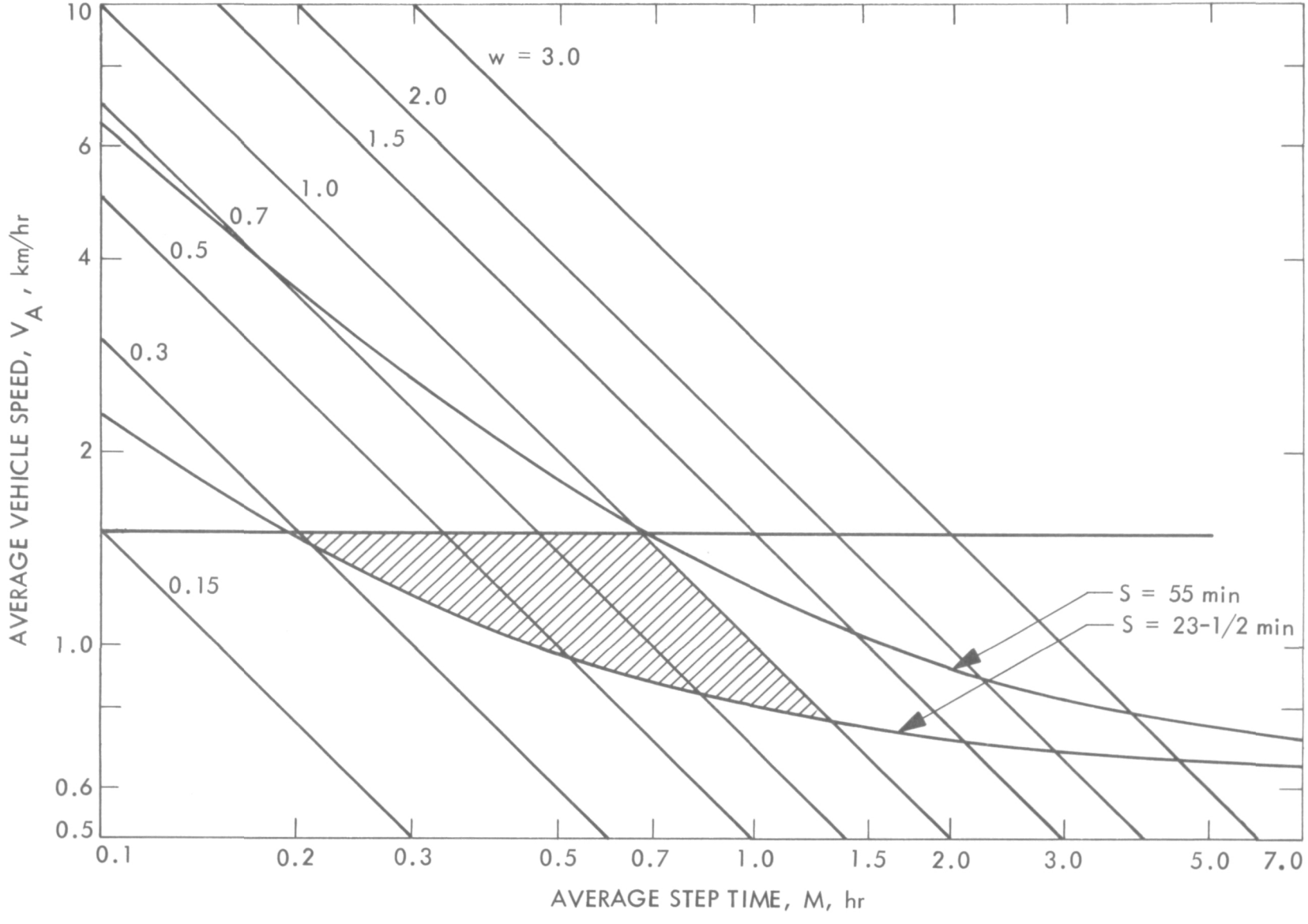

Figure V-75. Average Step Time Versus Average Vehicle Speed

landmarks used to locate LRV at the previous station. On the average this would be something more than the horizon distance of a 5-foot mast on a spherical Moon, or

$$W = 2.3 \text{ km.} \tag{28}$$

The second and more limiting factor is to keep navigation and guidance errors to the 10 percent estimated. These errors accumulate from the successive deflections of LRV from a straight path by craters and other terrain irregularities. Although some efforts have commenced in the Advanced Lunar Study to get a measure of these effects (see Crater Deflection Analysis), a firm estimate is at this writing unavailable. For the immediate purpose, the average step distance W is assumed to be in the neighborhood of one kilometer.

5. Crater Deflection Test

The matter of deflection of LRV from its course by passing through a crater becomes critical as one attempts to lengthen the average step distance W. For larger W, the likelihood increases for larger deviations from the planned path.

In a preliminary effort to quantify crater deflection, a model vehicle with four-wheel drive has been run over a conical crater in a fine sand somewhat approximating the grain size distribution of lunar soils (Fig. V-76). The dimensions of the vehicle and crater are listed in Table V-33.

The model vehicle was directed toward the crater parallel to a line through the crater center and at various distances, referred to as the offset parameter a (cf. Fig. V-6), from that line. Ten runs were made for each value of $\underline{a}$ at 3-in. intervals, with the reference line through the crater center changed frequently to obviate any systematic errors in the formation of the crater. After the vehicle had negotiated the slopes of the crater and stopped, the angular deflection was measured between the orientation of the vehicle and its original course. The mean $\bar{\delta}$ and standard deviation σ of these measurements are presented graphically as a function of $\underline{a}$ in Figs. V-77 and V-78. (The offset parameter $\underline{a}$ is normalized with respect to the crater diameter D, a ranging from -D/2 to +D/2.)

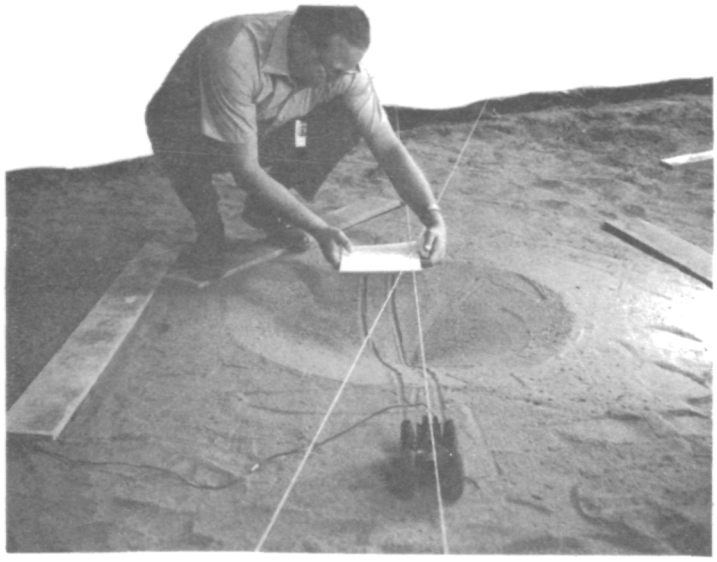

Figure V-76. Crater Deflection Test Setup

Table V-33. Crater Deflection Test Dimensions of Vehicle and Crater

Model Vehicle	Dimensions, in.
Wheel base	4-3/8
Wheel span (outer edges)	3-3/4
Tread width	1/2
Wheel diameter	3-1/4
Crater	
Diameter (D)	36
Depth (d)	6

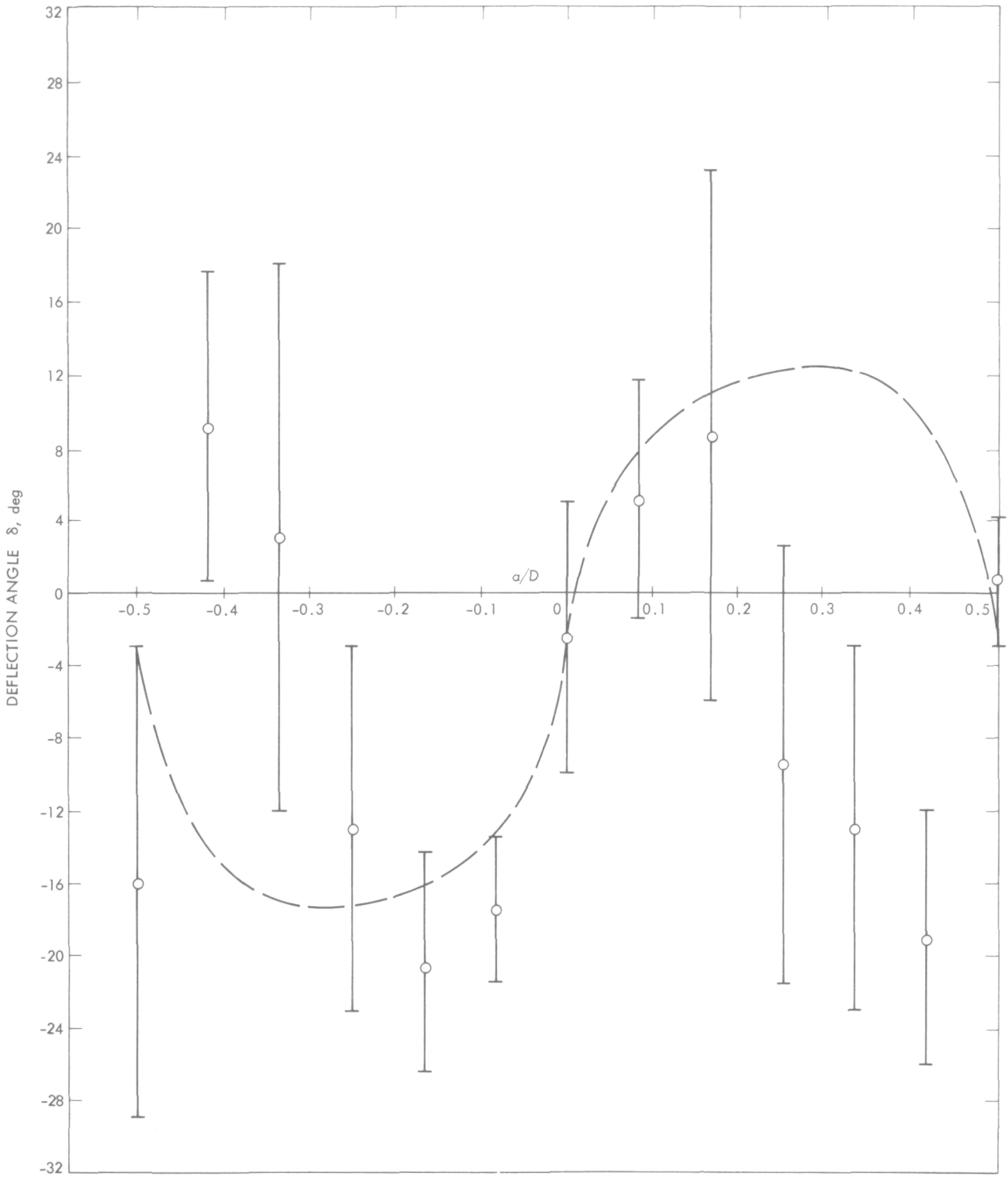

Figure V-77. Results of Crater Deflection Tests

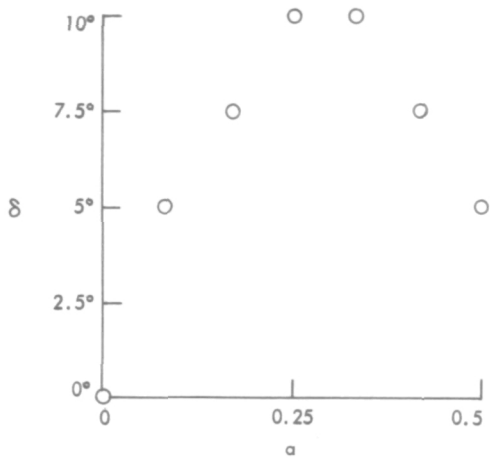

Figure V-78. Results of Shallow Crater Deflection Test

The significant thing about Figure V-77 is the reversal of the direction of deflection at approximately a = ±0.2 D. This reversal is due to wheel slippage on the uphill slopes that tends to draw the rear of the vehicle to the crater center. For $|a| < 0.2D$ the front of the vehicle is drawn toward the center, and deflection is that expected for an attractive scattering center. Therefore, as the wheels begin to slip, the vehicle alters course again for $|a| > 0.2D$.

Some confirmation of this explanation was obtained by a single set of runs in a much shallower crater. For the same diameter crater (D = 36 inches) but only 3-inch depth, values of the deflection angle δ obtained for positive a (measured to the right of the reference centerline) are plotted in Figure V-78. For these shallow slopes no slipping of wheels was observed. Although these data are not statistically significant, they do suggest a well-behaved function δ(a) like that shown as a broken line in Figure V-77.

A useful quantity is the expected angular deflection E(δ) for craters of various sizes. This can be calculated for the crater with the deflection data shown in Figure V-77 from the formula

$$E(\delta) = \int_{-D/2}^{D/2} \delta(a)p(a)\,da \qquad (29)$$

where the probability density p(a) is 1/D, and δ(a) is assumed to be normally distributed and given by

$$\delta(a) = \bar{\delta}(a) \pm \sigma(a) \qquad (30)$$

In order to adjust for an apparent systematic error in the data, each δ is increased by 2.5°. Evidently, the vehicle consistently turned somewhat to the right so that $\overline{\delta}(0) = 2.5°$. If this adjustment is made and equation (30) is used, the expectation of δ by numerical integration is

$$E(\delta) = 3.0° \pm 9.0° \tag{31}$$

The fact that the mean of $E(\delta)$ is not equal to zero indicates that not all systematic errors have been eliminated. However, if the assumption that $E(\delta)$ is normally distributed holds, and if equation (30) is examined without further qualification, the probability P that $E(\delta) \geq \delta$ is plotted in Fig. V-79.

It must be noted again that these results on the question of crater deflection are found on the basis of an extremely limited sample. The experiment, itself, is difficult to extend to the operation of a full scale LRV in the lunar environment. Certainly, more shallow craters imply less slipping and a less rapid decline of the probability P in Fig. V-79.

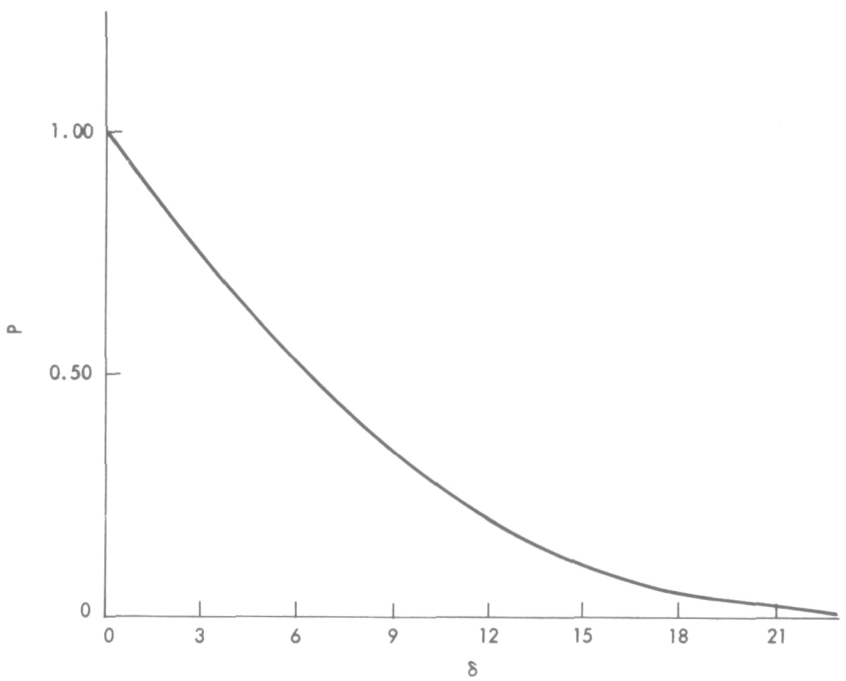

Figure V-79. Deflection Probability

O. WHEEL-SOIL INTERACTION STUDY AND TESTS

An outline is presented herein, of the basic theoretical concepts and analysis being used to determine the bearing capacity and the pressure-sinkage relationships of soft soil surfaces when subjected to uniform vertical loads. This study is being implemented by an exploratory testing program. The results of both analysis and tests will be used to evaluate mobility performance of the LRV. The conclusions will be valid for any environment as long as the soil mechanical properties are expressed in terms of friction and cohesion. (cf. Sec. V-F.)

The need of this analysis arises due to the practical impossibility of obtaining bearing capacity values and pressure-sinkage relationships by direct tests as done on Earth over potentially known and accessible environments. Faced with this problem, the objectives of this study are:

(1) Theoretical determination of the ultimate pressure load of horizontal or sloping lunar surfaces.

(2) Determination of soft soil surface pressure-sinkage relationships to evaluate lunar vehicle performance.

(3) Testing to see if the pressure-sinkage relationships can be predicted by using the ultimate pressure load.

This study relates mainly to the safety and performance of vehicles operating over horizontal soil surfaces or when climbing, descending, or traversing a sloping ground. For testing purposes and to verify the theory, use is made of a cohesionless soil (sand).

A possible extension of this study is outlined and refers to the ultimate load (vertical or inclined) that a lunar crater can support close to the crater rim.

1. Soil Bearing Capacity Problem

Currently there is no general and reliable theoretical formulation, based upon tests, which presents the influence of terrain slope on the soil bearing capacity. Available solutions provide only the ultimate bearing load applied uniformly on an infinitely long strip over a horizontal terrain. An exact solution of this problem was obtained by Sokolovsky who also considered inclined loads. An approximate solution to the same problem was obtained by Terzaghi (1943) and improved by Mayerhof (1951) who expanded the results (1953) to include

oblique loads over horizontal terrains. This author also studied the case of vertical loads applied on slopes considering either purely cohesive or cohesionless soils only, a limitation which restricts its general and practical application. Recently, Karafiath (1968) following Terzaghi's basic concepts and using Sokolovsky's intermediate results, formulated the ultimate (vertical or oblique) load on the slopes. No load optimization or tests were made to better define and verify the results. Since the problem on hand is of non-linear character and the methods of approximation resort to the principle of superposition, it is impossible to state the degree of approximation obtained.

As an attempt to solve the problem of ultimate load on sloping surfaces, it is considered that the application of limit load analysis of the theory of plasticity to soil mechanics will permit us to arrive at a satisfactory solution. In this context, the theorems of collapse load of limit analysis define upper and lower bound loads between which lies the ultimate load. A proper selection of both velocity and stress field pattern permits us to narrow down the interval of these bounds, and a better definition of the ultimate load is obtained. The identity of both the upper and lower bounds is a sufficient condition to define the true maximum load.

Plastic limit analysis theory was used in the study of the punch indentation problem of soils by Shield (1955). A rather large difference between bounds was obtained for friction angles between 30 and 40 degrees, of particular interest to lunar soils. Furthermore, the soil was considered weightless although this factor bears significantly on the ultimate load value. To obviate these limitations, the present analysis will consider the soil weight and further attempt to narrow down the interval between the limiting loads.

To this effect, a theoretical study was done and numerical results have been obtained which define the upper limit load of the lunar surface when subjected to a quasi-static vertical load applied on an infinitely long strip of known width, resting either on a horizontal surface or along a sloping terrain. The solution accounts for the influence of depth of penetration, soil weight, friction, and cohesion.

It is assumed that the lunar soil behaves as a rigid plastic material which follows the Coulomb-Mohr failure condition for solids and its associated flow rule. This criterion satisfies reasonably well the expected failure modes and

the character of the lunar soil as described by its mechanical properties based on Surveyor lunar experiments; the angle of internal friction is 37 ±2 degrees, Cohesion C is 0.06 psi and unit weight in the lunar gravitational field is 15.0 lb/cft ±2.0 lb/cft. A computer program was developed which accounts for all these factors.

This study, proceeding now, attempts to define the lower bound load which results from an appropriate selection of a stress field pattern.

After a satisfactory solution of the problem to account for vertical loads, the results will be extended to cover inclined loads.

It is further emphasized that the infinite strip direction is horizontal along the slope and not up, down or at the top of the slope (rim of a lunar crater). Each of these cases requires a separate study which can be done based on the same method of solution.

2. Extension of Analysis

The importance of the various stability conditions to which the LRV will be subjected as it traverses sloped surfaces cannot be over-emphasized. The sorting out, and overriding of obstacles can always be managed on a go - no go basis as long as the vehicle has the design power and discrimination capability to operate accordingly. When faced with the maximum support that the ground can provide, the soil mechanical properties, and lunar topography, slopes and regions of slope changes play an important role in disclosing the potential risks of the vehicle becoming immobolized. This may be due to excessive sinkage or due to the existance of weakening tension cracks around the periphery of a crater edge. In the latter case, a state of failure could result in a pronounced tilting of the vehicle accompanied by a loss of its stability. Within the same analytical framework, a possible extension of this study could cover the ultimate load a lunar crater edge can support.

In the application of the numerical data, extreme care should be exercised when trying to extend the results of an infinite strip to a finite circular, rectangular or elliptical load pattern. These factors should be interpreted in the light of the three-dimensional criteria of soil failure which, in the present state of theoretical soil mechanics, are still under discussion and experimentation. Nevertheless, an attempt will be made to better define and improve on the current available concepts.

3. Testing Program

The following exploratory testing program describes the basic information, methods and procedures required to corroborate the load-bearing capacity values and the pressure-sinkage relationships to be used in connection with lunar surface vehicle mobility studies. Specific information is given with reference to equipment handling, instrumentation, soil preparation and generation of testing data.

The purpose of these tests is to disclose the soil failure character and response (load versus displacement) of two principal soil surface types:

(1) Horizontal soil surface

(2) Sloping soil surface

In both cases the applied loads are uniform and vertical. In the case of horizontal surfaces the displacements are restricted to develop along the vertical direction only. For sloping surfaces the bearing plates are guided and displacements may occur simultaneously in the vertical and horizontal direction.

Plate-soil contact starts either on or at a specified depth below the surface. In all cases during the penetration process the bearing plates are maintained parallel to the original soil surface.

The objectives of the tests are:

(1) To verify the analytical approach which formulates the bearing capacity of horizontal and sloping terrain surfaces subjected to quasi-static uniform vertical loads.

(2) To find out if the bearing capacity of cohesionless soil surface slope can be predicted up to slopes equivalent to the soil angle of repose.

(3) To qualify the semiempirical procedure designed to estimate the pressure-sinkage relationships whereby a single continuous load penetration test may be approximated by a series of load bearing capacities as functions of the depth below the terrain surface.

(4) To compare the influences of plate size and geometry (rectangular, square, circular, and wheel shapes) on the soil bearing capacity and pressure-sinkage relations.

(1) Test Boxes. Two plywood boxes reinforced with peripheral aluminum corner angles are provided to contain the soil material (Fig. V-80). The inside box dimensions are 28 inches x 38 inches each having a depth of 30 inches and 40 inches, respectively. The 40 inch box is used to form soil slopes at 15 and 35 degrees. The 30 inch high box is used for horizontal surfaces. Box dimensions are established to minimize the wall boundary effects for the selected bearing plates. The walls are marked every half inch to control the soil surface level during sand pouring. Special aluminum guides are provided to support a metal straight edge which smooths the soil surface to prescribed heights and slopes. An overhead crane picks up the box by means of four steel cables attached to the corners and carries it to the load testing machine.

(2) Soil Hopper. A specially designed wood hopper 26 inches x 11.5 inches x 13 inches high permits the soil to flow down into the test box at a controlled rate and height while it can displace horizontally and/or vertically (Figs. V-81 and V-82). The bottom of the hopper has an adjustable gap which permits control of the sand flow. The soil is deposited in the test box under similar conditions of flow rate and height. This generates an artificial sand bed of homogeneous and reproducible granular structure over a wide range of densities.

(3) Soil Material. The soil material selected is an air dried, coarse, medium to fine white silica sand. Penetration tests are done on a compact sand in which a shear type failure can be produced by bearing plates.

The following tests, performed at Cal-Tech by Professor R. F. Scott, established the basic sand identification and properties. These test results will be used to evaluate the plate penetration tests on sand.

(a) Sieve analysis to define the grain size distribution.

(b) Maximum and minimum sand density to determine the parametric limits of soil behavior.

(c) Direct shear tests of sand for dense and loose conditions to determine the angle of internal friction as a function of relative density.

(d) Angle of repose of compacted sand to define the limiting slope and stability conditions of the sand surface.

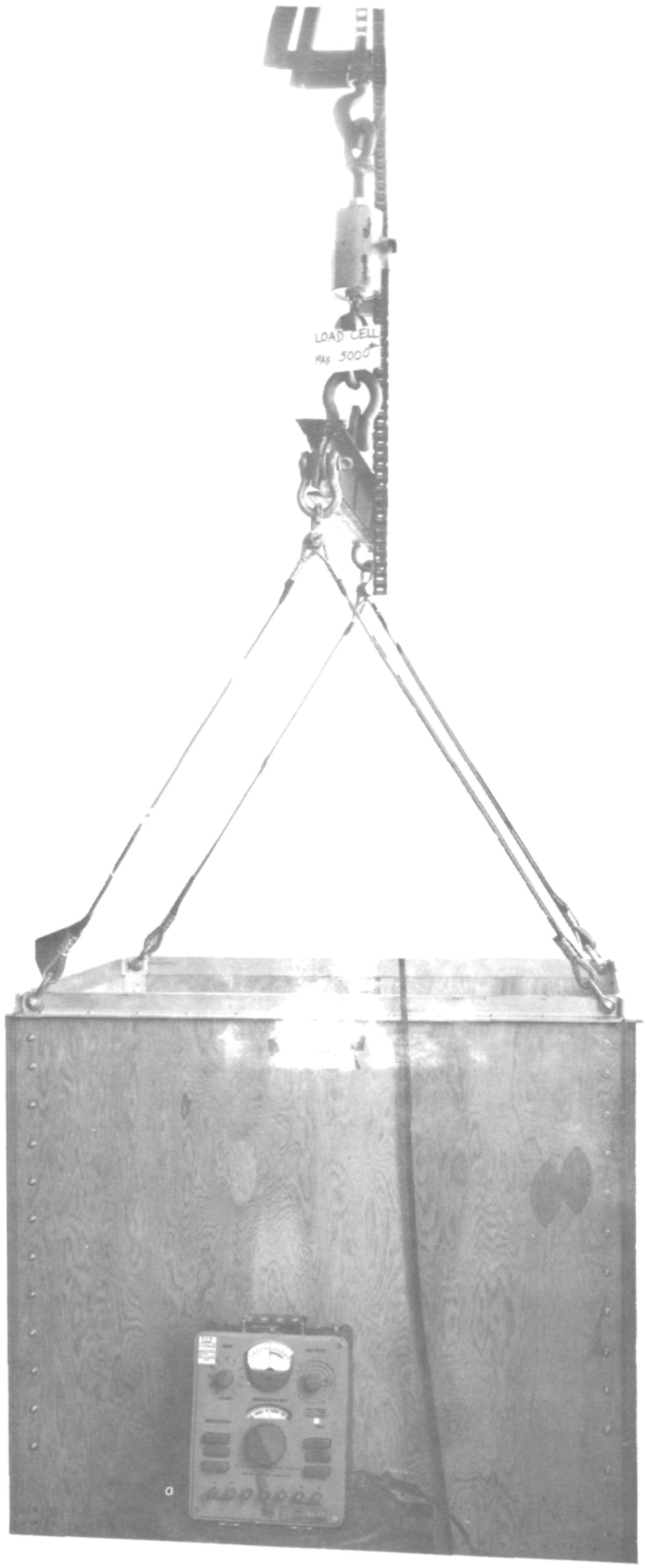

Figure V-80. Test Box

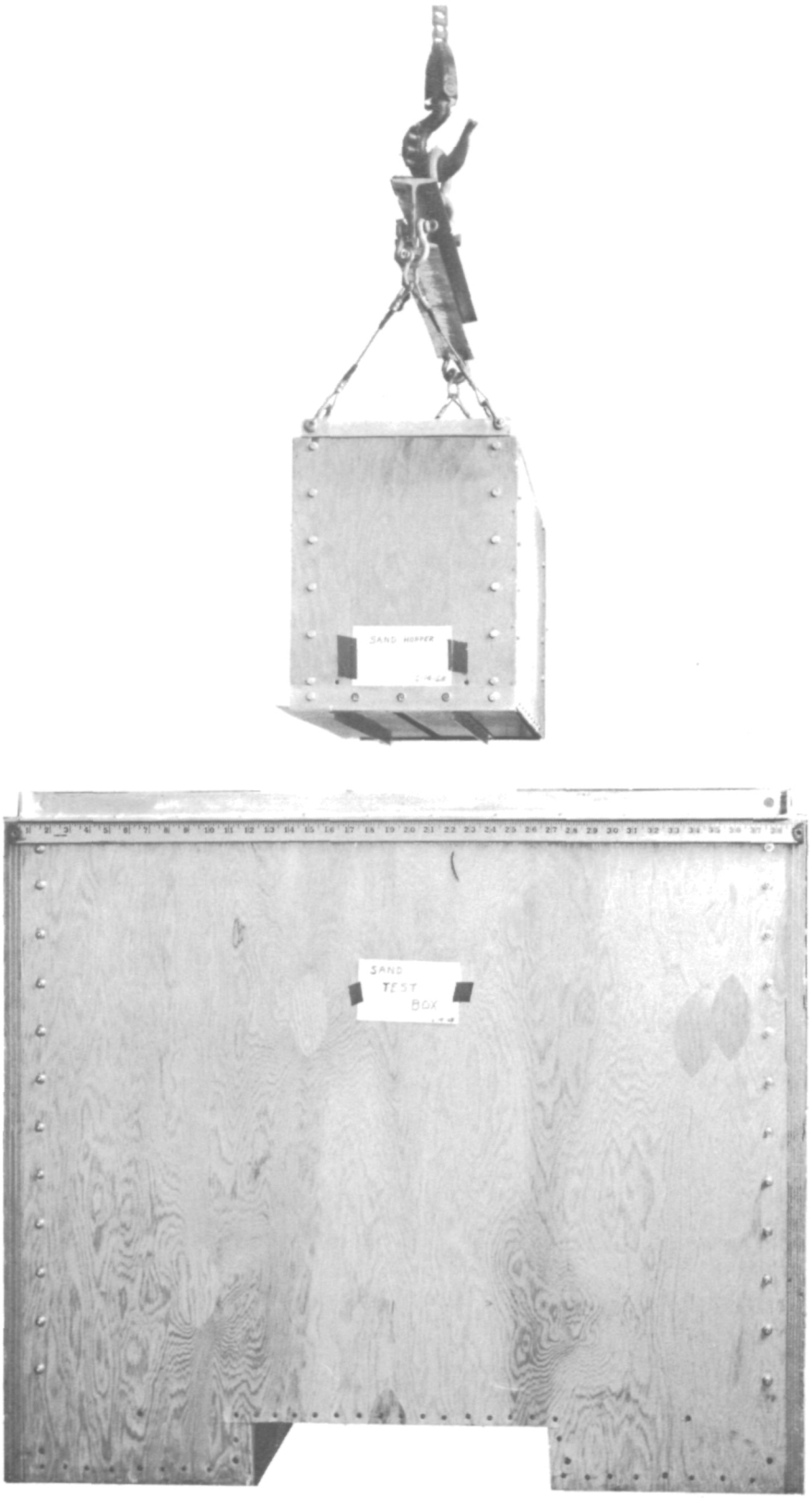

Figure V-81. Sand Hopper in Place Over Test Box

Figure V-82. Close-up of Sand Hopper

(4) Sand Bed Preparation. The most important controlling factors of soil placement relate to the uniformity and repeatibility of soil structure formation to set the test results on an equal basis. To this end a simple procedure using the soil hopper permits control of the sand density at all levels of soil bed preparation. The sand is compacted by its own weight falling through the hopper which can be displaced back and forth from a constant height (Fig. V-83).

The main factors controlling density of sand deposition are the rate of sand flow (weight deposited per unit time) and height of flow. For a constant flow height an increase of the rate of flow will decrease the density of the sand. The rate of flow has a more predominant influence in the soil density outcome than the variation of flow height. For instance, a height of 32 inches ±2.0 inches produces less than 1 percent variation in density. Dust conditions have been practically eliminated by selecting a sand mixture with less than 1 percent passing sieve No. 200 by weight and a maximum fall height of 32 inches.

After the box is filled to the prescribed level, its surface is smoothed out into either a horizontal or sloping configuration. Control weights are taken using a load cell and an SR-4 gage (Fig. V-80).

(5) Bearing Plates and Loading Ram. The bearing plates are made of aluminum. A variety of shapes and sizes can be used limited by the boundary influences of the testing box walls (Fig. V-84). Rectangular plate aspect ratio is 1 to 5 to simulate a uniformly loaded long strip in plane deformation.

A common fixture supports all bearing plates and a carriage permits unrestricted horizontal displacement to occur simultaneously with the vertical one. The horizontal carriage may be locked to produce only vertical displacements (Figs. V-85 and V-86).

4. Pressure-Sinkage Test

Test Box. The sand test box is set on the loading machine verifying that the bearing plate and soil surface are parallel. The compressive vertical load is applied at a penetration rate of 0.5 in/min and unloaded at .05 in/min. Loads, pressures and displacements are automatically and continuously recorded in two x-y plotters. One records load versus vertical displacement, the other pressure versus horizontal and vertical displacement.

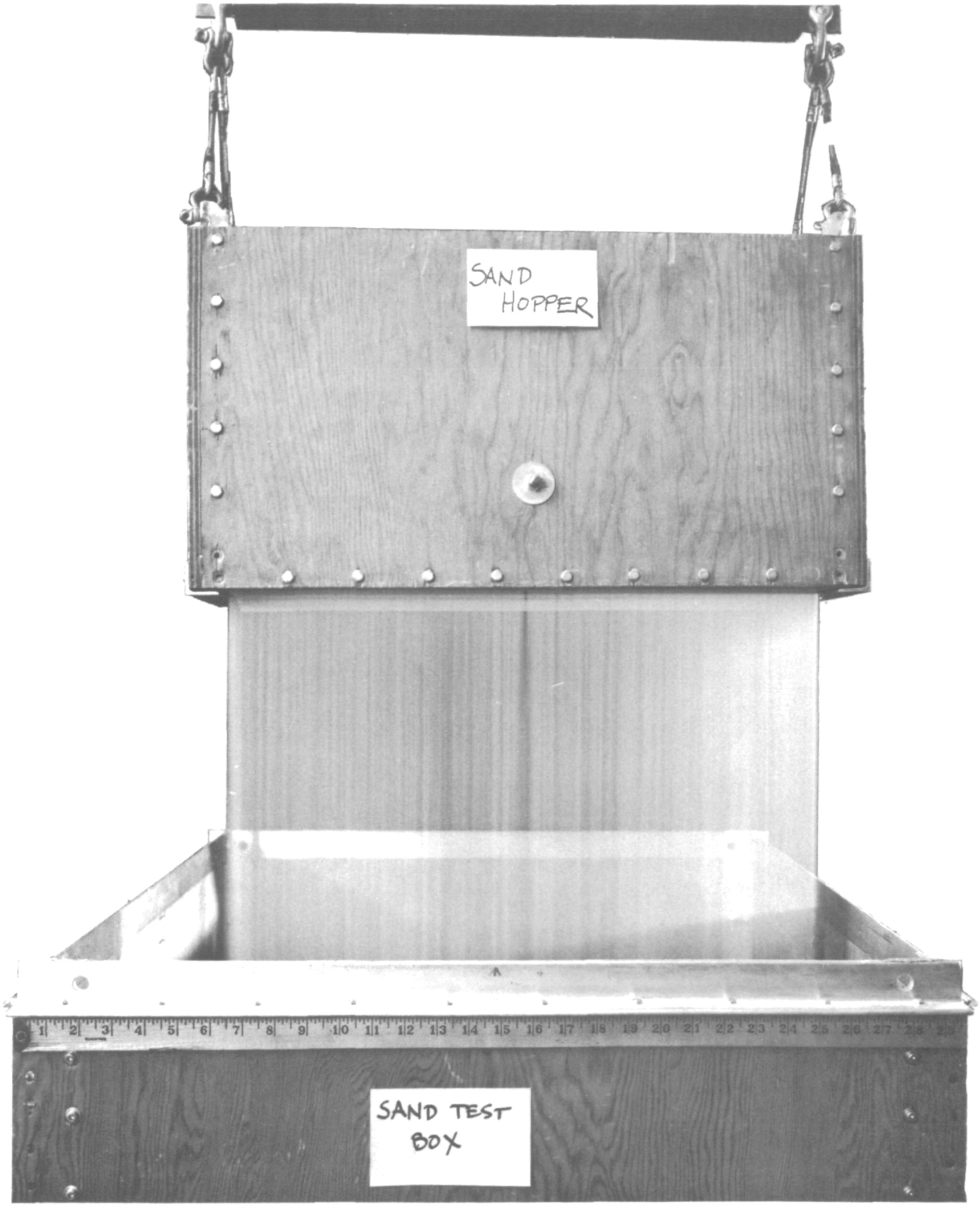

Figure V-83. Control of Sand Density

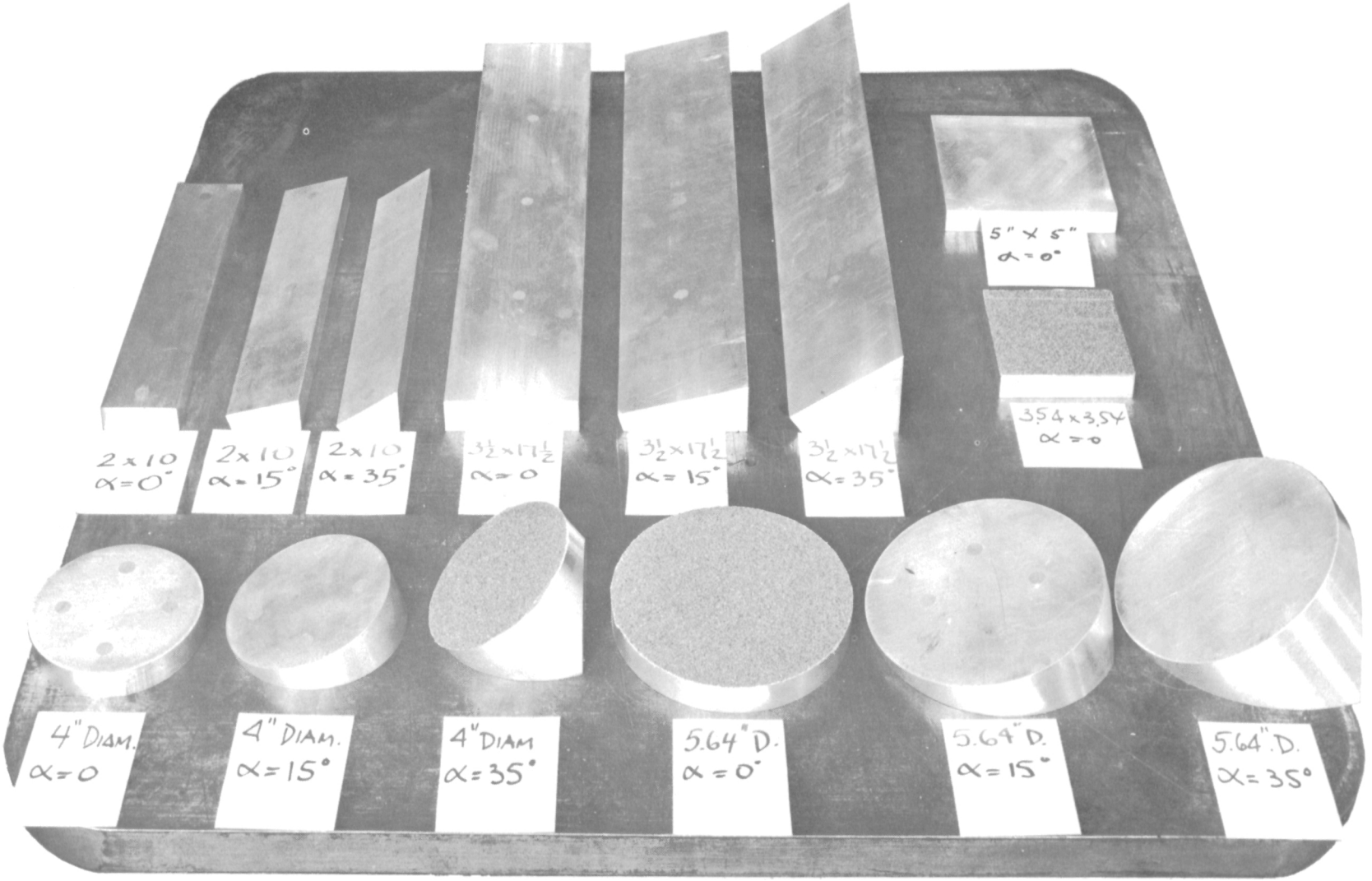

Figure V-84. Bearing Plate Configurations

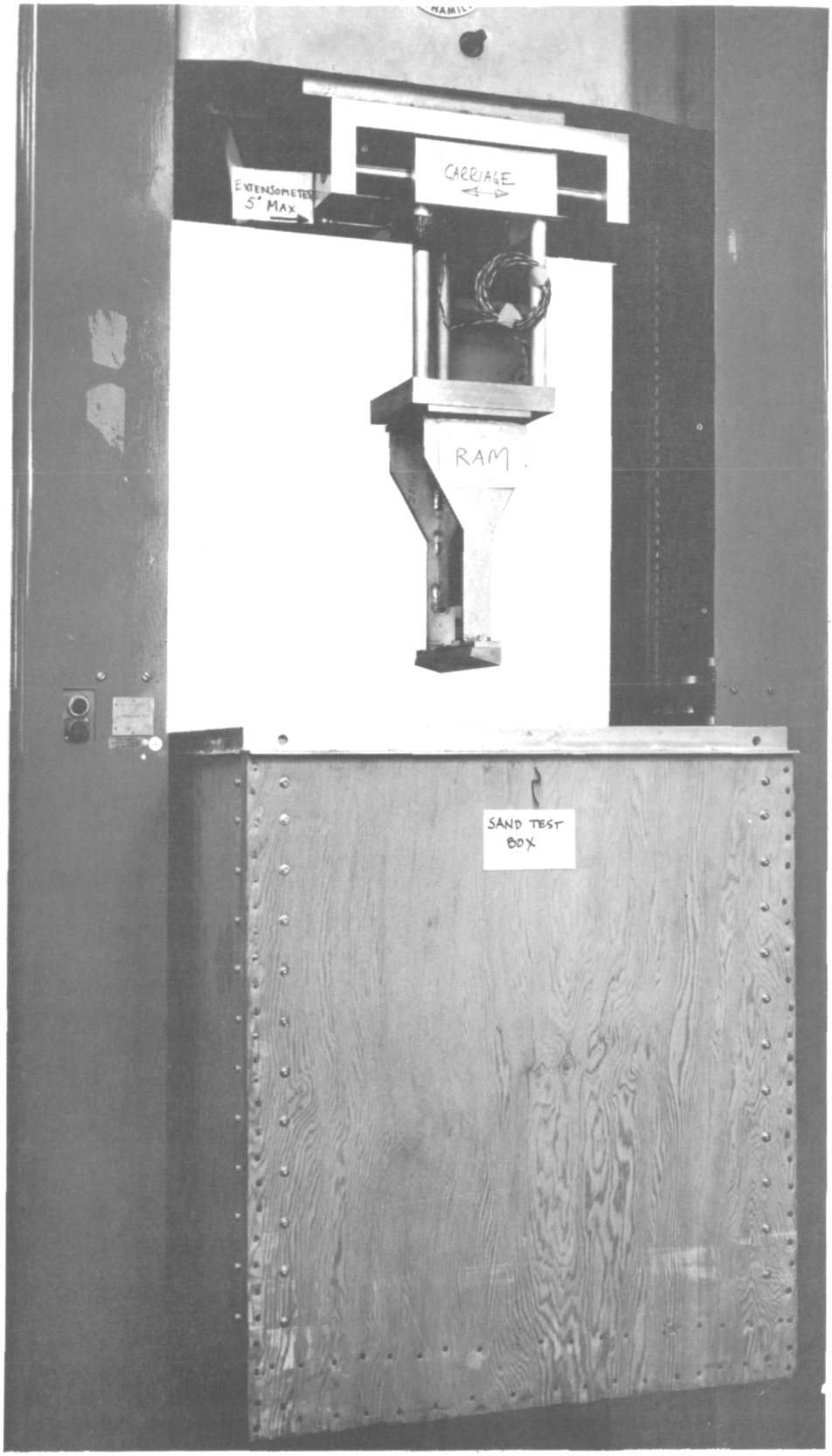

Figure V-85. Horizontal Carriage Fixture, Centered Position

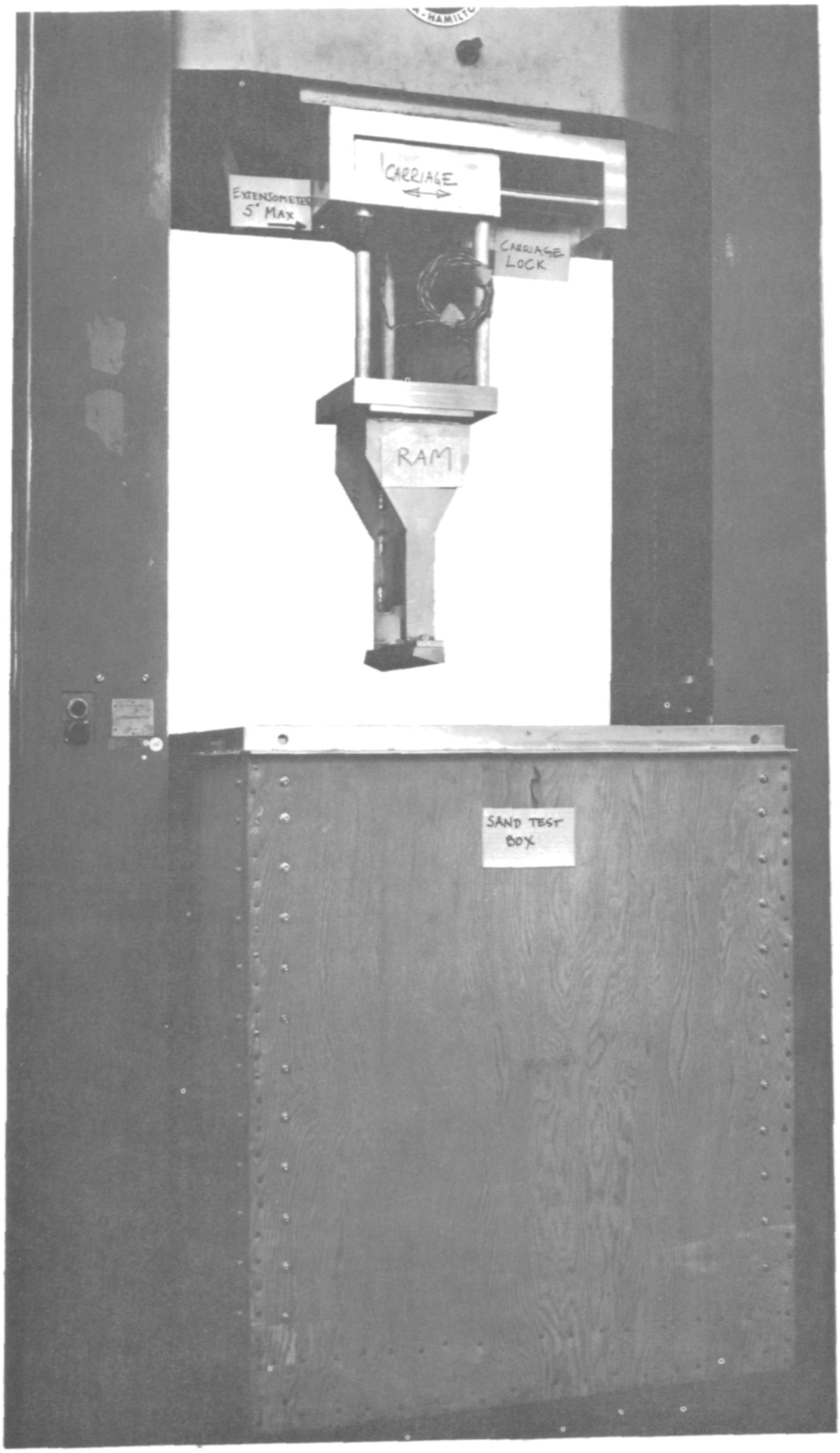

Figure V-86. Horizontal Carriage Fixture, Extreme Left Position

5. Testing Plan and Schedule (Table V-34)

Bearing Plate Tests. Four groups of bearing plate tests are planned. These are identified by their configuration as rectangular, square, circular, and wheel tests. A fundamental soil bearing test concept states that at least two load penetration tests are required on different sizes of the same plate configuration in order to determine significant pressure-sinkage relations. The minimum number of tests required results from the combination of plate shape, size, slope angle and initial plate level below the soil surface.

Table V-34. Test Plan for Plate Configuration

Plate Shape	Size (In)	Slope (Degrees)	Depth Below Soil Surface (In)	Number of Tests
Rectangular	2.00 x 10.00 3.50 x 17.50	0 15 35	0 1 2	18
Square	3.54 5.00	0	0 1 2	6
Circular (Diam)	4.00	0 15 35	0 1 2	18
Wheels	To be defined	0 15 35	0 1 2	18

6. Exploratory Test Results

Soil Tests. Some initial soil tests which were made to check out the experimental equipment are presented here for interest. These clearly demonstrate the effect of soil slope on the pressure-sinkage relationship and bearing capacity of loaded wheels and flat plates on frictional type soils.

The test wheels are shown in Figs. V-87 and V-88, sized 10 x 2.5 inches and 14 x 3.5 inches respectively. Segments of these wheels are attached to the loading ram (Fig. V-89) and load-penetration tests were made. Loads were applied vertically at a constant penetration rate of 0.5 in./min. on both horizontal as well as 15 degree sloped soil surfaces. Vertical as well as horizontal displacements were recorded using a special ball bearing supported loading carriage which permitted essentially free horizontal displacement of the loading fixture (Fig. V-90). Thus, the wheel segment follows the soil surface failure pattern simulating the free loaded stationary wheel of a roving vehicle traveling on the slope with little lateral restraint.

Results of these early tests for the wheels traveling along the 15 degree slope side as well as up the slope face are shown on Fig. V-91. With this limited information it is clear the slope effect on soil properties is considerable even at this low slope angle (15 deg) relative to the angle of repose (35 deg) and approximates the following expression:

$$\frac{P_\alpha}{P_H} = \left(1 - \frac{\alpha}{\phi}\right)^{1.5}$$

where

α = Surface slope

ϕ = Soil angle of internal friction (angle of repose approx.)

P_α = Load on sloped surface at given sinkage

P_H = Load on horizontal surface at given sinkage

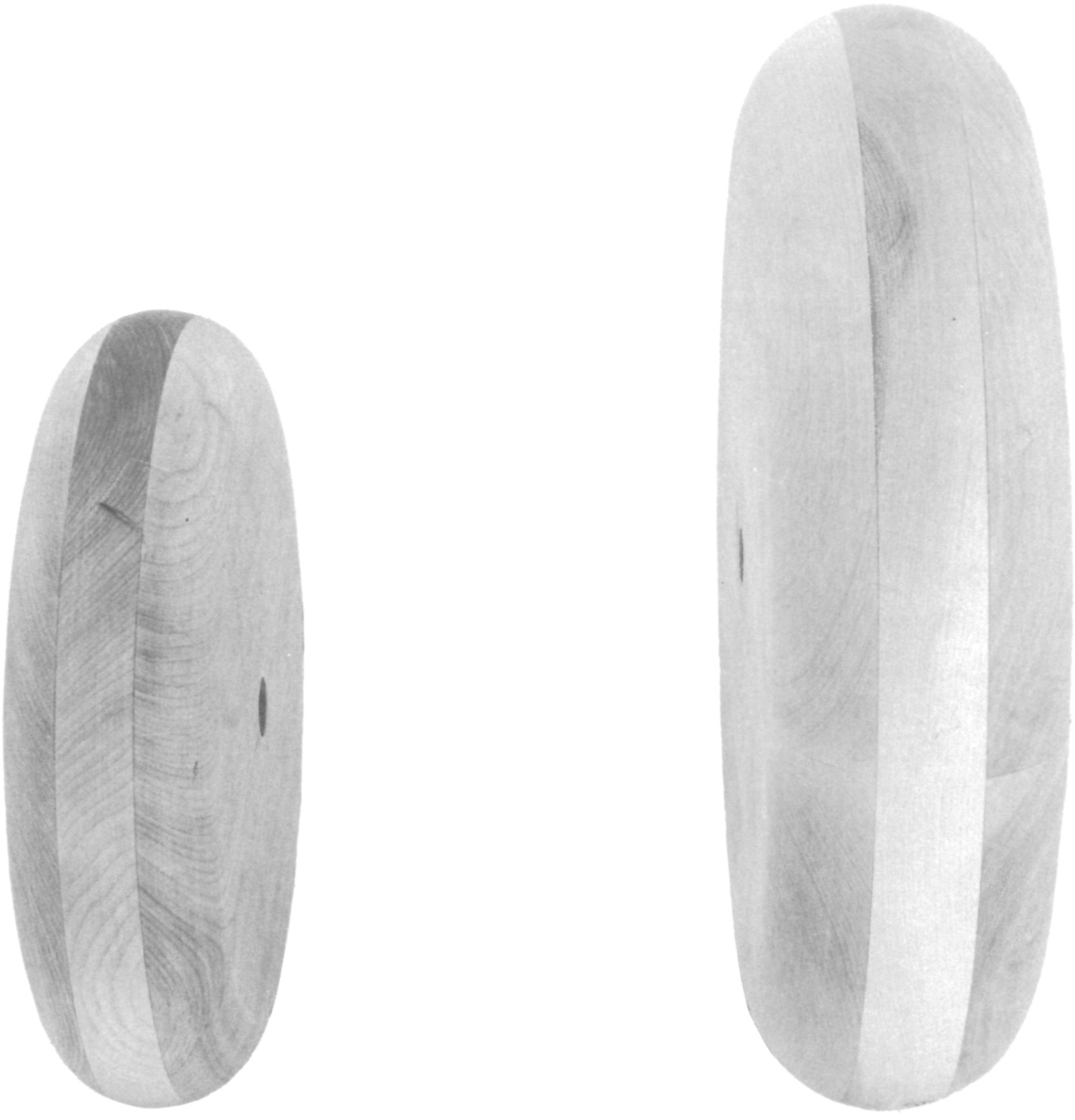

Figure V-87. Test Wheels, Front View

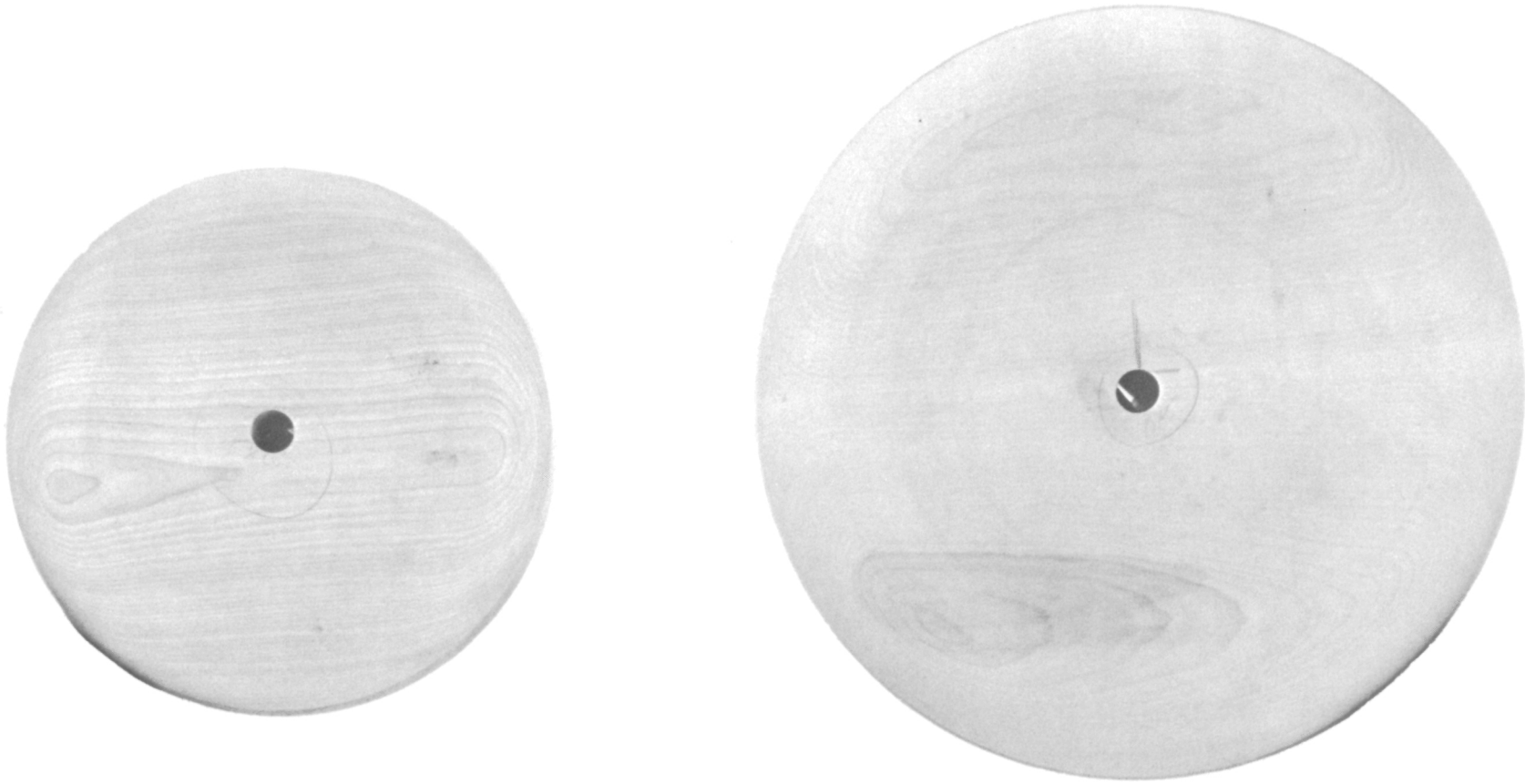

Figure V-88. Test Wheels, Side View

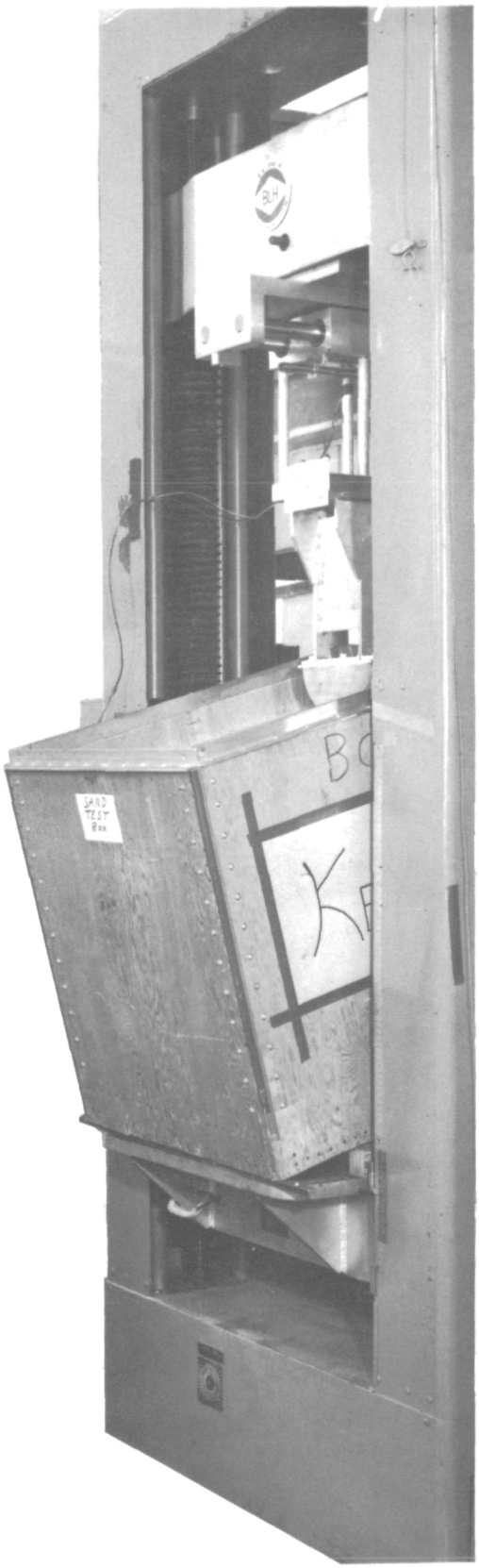

Figure V-89. Loading Ram with Wheel Segments Attached

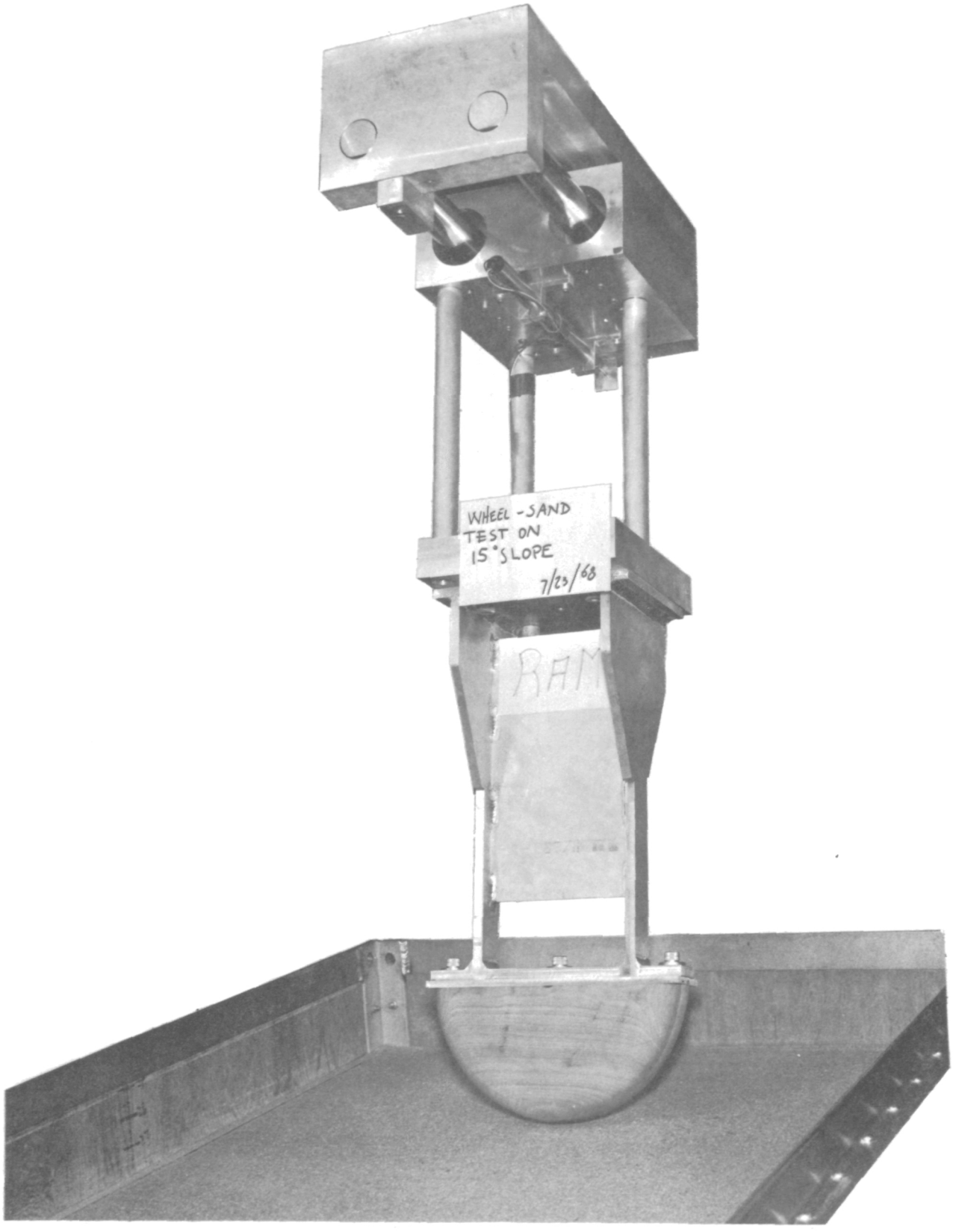

Figure V-90. Loading Ram Special Loading Carriage

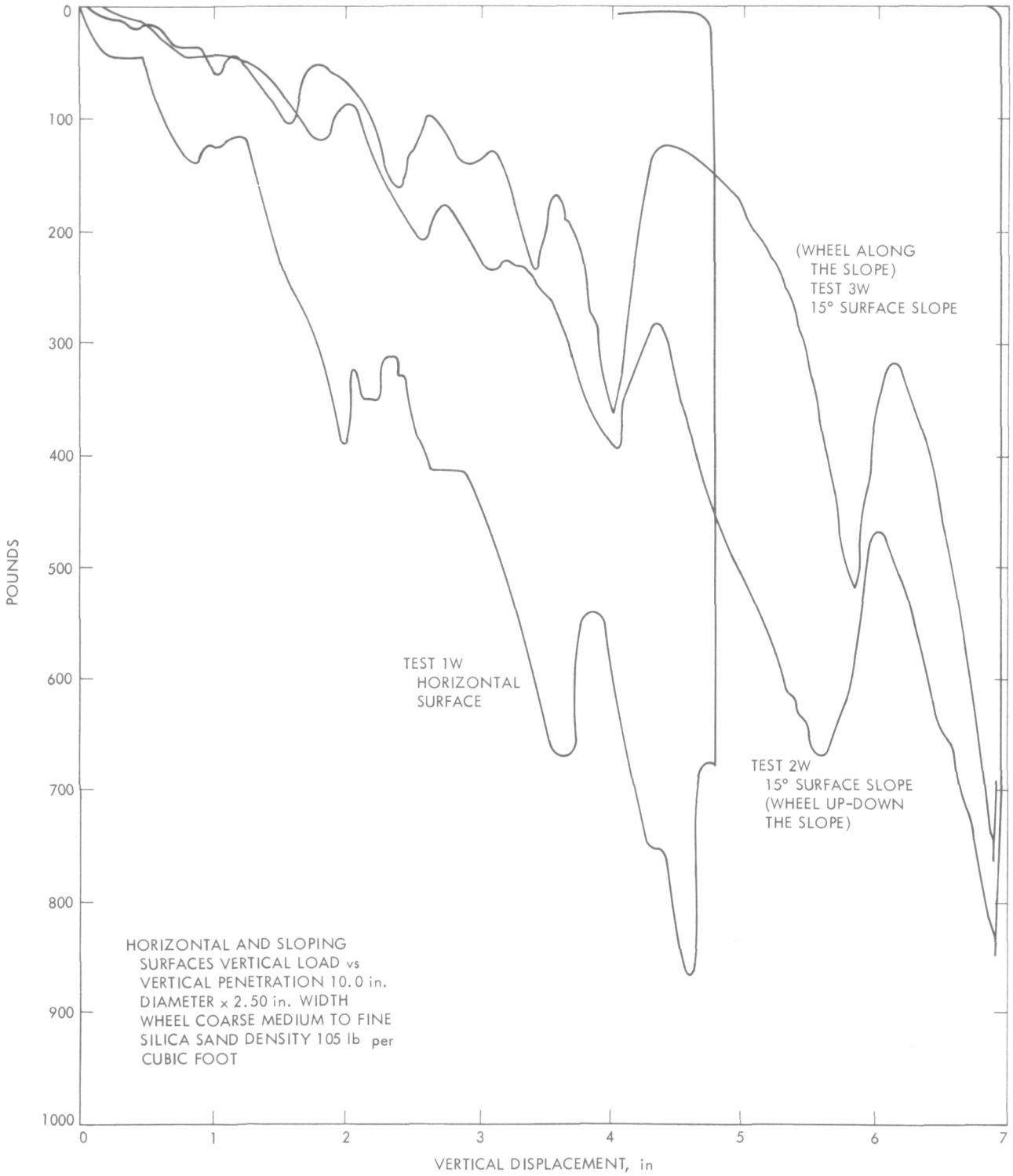

Figure V-91. Wheel Sinkage Test Results

This expression correlates reasonably well with the analytically developed equation where the slope effect was:

$$(1 + \frac{\alpha+\beta}{\phi})^{1.64}$$

Note: $\beta = 0$ and $\alpha = 15$ deg for the test conditions

Typical surface penetration failure patterns are shown as follows:

Figs. V-92, 93, 94	Horizontal Surface Tests - wheel along slope
Figs. V-95, 96, 97	15 degree Sloped Surface Tests - wheel along slope
Figs. V-98, 99	15 degree Sloped Surface Tests - wheel up down slope

Preliminary tests were also made with rectangular and circular plates with results as shown on Figs. V-100, 101, 102, and 103.

These exploratory results point out that:

(1) The effect of surface slope on frictional type soil properties is appreciable even at relatively low surface slopes compared to the angle of repose.

(2) Horizontal and vertical displacements are of comparable magnitudes and importance in sloped surface tests--whereas on horizontal surfaces the vertical displacements predominate.

Mobility Aspects. The practical implications of these results concern the following mobility aspects:

(1) Current mobility concepts refer only to horizontal terrains. These concepts will have to be re-evaluated and extended to include slope effects. In particular, new concepts of soil thrust, mobility resistance and slip on sloping terrains must be investigated to properly model and evaluate lunar vehicle mobility performance.

(2) The safety of the vehicle to perform on slopes is largely impaired due to excessive sinkage. Since vehicle design performance is highly dependent on slopes, further analysis and tests must be done to disclose preferred relative wheel-slope orientation to obtain optimum performance.

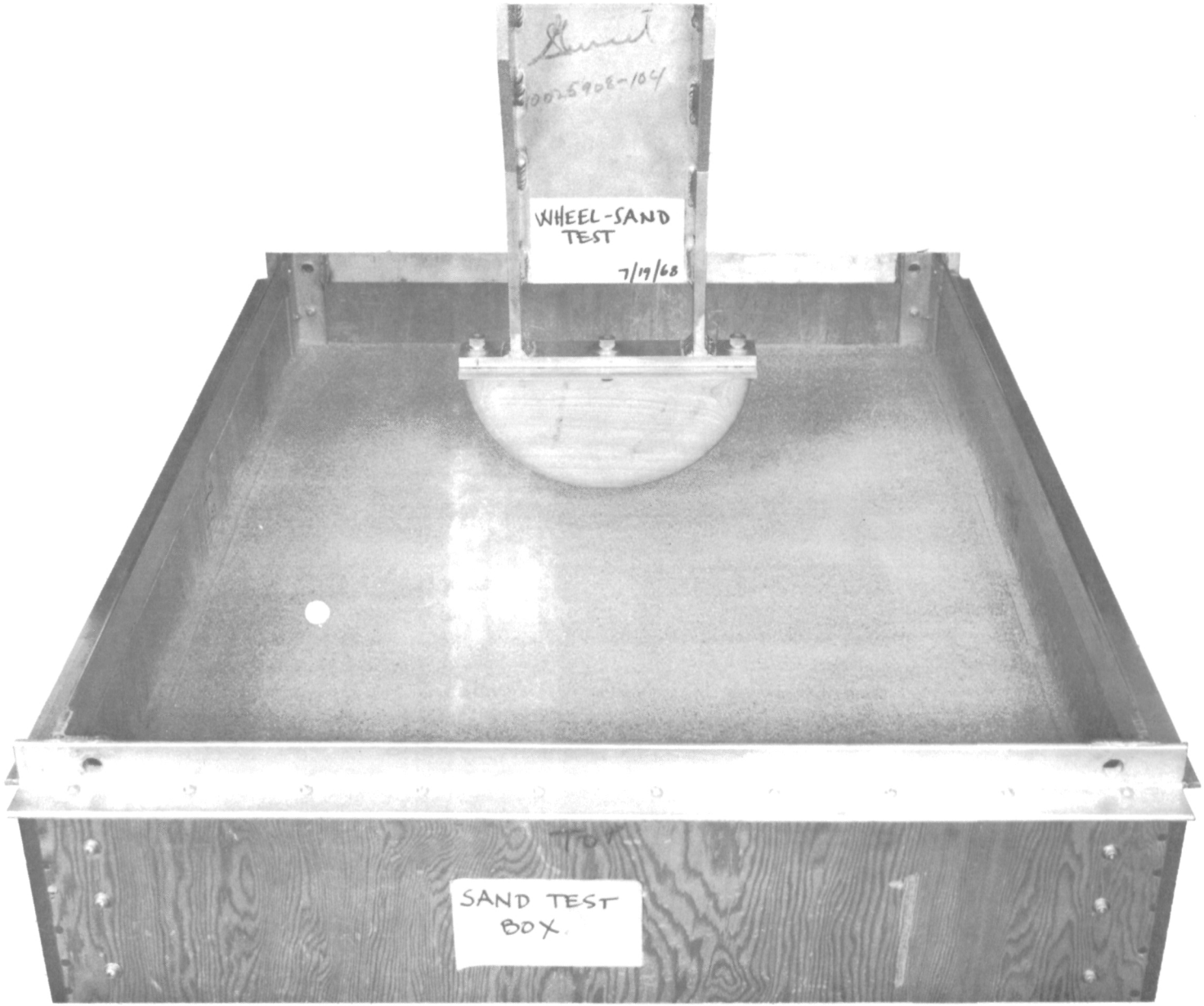

Figure V-92. Horizontal Surface Test (Wheel Along Slope) with Wheel Raised

Figure V-93. Horizontal Surface Test (Wheel Along Slope) with Wheel One-third Submerged

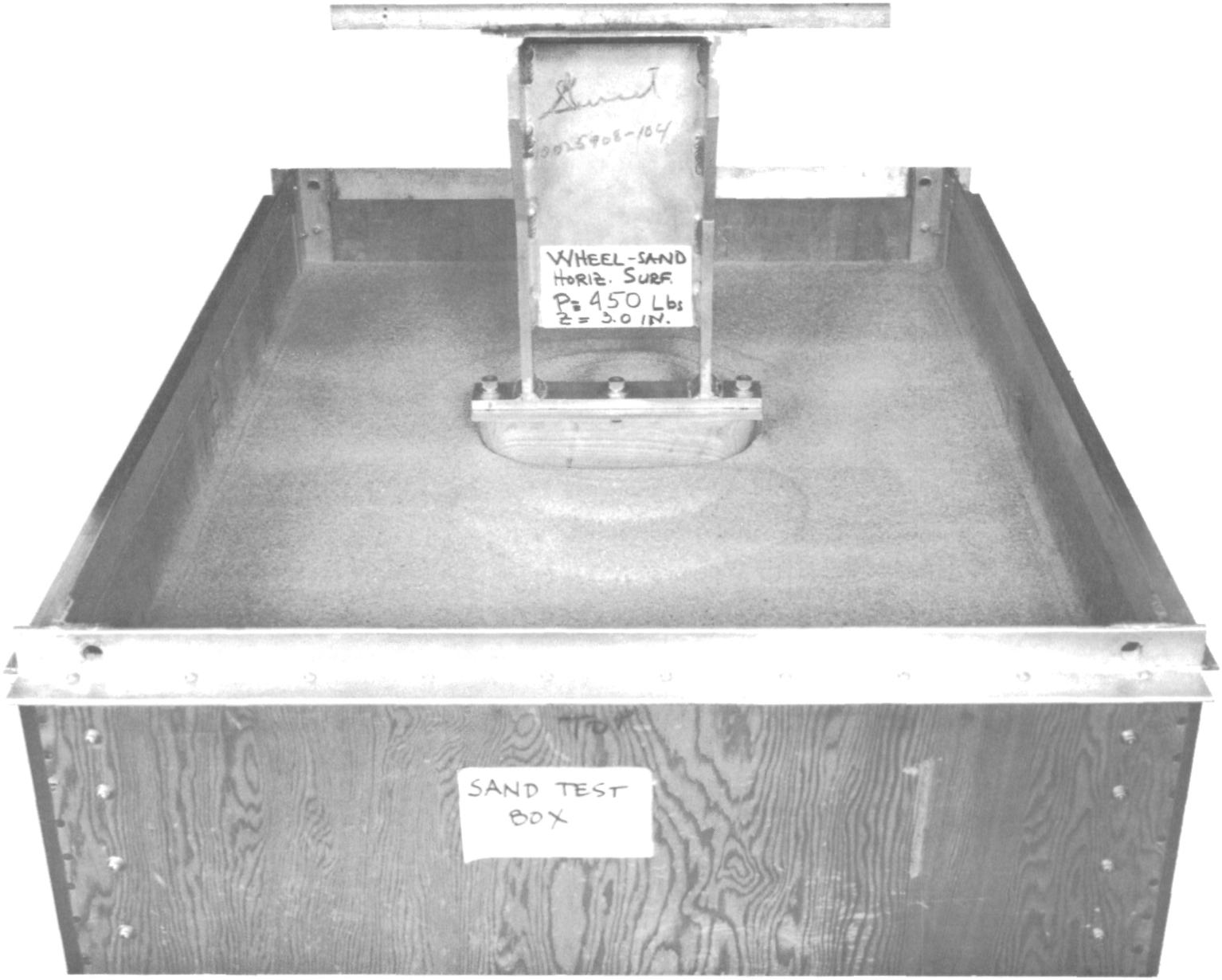

Figure V-94. Horizontal Surface Test (Wheel Along Slope) with Wheel Two-thirds Submerged

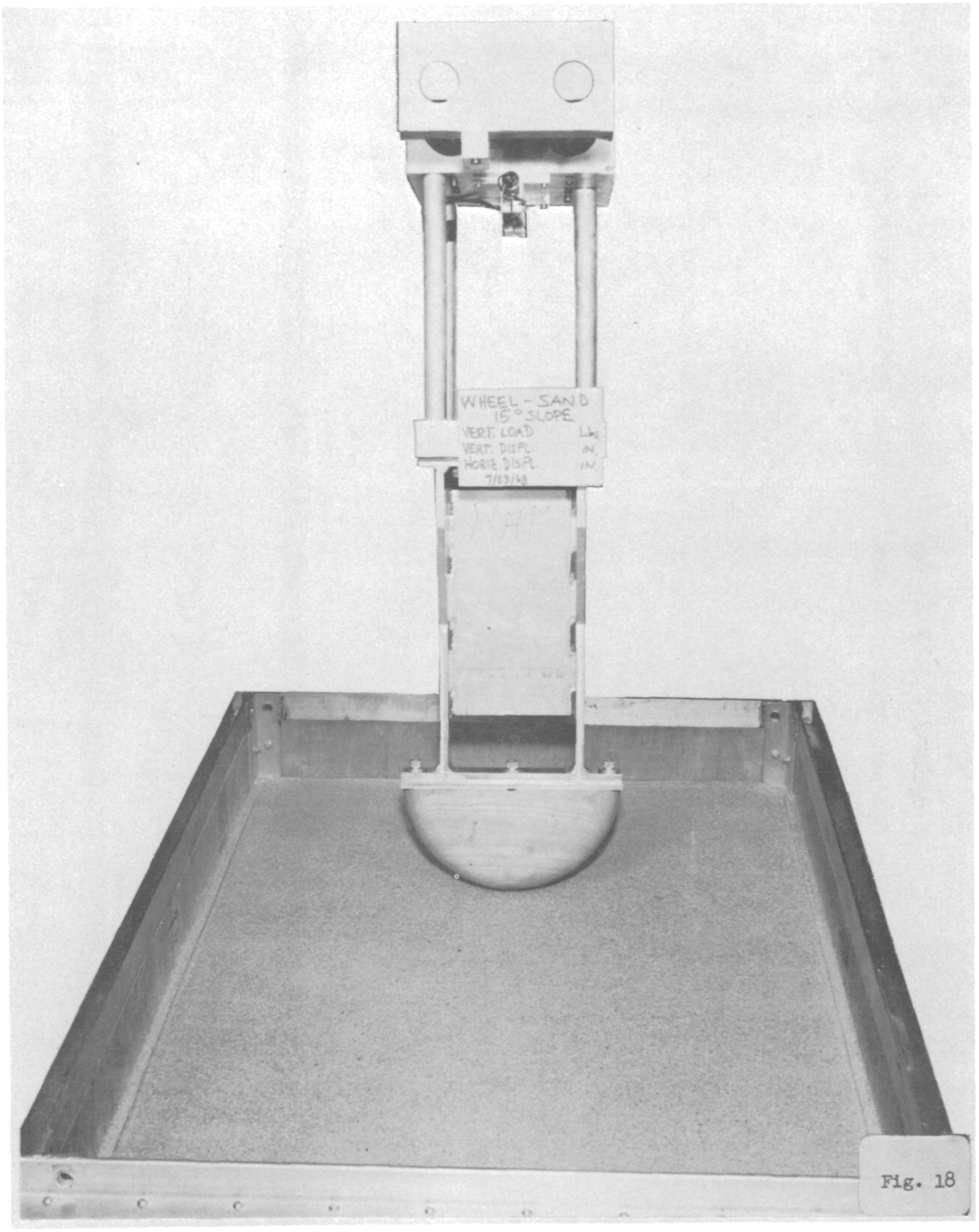

Figure V-95. Fifteen-degree Sloped Surface Test (Wheel Along Slope) with Wheel Raised

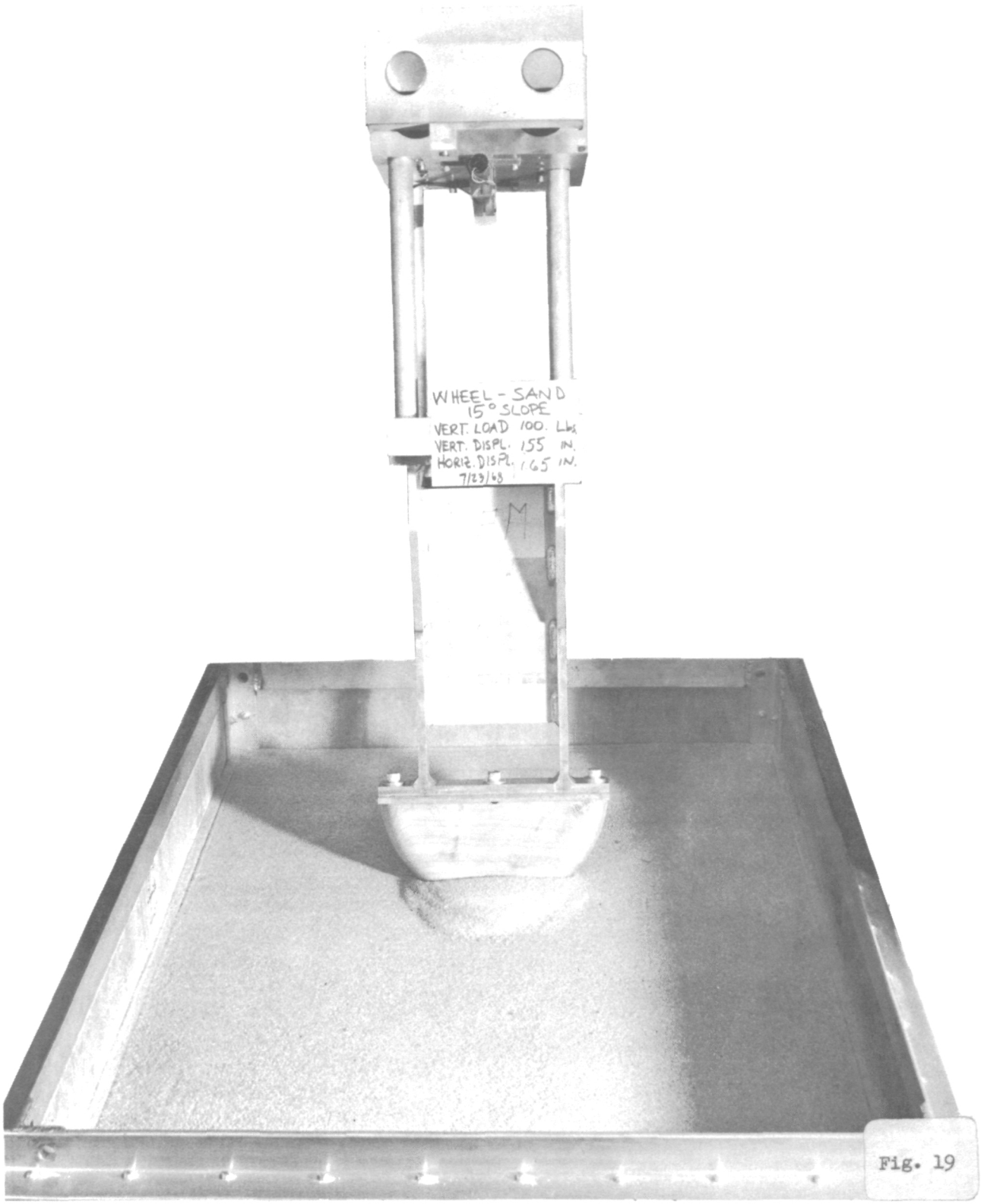

Figure V-96. Fifteen-degree Sloped Surface Test (Wheel Along Slope) with a 1.55 in. Vertical Displacement and a 1.65 in. Horizontal Displacement

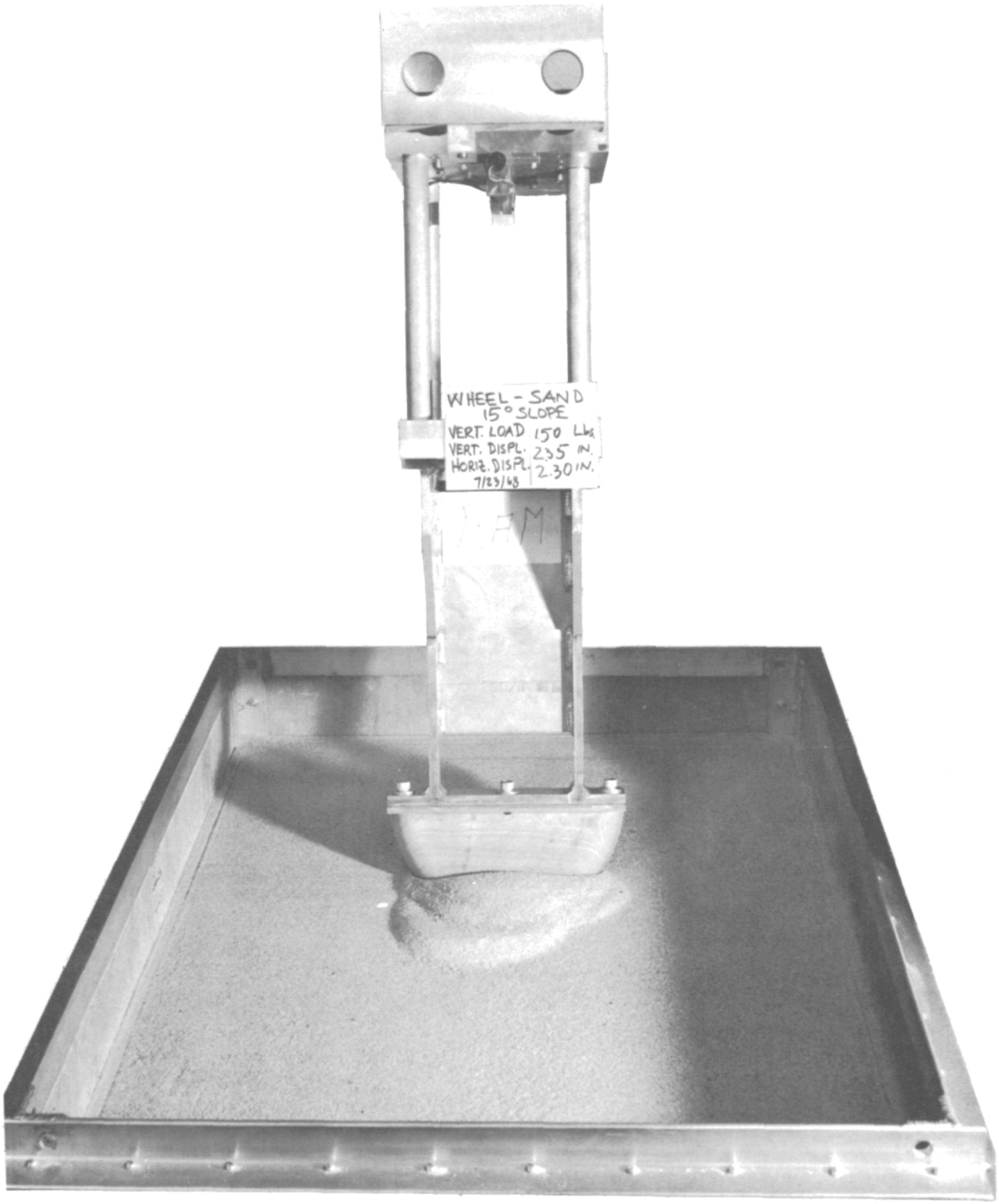

Figure V-97. Fifteen-degree Sloped Surface Test (Wheel Along Slope) with a 2.35 in. Vertical Displacement and a 2.30 in. Horizontal Displacement

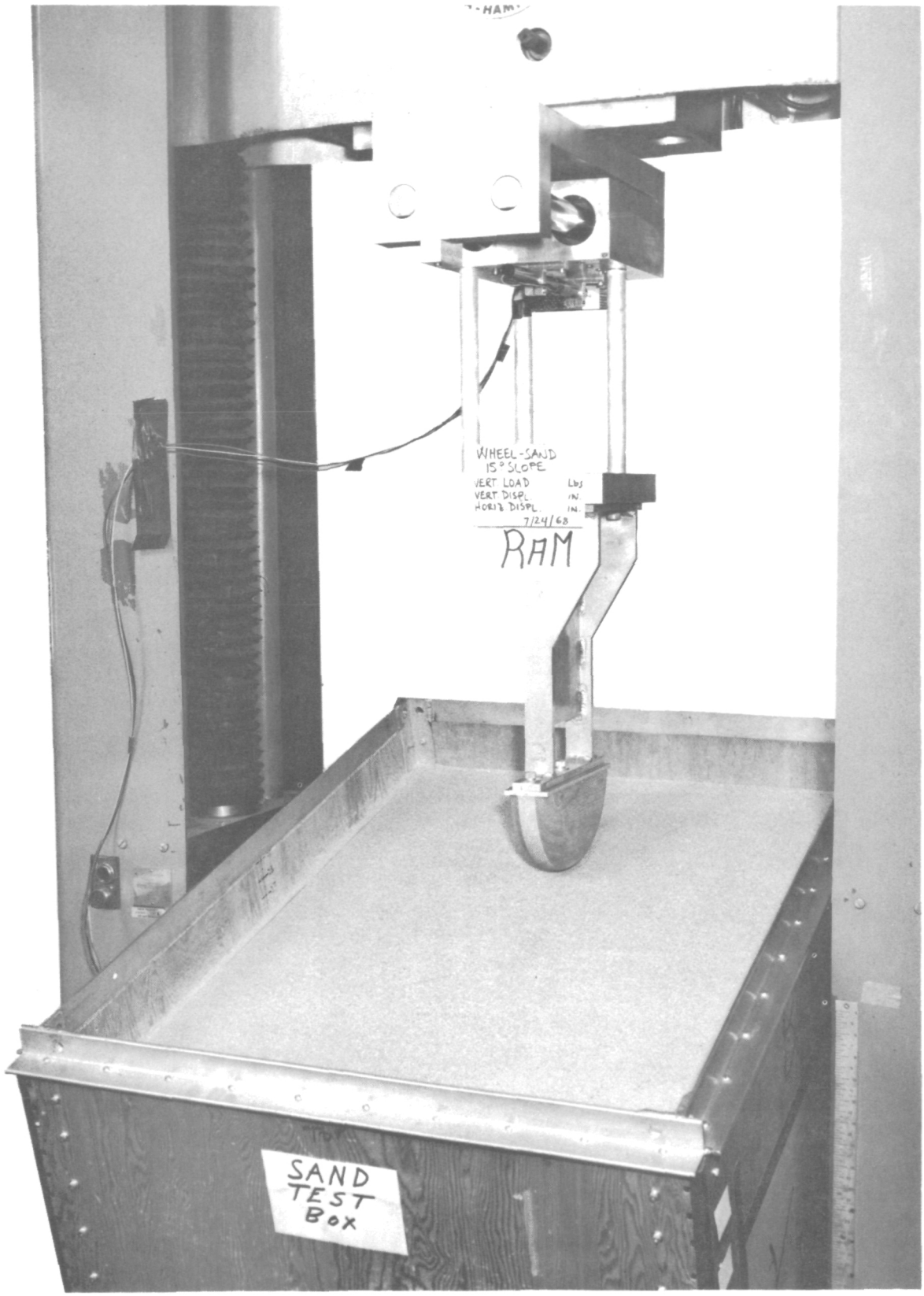

Figure V-98. Fifteen-degree Sloped Surface Test (Wheel Up-Down Slope) with Wheel Raised

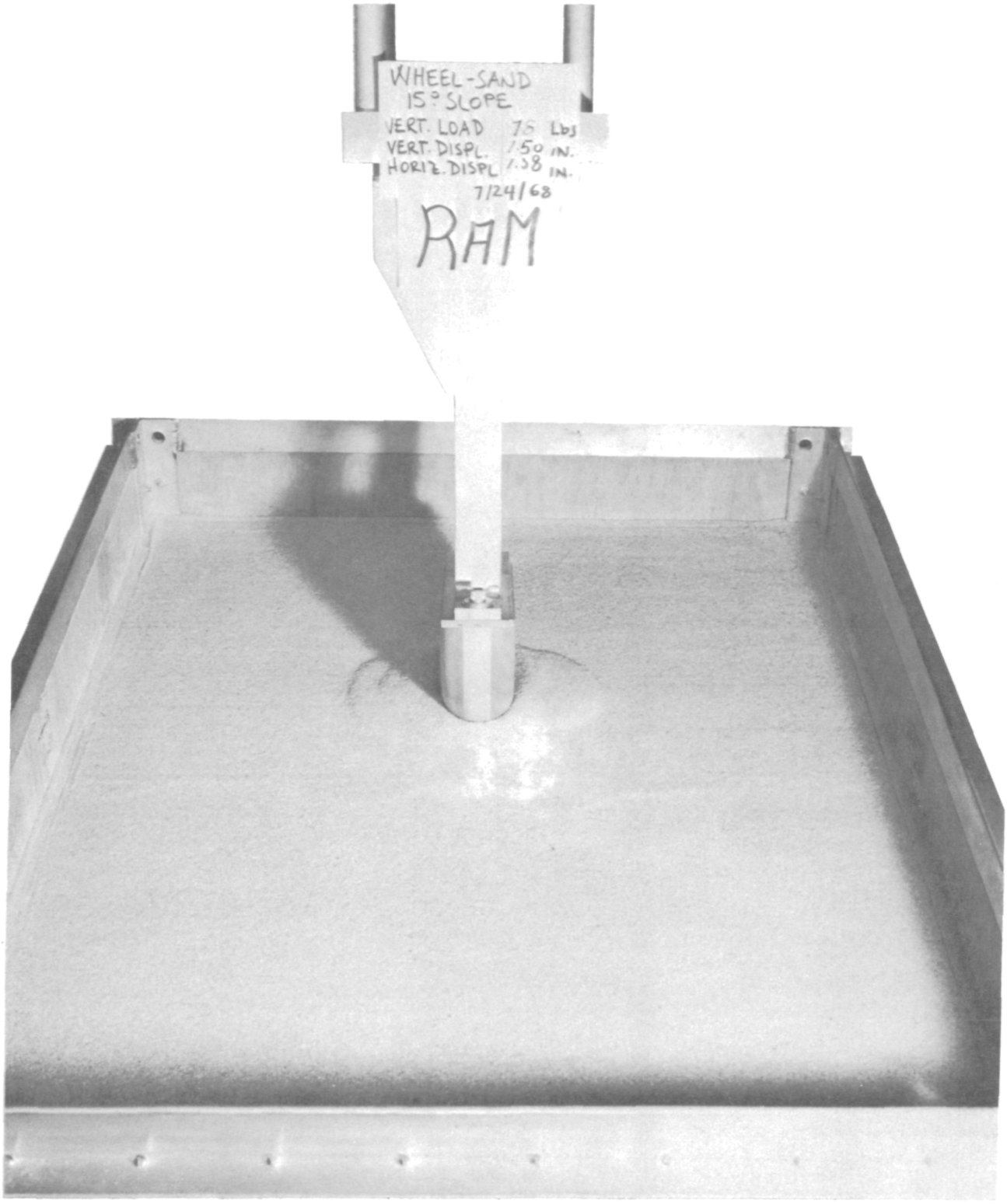

Figure V-99. Fifteen-degree Sloped Surface Test (Wheel Up-Down Slope) with a 1.50 in. Vertical Displacement and a 1.38 in. Horizontal Displacement

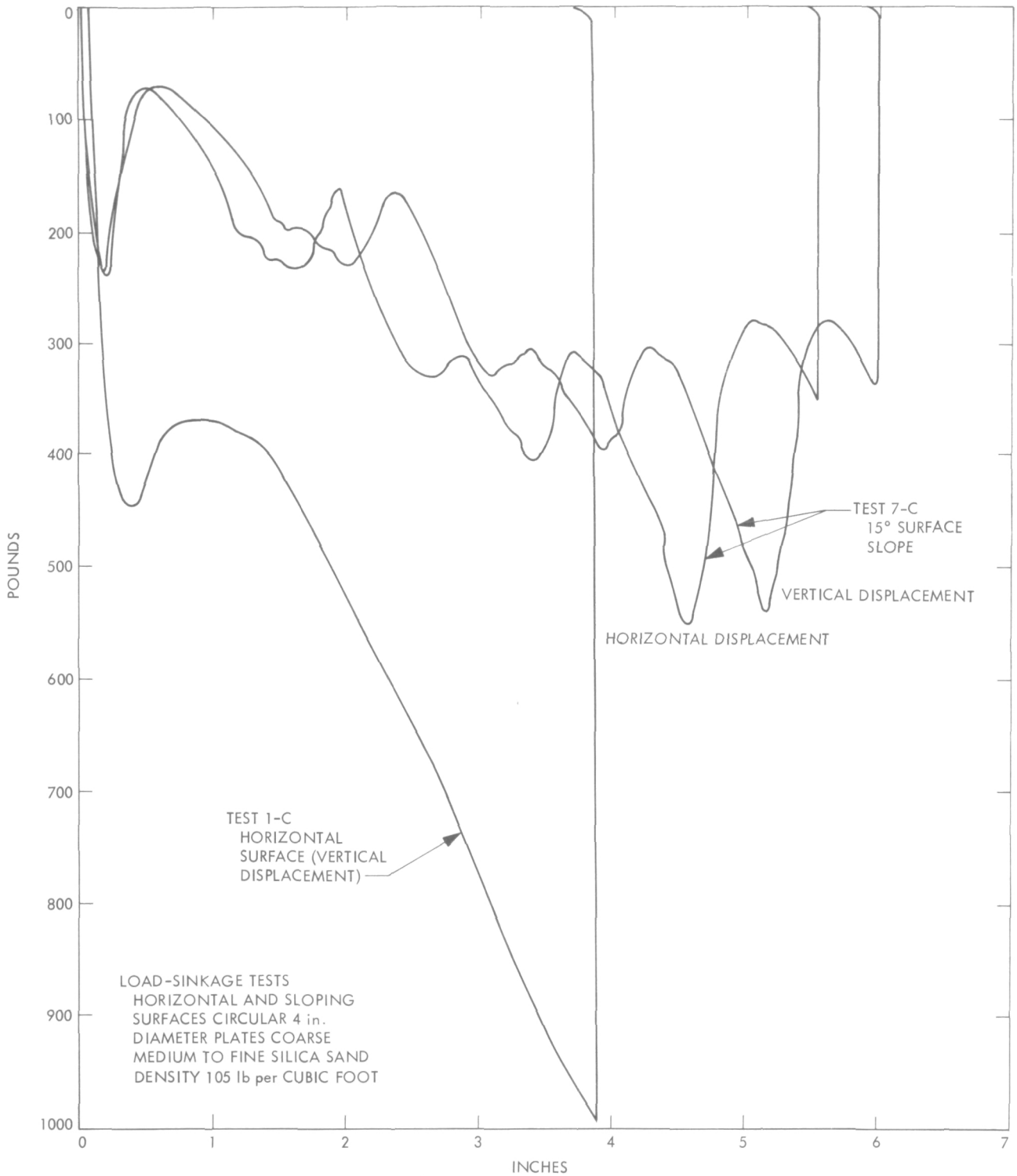

Figure V-100. Load Sinkage Test Results (Circular Plate)

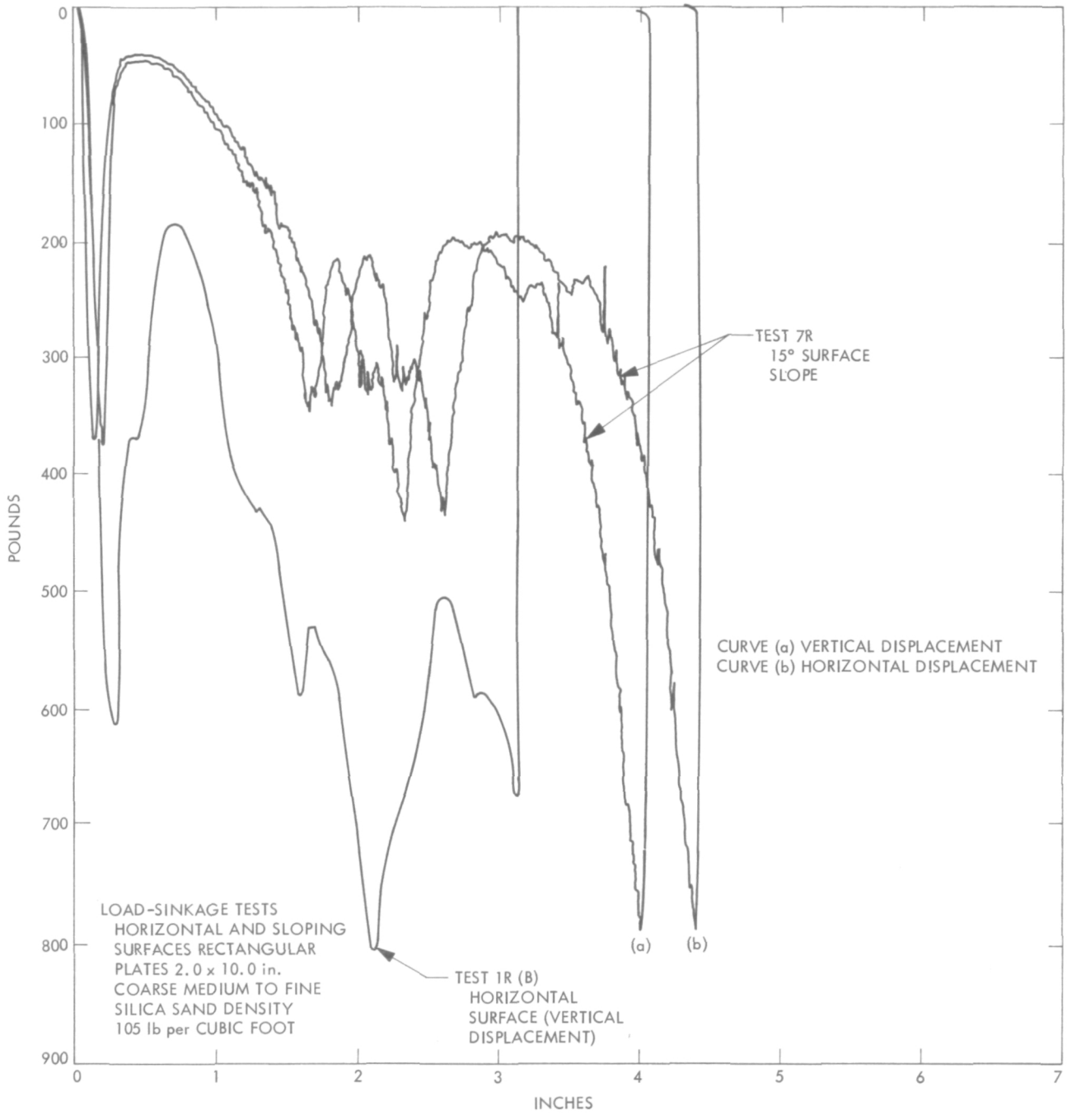

Figure V-101. Load Sinkage Test Results (Rectangular Plates)

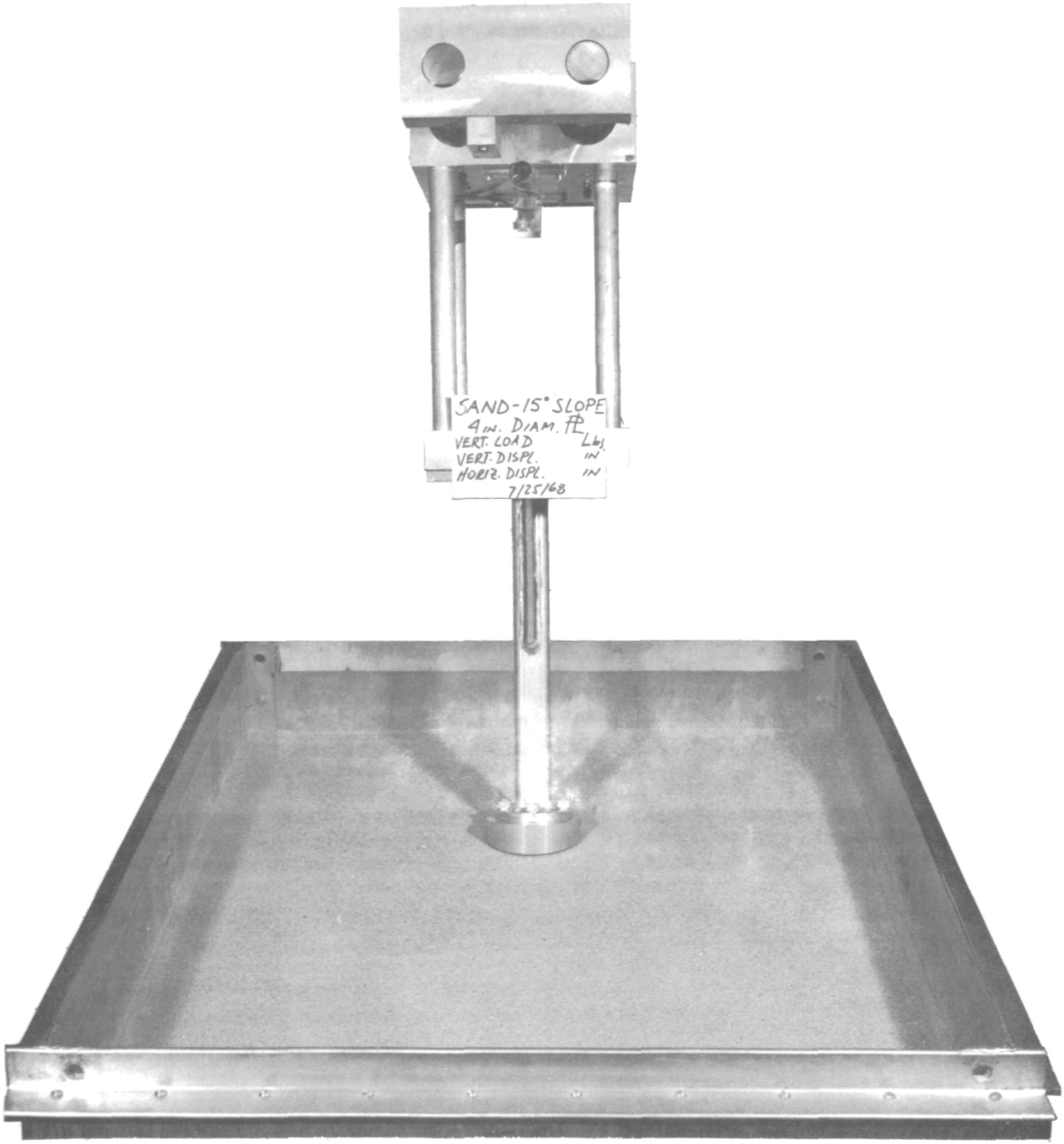

Figure V-102. Circular Plate Test Before Loading

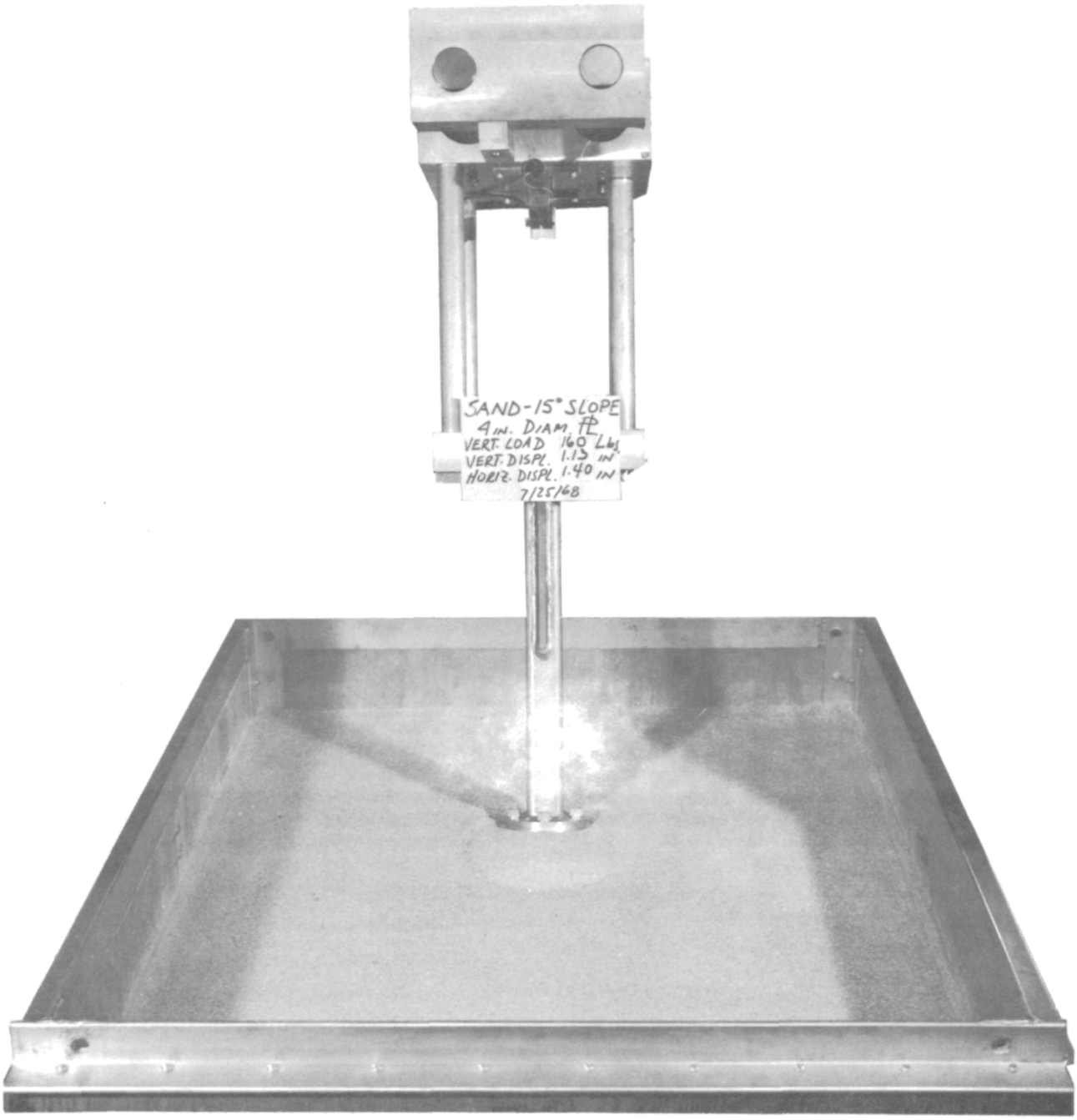

Figure V-103. Circular Plate Test After Loading

P. OPEN DESIGN ITEMS

Potential problems that have been identified but require further analysis are described in the following paragraphs.

1. Obstacle Encounter Analysis

The frequency with which LRV will encounter rocks of sufficient size to stop it can be estimated from counts of fragments scattered over the lunar surface in the vicinity of Surveyor spacecraft (cf Section IV.)

These counts from Surveyor photographs have been extended to cumulative distribution curves plotted in Fig. V-104. For purpose of this estimate the function describing Surveyor I data is used:

$$N = 5 \times 10^5 \, Y^{-2.2} \qquad (1)$$

where N is the number of fragments per 100 M^2 of diameter Y or larger and Y is measured in millimeters. This example is of an area more generously supplied with rocks than other Surveyor sites, but much less than the Surveyor VII highland site.

The frequency of encounter, ϕ, is computed by multiplying the frontal width X_i of an appropriate Section I of LRV by N. Figure V-48 shows the three pertinent sections and their frontal widths: wheels with tread width X_1 = 6 inches; wheel suspensions, each with width X_2 = 21 inches; and the under carriage with half-width X_3 = 8 inches.

The obstacle clearance capability is assumed equal to the diameter Y of the rock. The single wheel capability is shown in Fig. V-22 to vary with the coefficient of friction, but for this analysis Y_1 = 10 inches is assumed. For the suspension section Y_2 depends linearly on where on the strut a rock is encountered. For this design:

$$Y_2 = \frac{3}{7} X + 10 \qquad (2)$$

where Y_2 and x are in inches and x ranges from 0 to 21 inches. For the undercarriage Y_3 = 19 inches.

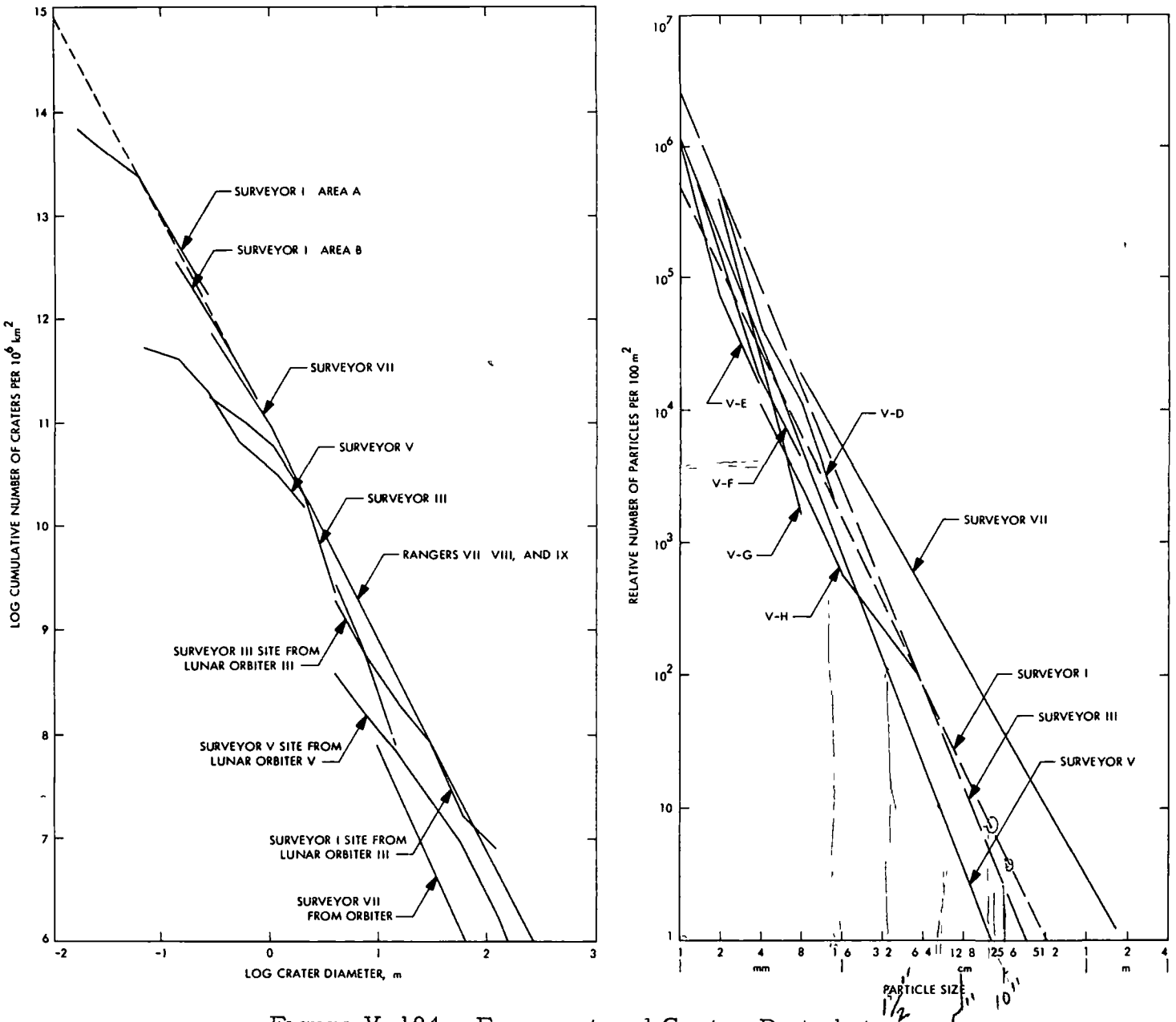

Figure V-104. Fragment and Crater Distribution

For wheels and undercarriage the contributions to are found simply by:

$$\phi_1 = 2X_1 N(Y_1)$$

$$= 2(0.15)(5 \times 10^3)(254)^{-2.2}$$

$$= 7.6 \times 10^{-3} \text{ per meter} \qquad (3)$$

and

$$\phi_3 = 2X_3 N(Y_3)$$

$$= 2(0.203)(5 \times 10^3)(482)^{-2.2}$$

$$= 2.6 \times 10^{-3} \text{ per meter} \qquad (4)$$

where the X's are in meters and Y's in millimeters.

Because of equation (2) ϕ_2 must be found from:

$$\phi_2 = \int_0^{x2} N(Y_2)\, dx \qquad (5)$$

Since

$$dx = 2.33 \times 10^{-3}\, dy_2 \qquad (6)$$

for x in meters and y in mm, equation (5) can be evaluated as follows:

$$\phi_2 = 2.33 \times 10^{-3} \int_{254}^{482} N(y_2)\, dy_2$$

$$= 11.7 \int_{254}^{482} y_2^{-2.2}\, dy_2$$

$$= 13.6 \times 10^{-3} \text{ per meter.} \qquad (7)$$

The total number of rocks capable of stopping LRV is then

$$\phi = \phi_1 + \phi_2 + \phi_3$$

$$= 2.38 \times 10^{-2} \text{ per meter} \qquad (8)$$

Stated conversely, this number means LRV stops for an obstacle every 42 meters. Luckily there are good reasons to believe further study will substantiate confidence in a ϕ smaller by an order of magnitude. These reasons are:

(1) Rocks and boulders are not distributed uniformly on the lunar surface but rather are concentrated in strewn fields inside craters and on their outer rims. By proper navigation of LRV many of these fields can be avoided.

(2) The cumulative distribution functions in Fig. V-104 are probably pessimistic for rocks 10 inches and larger. The grain size distributions of gravels and sediments on Earth are commonly normal (Choate, personal communication). One would obtain an approximation to the typical bell-shaped curve with grain size plotted on a logarithmic scale. Therefore, the cumulative distribution curve would not be a straight line as in Fig. V-104 but rather a curve with an increasingly negative slope in the larger fraction.

Extensive rock counts on Surveyor photographs are currently under way at JPL. The results of this effort should demonstrate or disprove the validity of a normal distribution of surface fragments.

(3) Finally, rocks are not spherical but ordinarily have a long dimension that lies flat on the ground. Since this is the dimension usually measured in rock counts, the dimension vertical to the ground and threatening to LRV is therefore something less. This observation holds especially for the larger fraction, which is of interest to the problem of obstacle encounter.

2. Solar Panel and High Gain Antenna Articulation

The articulation of the solar panel and high-gain antenna is described by either of two general designs. In one design both solar panel and antenna have two degrees of freedom. In the other the solar panel has three degrees of freedom and the antenna one.

First Design Concept. The first design concept can be interpreted from Fig. V-48. The solar panel can be driven in roll and in pitch. The antenna is attached to the narrow upper end of the solar panel and is capable of similar motion, hinged about an axis on the edge of the panel and about an axis in the plane perpendicular to the panel edge.

Second Design Concept. The second design concept is adapted from Surveyor and is illustrated in Fig. V-105. The solar panel has the same capability of being driven in pitch and in roll, but it may also be rotated about the sun line. The antenna rotates only about an axis parallel to or through the solar panel's upper edge.

The latter design allows a simplified Earth acquisition by the antenna after the solar panel is locked on the sun. The antenna is fixed at 180 degrees plus the known angle between Earth and Sun for the appropriate time of the lunar day, and the solar panel is rotated about the Sun line until Earth lock is obtained.

A more complete analysis will be made to resolve the problem of solar panel/antenna articulation

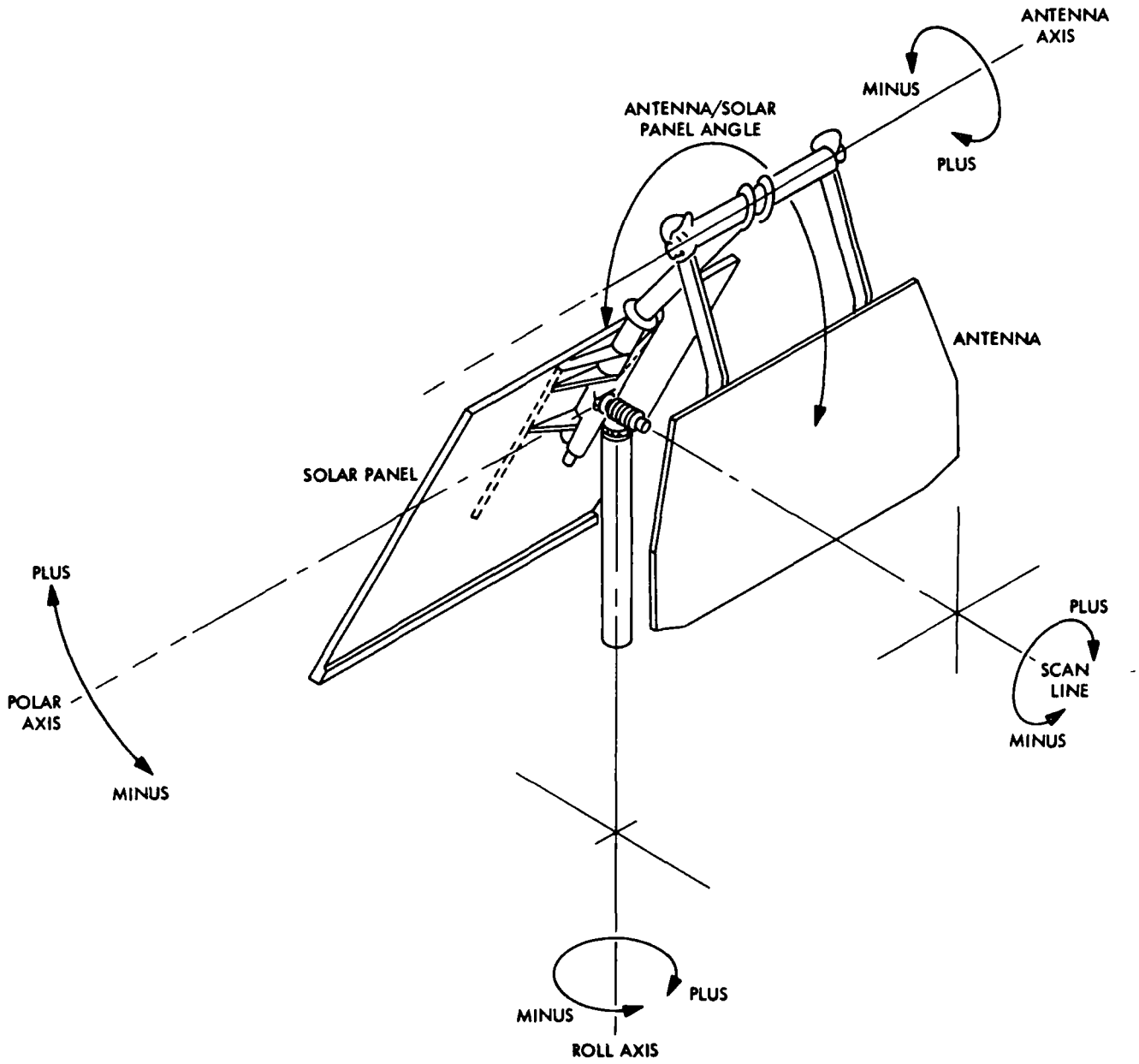

Figure V-105. Solar Panel and High-gain Antenna Secondary Design

Q. LRV MISSION EXTENSION

Recent studies of lunar exploration goals, both for science and for technology, indicate that traverses would have an expanding role in any continuing lunar exploration program. It is, therefore, important that the early technology developed in this field provide a good engineering basis for future growth as well as flexibility from the lunar delivery system standpoint.

1. Preliminary Review of LRV Growth.

A preliminary review has been made of the growth potential of the LRV design approach and the adaptability of the concepts to rovers of increased size and science capability. For this review the 500-600 pound integrated LRV was scaled up to sizes consistent with the capabilities of some candidate launch vehicles available as future lunar delivery systems. These include the Titan IIIC and Titan III-Centaur as well as advanced versions of Apollo systems. The estimated sizes of roving vehicles deliverable by these boosters are indicated in Table V-35 along with the Atlas Centaur LRV.

Table V-35. LRV Estimated Sizes

Delivery System	Injection Capability lb	LRV Weight lb
Atlas Centaur (Baseline)	2500 to 3000	500 to 600
Titan IIIC	5000 to 6000	1000 to 1200
Titan III-Centaur	10000 to 12000	2000 to 2500
Improved LM	(Strap-on)	500 to 1200

2. Results of Review.

These results suggested the investigation of three classes of rovers whose gross size and estimated payload capability are indicated in Table V-36.

The baseline design considers the Atlas Centaur and the Titan IIIC class LRV is described in Section V. L.

The design of the 2000 to 2500 pound class of LRV was next considered. However, due to the study limitations only some preliminary results are available at this time. These indicate that further scaling to this LRV size

Table V-36. Class of Rovers

Rover Class	Size (Wheelbase) (feet)	Weight lb	Payload, lb	
			4-wheel	6-wheel
Atlas Centaur	5	500 to 600	50 to 100	25 to 50
Titan IIIC	6 to 7	1000 to 1200	200 to 300	150 to 250
Titan III Centaur	7 to 8	2000 to 2500	400 to 700	300 to 600

seems acceptable for adaptation to the Titan III Centaur as well as a future extended Apollo with the following ramifications:

(1) Titan III Centaur Adaptation. A new Titan shroud with a 12 to 15 foot diameter will probably be necessary to house this large LRV concept.

(2) Apollo Adaptation. Increased center of gravity offset due to added LRV weight may cause attitude control difficulties. Wheels plus suspension system will probably have to be stowed to provide LM separation clearances. Interference with the control motor exhaust may cause attitude control and local heating problems on the LM.

3. Conclusions

The results of this preliminary study indicate that the LRV concept provides a sound engineering basis for growth potential in lunar roving technology. Besides adapting to roving vehicles of larger size and capability, these enlarged LRV concepts indicate a flexibility to lunar delivery systems by either unmanned boosters or the Apollo extension modes.

It may be that the use of a number of smaller LRVs, roving in diverse areas, may compete favorably with fewer but larger LRVs with more limited area coverage in a finite program from the science, cost, or schedule standpoint.

The flexibility of the various LRVs to multiple delivery by the various booster systems, of course, is a pertinent part of this tradeoff study. Here the doubling of size of the LRVs provides an advantage for multiple delivery as indicated in Table V-37.

Table V-37. Delivery Mode Flexibility

Booster/Rover Weight	500 Class	1000 Class	2000 Class
Atlas Centaur	Single	--	--
Titan IIIC	Twin	Single	--
Titan III Centaur	Multiple	Twin	Single
Apollo Ext.	Twin	Single	--

Table V-37 shows that weight would not be the primary constraint in a multiple delivery mode, the desirability of such an operation would depend more on the operational and duty-cycle problems attending multiple and simultaneous roving missions.

R. SUMMARY OF LRV BASELINE DESIGN

The baseline design of an automated Lunar Roving Vehicle (LRV) studied in this report has emerged with certain salient characteristics. Although the scaling of this baseline to larger vehicles has been considered, baseline LRV in this report means a vehicle of the size and operating characteristics described in Tables V-38 through V-42. All data in these tables describe LRV in its roving configuration. (cf. Fig. V-48).

Table V-38. LRV Mechanical Characteristics

Weight on Earth	540 pounds
Number of wheels	4
Wheel diameter	28 inches
Wheel base	60 inches
Wheel tread	64 inches
Soft soil slope climbing capability	30 - 35 degrees
Soft soil obstacle climbing capability	8 - 10 inches
Minimum turning radius	0 or 15 feet
Stability limit	40 - 45 degrees
Undercarriage clearance	35 degree crater ledge
Steering	4-wheel Ackerman
Lunar delivery and descent system	Atlas/Centaur – Surveyor type
Alternate delivery and descent system	Apollo LM strap-on

Table V-39. LRV Guidance Characteristics

Mission range	1500 kilometers
Mission duration	1 year
Average speed	1.0 - 1.5 km/hr
Average step distance	0.5 - 1.0 km
Navigation scheme	Piloting by landmark
Control scheme	Ground command with minimum of on-board logic
Hazard detection scheme	Inclinometers, motor-current monitors, and tactile detectors
Hazard avoidance scheme	Route planning and TV examination of local terrain

Table V-40. LRV Telecommunications Characteristics

Radio	S-band transponder with turn-around ranging
Transmitter power output	
Low power	0.5 watt
High power	20 watts
Antennae	Omni and steerable directional
Beam width of directional antenna	22 degrees
Telemetry	Analog and digital

Table V-41. LRV Energy Characteristics

Electrical energy sources	Solar panel and battery
Solar panel power	200 watts
Solar panel orientation	Steerable
Battery capacity	680 watt-hours
Thermal energy sources	Radioisotope heaters
Thermal power	17.5 watts

Table V-42. LRV Scientific Payload Characteristics

Payload weight	91 pounds
Payload complement	Photo-imaging; sampling tools and sample handling and storage; and discriminatory instruments
Photo-imaging	Vidicon and/or facsimile
Bulk sampler	100 cubic centimeters per load of particulate material up to 3 centimeters diameter
Hardrock drill and particulate sampler	400 cubic centimeters per load of pulverized material less than 1 mm diameter
Subsurface soil auger	Borehole 1 meter deep and 1 inch in diameter, cuttings acquired by bulk sampler
Instruments	X-ray diffractometer, alpha scattering/ X-ray spectrometer, and hygrometer

REFERENCE LIST

Section V

V-1 JPL ASD 760-5.
JPL "A Program Analysis for Lunar Exploration " JPL 25 July 1967.

V-2. United States Geological Survey.
Bailey, N G and Ulrich, G E "Apollo Applications Program Field Test 8", Technical Letter: Astrogeology 26, Flagstaff, Arizona, April 1967

V-3. AC Electronics TR68-20.
Miller, B P "Analysis of Remote Control Systems for Lunar Vehicles." AC Electronics - Defense Research Laboratories, General Motors Corporation, Santa Barbara, California May 1968.

V-4 Proceedings of Second Space Congress
Streicher, M "Lunar Surface Navigation for a Roving Vehicle (MOLAB) "
Proceedings of Second Space Congress, CCTS, Cocoa Beach, Florida. 5 through 7 April 1965

V-5. Spradley, L H , et al
"Surveyor I: Location and Identification " Science, Volume 157 11 August 1967.

V-6. JPL ASD 760-9.
Internal Advanced Study Document, Baseline Design Document for LRV, 1967.

V-7. JPL TR 32-1264, "Surveyor VII Mission Report."
Parts I through III (Part II published 15 March 1968, Parts I and III publication pending winter-1968).

V-8. Collins, D. H., ed.
"Batteries; Research and Development in Nonmechanical Electrical Power Sources." Pergamon, New York, 1963.

V-9. Hughes Aircraft Co. SSD 78137R.
Knudson, H. E. and Tuchscher, J. S. "Surveyor Spacecraft Thermal Control." August 1967.

V-10. Hughes Aircraft Co. SSD 7811R
"Lunar Night Survival Study Report. July 1967.

V-11. Soviet Technical Paper (Moscow, Tekhnika Kino i Televideniya, No. 1)
Selivanov, A. S., Govorov, V. M., Titov, A. S., Chemodanov, V. P.
"Lunar Station Television Camera," pp. 9 through 17. Moscow, January 1968.

REFERENCE LIST

Section V (contd)

V-12. Journal of Geophysical Research.
Adams, J. and Filice, A. "Spectral Reflectance 0.4 to 2.0 Microns of Silicate Powders," volume 5, p. 5705 through 5715. 31 August 1967.

V-13 JPL TR 32-1023.
JPL "Surveyor I Mission Report: Part 1, Mission Description and Performance," pp 81 through 88 (Television) JPL 31 August 1966

V-14 JPL ASD 760-3
Brereton, R G et al. "Scientific Instruments for Lunar Exploration, Part B: Surveyors, Roving Vehicles, and Rough-Landed Probes." JPL May 1967.

V-15. JPL TR 32-1248
Dunne, J A and Nickle, N A "The Lunar and X-ray Diffraction Program: A Summary." JPL 15 March 1968.

V-16 IAS Paper 63-50.
Roberts, L "The Action of a Hypersonic Jet on a Dust Layer " IAS 31st Annual Meeting, New York, 21 January 1963

V-17. JPL PD-54.
Surveyor Project Lunar Scientific Model, Jaffe, L D., JPL, December 15, 1966.

V-18. NASA TM X-53661.
Vaughn, Jr., O. H. "Lunar Environment: Design Criteria Model for Use in Lunar Surface Mobility Studies. NASA George C. Marshall Space Flight Center, Huntsville, Alabama, September 1967.

APPENDIX A

DESCRIPTION OF NUCLEAR MAGNETIC RESONANCE SPECTROMETER

APPENDIX A

DESCRIPTION OF NUCLEAR MAGNETIC RESONANCE SPECTROMETER

A. NMR FUNDAMENTALS

Nuclear Magnetic Resonance (NMR) is a field of spectroscopy that exploits the fact that many of the isotopes of the elements possess magnetogyric properties. Thus, when material containing nuclei having this intrinsic magnetogyric property is placed in an external static magnetic field and is simultaneously exposed to an oscillating electromagnetic field of the proper frequency (in the radio frequency range), certain information about the nuclei can be ascertained.

It can be determined what nuclear species are present in the sample by merely noting the value of the magnetic field and the frequency at which the absorption of the radio frequency energy takes place. For the hydrogen nucleus (proton) in a field of 1000 gauss the absorption of rf energy occurs at 4.257 megahertz. One can determine not only the presence of the various nuclear species, but also the number of nuclei present in the sample by measuring the intensity of the NMR absorption line. It is a well-known fact that the intensity of the line is directly proportional to the number of nuclei present in the sample. Finally, the width and shape of the NMR absorption line yield information about the molecular structure in which the nuclei under study are located.

B. APPLICATION OF NMR

Water contains one atom of O^{18} (which does not contain a magnetic moment and thus does not exhibit an NMR absorption signal) and two protons (which have relatively strong NMR absorption signals). Thus the presence of water in a sample can be determined by merely measuring the proton NMR signal. The intensity of the signal gives a direct measurement of the number of protons present in the sample, and the width and shape of the line give information on the chemical environment in which the protons are located. That is, the width and shape of the line determine whether the protons are in free water (liquid state), absorbed water, or water of hydration. If organic molecules are present, their protons exhibit a resonance line of still different form. A more sophisticated NMR spectrometer could differentiate and identify various organic compounds.

In free water the NMR absorption signal appears as a single narrow line with a width of the order of 0.1 to 3 milligauss. For absorbed water the width of the line depends on the thickness of the layer of water and can vary from approximately 10 milligauss to 1 or 2 gauss. Protons located in organic solids exhibit line widths in the range of 2 to 4 gauss. Finally, protons located in water of hydration have line widths of the order of 15 gauss. In addition, the lines that result from water of hydration have some complexity, usually exhibiting two or more broad peaks that depend on the crystal structure of the hydration water molecules.

A laboratory type NMR spectrometer has been used to measure the moisture content of terrestrial rock and soil samples and it has been demonstrated that water contents as low as 0.05 percent by weight are easily measured.

C. FLIGHT TYPE NMR

For the past several years personnel of the Low Temperature Physics Group in the Physics Section at JPL have been conducting experiments to ascertain the feasibility of using a flight type nuclear magnetic resonance spectrometer for the detection of water on the lunar and planetary surfaces (Ref. III-15).

Figure A-1 is a diagram of an NMR marginal oscillator that was built as a breadboard model of a possible flight type instrument. The soil sample is in a test tube that is placed in the tank coil of the marginal oscillator. The actual electronic components weigh a small fraction of a pound, and the system needs only a few milliwatts of power. Not shown is the several-thousand-gauss permanent magnet that completes the assembly. This spectrometer was able (using an electromagnet) to measure water in soil samples in the range down to 0.5 percent by weight.

Figure A-2 shows a block diagram of an NMR spectrometer system. As can be seen, it consists of a magnet of the order of several thousand gauss in strength and a radio-frequency marginal oscillator. The sample is placed in the tank coil of the marginal oscillator, which operates at the resonant frequency corresponding to the Larmor condition $\omega = H$ for the nuclei under study. When the Larmor condition is satisfied, power is absorbed by the nuclear spin

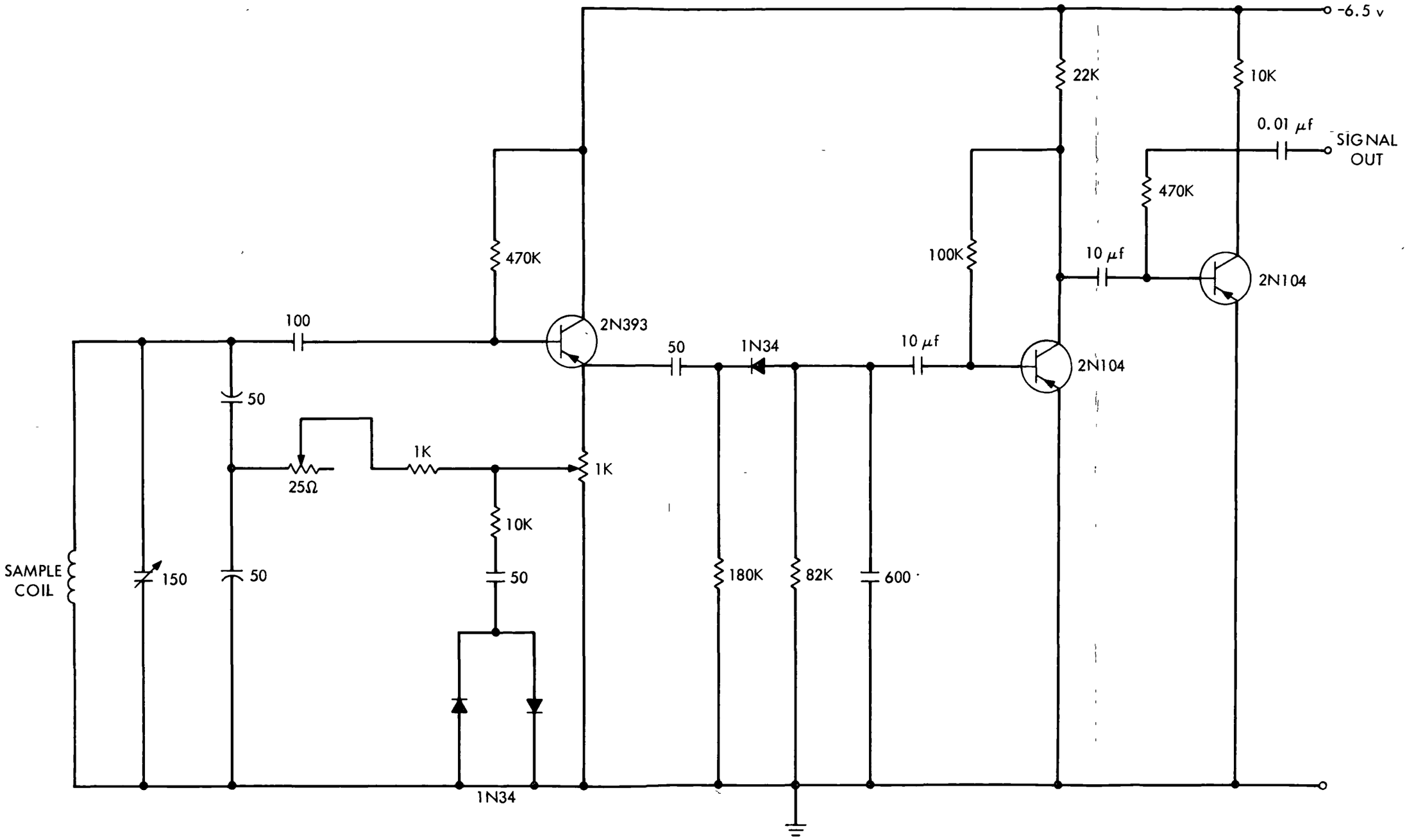

Figure A-1. NMR Marginal Oscillator, Schematic Diagram

Page intentionally left blank

Page intentionally left blank

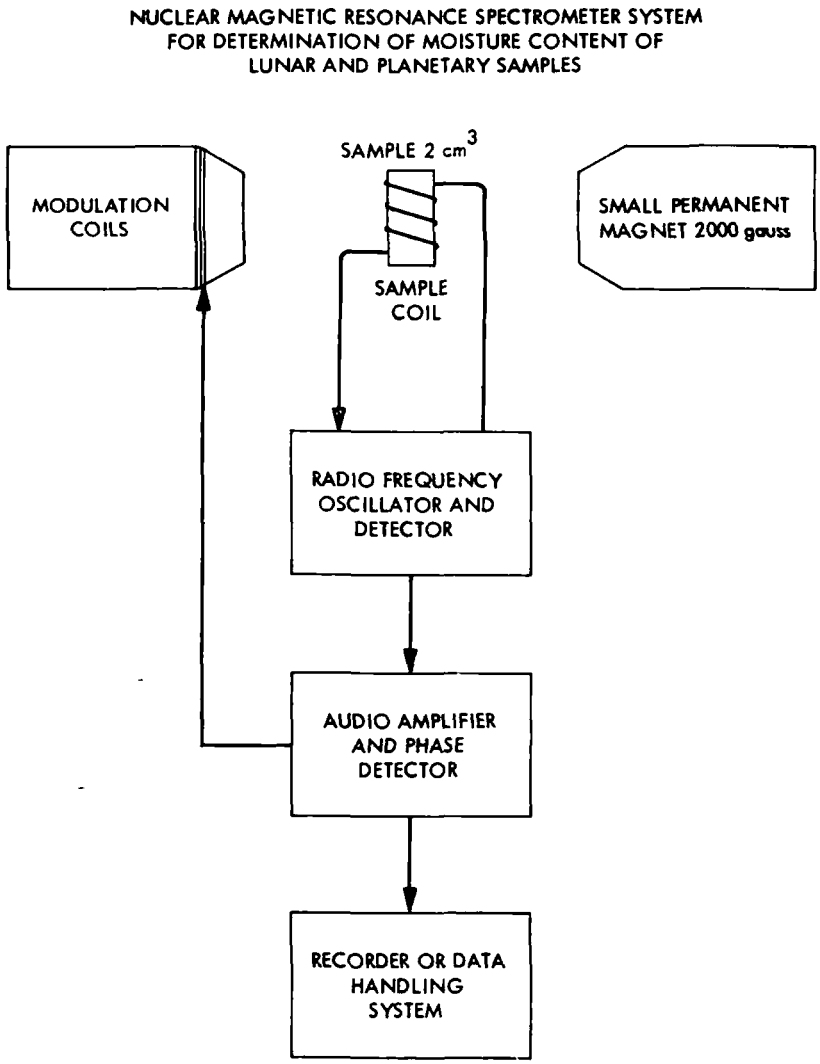

Figure A-2. NMR Spectrometer System Block Diagram

system, and this lowers the oscillation level of the marginal oscillator. This decrease in oscillation level is amplified and can be displayed on a chart recorder or digitized for appropriate data handling techniques. The absorption line shape can be studied by slowly changing either the magnetic field or the oscillator's frequency.

A complete water detection system could be integrated into a lunar roving vehicle. The experiment would be made preferably in the high latitudes of the Moon where subsurface water is more likely to be found (Ref. III-12 and III-13). Samples for the NMR spectrometer would be obtained by either drilling or digging into the surface. Samples from various depths would be placed one at a time in the spectrometer for analysis to obtain a moisture profile for the drill site. Of course it would be necessary to seal the samples from vacuum if measurements of both free and bound volatiles were desired. Since NMR is a nondestructive method of analysis, the samples would then be available for other experiments.

The research effort to date has demonstrated that NMR techniques can be used to measure the water content of lunar and planetary samples with water present at 0.05 percent or greater. A flight type instrument that requires only a few milliwatts of power excluding samples can be constructed with adequate sensitivity. The total weight of such an instrument is limited mainly by the size of the magnet that is used (the order of a few pounds).

In addition, the NMR technique has the unique capability of being able to detect and differentiate between free water, absorbed water and crystalline water of hydration in minerals. Also, the NMR technique has less ambiguity in the calibration of the instrument than say the thermal neutron method. Another competitive technique of moisture detection is the differential thermal analysis method. The DTA technique can differentiate between the various forms of water in water of hydration, free water, etc., as can NMR, however, the DTA requires considerably more power to operate than the NMR technique.

APPENDIX B

DESCRIPTION OF 3-D QUADRUPOLE ION GAGE/MASS SPECTROMETER

APPENDIX B

DESCRIPTION OF 3-D QUADRUPOLE ION GAGE/MASS SPECTROMETER

The basic instrument is a three-dimensional quadrupole mass spectrometer first explored by Fischer, et al. in 1959. It has the ability to ionize gaseous species within a three-dimensional quadrupole field and sustain these ions in stable orbits for extended periods of time (up to several days). This storage technique then allows a high signal to noise ratio to be developed through the use of long sample integration times. To avoid confusion it should be mentioned that in the finely tuned mode only one mass species can be stored at a time, and this species must be "read out" before the storage of the next species. Operated in a broadly tuned mode, the instrument functions as an ion gage, and will collect and store a wide range of mass species at a time. The resulting "read out" will be a function of the collection time and the total pressure.

It is believed that the total analyzer (which incorporates a volume of only one cubic inch) could be constructed mainly out of high transmission grid material, therefore allowing gaseous sampling from greater than a 2π solid angle and at the same time minimizing the degassing from solid surfaces. This results in a totally "nude" mass spectrometer rather than only a nude ion source as has been previously proposed. If the analyzer were placed near the apex of a conical electronics package almost the entire primary gas evolution from the package could be eliminated when placed on the surface of the Moon. If the instrument were placed on a spacecraft then the cone angle would need to be such that it shadowed the analyzer from the spacecraft as well.

The basic instrument appears to be quite amenable to a radioactive reduced capillary cold ionizing electron emitter as well as the Bendix type electron multiplier (Channeltron) ion detector. Both of these devices are extremely small and would present minimal surface areas as a source of degassing.

The one disadvantage of the three-dimensional quadrupole is that no proven technique has been devised to analyze an ionized atmosphere. At the present time the ions must be created within the three-dimensional quadrupole field to obtain stable orbits.

A typical mode of operation, in the search for outgassing during an LRV traverse, or when drilling a hole, would be to first operate as an ion gage, reading out periodically, looking for increases above previous background readings. If an increase were noted then one would step scan (mass spectrometer mode) through the desired mass range at constant integration times and determine the total charge collected at each mass number. A feedback logic system could be used to determine maximum integration times at each mass in later scans to enhance the signal to noise ratio. The total charge collected at each mass setting would be a measure of the number density of that particular species.

By the time of a possible LRV mission, lunar atmospheric compositional measurements may already have been made. If not, or if additional measurements are desired, this instrument will also have that capability.

Quadrupole Fundamentals. Mass selective ion storage in electrodynamic quadrupole fields has been used in conjunction with an efficient ion drawout system as a mass spectrometer. The three-dimensional, quadrupole fields are provided by rf and dc voltages applied to surfaces that are hyperboloids of revolution (Ref. III-16 and III-17). Ions are stored in the field and then are pulsed out of the storage volume into an electron multiplier at selected repetition rates. Consequently at low pressures the ion current may be integrated over long periods of time. Using a low resolution mode, ions have been trapped for several days in an active volume of less than one cubic inch.

The three dimensional, quadrupole fields are generated by the electrode structure shown in Fig. B-1. A cross-section is shown through a plane containing the z-axis. The surfaces are hyperboloids of revolution, obtained in the figure by rotation about the z-axis. An rf voltage of 1.8 MHz is applied to the ring electrode. The two cap electrodes at the top and bottom are held at a negative dc potential with respect to the midpoint of the ring potential. The ratio of rf to dc potential is chosen so that the mass scanning line intersects close to a corner of the stable region in the a-q diagram, that is, the region of bounded solutions to the Mathieu equation of motion. The mass spectrum is scanned by varying the voltages, while keeping the voltage ratio constant. Each e/m ratio ion is brought in turn, into the stable region, and the mass spectrum appears as equally spaced peaks.

Stored ions are pulsed out of the trap by applying a voltage pulse to one of the cap electrodes. This electrode is perforated, and ions pass through it and impinge on an electron multiplier. Voltage pulses from the multiplier may be amplified, and a peak-reading circuit can be used to drive an X-Y recorder. The electron ionizing beam may be pulsed off before the ion drawout pulse so that effects due to soft X-rays and metastable ions are eliminated.

Figure B-2 presents an ion-storage decay curve, taken with a total background pressure of 3×10^{-10} torr. The rf and dc voltages were chosen so that CO^+ ions would be near the center of the region of stable motion. After an ionizing period of 10 sec, the electron filament was disconnected from the battery. Ions formed during the ionizing period were stored for times corresponding to the abscissa, and were then pulsed out of the trap into the electron multiplier. The corresponding peak height is given as the ordinate. Note the log-log coordinates. The straight line decay, with a gradual flattening of the curve at short times is consistent with the hypothesis that the ion loss mechanism is dominated by ion-ion scattering.

A mass spectrum, from masses 16-44, is shown in Fig. B-3. The total pressure was 5×10^{-8} torr, and the ion storage time was 25 msec. The resolution $m/\Delta m$ is 130, where Δm is the width of the peak at half-maximum amplitude.

A detailed account of this work, and of the theoretical basis for ion mapping in three-dimensional quadrupole fields, is to be published in the Journal of Vacuum Science and Technology.

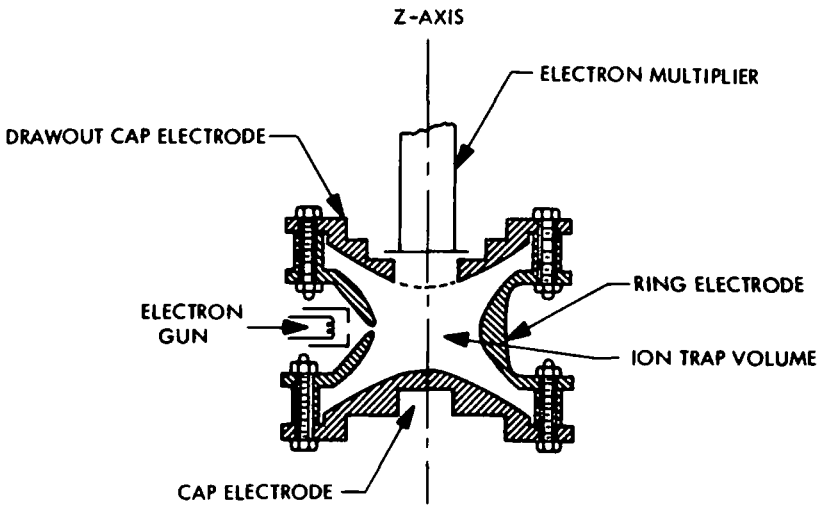

Figure B-1. Quadrupole Electrode Structure

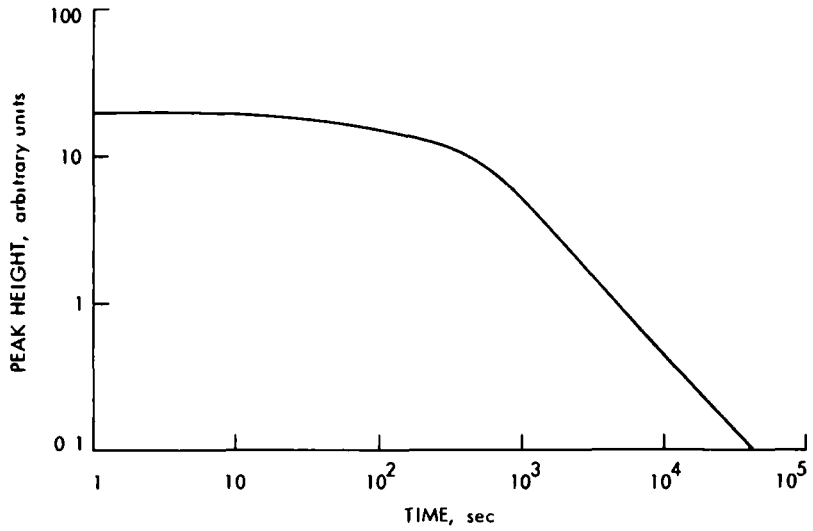

Figure B-2. Ion Storage Decay Curve

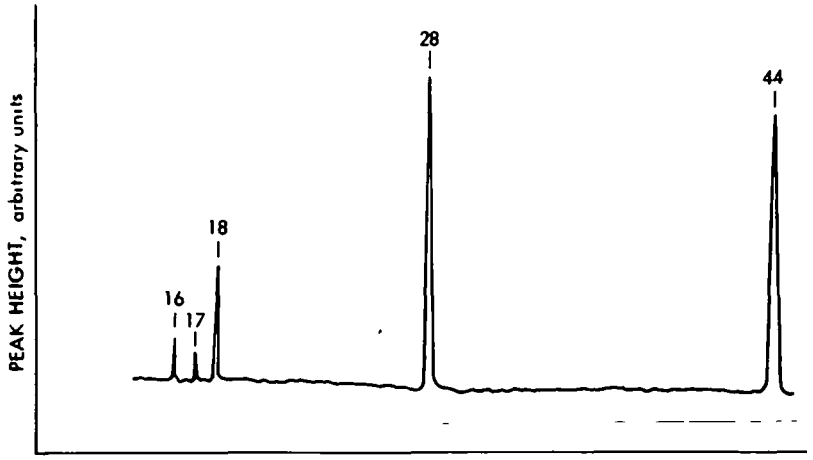

Figure B-3. Mass Spectrum

APPENDIX C

LRV SEQUENCE OF EVENTS

Table C-1. Post Landing Events (Sheet 1 of 2)

LRV SEQUENCE OF EVENTS

POST LANDING EVENTS

EVENTS	FROM	TO	RESPONSE	INDICATION	POWER	TIME
POST LANDING T/M ENG ASSESSMENT	DC*	T/M	CYCLE THRU ALL ENG T/M MODES			
UNLOCK S/P POSITION	DC	PYRO				
POSITION S/P (AUTO MODE)	DC	G+C	NULL S/S ERROR	S/S ERROR S/P POS POTS S/P VOLT + AMP		
DEPLOY TV BOOM	DC PYRO	PYRO DEV		SQUIB CURRENT LIMIT SWITCH		
HIGH PWR RF	DC	RFS	XMTR OUTPUT INCREASE TO 20 WATTS			
POST LANDING IMAGE ASSESSMENT	OPER					

NOTE- USING THE COMMANDS AND PROCEDURES DEVELOPED FOR LOW RESOLUTION PICTURES CONDUCT AN AREA SURVEY TO VERIFY THE SAFETY AND DESIRABILITY OF JETTISONING THE A FRAME

POSITION SOLAR PANEL (MANUAL)	OC**	CC+S
	OC	CC+S
	DC	CC+S

NOTE- REQUIRED ONLY IF CLEARANCE NEEDED FOR A FRAME JETTISON

* Discrete Command
** Quantitative Command

Table C-1 Post Landing Events (Sheet 2 of 2)

EVENTS	FROM	TO	RESPONSE	INDICATION	POWER	TIME
JETTISON A FRAME	DC	PYRO	FIRE PIN PULLER	SQUIB CURRENT		
	PYRO	DEV	EJECT A FRAME	LIMIT SWITCH		
NOTE- DECISION TO NOT JETTISON A FRAME IF TERRAIN AND SUBSYSTEM STATUS SO INDICATES						
POSITION S/P (AUTO MODE)	DC	G+C	NULL S/S ERROR	S/S ERROR S/P POS POTS S/P VOLT + AMP		
UNLOCK HI-GAIN ANTENNA	DC	PYRO				
POSITION HI-GAIN ANT	QC	CC+S	STORE ELEVATION			
	QC	CC+S	STORE AZIMUTH			
	DC	CC+S	OUTPUT PULSES			
	CC+S	DEV		POSITION POTS		
NOTE-1 QC DETERMINED FROM S/P POITION AND INCLINOMETER ANGLES 2 POSITIONING MAY BE AUTOMATIC USING AGC FROM REDUNDANT RECEIVER						
TRANSFER TO HI-GAIN ANTENNA	DC	RFS		INCREASE IN SIGNAL STRENGTH		
DEPLOY OBSTACLE DETECTOR	DC	PYRO	FIRE PIN PULLERS	SQUIB CURRENT		

Table C-2. Site Identification Events (Sheet 1 of 3)

SITE IDENTIFICATION EVENTS

EVENT	FROM	TO	RESPONSE	INDICATION	POWER	TIME
TV POWER ON	DC	TV				4
NOTE- RANGING POWER ON WITH TV POWER ON						
FTS TO TV MODE	DC	FTS				4
360 DEG WIDE ANGLE SCAN PREPARATION						
A- SELECT WIDE ANGLE	DC	TV				4
B- SEL HI RESOLUTION	DC	TV				4
C- SEL SHUTTER SPEED	DC	TV				4
D SEL APERTURE	DC	TV				4
NOTE- 1 INITIAL SETTING ESTIMATED BY GROUND COMPUTATION FROM SUN ANGLE (S/P POSITION), TIME OF DAY, AND BEARING OF FIRST PICTURE						
2 SUCCESSIVE SETTINGS OBTAINED FROM BRIGHTNESS OF PREVIOUS PICTURE						
PERFORM SCAN						
A CMD TV AZIMUTH	QC	CC+S	STORE MAGNITUDE			4
	DC	CC+S	INITIATE POSITIONING			4
B CMD TV ELEVATION	QC	CC+S	STORE MAGNITUDE			4
	DC	CC+S	INITIATE POSITIONING			4
NOTE- REQUIRES GND COMPUTATIONS USING LRV T/M TO GENERATE POSITION QC THAT ACCOMMODATES LRV TILT						

Table C-2. Site Identification Events (Sheet 2 of 3)

EVENTS	FROM	TO	RESPONSE	INDICATION	POWER	TIME
C WAIT FOR POSITION	OPER			POSITION POTS		9
NOTE- WAIT TIME FOR POSITIONING ASSUMES 4 DEG PER SEC RATE AND MAX DISPLACEMENT OF 52 DEG IN AZIMUTH AND 37 DEG IN ELEVATION						
2 SHUTTER OR APERTURE MAY BE CHANGED DURING WAIT						
D INITIATE PICTURE	DC	TV				4
E WAIT FOR READOUT						6
F REPEAT STEPS A THRU E 6 TIMES						210
IDENTIFY LANDMARKS AND GROSS LOCATION	OPER					480
NOTE 1 REQUIRES RETENTION AND DISPLAY OF PICTURES IN SFOF						
2 MAY REQUIRE LRV MOVEMENT IF LANDMARKS NOT VISIBLE (SEE NONSTANDARD SEQUENCE)						
PREPARE FOR NARROW ANGLE LANDMARK SURVEY						
A SEL NARROW ANGLE	DC	TV				4
B SEL APERTURE	DC	TV				4
C SEL SHUTTER SPEED	DC	TV				4

Table C-2. Site Identification Events (Sheet 3 of 3)

EVENTS	FROM	TO	RESPONSE	INDICATION	POWER	TIME
PERFORM NARROW ANGLE SURVEY						
A CMD TV AZIMUTH	QC	CC+S	STORE MAGNITUDE			4
	DC	CC+S	INITIATE POSITIONING			4
B CMD TV ELEVATION	QC	CC+S	STORE MAGNITUDE			4
	DC	CC+S	INITIATE POSITIONING			4
C WAIT FOR POSITION	OPER					12
NOTE- POSITIONING TIME ASSUMES 4 DEG PER SEC AND MAXIMUM DISPLACEMENT IN AZIMUTH OF 315 DEG FOR FOUR PICTURES						
D INITIATE PICTURE	DC					4
NOTE- INITIATION OF PICTURE ALSO INITIATES NAVIGATION RANGING						
E WAIT FOR READOUT						6
F REPEAT STEP A THRU E 3 TIMES						114
RANGE TO LANDMARKS	DC		NARA			
NOTE- THIS STEP USED TO REPEAT RANGING MEASUREMENT WITHOUT REPEATING TV						
PINPOINT LOCATION ON MAP	OPER					300

Table C-3 Commanded Traverse Events (Sheet 1 of 3)

COMMANDED TRAVERSE EVENTS

EVENTS	FROM	TO	RESPONSE	INDICATION	POWER	TIME
SELECT BEARING AND STEP DISTANCE	OPER					40
LOW POWER RF	DC	RFS		DECREASE SIGNAL STRENGTH		4
TRANSFER TO OMNI ANT	DC	RFS		DECREASE SIGNAL STRENGTH		4
INSERT TURN PARAMETERS	QC	CC+S				4
	CC+S	MOB	TURN DIRECTION	LIMIT SWITCH		
	CC+S	MOB	TRAV DIRECTION	LIMIT SWITCH		

NOTE- 1 ONE QC CONTAINS TRAVERSE DIRECTION, TURN DIRECTION AND TRAVERSE DISTANCE
2 ONE POSITION STEERING PRESENT PLAN. MULTIPLE POSITION INCLUDING 45 DEG COULD BE SUBJECT OF FUTURE STUDY

INITIATE TURN	DC	CC+S		COMMAND EVENT		4
	CC+S	MOB	TRAVERSE START	MOTOR CURRENT		
	CC+S	ODOM	RESET ODOMETER	ODOMETER OUTPUT		
STOP TURN	ODOM	CC+S	TRAVERSE STOP	CC+S EVENT		4

NOTE- TIME ESTIMATE BASED ON 20 DEG AVERAGE TURN, 15 FT TURN RADIUS, AND 1.5 KM/HR

HIGH POWER RF	DC	RFS	INCREASE PWR OUTPUT	INCREASE SIGNAL STRENGTH		4
NARROW ANGLE TV SURVEY OF LANDMARKS						48

NOTE-1 INCLUDES AUTOMATIC RANGING
2 REQUIRED TO VERIFY NEW BEARING
3 USE TV PROCEDURES DEVELOPED FOR SITE IDENTIFICATION
4 TIME IS 16 SEC FOR TV POSITION COMMANDS + 22 SEC WAIT + 4SEC FOR INITIATE COMMAND + 10 SEC READ OUT

Table C-3. Commanded Traverse Events (Sheet 2 of 3)

EVENTS	FROM	TO	RESPONSE	INDICATION	POWER	TIME
VERIFY NEW BEARING	OPER					30
LOW POWER RF	DC	RFS				4
TV AND RANGING OFF	DC	TV NARA				4
FTS TO TRAVERSE MODE	DC	FTS				4
INSERT TRAV PERAMETERS	QC	CC+S				4
OPTIMIZE SOLAR PANEL POINTING	QC	CC+S		QC VERIFICATION		4
	QC	CC+S				4
	DC	CC+S				4
	CC+S	DEV		POSITION POTS		
WAIT FOR POSITION	OPER					4
NOTE- OPTIONAL SEQUENCE TO OPTIMIZE SOLAR PANEL POINTING OVER UNEVEN TERRAIN						
INITIATE TRAVERSE	DC	CC+S	APPLY POWER TO WHEEL MOTORS	COMMAND EVENT MOTOR CURRENT ODOMETER OUTPUT		4
STOP TRAVERSE	ODOM	CC+S	REMOVE POWER FROM WHEEL MOTORS	CC+S EVENT		
POSITION SOLAR PANEL (AUTO)	CC+S	G+C	NULL S/S ERROR	S/S ERROR S/P POS POTS S/P VOLT + AMP		10
DETERMINE HI-GAIN ANTENNA POINTING PARAMETERS	OPER		COMPUTATION BY GROUND COMPUTER			10

Table C-3. Commanded Traverse Events (Sheet 3 of 3)

EVENTS	FROM	TO	RESPONSE	INDICATION	POWER	TIME
POSITION HI-GAIN ANT	OC	CC+S				4
	OC	CC+S				4
	DC	CC+S				4
TRANSFER TO HI-GAIN ANTENNA	DC	RFS		INCREASE IN SIGNAL STRENGTH		4
HIGH POWER RF	DC	RFS	RF POWER OUTPUT INCREASE TO 20 WATTS			4

Table C-4. Science Sampling Events (Sheet 1 of 2)

SCIENCE SAMPLING EVENTS

EVENT	FROM	TO	RESPONSE	INDICATION	POWER	TIME
IDENTIFY DESIRABLE SAMPLING SPOT	OPER					
NOTE-1 CHOICE OF LOCATION MAY BE BASED ON DATA FROM LRV OR DATA FRM OTHER SOURCES 2 DESIRABLE FEATURES MAY INCLUDE SURFACE PARTICULATE- ROCKS- OUTCROPPINGS- ETC-						
TRAVERSE TO EXACT LOCATION TO BE SAMPLED						
NOTE- USE NORMAL TRAVERSE SEQUENCES						
PHOTOGRAPH SAMPLE SPOT						
NOTE- USE NORMAL NARROW ANGLE TV PROCEDURES						
SELECT SAMPLER TYPE (SCOOP,DRILL OR AUGER)	OPER					
FTS TO SCIENCE SAMPLE MODE	DC					
POSITION SAMPLER						
NOTE- POSITIONING SEQUENCE DEPENDS ON TYPE SAMPLER SELECTED AND WILL CONSIST OF A SERIES OF DC AND DC POSITIONING COMMANDS						
TV VERIFICATION OF SAMPLER POSITION						
NOTE-1 USE NORMAL TV PROCEDURES 2 REQUIRES OPERATIONS EVALUATION						
COMMAND SAMPLE ACQUISITION TIME	OC	CC+S				

Table C-4. Science Sampling Events (Sheet 2 of 2)

EVENTS	FROM	TO	RESPONSE	INDICATION	POWER	TIME
COMMAND SAMPLE ACQUISITION MODE	DC	SPLR	START SAMPLE PROCESS	COMMAND EVENT		
		CC+S	START TIME			
	CC+S	SPLR	STOP SAMPLE PROCESS	CC+S EVENT		
VERIFY ADEQUATE SAMPLE						
NOTE-1 USE NORMAL TV PROCEDURES 2 REQUIRES OPERATIONS EVALUATION						
DETERMINE DISPOSITION OF SAMPLE (STORE, ANALYZE, OR DUMP)						
NOTE-1 DUMP CONSISTS OF SAMPLE TRANSFER WITHOUT SAMPLE CUP IN PLACE						

Table C-5. Science Sample Handling Events

SCIENCE SAMPLE HANDLING EVENTS

EVENT	FROM	TO	RESPONSE	INDICATION	POWER	TIME
SELECT STORAGE POSITION	DC DC	SH+S SH+S	ROTARY POSITION VERTICAL POSITION	POS POTS OR SWITCHES		
NOTE-1 ROTARY POSITIONS TOTAL 20 (ONE FOR SAMPLE RECEIPT, ONE FOR EACH INSTRUMENT, AND 17 FOR STORAGE) 2 VERTICAL POSITIONS TOTAL 7 3 IF SAMPLE IS TO BE DUMPED THIS EVENT NOT REQUIRED						
EXTEND CUP ARM	DC	SH+S		LIMIT SWITCH		
GRASP SAMPLE CUP	DC	SH+S		LIMIT SWITCH		
RETRACT CUP ARM	DC	SH+S		LIMIT SWITCH		
SELECT SAMPLE RECEIPT POSITION	DC DC	SH+S SH+S	ROTARY POSITION VERTICAL POSITION	POSIT POTS OR LIMIT SWITCHES		
EXTEND CUP ARM	DC	SH+S		LIMIT SWITCH		
SAMPLER TO SAMPLE TRANSFER POSITION	DC	SPLR		LIMIT SWITCH		
SAMPLE TRANSFER	DC	SPLR				
NOTE- MAY REQUIRE A TIME FROM CC+S						
RETRACT CUP ARM	DC	SH+S		LIMIT SWITCH		
NOTE- AFTER SAMPLE HAS BEEN TRANSFERRED TO SAMPLE CUP, SAMPLE MAY BE DUMPED BY INVERTING SAMPLE CUP						
SELECT STORAGE POSITION	DC DC	SH+S SH+S	ROTARY POSITION VERTICAL POSITION	POSIT POTS OR LIMIT SWITCHES		
EXTEND CUP ARM	DC	SH+S		LIMIT SWITCH		
RELEASE SAMPLE CUP	DC	SH+S		LIMIT SWITCH		
RETRACT CUP ARM	DC	SH+S		LIMIT SWITCH		

Table C-6 Lunar Night Sequence (Sheet 1 of 2)

LUNAR NIGHT SEQUENCE

EVENTS	FROM	TO	RESPONSE	INDICATION	POWER	TIME
POSITION SOLAR PANEL	OC	CC+S		OC VERIFICATION		4
	OC	CC+S				4
	DC	CC+S				4
	CC+S	DEV		POSITION POTS		
POSITION ARTICULATED RADIOISOTOPE HEATERS						
TURN ELECTRONICS POWER OFF	DC					
PREPARE PLAN FOR INITIAL SUNRISE OPERATION	OPER					
RECEIVER POWER ON (AUTOMATIC ON BOARD REDUNDANT SWITCH)						
POSITION S/P (AUTO) (BATTERY CHARGING STARTS)	DC	G+C	NULL S/S ERROR			
COMMAND TRANSMITTER AND FTS POWER ON	DC	PWR				
NOTE- ELECTRIC HEATERS MAY BE COMMANDED ON TO EXPEDITE WARMUP OF LOCAL AREAS						
ENG T/M ASSESSMENT	DC	FTS	CYCLE THRU ALL ENG T/M MODES			

Table C-6. Lunar Night Sequence (Sheet 2 of 2)

EVENTS	FROM	TO	RESPONSE	INDICATION	POWER	TIME
IMAGING ASSESSMENT NOTE- USE THE PROCEDURES DEVELOPED FOR IMAGING SURVEYS TO ASSESS THE LRV EXTERIOR CONDITION						
SCIENCE OPERATION NOTE- USE AVAILABLE TIME WHILE WAITING FOR THE BATTERY TO CHARGE TO PERFORM SCIENCE EXPERIMENTS PLANNED DURING NIGHT						
BATTERY CHARGE COMPLETE NOTE- BATTERY STATUS DETERMINED BY OPERATIONS FROM T/M DATA						

Table C-7. Alternate Lunar Night Sequence With RTG

ALTERNATE LUNAR NIGHT SEQUENCE WITH RTG

EVENTS	FROM	TO	RESPONSE	INDICATION	POWER	TIME
POSITION SOLAR PANEL	OC	CC+S		OC VERIFICATION		4
	OC	CC+S				4
	OC	CC+S				4
	CC+S	DEV		POSITION POTS		
ACTIVATE RTG THERMAL CONTROL SYSTEM	OPER					
COMMAND MAIN POWER OFF						
NOTE- RECEIVER, TRANSMITTER, FTS AND SELECTED SCIENCE MAY REMAIN ON AS A FUNCTION OF AVAILABLE POWER						
PREPARE PLAN FOR INITIAL SUNRISE OPERATION	OPER					
POSITION S/P (AUTO) (BATTERY CHARGING STARTS)	OC	G+C	NULL S/S ERROR			
ENG T/M ASSESSMENT	OC	FTS	CYCLE THRU ALL ENG T/M MODES			
IMAGING ASSESSMENT						
NOTE- USE THE PROCEDURES DEVELOPED FOR IMAGING SURVEYS TO ASSESS THE LRV EXTERIOR CONDITION						
SCIENCE OPERATION						
NOTE- USE AVAILABLE TIME WHILE WAITING FOR THE BATTERY TO CHARGE TO PERFORM SCIENCE EXPERIMENTS PLANNED DURING NIGHT						
BATTERY CHARGE COMPLETE						
NOTE- BATTERY STATUS DETERMINED BY OPERATIONS FROM T/M DATA						

Table C-8 Nonstandard Sequence (Sheet 1 of 3)

NONSTANDARD SEQUENCE

LOCATION OF LRV AT END OF TRAVERSE STEP DOES NOT PROVIDE ADEQUATE VIEW

EVENT	FROM	TO	RESPONSE	INDICATION	POWER	TIME
360 DEG SCAN HAS BEEN COMPLETE PER STANDARD SEQUENCE						
EVALUATE 360 DEG SCAN AND SELECT ALTERNATE LOCATION	OPER					90
NARROW ANGLE SURVEY OF ALTERNATE LOCATION						
A CMD TV AZIMUTH	OC DC	CC+S CC+S	STORE MAGNITUDE INITIATE POSITIONING			4
B CMD TV ELEVATION	OC DC	CC+S CC+S	STORE MAGNITUDE INITIATE POSITIONING			4
C SEL NARROW ANGLE	DC	TV				4
D SEL APERTURE	DC	TV				4
E SEL SHUTTER SPEED	DC	TV				4
F INITIATE PICTURE	DC	TV				4
E WAIT FOR READOUT	OPER					6
EVALUATE NARROW ANGLE SURVEY	OPER					
SELECT BEARING AND STEP DISTANCE	OPER					
LOW POWER RF	DC	RFS		DECREASE SIGNAL STRENGTH		4

Table C-8. Nonstandard Sequence (Sheet 2 of 3)

EVENTS	FROM	TO	RESPONSE	INDICATION	POWER	TIME
TRANSFER TO OMNI ANT	DC	RFS		DECREASE SIGNAL STRENGTH		4
INSERT TURN PARAMETERS	OC CC+S	CC+S MOB	TURN DIRECTION	LIMIT SWITCH		4
INITIATE TURN	DC CC+S	CC+S MOB	TRAVERSE START	COMMAND EVENT MOTOR CURRENT ODOMETER OUTPUT		4
STOP TURN	ODOM	CC+S	TRAVERSE STOP	CC+S EVENT		
FTS TO TRAVERSE MODE	DC	FTS				4
INSERT TRAV PARAMETERS	QC	CC+S				4
INITIATE TRAVERSE	DC	CC+S	APPLY POWER TO WHEEL MOTORS	COMMAND EVENT MOTOR CURRENT ODOMETER OUTPUT		4
STOP TRAVERSE	ODOM	CC+S	REMOVE POWER FROM WHEEL MOTORS	CC+S EVENT		
POSITION SOLAR PANEL (AUTOMATIC)	CC+S	G+C	NULL S/S ERROR	S/S ERROR S/P POS POTS S/P VOLT + AMP		10
DETERMINE HI-GAIN ANT POINT PARAMETERS	OPER		COMPUTATION BY GROUND COMPUTER			10
POSITION H-GAIN ANT	QC QC DC	CC+S CC+S CC+S				

Table C-8. Nonstandard Sequence (Sheet 3 of 3)

EVENTS	FROM	TO	RESPONSE	INDICATION	POWER	TIME
TRANS TO HI-GAIN ANT	DC	RFS		INCREASE SIGNAL		4
HIGH POWER RF	DC	RFS	20 WATTS RF POWER	INCREASE SIGNAL		4
RETURN TO STANDARD SITE IDENTIFICATION SEQUENCE	OPER					

Table C-9. Emergency Stop From "X" Reason (Sheet 1 of 2)

EVENTS	FROM	TO	RESPONSE	INDICATION	POWER	TIME
EMERGENCY STOP FROM						
(A)LOSS OF AGC VOLTAGE	RFS	G+C	TRAVERSE STOP			
NOTE- 1 TWO-WAY RF LOCK REQUIRED DURING TRAVERSE 2 RECEIVER ANTENNA PLACEMENT ON LRV MUST BE SUCH THAT UP-LINK COMMUNICATIONS CAN BE ESTABLISHED AFTER LRV STOP 3 BACK-UP OF LRV NOT ALWAYS DESIRABLE 4 PROBABLE LOSS OF DOWN LINK T/M						
(B)EXCESS LRV TILT	INCL	G+C	TRAVERSE STOP			
(C)SHARP SURFACE SLOPE CHANGE (NEG OR POS)	OBST	G+C	TRAVERSE STOP			
(D)EXCESS SURFACE PENETRATION	DC	G+C	TRAVERSE STOP			
NOTE- DETERMINED BY GROUND COMPUTATION FROM TELEMETERED POWER REQUIREMENT AND INDICATED SURFACE SLOPES						
(E)EXCESS WHEEL SLIP	CC+S	G+C	TRAVERSE STOP			
NOTE- DETERMINED BY ODOMETER UNBALANCE						
POSITION SOLAR PANEL						
A LOSS OF AGC	RFS	G+C				
	G+C	DEV	AUTO SUN SEARCH	S/S ERROR		
B EMERGENCY STOP FROM OTHER CAUSE	DC	G+C				
	G+C	DEV	AUTO SUN SEARCH	S/S ERROR		
POSITION HI-GAIN ANT	OC	CC+S				
	OC	CC+S				
	DC	CC+S				
NOTE- IF AUTO ANTENNA POSITIONING IS AVAILABLE, LOSS OF AGC MAY BE USED TO INITIATE SEARCH						
HIGH POWER RF	DC	RFS	20 WATT RF POWER	INCREASE SIGNAL		

Table C-9. Emergency Stop From "X" Reason (Sheet 2 of 2)

EVENTS	FROM	TO	RESPONSE	INDICATION	POWER	TIME
IMAGING ASSESSMENT NOTE- USE STANDARD IMAGING PROCEDURES TO PROVIDE PICTURES FOR SITUATION ASSESSMENT						
ASSESS SITUATION AND DEVELOP CORRECTIVE PROCEDURE	OPER					

APPENDIX D

SURVEYOR MIDCOURSE AND LUNAR LANDING SYSTEM

APPENDIX D

SURVEYOR MIDCOURSE AND LUNAR LANDING SYSTEM

The primary objective of the Surveyor propulsion is to provide the appropriate velocity changes required by the spacecraft after separation from the Atlas-Centaur boost vehicle. Such velocity changes are necessary for midcourse trajectory corrections as well as for the main and vernier deceleration phases of soft landing on the lunar surface.

To accommodate these requirements, a fixed high-thrust propulsion system and a variable, low-thrust propulsion system are provided. The high-thrust system (main retro-propulsion) consists of a solid propellant rocket motor that supplies the major portion of the impulse required to decelerate the spacecraft when approaching the Moon. The low-thrust system (vernier propulsion) consists of three liquid bi-propellant engines, coupled with the associated pressurization and propellant feed systems. This system supplies the forces required for midcourse velocity correction, for attitude control during the retro deceleration phase of terminal descent and, after retro-rocket burnout, for the final deceleration to the lunar surface.

During a typical Surveyor flight, a midcourse maneuver is performed 15 hours after launch. At this time the spacecraft is oriented so that the vernier engines thrust in the desired direction. Upon command, these engines are then ignited and fired for a predetermined time to produce the desired velocity vector correction. Midcourse correction capability is limited to a maximum of 164 ±1.3 fps and a minimum of 6.6 ±1.3 fps. Differential throttling of the three engines and hinging one of the engines stabilizes the spacecraft during the correction.

The nominal lunar approach and terminal descent sequence may be described briefly as follows. Approximately 63 hours after launch, the spacecraft is commanded to roll and pitch, or yaw, from its Sun/Canopus locked cruise attitude into a position in which the main retro thrust axis approximately coincides with the velocity vector. Sixty miles above the lunar surface, a radar sensor called the altitude marking radar (AMR) (Fig. D-1) generates a signal which triggers the following automated descent sequence: (1) The three engines of the vernier propulsion system are ignited. These liquid propellant engines,

each of which is capable of being throttled within a thrust range from approximately 30 to 104 pounds, provide stabilization during the main retro motor burn. One second later, the 10,000 pound thrust solid-propellant main retro motor is ignited and burns for approximately 40 seconds. This reduces the spacecraft velocity from 8,700 ft/s to 350 ft/s at approximately 26,000 feet altitude. The main retro motor case is then ejected, while the vernier propulsion system continues to stabilize the spacecraft, developing a constant resultant thrust of 90 percent of the lunar spacecraft weight, in other words the spacecraft is free falling in a one-tenth lunar gravity field. In the meantime, the Radar Altimeter and Doppler Velocity Sensors (RADVS) have acquired the lunar surface. About two seconds after retro motor case ejection, the RADVS system takes control of the further spacecraft descent, this system determines the spacecraft altitude and velocity relative to the lunar surface by means of four radar beams which are oriented as shown in Fig. D-2. The RADVS measurements are fed into a closed-loop automatic control system which commands the three vernier thrust levels such that the spacecraft acquires and is subsequently guided along a segmented straight line approximation of the "gravity turn" trajectory. This trajectory has two properties which are highly desirable for a dynamically smooth landing. First, it aligns the thrust and velocity directions, i.e., the spacecraft moves along its Z-direction only (see Fig. D-2 for spacecraft coordinates). Second, as the velocity approaches zero, the flight path direction (and, hence, the spacecraft Z-axis) is turned toward the lunar vertical. Because of control loop saturation, the spacecraft cannot always follow the trajectory segments precisely. However, in each segment, the actual trajectory intersects the pre-programmed line at a point called the acquisition point, from which point very close tracking ensues.

The final segment of the descent profile, together with the actual trajectory, is shown in Fig. D-3. After acquisition, which occurs at approximately an altitude of 80 feet, the straight line is followed until the velocity reaches 10 ft/sec at approximately an altitude of 43 feet. At this point, the RADVS system generates a signal (10-ft/s mark) which causes the RADVS control as well as the gravity turn descent profile to be abandoned and initiates the following automatic final descent sequence. The control is switched to a gyro-controlled inertial hold mode, and the vernier engines are commanded to decelerate the spacecraft rapidly to 5-ft/s vertical velocity. The spacecraft then descends

with this velocity held constant until, at an altitude of 13 feet, a second signal is generated (13-foot mark), turning the vernier engines off. Consequently, the spacecraft falls free until the surface is encountered, increasing its vertical velocity to nominally 12.6 ft/s. Since the gravity turn descent was abandoned at 10 ft/s, the spacecraft Z-axis is not precisely vertical at this time, in which position it remains during the inertial hold mode. This introduces a horizontal velocity at touchdown because of vernier thrusting in this tilted position between the 10 ft/s and the 13-foot mark.

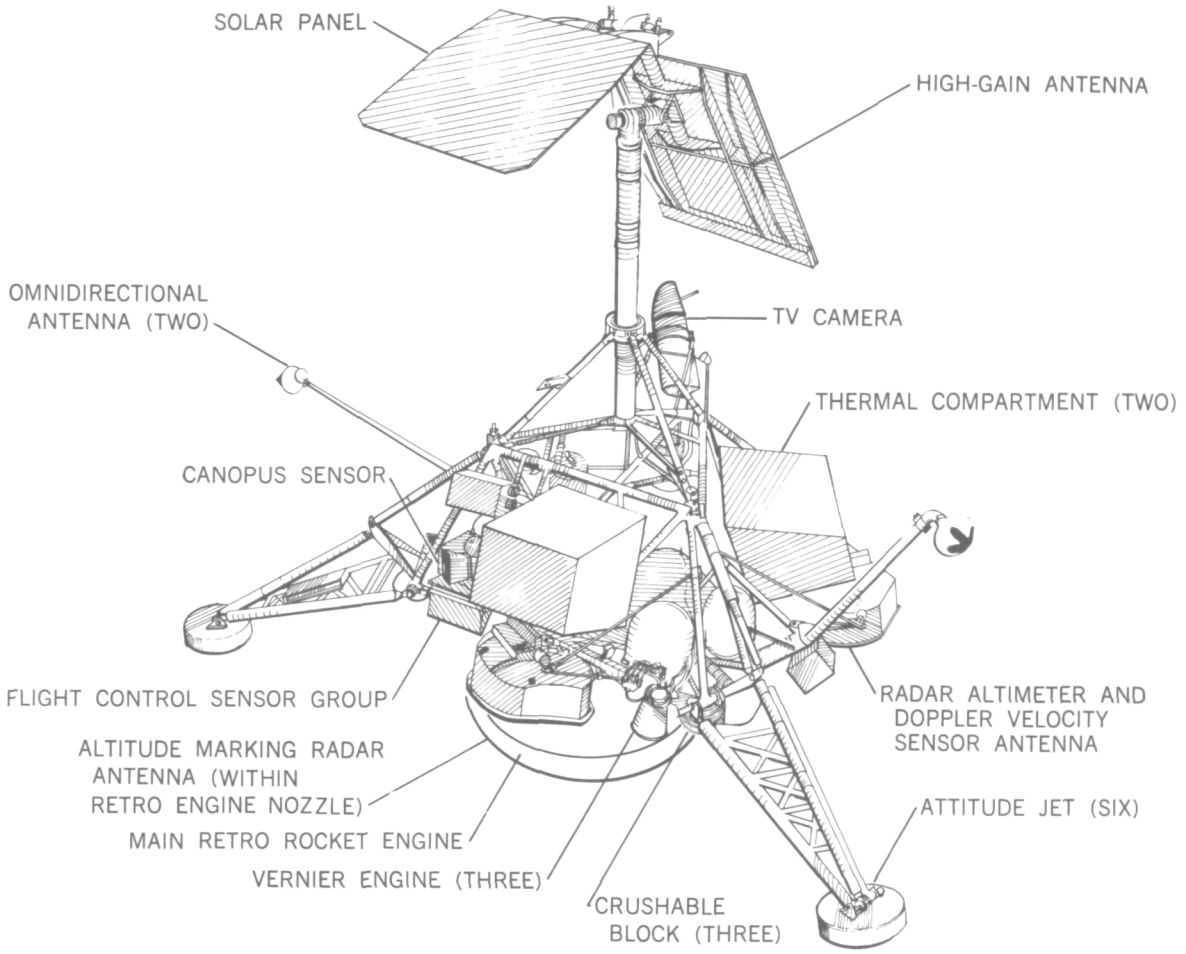

Figure D-1. Surveyor I Spacecraft Configuration

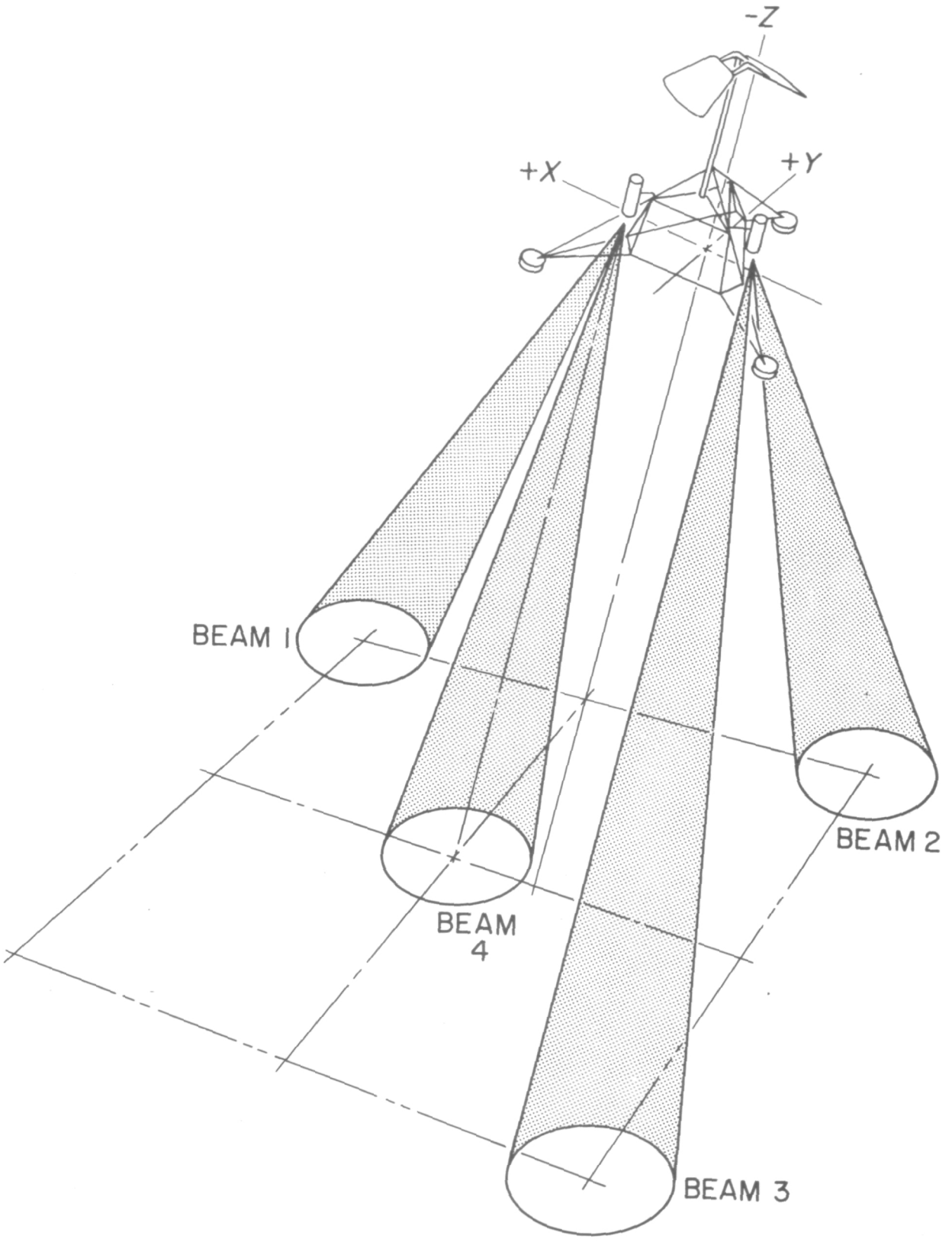

Figure D-2. RADVS Beam Orientation

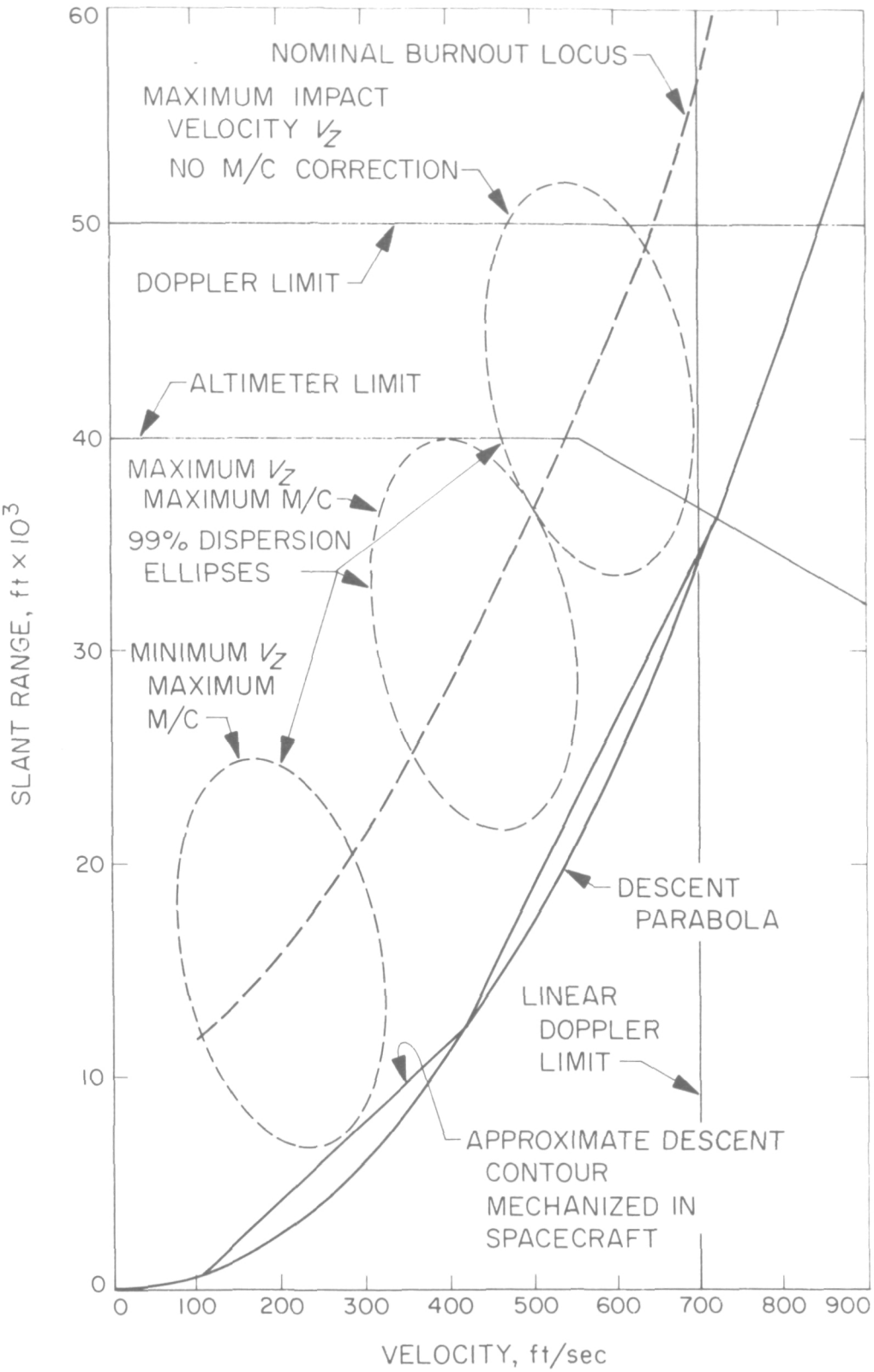

Figure D-3. Terminal Descent Velocity Profile

APPENDIX E

CIRCUIT LISTINGS

APPENDIX E

CIRCUIT LISTINGS

The procedure has been to number the circuits in ascending numerical order and list them in tabular form. The subsystem numbers have been assigned in accordance with the following code:

Table E-1. Subsystem Number Code

Reference Number	Subsystem	Abbreviation
001	Structure	STRU
002	Radio frequency	RFS
003	Flight command	FCS
004	Power	PWR
005	Central computer and sequencer	CC&S
006	Flight telemetry	FTS
007	Guidance and control	G&C
008	Pyrotechnics	PYRO
009	Cabling	CABL
010	Propulsion	PROP
011	Temperature control	T/C
012	Mechanical devices	DEV
013	Mobility	MOB
014	Navigation ranging	NARA
030	Science sampler	SPLR
031	Sample handling and storage	SH&S
036	Television	TV
072	Inclinometer	INCL
073	Accelerometer	ACCL
074	Obstacle detector	OBST
075	Sun sensors	SS

Table E-2 defines the following:

SUB SUB NO.

This column identifies the two interfacing subsystems by subsystem number.

FROM-TO

The direction of signal flow between subsystems is given by the "FROM" and "TO" columns, in which the subsystems are referred to by their standard abbreviations.

CIRCUIT NAME

The names of the circuits are given under the column called "CIRCUIT NAME" and if the circuit is associated with a ground command, it is identified at the beginning of the name by the letters "DC" or "QC".

USE OF LISTINGS

An example of the use of the listing is as follows:

To find all the circuits between the Radio Frequency Subsystem and the Flight Command Subsystem, it is first necessary to determine the reference number for the RFS, which is 002. The reference number for the FCS is 003. Since 002 is the lower number, these circuits will be found under 002-003 in the listing. All circuits forming the RFS-FCS interface are listed together at this point.

Table E-2. Functional Block Diagram Circuit List 6/25/68 (Sheet 1 of 5)

SUB SUB NO	FROM	TO		CIRCUIT NAME	REMARKS
002-003-001	FCS	RFS	DC	PWR SWITCH	
002-003-002	FCS	RFS	DC	ANT XFER	
002-003-003	RFS	FCS	COMMAND DATA		
002-003-004	FCS	RFS	DC	TRANSMITTER POWER ON/OFF	
002-005-001	RFS	CC+S	SIGNAL STRENGTH		
002-006-001	FTS	RFS	T/M MODULATION		
003-004-001	FCS	PWR	DC	PWR SWITCHING	
003-005-001	FCS	CC+S	QC	S/P ELEVATION	
003-005-002	FCS	CC+S	QC	S/P AZIMUTH	
003-005-003	FCS	CC+S	DC	S/P MANUAL POSITION	
003-005-004	FCS	CC+S	QC	ANT ELEVATION	
003-005-005	FCS	CC+S	QC	ANT AZIMUTH	
003-005-006	FCS	CC+S	DC	ANT MANUAL POSITION	
003-005-007	FCS	CC+S	QC	TV ELEVATION	
003-005-008	FCS	CC+S	QC	TV AZIMUTH	
003-005-	FCS	CC+S	DC	TV MANUAL POSITION	
003-005-	FCS	CC+S	QC	TRAVERSE COMMAND	INCLUDES TRAVERSE DIRECTION AND MAGNITUDE PLUS TURN DIRECTION
003-005-	FCS	CC+S	DC	STOP TRAVERSE	
003-005-	FCS	CC+S	DC	START TRAVERSE	
003-005-	FCS	CC+S	QC	SAMPLER POSITION AZIMUTH	INCLUDES RIGHT/LEFT AND MAGNITUDE
003-005-	FCS	CC+S	QC	SAMPLER POSITION ELEVATION	INCLUDES UP/DOWN AND MAGNITUDE
003-005-	FCS	CC+S	QC	SAMPLER POSITION EXTENSION	INCLUDES EXTEND/RETRACT AND MAGNITUDE
003-005-	FCS	CC+S	QC	SAMPLE ACQUISITION TIME	
003-006-	FCS	FTS	DC	MODE CHANGE	
003-006-002	FCS	FTS	COMMAND EVENT MONITOR		
003-006-003	FCS	FTS	DC	POWER ON/OFF	

Table E-2. Functional Block Diagram Circuit List 6/25/68 (Sheet 2 of 5)

SUB SUB NO	FROM	TO		CIRCUIT NAME	REMARKS
003-007-001	FCS	G+C	DC	S/P AUTO POSITION ON/OFF	
003-007-002	FCS	G+C	DC	EMERGENCY OVERRIDES	MAY BE A FAMILY OF COMMANDS
003-007-003	FCS	G+C	DC	POSITION T/C HEATERS	
003-008-	FCS	PYRO	DC	UNLOCK S/P	
003-008-	FCS	PYRO	DC	DEPLOY TV BOOM	
003-008-	FCS	PYRO	DC	A FRAME JETTISON	
003-008-	FCS	PYRO	DC	UNLOCK ANTENNA	
003-008-	FCS	PYRO	DC	DEPLOY OBSTACLE DETECTOR	
003-014-	FCS	NARA	DC	RANGING MANUAL OVERRIDE	USED TO REPEAT RANGE MEASUREMENT WITHOUT REPEATING TV
003-030-	FCS	SPLR	DC	SELECT SCOOP (ON/OFF)	
003-030-	FCS	SPLR	DC	SELECT DRILL (ON/OFF)	
003-030-	FCS	SPLR	DC	SELECT AUGER (ON/OFF)	
003-030-	FCS	SPLR	DC	SAMPLE ACQUISITION START	STOP CONTROLLED BY CC+S
003-030-	FCS	SPLR	DC	INITIATE SAMPLE TRANSFER	
003-030-006	FCS	SPLR	DC	SAMPLE TRANSFER POSITION	
003-031-	FCS	SH+S	DC	ROTARY STORAGE POSITION	
003-031-	FCS	SH+S	DC	VERTICAL STORAGE POSITION	
003-031-	FCS	SH+S	DC	EXTEND CUP ARM	
003-031-	FCS	SH+S	DC	GRASP SAMPLE CUP	
003-031-	FCS	SH+S	DC	RETRACT CUP ARM	
003-031-	FCS	SH+S	DC	RELEASE SAMPLE CUP	
003-036-	FCS	TV	DC	TV PWR ON/OFF	
003-036-	FCS	TV	DC	FIELD OF VIEW	
003-036-	FCS	TV	DC	RESOLUTION CONTROL	
003-036-	FCS	TV	DC	SHUTTER SPEED CONTROL	
003-036-	FCS	TV	DC	SHUTTER CONTROL	

Table E-2. Functional Block Diagram Circuit List 6/25/68 (Sheet 3 of 5)

SUB SUB NO	FROM	TO	CIRCUIT NAME	REMARKS
003-036-007	FCS	TV	DC APERTURE CONTROL	
004-098-	PWR	ALL	VOLTAGES AND CURRENTS	
005-006-	CC+S	FTS	T/M TRAVERSE START/STOP	
005-006-	CC+S	FTS	T/M ODOMETER	
005-006-	CC+S	FTS	T/M STEERING COMMANDS	
005-006-004	CC+S	FTS	CC+S EVENT MONITOR	
005-007-	CC+S	G+C	SOLAR PANEL POSITIONING	
005-007-	G+C	CC+S	EMERGENCY STOP TRAVERSE	
005-012-	CC+S	DEV	ANTENNA POSITIONING	
005-013-	CC+S	MOB	TURN DIRECTION	
005-013-	CC+S	MOB	TRAVERSE START/STOP	
005-013-	CC+S	MOB	TRAVERSE DIRECTION	
005-030-	SPLR	CC+S	START SAMPLE ACQUISITION	
005-030-	CC+S	SPLR	STOP SAMPLE ACQUISITION	
005-030-	CC+S	SPLR	POSITIONING COMMANDS	
005-036-	CC+S	TV	POSITIONING COMMANDS	
005-071-	ODOM	CC+S	OUTPUT PULSES	
005-071-	CC+S	ODOM	RESET	
006-007-001	G+C	FTS	SUN SENSOR ERROR	
006-008-	PYRO	FTS	T/M SQUIB CURRENTS	
006-012-	DEV	FTS	T/M SOLAR PANEL POSITION	

Table E-2. Functional Block Diagram Circuit List 6/25/68 (Sheet 4 of 5)

SUB SUB NO	FROM	TO	CIRCUIT NAME	REMARKS
006-012-	DEV	FTS	T/M HI GAIN ANTENNA POSITION	
006-012-	DEV	FTS	T/M TV BOOM POSITION	
006-013-001	MOB	FCS	MOTOR CURRENT	
006-014-	NARA	FTS	RANGE DATA	
006-031-	SH+S	FTS	T/M VERTICAL POSITION	
006-031-	SH+S	FTS	T/M ROTARY POSITION	
006-031-007	SH+S	FTS	CUP ARM EXTEND/RETRACT T/M	
006-031-008	SH+S	FTS	SAMPLER IN TRANSFER POSITION	
006-036-	TV	FTS	T/M TV POSITION	
006-036-	TV	FTS	VIDEO DATA	
006-072-	INCL	FTS	T/M INCLINOMETER OUTPUTS	
006-073-	ACCL	FTS	T/M ACCELEROMETER OUTPUTS	
006-074-	OBST	FTS	T/M OBSTACLE DETECTOR OUTPUTS	
006-075-	SS	FTS	T/M SUN SENSOR OUTPUTS	
007-011-001	G+C	T/C	POSITION HEATERS	
007-012-	G+C	DEV	S/P POSITION COMMANDS	
007-072-	INCL	G+C	INCLINOMETER OUTPUTS	
007-073-	ACCL	G+C	ACCELEROMETER OUTPUTS	
007-074-	OBST	G+C	OBSTACLE DETECTOR OUTPUTS	

Table E-2. Functional Block Diagram Circuit List 6/25/68 (Sheet 5 of 5)

SUB SUB NO	FROM	TO	CIRCUIT NAME	REMARKS
007-074-	G+C	OBST	OBSTACLE DETECTOR CONTROL	
007-075-	SS	G+C	SUN SENSOR OUTPUT	
008-012-001	PYRO	DEV	EJECT A FRAME	
014-036-	TV	NARA	PWR ON/OFF CONTROL	
014-036-	TV	NARA	RANGING CONTROL	
036-072-	INCL	TV	INCLINOMETER OUTPUTS	
- -	INCL	TV	INCLINOMETER OUTPUTS	
- -	INCL	TV	INCLINOMETER OUTPUTS	